

Identifying RING-type E3s involved in nutrient stress responses in *Arabidopsis thaliana*

by

Erin MacKinnon

A thesis submitted in partial fulfillment of the requirements for the degree of

Master of Science

at

Dalhousie University

Halifax, Nova Scotia

March 2024

This thesis is dedicated to everyone who has helped these past two years.

TABLE OF CONTENTS

LIST OF TABLES	iv
LIST OF FIGURES	v
ABSTRACT	vi
LIST OF ABBREVIATIONS USED	vii
ACKNOWLEDGEMENTS	xiii
CHAPTER 1: INTRODUCTION	1
1.1 The Ubiquitin Proteasome System	1
1.1.1 Ubiquitin ligases	3
1.1.2 RING-type E3s	5
1.2 The UPS and abiotic Stress	6
1.3 Iron	8
1.4 Nitrogen	14
1.5 Phosphorus	17
1.6 Objectives	20
CHAPTER 2: <i>Arabidopsis</i> E3s ATL12 and ARI12 are involved in regulating the response to Fe stress	
Abstract	22
Introduction	23
Materials and Methods	27
Results	36
Discussion	47
Supplementary Material	55
CHAPTER 3: RING-type E3 WAVH1 is required for optimal root growth and gravitropism under nitrogen limitation in <i>Arabidopsis thaliana</i>	
Abstract	60
Introduction	61
Materials and Methods	66
Results	73
Discussion	86
Supplementary Material	92
CHAPTER 4: CONCLUSIONS AND FUTURE DIRECTIONS	98
REFERENCES	101
APPENDIX A: Selecting candidate RING-type E3s	120
APPENDIX B: Phenotypic analysis of eight RING-type E3 mutants in nutrient stress assays	124
APPENDIX C: Review Article - The Ubiquitin Proteasome System and Nutrient Stress Response	132

LIST OF TABLES

CHAPTER 2

Table 1. Candidate RING-type E3s	27
Table 2. Composition of treatments for nutrient stress assays.....	28
Table 3. Primers used in PCR genotyping.....	30
Table 4. Primers used in RT-PCR.....	31
Table 5. Fe content quantification standards.....	35

CHAPTER 3

Table 1. Candidate RING-type E3s.....	66
Table 2. Composition of treatments for nutrient stress assays	67
Table 3. Primers used in PCR genotyping.....	69
Table 4. Primers used in RT-PCR.....	70

LIST OF FIGURES

CHAPTER 1

Figure 1. The Ubiquitin Proteasome System (UPS)	3
Figure 2. Simplified representation of different types of E3s.....	4
Figure 3. Simplified schematics of a RING domain.....	6
Figure 4. Fe uptake strategies.....	11
Figure 5. The UPS and Fe stress response.....	13
Figure 6. The UPS and N stress response.....	16
Figure 7. The UPS and P stress response.....	19

CHAPTER 2

Figure 1. Genotyping ATL12 and ARI12 T-DNA insertion mutants.....	36
Figure 2. Phenotypic analysis of <i>atl12-1</i> and <i>ari12-1</i> under iron (Fe) stress.....	38
Figure 3. Survival rates of <i>atl12-1</i> , <i>ari12-1</i> , and wild type (WT) on Fe deficient soil.....	40
Figure 4. Survival rates of <i>ari12-1</i> and WT on Fe excess soil.....	41
Figure 5. Rhizosphere acidification ability and FRO2 activity of <i>atl12-1</i> , <i>ari12-1</i> , and WT.....	42
Figure 6. Analysis of electrolyte leakage under Fe stress.....	44
Figure 7. Lower <i>FIT</i> and <i>IRT1</i> transcript levels and IRT1 protein levels in <i>atl12-1</i> under Fe deficiency compared to WT.....	45
Figure 8. <i>ari12-1</i> demonstrates higher whole seedling Fe content after Fe excess treatment compared to <i>atl12-1</i> and WT	46
Figure 9. Possible feedback loop involving ATL12 and FIT	49
Figure 10. Simplified schematics of the possible role of ARI12.....	53

CHAPTER 3

Figure 1. Genotyping <i>WAVH1</i> T-DNA insertion mutants	73
Figure 2. Phenotypic analysis of <i>wavh1-1</i> under nitrogen (N) and phosphorus (P) stress.....	75
Figure 3. Analysis of root gravitropic response under N and P stress.....	76
Figure 4. Lugol's staining on <i>wavh1-1</i> and wild type (WT) root tips	77
Figure 5. RT-PCR analysis of genes involved in the response to N limitation.....	78
Figure 6. Analysis of <i>wavh1-1</i> and WT lateral root elongation and emergence	80
Figure 7. Analysis of <i>wavh1-1</i> and WT primary root length when exposed to excess epibrassinolide brassinosteroids	81
Figure 8. Analysis of <i>wavh1-1</i> and WT primary root growth pattern when exposed to excess epibrassinolide brassinosteroids	82
Figure 9. Analysis of <i>wavh1-1</i> and WT root growth when exposed to brassinazole.....	84
Figure 10. Analysis of <i>wavh1-1</i> and WT root gravitropism when exposed to brassinazole.....	85
Figure 11. WAVH1 promoting lateral root emergence in Arabidopsis.....	89

ABSTRACT

The Ubiquitin Proteasome System (UPS) is a key molecular mechanism plants utilize to facilitate changes to the proteome. The UPS encompasses ubiquitination, the attachment of ubiquitin (Ub) molecule(s) to a target substrate, followed by the degradation of the modified substrate by the 26S proteasome. Ubiquitin ligases, or E3s, are central to the UPS as they govern specificity of substrate selection, interacting with the substrate directly and mediating ubiquitination. The UPS has emerged as an important regulator of the uptake and translocation of nutrients through mediating the degradation of enzymes, transporters, ion channels, signalling proteins, and transcription regulators in response to fluctuating nutrient levels. Inability to maintain nutrient homeostasis is detrimental due to suboptimal nutrient levels impacting processes vital to plant growth and development, such as carbon fixation, hormonal signalling, and synthesis of nucleic acids and amino acids. In addition, the effects of other abiotic stresses, such as drought, can be minimized by optimizing nutrition, which influences photosynthetic and physiological processes, and promotes water circulation. As the frequency and duration of stress conditions increases with climate change, plants rely more heavily on the UPS to maintain homeostasis of all essential nutrients, including the macronutrients nitrogen (N) and phosphorus (P), and the micronutrient iron (Fe). In this thesis I analyze the role of eight RING-type E3s in facilitating responses to excess and deficient levels of N, P, and Fe, using the model species *Arabidopsis thaliana* (*Arabidopsis*). I carried out in depth analyses of the role of three of these E3s, ARABIDOPSIS TOXICOS EN LEVADURA 12 (ATL12), ARIADNE 12 (ARI12), and WAVY GROWTH 3 (WAV3) Homolog 1 (WAVH1). I present evidence for the involvement of ATL12 in the Iron Deficiency Response (IDR) and discuss a model in which ATL12 participates in a feedback loop with FIT to promote Fe uptake under Fe deficiency. Under Fe deficiency, *ATL12* loss-of-function mutants exhibit lower *FIT* transcript levels, as well as lower *IRT1* transcript levels and IRT1 protein abundance, while simultaneously demonstrating longer roots and higher survival rates compared to WT. I also show that the E3 ARI12 is involved in the response to Fe stress. *ARI12* loss-of-function mutants exhibit a higher Fe content after exposure to excess Fe levels and exhibit significantly longer roots under Fe deficient and excess conditions when compared to WT. Results suggest that ARI12 regulates the abundance of an unknown IDR protein, and that *ARI12* expression is suppressed under Fe deficiency to allow its target protein to accumulate as part of the IDR. In this work I also propose a model where WAVH1 is involved in brassinosteroid (BR) signalling to regulate root growth. Results suggest that proper *WAVH1* function is required for proper primary root (PR) growth and root gravitropic abilities under severe N limitation, with *WAVH1* loss-of-function mutants exhibiting a significantly shorter PR length and larger root reflex angle in response to a 90° rotation compared to WT under severe N limitation. Mutants also exhibited significantly lower lateral root (LR) emergence suggesting that *WAVH1* function is also needed for this process, especially under severe N limitation. These significant differences are removed when seedlings are treated with brassinazole (BRZ), a BR biosynthesis inhibitor. This thesis attempts to fill in some of the many gaps in current knowledge of nutrient stress response in plants. The UPS is a highly conserved eukaryotic system, and therefore this knowledge will be of interest to researchers in other fields of research beyond the plant sciences.

LIST OF ABBREVIATIONS USED

-Fe	Fe deficient treatment
-N	N deficient treatment
-P	P deficient treatment
++Fe	Fe excess treatment
++N	N excess treatment
++P	P excess treatment
ABCG37/PDR9	ATP-binding cassette g37
ABRC	Arabidopsis Biological Resource Center
AAK6	Arabidopsis Adenylate Kinase 6
ACT1	ACTIN1
ADP	Adenosine diphosphate
AHA2	H ⁺ -ATPase 2
Al	Aluminium
AMT	Ammonium Transporter
Arabidopsis	<i>Arabidopsis thaliana</i>
ARI12	ARIADNE 12
AtFER1	Arabidopsis Ferritin 1
AtIPS1	Arabidopsis Induced by Phosphate Starvation 1
ATL12	Arabidopsis Toxicos en Levadura 12
ATP	Adenosine triphosphate
B	Boron
BAK1	BRI1-ASSOCIATED KINASE RECEPTOR 1
BES1	BRI1 EMS SUPPRESSOR 1
bHLH	Basic Helix-Loop-Helix
BL	Epibrassinolide brassinosteroids
BP	Bromocresol Purple
BR	Brassinosteroid
BRI1	BRASSINOSTEROID-INSENSITIVE 1

BRZ	Brassinazole
BSK2/3	Brassinosteroid Signalling Kinase 2/3
BTS	BRUTUS
BTSL1/2	BTS-Like 1/2
BZR2	BRASSINAZOLE-RESISTANT 2
C	Carbon
Ca	Calcium
CaCO	Calcium carbonate
CBL	Calcineurin B-Like
CC	Columella Cells
Cd	Cadmium
cDNA	Complementary DNA
CIPK14/23	CBL Interacting Protein Kinase 14/23
CK	Cytokinins
Cl	Chlorine
CLC	Chloride channel
Co	Cobalt
CO₂	Carbon dioxide
Col-0	<i>Arabidopsis thaliana</i> ecotype Columbia
COP1	CONSTITUTIVELY PHOTOMORPHOGENIC 1
CP	Core Protease
CRL	Cullin-RING Ub Ligase
Cu	Copper
Cul	Cullin
DNA	Deoxyribonucleic acid
E1	Ub activating enzyme
E2	Ub conjugating enzyme
E3	Ub ligase
EC1	Initial electrical conductivity
EC2	Final electrical conductivity
EDA40	EMBRYO DEVELOPMENT ARREST 40

EIL1	ETHYLENE INSENSITIVE3-LIKE1
EIN3	ETHYLENE INSENSITIVE3
EL	Electrolyte leakage
ERF53	Ethylene Response Factor 53
ERiN	E3 RING-type involved in Nutrition
EZ	Elongation Zone
Fe	Iron
Fe-EDDHA	Ethylene diamine-N,N bis(2hydroxyphenylacetic acid) Ferric sodium complex
Fe-EDTA	Ferric ethylenediaminetetraacetic acid
Fe²⁺	Ferrous Fe
Fe₂O₃	Hematite
Fe³⁺	Ferric Fe
FeOOH	Goethite
FIT	FER-like Fe-deficiency Induced Transcription factor
FMC	Fe mobilizing coumarins
FRD3	Ferric Reductase Defective 3
FRO2	Ferric Reduction Oxidase 2
FW	Fresh weight
H	Hydrogen
HECT	Homologous to the E6-AP Carboxyl Terminus
IBR	In Between RING
ICP-OES	Inductively Coupled Plasma Optical Emission Spectroscopy
IDF1	IRT1 Degradation Factor 1
IDR	Iron Deficiency Response
IDRP	Iron Deficiency Response Protein
IDT	Integrated DNA Technologies
IERP	Iron Excess Response Protein
IMA	IRON MAN
IRT1/2	Iron-Regulated Transporter 1/2
JA	Jasmonic Acid

K	Potassium
K (6, 11, 27, 29, 33, 48, 63)	Lysine residue 6, 11, 27, 29, 33, 48, 63
LR	Lateral Root
LRR-RLK	Leucine-Rich Repeat Receptor-Like protein Kinase
Met1	Methionine residue 1
Mg	Magnesium
miRNA	MicroRNA
Mn	Manganese
Mo	Molybdenum
MS	Murashige and Skoog
MYC2/JAI1	JASMONATE INSENSITIVE 1
N	Nitrogen
NCBI	Nation Center for Biotechnology Information
NH₄⁺	Ammonium
Ni	Nickel
NLA	Nitrogen Limitation Adaptation
NLP3/6/7	NIN-Like Protein 3/6/7
NO	Nitric oxide
NO₃⁻	Nitrate
NPF	NRT1/PTR transporter family
NRAMP	Natural Resistance-Associated Macrophage Proteins
NRT1/2	Nitrate Transporter 1/2
NUE	Nitrogen Use Efficiency
OsHRZ1/2	<i>Oryza sativa</i> Hemerythrin motif-containing RING- and Zinc-finger protein 1/2
OsNBIP1	<i>Oryza sativa</i> NRT1.1B interacting protein 1
P	Phosphorus
PHO1/2	PHOSPHATE 1/2
PHR	Phosphate Starvation Response
PHT	Phosphate Transporter
Pi	Inorganic phosphate

PM	Plasma Membrane
PR	Primary Root
PRU1	Phosphate Response Ubiquitin E3 Ligase 1
PSI	Pi Starvation Induced
PTR	Peptide Transporter
PUB12/13	PLANT U-BOX 12/13
PYE	POPEYE
RA	Rhizosphere Acidification
RBR	RING-Between-RING
RGLG1/2	RING domain ligase 1/2
Rice	<i>Oryza sativa</i>
RING	Really Interesting New Gene
RNA	Ribonucleic acid
ROS	Reactive Oxygen Species
RP	Regulatory Particle
RSA	Root System Architecture
RT-PCR	Reverse Transcription - PCR
S	Sulfur
SDEL1/2	SPX4 degradation E3 ligases 1/2
SIGNAL	Salk Institute Genomic Analysis Laboratory
SLAC1	Slow Anion Channel-Associated 1
SLAH	SLAC1 Homolog
T-DNA	Transfer-DNA
TCP20	TEOSINTE BRANCHED1/CYCLOIDEA/PROLIFERATING CELL FACTOR 20
Ub	Ubiquitin
UPS	Ubiquitin Proteasome System
URI	UPSTREAM REGULATOR OF IRT1
UV	Ultraviolet
WAV3	Wavy Growth 3
WAVH1/2	WAV3 Homolog 1/2

WB	Western Blot
WT	Wild-Type
ZIP	ZRT-IRT-like proteins
Zn	Zinc
ZRT	Zn-Regulated Transporter

ACKNOWLEDGEMENTS

Firstly, I would like to thank my supervisor, Dr. Sophia Stone. I have no idea where I would be today if you had not given me this opportunity. Thank you for entrusting me with this project and for your unwavering encouragement and support these past two years.

I would also like to thank everyone at Dalhousie who has ever offered me informational, emotional, or financial support. I would like to especially thank all the past and present members of the Stone Lab, including Michon McDonald, Sophia Tonks, Alison Tran, Dona Nelson, and Raja Wairavan. And thank you to my committee, Dr. Andrew Schofield, Dr. Lord Abbey, and Dr. David Chiasson. Thank you all for taking the time out of your lives to help me in my pursuit of this degree.

I would also like to express a special thanks to all my family and friends. This thesis could not have been completed without the constant influx of emotional support and encouragement that you have all provided me these past two years. You are all under no obligation to read this thesis (maybe look over the abstract).

And finally, I would like to thank the plants. Sorry that I had to kill all of you.

CHAPTER 1: INTRODUCTION

1.1 The Ubiquitin Proteasome System

The Ubiquitin Proteasome System (UPS) is an ATP-dependent protein degradation pathway that plants use to alter their proteome content, triggering the appropriate cellular changes to promote stress tolerance (Stone and Callis, 2007; Vierstra, 2009; Callis, 2014). The UPS involves the ubiquitination of a selected substrate followed by proteasomal degradation of the modified protein (Figure 1). Ubiquitination is a post-translational modification where ubiquitin (Ub), a small, highly conserved 76-amino acid eukaryotic protein, is covalently attached to a substrate (Callis, 2014). Ubiquitination requires the sequential actions of three types of enzymes: ubiquitin activating enzyme (E1), ubiquitin conjugating enzyme (E2), and ubiquitin ligase (E3). The E1 initiates the enzymatic cascade, hydrolysing ATP and binding to the Ub protein. The E1 and E2 interact to promote the transfer of the Ub from the E1 to the E2, forming an E2-Ub intermediate. The E3 interacts with the E2-Ub intermediate and facilitates the transfer of Ub to the substrate protein.

There are three possible outcomes of this enzymatic cascade: 1) monoubiquitination (attachment of one Ub); 2) polyubiquitination (attachment of two to more Ub proteins in a polyubiquitin chain); or 3) or multi- monoubiquitination (attachment of multiple Ub proteins at different sites) of the substrate (Figure 1) (Pickart and Eddins, 2004; Sadowski and Sarcevic, 2010). There is a degree of structural plasticity in polyubiquitination due to the flexibility of chain conformations which is caused by different linkages used to generate Ub chains. Ub-Ub linkages can be created using eight different sites, including seven lysine residues (K6, K11, K27, K29, K33, K48, and K63) and the N-terminal methionine (Met1) (Miricescu et al., 2018; Dittmar and

Winklhofer, 2019;). These different chain conformations are theorized to have distinct influence over the fate of the modified substrate. For example, a K63 linked chain is associated with non-proteasomal outcomes such as endocytosis, while a K48 linked chain is considered a signal for degradation by the 26S proteasome, a large multi-catalytic multi-subunit protease (Thrower et al., 2000; Varadan et al., 2002; Duncan et al., 2006). The attachment of Ub is reversible via the actions of deubiquitylating enzymes (DUBs) which cleave the isopeptide bond between Ub molecules to dismantle chains and remove ubiquitin from substrate proteins, acting as alternate regulators of ubiquitination (Komander, 2010).

The most well-understood function of ubiquitination is flagging proteins for degradation via the 26S proteasome, a compartmentalized complex composed of a hollow cylindrical 20S Core Protease (CP) capped at one or both ends by a 19S Regulatory Particle (RP) (Figure 1) (Bard et al., 2018). Protease activity is located on the β subunits of the two inner rings of the CPs four stacked heptameric rings. The polyubiquitin chains on the substrate are recognized by the RP, which unfolds the protein and directs it into the CP for proteolysis. The resulting peptides are expelled by the 26S proteasome and the Ub molecules are recycled.

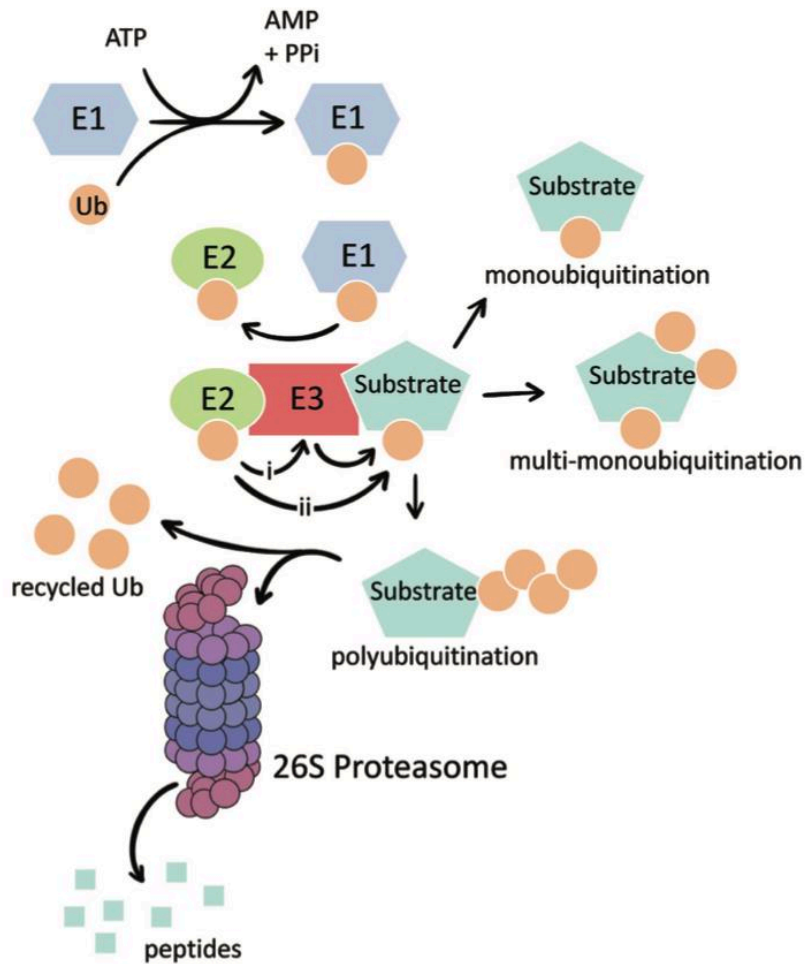


Figure 1. The ubiquitin proteasome system (UPS). The E1, E2, and E3 enzymes facilitate attachment of one or more ubiquitin (Ub) molecules to the target substrate. Ubiquitination of the target occurs through transfer of Ub from the E2 to the E3 prior to attachment to the substrate (i) or direct transfer of Ub to the substrate (ii). The enzymatic cascade results in the monoubiquitination (one Ub at one site), multi-monoubiquitination (multiple Ubs at different sites), or polyubiquitination (multiple Ubs forming a chain) of the substrate. Substrates destined for degradation are recognized and degraded by the 26S proteasome. The Ub is removed and recycled.

1.1.1. Ubiquitin ligases

E3s mediate the transfer of Ub from the E2 to the target substrate through the formation of an isopeptide bond between the C-terminal carboxyl group of the Ub and the amino group of a residue on the target substrate. Specificity of the ubiquitination pathway can be attributed to the

extensive and diverse collection of E3s. For example, the *Arabidopsis thaliana* (Arabidopsis) genome is estimated to encode for over 1500 single subunit ubiquitin ligases or components of E3 complexes (Vierstra, 2012; Callis 2014). To interact with the E2-Ub intermediate, single subunit E3s will employ a Really Interesting New gene (RING), Homologous to E6AP C-terminus (HECT) or U-box domain (Figure 2). Complex E3s will utilize a scaffold Cullin (Cul) protein interacting with a substrate-recognition component, with or without an adaptor subunit, and an E2-binding RING domain protein (Figure 2). Most ubiquitin ligases facilitate the transfer of Ub from the E2 directly to the substrate, with the exceptions being the single subunit HECT-type and RING-between-RING (RBR)-type E3s that accepts Ub from the E2 prior to transferring the Ub to the substrate (Figure 2). The ability of a single E3 to regulate the abundance of multiple substrates contributes to the pervasiveness of ubiquitin-dependent regulation in cellular function. Furthermore, multiple E3s may target one specific substrate for ubiquitination, depending on the environment.

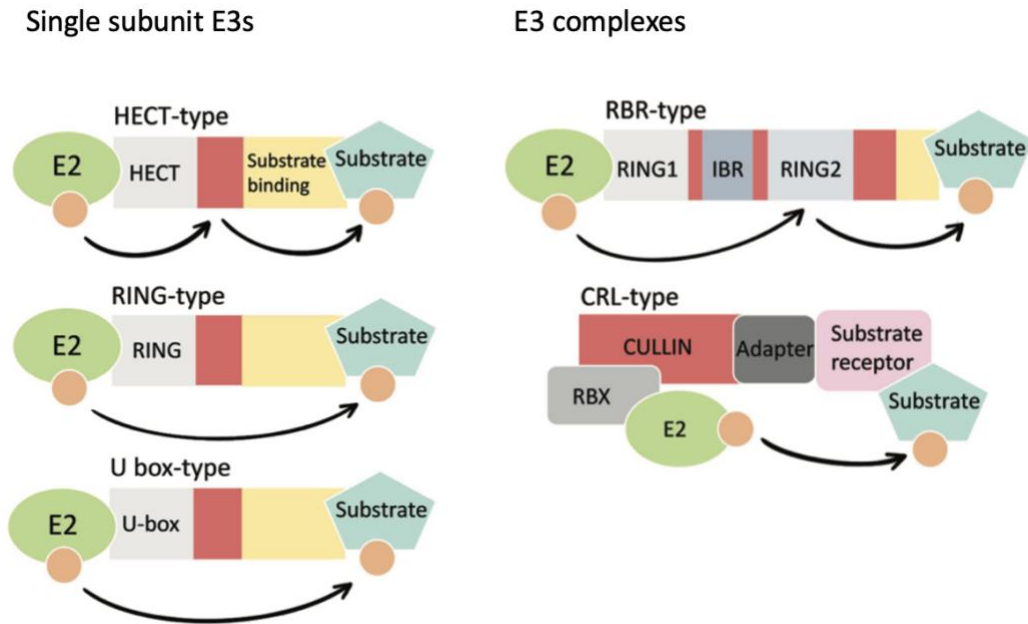


Figure 2. Schematics representation of different E3 types. E3s utilize a RING (Really Interesting New gene), HECT (Homologous to E6AP C-terminus), or U-box domain to interact with the E2. Single subunit HECT and RING-in-between-RING (RBR) type E3s accept the Ub from the E2 then transfers the Ub to the substrate. Other E3s interact with the Ub-E2 intermediate to mediate transfer of the Ub directly from the E2 to the target substrate. Complex E3 Cullin (Cul)-RING ubiquitin ligases (CRLs) utilize different subunits to interact with the E2 and substrate.

1.1.2. RING-type E3s

This thesis will focus on the E3s which contain a RING domain, which are characterized by the presence of an 8-ligand cysteine-rich domain that coordinates two zinc (Zn) atoms (Figure 3). These E3s include RING-type E3s and the RBR-type E3 complexes. There are approximately 500 RING-type E3s predicted to be encoded in the *Arabidopsis* genome, comprised of seven different classes: RING-HC, RING-H2, RING-V, RING-C2, RING-D, RING-S/T and RING-G; these seven classes differ very minimally in structure and can be distinguished by the amino acids in positions 2, 4, 5, and 6 within the domain, as well as the number of amino acids in between them (Figure 3) (Kosarev et al., 2002; Stone et al., 2005; Jiménez-López et al., 2018). For example, RING-H2 contains a Histidine (His) residue at position 5, whereas RING-D has an aspartate (Asp) residue (Stone et al., 2005). There are approximately 42 genes that encode for RBR-type proteins in the *Arabidopsis* genome, these 42 genes are divided into four subgroups: ARA54 (1), ARIADNE (ARI) (16), Plant I (3), and Plant II (22) (Marín, 2010). RBR-type E3 complexes are more structurally elusive than single subunit RING-type E3s and are characterized by the presence of three consecutive RING domains: RING1-IN BETWEEN RING (IBR)-RING2 (Marín, 2010). RING-type E3s interact with the E2-Ub intermediate to facilitate the transfer of Ub directly to the substrate, whereas the RBR-type E3s interact with the E2-Ub intermediate and mediate the transfer of Ub from the E2 to the RING2 and then to the substrate.

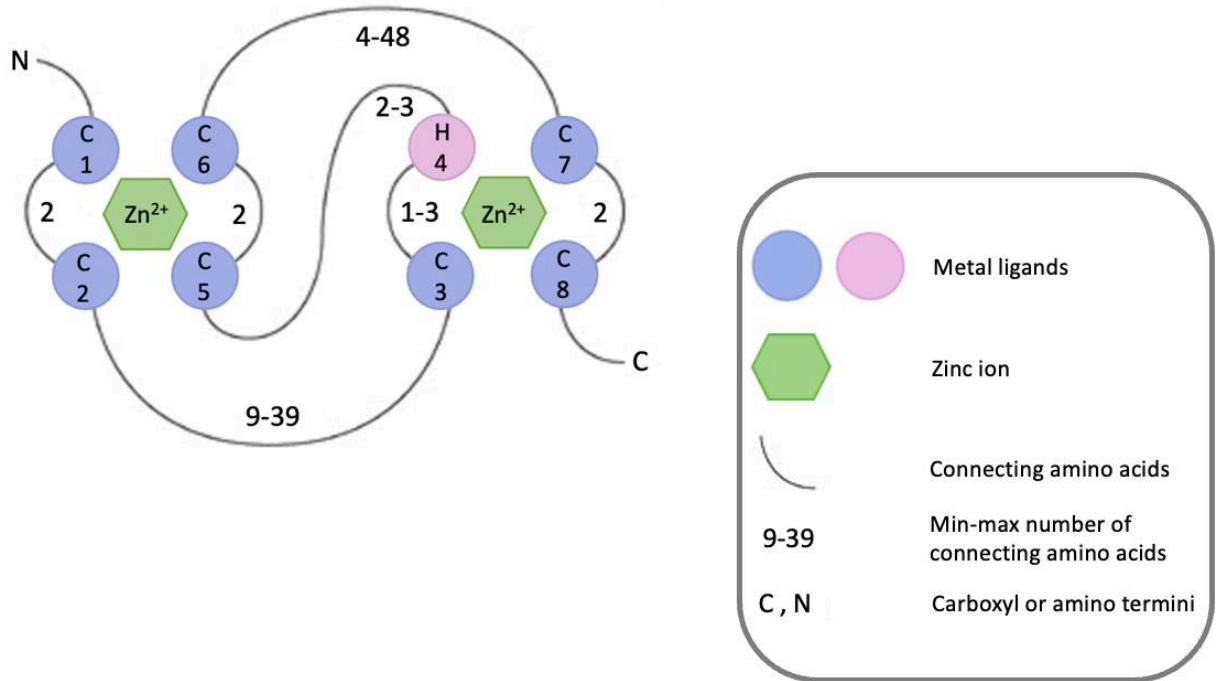


Figure 3. Schematics of the structure of prototypical RING domain (RING-HC type). The metal-ligand pairs 1 (1 and 2) and 3 (5 and 6) coordinate one zinc ion, while pairs 2 (3 and 4) and 4 (7 and 8) coordinate a second zinc atom in a cross-brace arrangement. There are seven different RING domain classes: RING-HC, RING-H2, RING-V, RING-C2, RING-D, RING-S/T and RING-G. These classes differ very minimally in structure and can be distinguished by which amino acids are in positions 2, 4, 5, and 6, as well as the number of amino acids in between them.

1.2 The UPS and Abiotic Stress

The UPS has been established as an important regulator of plant response to many abiotic stresses including drought/flooding, extreme heat, and high salinity (Stone, 2019; Melo et al., 2021). The UPS allows plants to efficiently regulate many aspects of cellular function via the degradation of numerous proteins including enzymes, transporters, ion channels, signalling proteins (e.g., kinases and receptors), and transcription regulators (e.g., transcription factors, co-activators, and repressors) (Trujillo and Shirasu, 2010; Sadanandom et al., 2012; Adams and Spoel, 2018; Stone, 2019). In response to internal/external cues, ubiquitination of a substrate can be promoted or inhibited, causing increased protein degradation or stabilization, respectively. The

UPS allows inhibition of a cellular response via degradation of a positive regulator or promotion of a response through the degradation of a negative regulator. For example, in the absence of drought stress, the RING-type E3s RING Domain Ligase 1 and 2 (RGLG1/2) ubiquitinate Ethylene Response Factor 53 (ERF53), a drought-induced transcription factor that regulates the expression of a plethora of drought-response genes (Cheng et al., 2016). Ubiquitination prevents the accumulation of ERF53, which inhibits the promotion of the drought stress response under favourable conditions. During exposure to drought stress, RGLG2 is translocated out of the nucleus, allowing ERF53 to accumulate and activate the expression of downstream targets and increasing stress tolerance (Hsieh et al., 2013; Cheng et al., 2016).

As climate change intensifies it is increasing the abiotic stresses that plants must tolerate, such as drought, flooding, and extreme temperatures (Eckardt et al., 2023). In addition to directly affecting plant growth, these climatic shifts also influence plant health through the alteration of soil properties such as temperature, moisture, salinity, and pH, which, among other issues, impacts the acquisition of essential nutrients (Haynes and Swift, 1986; Pregitzer and King, 2005; Brown et al., 2006; Jiang et al., 2017; Gelybó et al., 2018; Niena, 2019). Decreased nutrient availability and uptake is detrimental, as the effects of other abiotic stresses can be minimized by optimizing nutrition, which influences water circulation, photosynthesis, and other physiological processes (Ahanger and Ahmad, 2019). As the frequency and duration of stress conditions increases, plants rely heavily on the UPS to maintain nutrient homeostasis.

Nutrients in the soil are essential for plant growth and development, as well as crop yield. Plants require many different mineral elements for proper growth and development, and these essential macro and micronutrients are either bound to a soil particle or soluble in the soil water. The primary macronutrients, nitrogen (N), phosphorus (P), and potassium (K), are required in large

amounts relative to secondary macronutrients, calcium (Ca), magnesium (Mg) and sulphur (S), and micronutrients. Micronutrients are required in low levels, but extremely low levels will cause deficiencies, and excess levels will induce toxicity. Therefore, maintaining optimal levels of the essential micronutrients, which includes chlorine (Cl), boron (B), iron (Fe), manganese (Mn), copper (Cu), Zn, nickel (Ni) and molybdenum (Mo), are critical for plant success. The success of a plant largely depends on the ability to maintain homeostasis of all these essential nutrients, which relies on availability in the soil as well as absorption from the rhizosphere and transport throughout their intricate system of xylem and phloem to the tissues in need. Ub-dependent proteolysis is emerging as an important regulator of the absorption of nutrients from the rhizosphere and translocation from the root to shoot (Zelazny et al., 2011; Yates and Sadanandom, 2013). Failure to properly regulate the uptake and transport of nutrients results in deficient or excess stress conditions, which inhibit plant growth and development, decrease immunity, and ultimately reduce yield (Smith et al., 2022; Tripathi et al., 2022). This thesis will focus on the homeostasis of N, P, and Fe, three essential nutrients with strictly regulated uptake.

1.3 Iron

Fe is an essential micronutrient for all plants and its uptake, as a heavy metal, is strictly regulated through the actions of various molecular mechanisms. The UPS is quickly emerging as a significant regulator of Fe uptake in multiple plant species including *Arabidopsis* and *Oryza sativa* (rice). Adequate Fe levels are essential for N fixation, DNA replication and repair, because it functions as a cofactor to multiple DNA repair enzymes (including helicases, nucleases, glycosylases, demethylases), and the electron transport chain (Pushnik et al., 2008; Zhang, 2014). Fe is also vital to chlorophyll biosynthesis since it is a major component of chlorophyll, and low

levels of Fe will induce chlorosis due to insufficient chlorophyll production (Li et al., 2021). However, high Fe levels will inhibit proper function of the chloroplast and thylakoids because high levels are toxic. Fe toxicity stunts plant growth due to the formation of reactive oxygen species (ROS) that inhibit root development, which in turn impacts the uptake of other nutrients, causing the deficiency of other essential nutrients (Zahra et al., 2021; Harish et al., 2023). The uptake of Fe is facilitated by different strategies involving enzymes, specialized channels, and transporter proteins, which are present in the plasma membrane (PM). The main transporters of Fe in non-grass plants are the Natural Resistance-Associated Macrophage Proteins (NRAMPs), specifically AtNRAMP1, and the Zn-Regulated Transporter (ZRT)- Iron-Regulated Transporter (IRT)-like Proteins (ZIP). There are 15 ZIP proteins encoded by the Arabidopsis genome, with the most well-studied being IRT1 and 2 (Grotz et al., 1998). IRT1/2 are heavily involved in the uptake of Fe under deficient conditions (Vert et al., 2001; Vert et al., 2002). Studies report the AtNRAMP family of transporters are mostly involved in the intracellular mobilization of Fe (Thomine et al., 2003; Lanquar et al., 2005; Li et al., 2019). However, there is one member of this family, AtNRAMP1, which was found to cooperate with IRT1 to increase Fe uptake under Fe deficiency (Castaings et al., 2016; Agorio et al., 2017). Curie et al. (2000) suggests that the AtNRAMP transporters are not present in the PM. However, more recent studies suggest that AtNRAMP1 although found in cytoplasmic granular structures are located at the PM in epidermal cells (Agorio et al., 2017).

There are two main forms of Fe available to plants in soil: ferric iron (Fe^{3+}), and the more readily available form, ferrous iron (Fe^{2+}). And although Fe is abundant in most well-aerated soils, the activity of Fe is relatively low because it primarily forms insoluble ferric oxides and hydroxide minerals, such as goethite (FeOOH) and hematite (Fe_2O_3) at neutral pH levels (Kobayashi and

Nishizawa, 2012). To compensate for this, dicots utilize a reduction-based strategy (Strategy I) to increase Fe solubility through the sequential actions of multiple proteins (Figure 4A). First, the PM-localized complex H⁺-ATPase 2 (AHA2) pumps protons into the soil to decrease the pH of the rhizosphere (Connolly et al., 2003; Santi and Schmidt 2009; Martín-Barranco et al., 2020). Low Fe also activates the FER-like Fe-deficiency Induced Transcription factor (FIT) which promotes the expression of *Ferric Reduction Oxidase 2 (FRO2)*, and *IRT1*. Rhizosphere acidification mobilizes immobile Fe³⁺, which is then reduced to Fe²⁺ by FRO2. Fe²⁺ is then imported by IRT1 and other Fe transporters. There are other, more elusive, regulators and mechanisms, including the bHLH transcription factor POPEYE (PYE), another major regulator of Fe deficiency response which negatively regulates the expression of *bHLH Ibs* (Pu and Liang, 2023). A second strategy (Strategy II-like) is coming to light in non-grass plants involving PM-localized protein ATP-binding cassette g37 ABCG37/PDR9 secreting Fe mobilizing coumarins (FMCs) into the rhizosphere and chelating Fe³⁺, and evidence suggests that Fe³⁺-FMC complexes are up taken via an unknown ATP-dependent mechanism (Figure 4B) (Fourcroy et al., 2014; Li et al., 2023). These two strategies allow for the solubilization of insoluble Fe. Under Fe sufficient or excess conditions, the Fe deficiency response genes are deactivated to decrease Fe uptake. Excess Fe is a problem increased by anaerobic and acidic soil conditions and is a major threat to plant growth and development, inhibiting root growth, which further impacts the uptake of other essential nutrients (Becker and Asch, 2005). To mitigate the negative effects of both excessively low and high Fe levels, plants utilize the UPS to target repressors of the Fe deficiency response to promote uptake when levels in the rhizosphere are low, and to target components of the Fe deficiency response genes when sufficient levels are detected. The UPS is required to maintain the vital homeostasis of Fe.

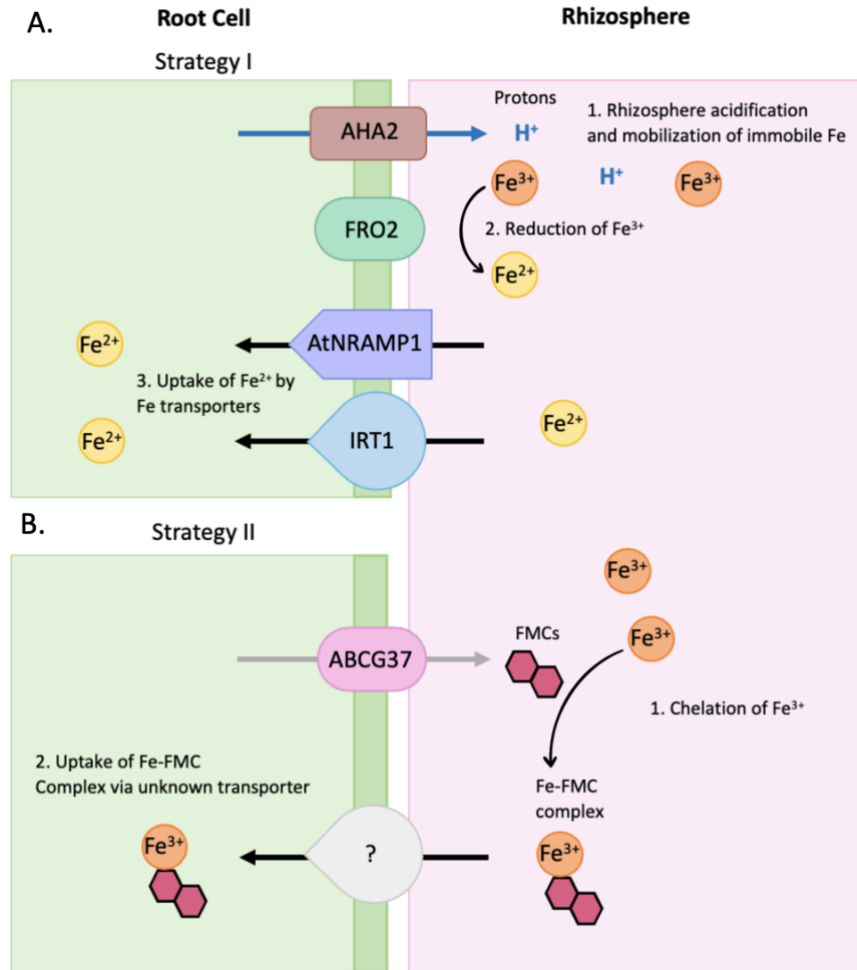


Figure 4. Simplification of rhizosphere acidification strategies utilized by dicots to increase iron (Fe) uptake when low Fe levels are detected in the rhizosphere. **(A)** Strategy I involves PM-localized protein AHA2 excreting protons into the rhizosphere, causing acidification, and mobilizing immobile Fe^{3+} . Insoluble Fe^{3+} is then reduced to soluble Fe^{2+} by FRO2, and Fe^{2+} is then transported across the PM by IRT1 and other metal transporters, like AtNRAMP1. **(B)** Strategy II involves ATP-binding cassette g37 ABCG37/PDR9 secreting Fe mobilizing coumarins (FMC) into the rhizosphere and chelating Fe^{3+} , and an unknown ATP-dependent mechanism up-taking the Fe^{3+} -FMC complexes.

Fe deficiency activates FIT, which is a major regulator among a group of basic helix-loop-helix (bHLH) transcription factors that control the expression of hundreds of Iron Deficiency Response Genes (IDRGs) (Colangelo and Gueriot, 2004; Mai et al., 2016). Approximately 500 FIT-regulated genes are encoded by the Arabidopsis genome (Kosarev et al., 2002; Stone et al.,

2005). FIT is a major regulator among a group of basic helix-loop-helix (bHLH) transcription factors that control the expression of multiple IDRGs (Colangelo and Guerinot, 2004; Mai et al., 2016). Upregulation of *IRT1* via FIT under Fe deficiency promotes Fe uptake (Figure 5A); IRT1 also transports other essential cations, including Zn, Mn, cadmium (Cd) and cobalt (Co) (Vert et al., 2002). Under Fe sufficient and excess conditions, IRT1 is ubiquitinated by the RING E3 IRT1 Degradation Factor 1 (IDF1), to limit uptake of the micronutrient (Figure 5B) (Barberon et al., 2011; Shin et al., 2013; Dubeaux et al., 2018). Sufficient Fe also promotes the ubiquitination of FIT by the RING E3s BRUTUS (BTS)-Like 1 and 2 (BTSL1/2) to prohibit nutrient uptake (Rodríguez-Celma et al., 2019). Higher concentrations of other metals, including Zn, Mn, and Co, also promotes the monoubiquitination of IRT1 prior to IDF1-mediated polyubiquitination to generate a 63-lysine chain (Barberon et al., 2011; Dubeaux et al., 2018). Monoubiquitination and polyubiquitination both decrease the levels of IRT1 in the PM via increasing degradation and internalization in the vacuole. High levels of non-iron metals also promote the Calcineurin B-Like (CBL) Interacting Protein Kinase 23 (CIPK23)-dependent phosphorylation of IRT1, triggering the IDF1-mediated ubiquitination of IRT1 (Dubeaux et al., 2018). AHA2 and FRO2 are also ubiquitinated, however the modification does not promote degradation and is suggested to regulate enzyme function (Martín-Barranco et al., 2020). Low iron in the rhizosphere activates a cascade of bHLH regulators which causes the expression and activation of FIT. In the absence of low Fe stress bHLH105 and bHLH115, two bHLH transcription factors involved in FIT activation, are targeted for Ub-mediated proteasomal degradation by the RING-type E3 BTS; this inhibits the activation of the Fe deficiency response (Selote et al., 2015). When low Fe is detected, the interaction with bHLH105 and bHLH115 is disrupted by IRON MAN (IMA) peptides that bind to BTS, which ultimately promote accumulation of the bHLHs and activation of the Fe deficiency

response (Grillet et al., 2018; Li et al., 2021). In rice there are two E3s like BTSL1 and BTSL2 which function as negative regulators of the Fe-deficiency response: Hemerythrin motif-containing RING- and Zinc-finger protein 1 (OsHRZ1) and OsHRZ2 (Kobayashi et al., 2013; Rodríguez-Celma et al., 2019). BTSL1/2 and OsHRZ1/2 have been shown to bind Fe and Zn, which suggests that these Ub ligases also function as metal sensors (Kobayashi et al., 2013; Selote et al., 2015; Rodríguez-Celma et al., 2019). Evidence shows OsHRZ1/2 are also vital for limiting the uptake of non-iron metals under excess Fe; this further suggests that these E3s have a role in Fe sensing (Aung et al., 2018).

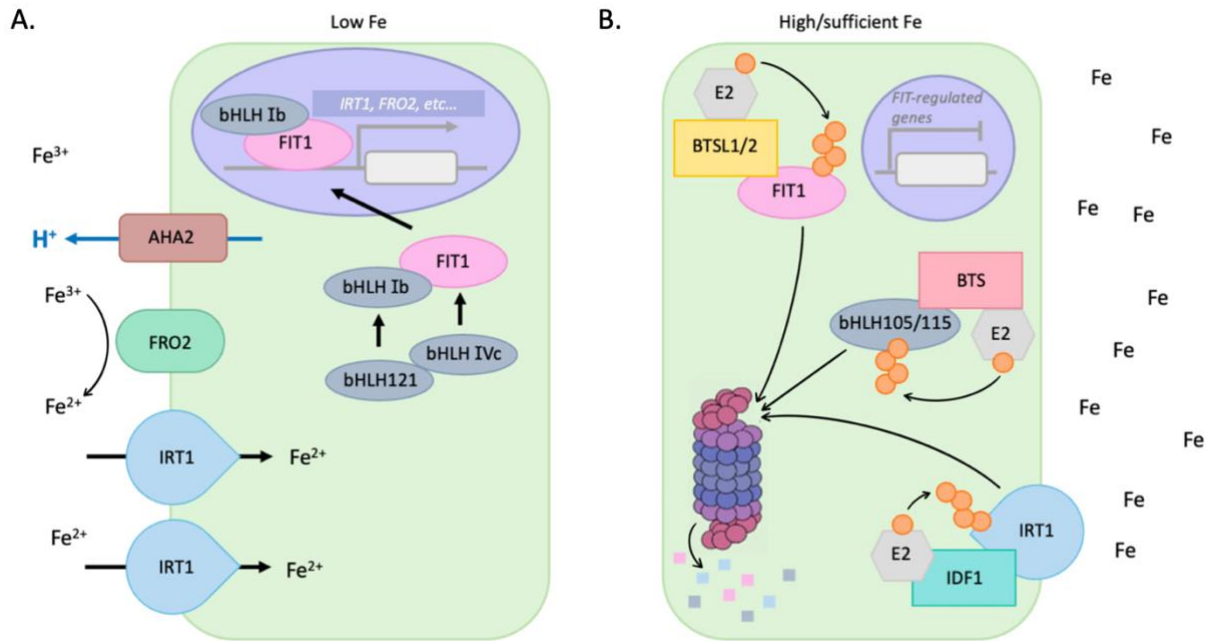


Figure 5. Simplified representation of the role of select E3s from Arabidopsis in regulating iron (Fe) uptake. **(A)** When Fe levels are low a cascade of bHLH transcription factors activates the FER-Like Iron Deficiency-Induced Transcription Factor (FIT) enters the nucleus and promotes the transcription of multiple Fe deficiency response genes including the Iron-regulated Transporter 1 (IRT1), Reduction Oxidase 2 (FRO2), and AHA2. **(B)** When exposed to high or sufficient Fe, FIT is ubiquitinated by BRUTUS-LIKE 1 or 2 (BTSL1/2), which prevents the transcription of IRT1 and other Fe deficiency response genes to limit Fe uptake. The E3 BTS targets bHLH IVc genes bHLH105 and bHLH115, which work upstream of FIT. In addition, IRT1 proteins are ubiquitinated by the IRT1 Degradation Factor 1 (IDF1) another RING-type E3 to further limit Fe uptake.

1.4 Nitrogen

N is the macronutrient required in the largest amount by plants. It is a major component of amino acids, nucleotides, and chlorophyll, therefore heavily contributing to photosynthetic processes and fruiting success. N is also essential for the metabolism of sugar, controlling sugar levels which regulate the expression of genes vital for various developmental and physiological processes (Sato et al., 2009; Zhang et al. 2020). Leaf N content and photosynthetic capacity are positively correlated, with N deficiency stress causing decreased photosynthetic rates (Hikosaka et al., 2004; Sage and Pearcy, 1987; Khamis et al., 1990). N levels too high or low inhibit total biomass production and overall plant success (Costa et al., 2002). Whenever adequate levels of N are not available it will limit growth, development, and crop yield. Plants uptake both inorganic forms of N, as nitrate (NO_3^-) and ammonium (NH_4^+), and organic forms of N, as the amino acids in the soil (Zhang et al., 2020). There are four groups involved in nitrate uptake and translocation in Arabidopsis; the Nitrate Transporter 1 (NRT1)/ Peptide Transporter (PTR), NRT2, Chloride Channel (CLC), and Slow Anion Channel-Associated 1 (SLAC1)/ SLAC1 Homolog (SLAH) transporter families (Krapp et al., 2014). The NRT1/PTR (NPF) transporter family is one of the most extensive collections of transporters in the plant kingdom. The NPF family contains 53 transporters which are predominantly low-affinity transporters involved in sensing, uptake, and translocation of NO_3^- and dipeptides (Almagro et al., 2008; Krapp et al., 2014). The SLAC1/SLAH family contains seven slow-type anion channels, which exhibit a strong preference for transporting nitrate (Schroeder and Keller, 1992; Schmidt and Schroeder, 2014; Krapp et al., 2014). The NRT2 family contains seven high-affinity nitrate transporters, four of which (NRT2;1, NRT2;2, NRT2;4; NRT2;5) are expressed in Arabidopsis roots under Nitrogen limitation (Kiba and Krapp, 2016). Research shows that upwards of 95% of high affinity nitrate influx can be attributed to these NRT2

transporters (Kiba et al., 2012; Lezhneva et al., 2014). The CLC family contains seven chloride channels which facilitate NO_3^- transport and vacuole storage, contributing to N use efficiency (NUE) (He et al., 2022; Liao et al., 2018). The ammonium transporters (AMT) mediate the acquisition of ammonium from the rhizosphere and are essential to plants growing in flooded or acidic soils where ammonium is the dominant form of N available (Ludewig et al., 2007). There are six members of the AMT family in Arabidopsis, all encoding ammonium transporters of different affinities and transport capacities (Yuan et al., 2007; Kiba and Krapp, 2016). N limitation de-represses the expression of AMT1;1, AMT1;2, AMT1;3, AMT1;5, and AMT2;1 (Kiba and Krapp, 2016; Yuan et al., 2007).

There are multiple E3s which have been identified as regulators of N uptake in Arabidopsis and rice. For example, the RING-type E3 Nitrogen Limitation Adaptation (NLA) is a major component in regulating the molecular response to N deficiency (Peng et al., 2007; Kant et al., 2011; Liu et al., 2017). NLA is predominantly localized to the PM, and during exposure to high N levels it mediates the ubiquitin-dependent degradation of the N transporter NRT1.7 (Figure 6) (Liu et al., 2017; Hannam et al., 2018). NRT1.7 is a low-affinity nitrate transporter expressed in the phloem where it is heavily involved in source-to-sink remobilization of nitrate (Fan et al., 2009). Abnormally high levels of NO_3^- exhibited in senescent leaves of *nrt1.7* mutants indicates that NRT1.7 is a significant facilitator of phloem loading to remobilize nitrate (Sakuraba, 2022). Under N deficiency, NLA protein levels decrease via microRNA (miRNA)-dependent translational repression, which diminishes negative regulation of NRT1.7 and promotes N mobilization through increased NRT1.7 levels (Liu et al., 2017). Peng et al. (2007) demonstrates that when exposed to N deficiency, NLA mutants displayed premature senescence which suggests hypersensitivity to N stress. The RING-type E3 NRT1.1B interacting protein 1 (OsNBIP1) in rice targets the repressor

protein SPX4 for degradation via the 26S proteasome, alleviating the inhibition of Nin-Like Protein 3 (NLP3) which promotes the expression of multiple N-responsive genes (Figure 6) (Hu et al., 2019).

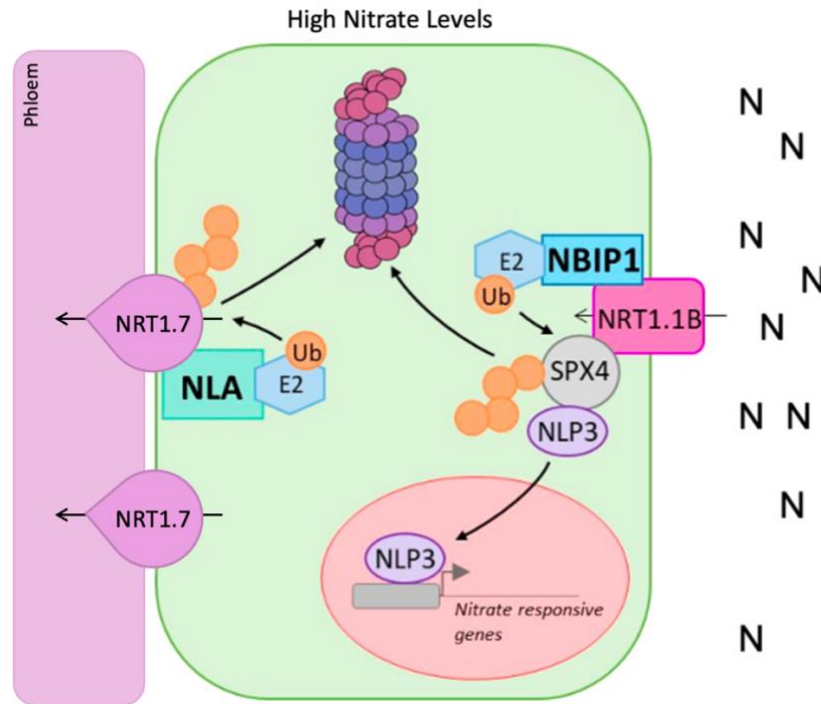


Figure 6. Simplified representation of the role of select E3s from *Arabidopsis thaliana* (Arabidopsis) and *Oryza sativa* (rice) in regulating nitrogen (N) uptake. In *Arabidopsis thaliana*, under high N, the Nitrogen Limitation Adaptation (NLA), an E3, mediates ubiquitin-dependent degradation of Nitrate Transporter 1.7 (NRT1.7) to avoid N overaccumulation. In rice the transceptor NRT1.1B recruits the E3 NRT1.1B interacting protein1 (NBIP1), which ubiquitinates SPX4 allowing the transcription factor NIN-Like Protein 3 (NLP3) to enter the nucleus and promote expression of N-responsive genes.

The UPS is also an established regulator of maintaining ideal carbon (C) to N ratio. The calculated coordination of C to N levels is vital to plant success, since under high C/low N stress conditions the C/N response inhibits post-germinative growth (Sato et al., 2009). An ideal C/N ratio is also necessary to optimize the utilization of CO₂ in plants, which is vital for the success of an ecosystem (Zheng, 2009). Two RING-type E3s in Arabidopsis, Arabidopsis tóxicos en levadura

(ATL) 6 and 31, are negative regulators of the C/N response, which plants utilize to balance C and N levels during early growth (Sato et al., 2009; Sato et al., 2011). When exposed to high C/N stress, 14-3-3 χ protein levels increase, which promotes the arrest of early seedling growth (Sato et al., 2011). ATL31 is an established mediator of the Ub-dependent degradation of 14-3-3 χ , with ATL31-mediated degradation of 14-3-3 χ increasing under normal C/N levels (Sato et al., 2011; Yasuda et al., 2014; Yasuda et al., 2017). This prevents 14-3-3 χ from accumulating, attenuating the C/N stress response (Sato et al., 2011). Upon detection of C/N stress, CIPK14, mediates the phosphorylation of ATL31; this stabilizes ATL31 levels, allowing 14-3-3 χ to accumulate to promote the response to C/N stress (Yasuda 2017).

1.5 Phosphorus

P is the macronutrient required in the second largest amount by plants. It is a key component of macromolecules, such as proteins, nucleic acids and the energy units ATP and ADP. Optimal levels are essential to support photosynthetic processes, metabolism of nitrogen, carbohydrates, and fat, and other ATP-dependent pathways (López-Arredondo et al., 2014). P deficiency also decreases leaf surface area, in turn decreasing CO₂ acquisition (Høgh-Jensen et al., 2002). The main forms of P available are the inorganic orthophosphates: H₂PO₄⁻ and HPO₄²⁻. Maintaining P homeostasis is important as low P levels greatly reduces root growth and net photosynthesis, and levels too high causes P toxicity. In Arabidopsis, there are four families of Phosphate Transporters (PHTs), PHT1-PHT4. Intracellular transport and uptake of inorganic phosphate (Pi) from soil are dependent on these transporters (Młodzińska and Zboińska, 2016). The PHT1 family comprises nine high affinity Pi transporters. Of the nine members, PM localized PHT1;1, PHT1;2, PHT1;3 and PHT1;4 transporters are primarily involved in the acquisition of Pi

from the rhizosphere (Shin et al., 2004; Ayadi et al., 2015). Translocation of Pi from source to sink is dependent on PHT1;5 transporters, and PHT1;8 and PHT1;9 work to mediate the acquisition of Pi during phosphorus starvation (Nagarajan et al., 2011).

In rice and Arabidopsis, the expression of Pi-starvation induced (PSI) genes including PHT1s are regulated by a family of Phosphate Starvation Response (PHR) transcription factors (Bustos et al., 2010). In *Oryza sativa*, OsSPX4 interacts with OsPHR2 when exposed to excess or sufficient Pi levels, inhibiting the transcription of many PSI genes (Figure 7A) (Lv et al., 2014). Under Pi-starvation, the repressor SPX4 is ubiquitinated by the RING-type ubiquitin ligases SPX4 degradation E3 ligases 1 (SDEL1) and SDEL2 (Ruan et al., 2019). SPX4 is then degraded by the 26S proteasome, allowing OsPHR2 to enter the nucleus, increasing the expression of PSI genes (Figure 7b) (Ruan et al., 2019). The ubiquitination of SPX4 also promotes to the activation of OsPHR2, the homolog of AtPHR1, and upregulating PSI genes under P deficiency (Hu et al., 2019). The N-stress responsive E3 NLA also plays a role in regulating P homeostasis, regulating the abundance of PHT1 proteins at the PM to limit or increase uptake under P excess or deficiency, respectively (Kant et al., 2011; Lin et al., 2013). Under P excess or sufficient conditions, loss of NLA function caused toxicity, due to the accumulation of PHT1s at the PM (Lin et al., 2013). The E3 NLA works with the E2 Phosphate 2 (PHO2) to mediate the Ub-dependent proteasomal degradation of the transporter PHT1;4 to limit Pi uptake when exposed to excess Pi (Figure 7A) (Lin et al., 2013; Park et al., 2014). P deficiency induced miRNAs modulate NLA and PHO2 levels, allowing for the accumulation of PHTs under low Pi or the increased ubiquitination of PHTs under Pi excess (Bari et al., 2006; Kant 2011; Lin et al., 2013). This increase in miRNA levels under Pi deficiency requires PHR1 (Bari et al., 2006). The homeostasis of P is also maintained by the F-Box E3 Phosphate Response Ubiquitin E3 Ligase 1 (PRU1) promoting the ubiquitin-

dependent degradation of WRKY6, a transcription factor that inhibits the transcription of *Phosphate 1 (PHO1)* (Chen et al. 2009; Lin et al., 2013; Ye et al., 2018). When exposed to low P, *PHO1* is expressed, increasing the root-to-shoot loading of P (Hamburger, 2002). The proteasomal degradation of WRKY6 via ubiquitination by PRU1 increases the abundance of PHO1, which increases the movement of P into root xylem (Figure 7B).

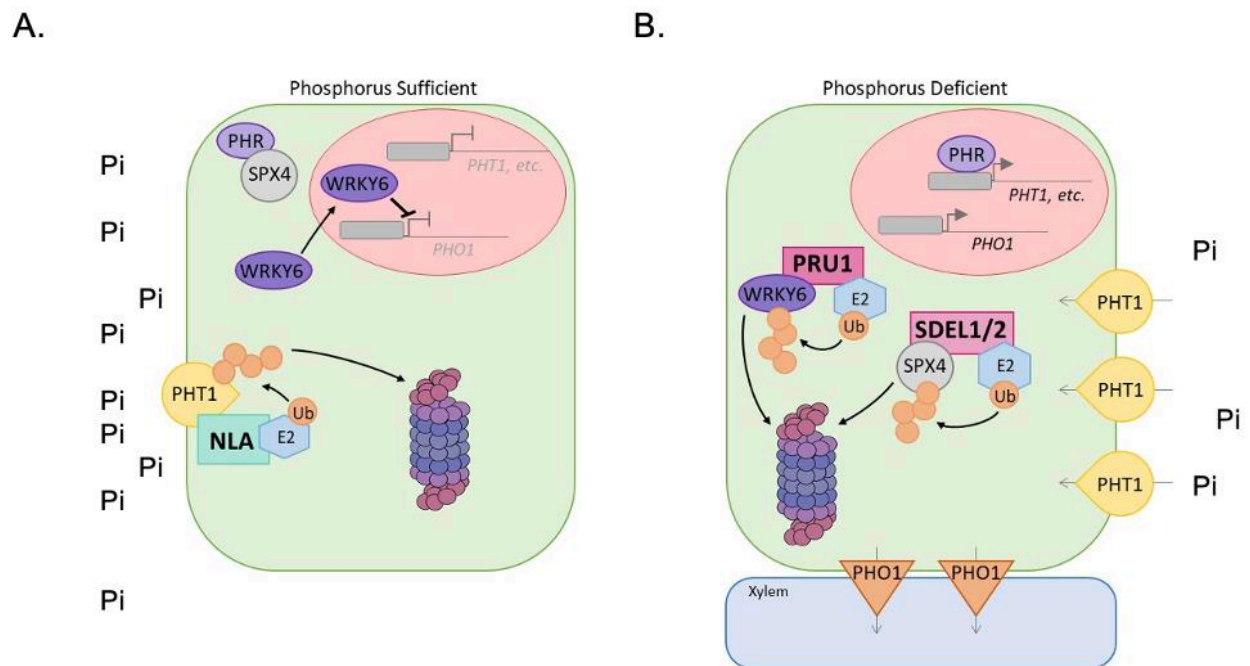


Figure 7. Simplified representation of the role of select E3s from *Arabidopsis thaliana* and *Oryza sativa* in regulating phosphorus (P) uptake. **(A)** Under Pi sufficient conditions, E3 Nitrogen Limitation Adaptation (NLA) ubiquitinates Phosphate Transporter 1 (PHT1) inorganic phosphate transporters facilitating degradation by the 26S proteasome to reduce uptake and prevent Pi overaccumulation. **(B)** Under P limiting stress conditions, E3s SDEL1 and SDEL2 mediate the degradation of SPX4, which allows the transcription factor Phosphate Starvation Response 1 (PHR1/2) to activate the expression of PSI genes such as Phosphate Transporter 1 (PHT1). Also, the Phosphate Response Ubiquitin E3 Ligase 1 (PRU1) mediates degradation of the repressor WRKY6, which relieves inhibition of Phosphate 1 (PHO1) transcription. Increase in PHO1 transporter abundance promotes loading of Pi into the root xylem.

1.6 Objectives

This thesis will explore the role of the UPS in regulating the uptake of N, P and Fe, as well as plant response to limited and excess nutrient conditions using *Arabidopsis thaliana* as a model species. The overall objective is to identify novel Arabidopsis RING-type and RBR-type E3s, which are involved in uptake and response to these nutrient stresses. To complete this objective, there were five main aims, 1: Select candidate RING-type E3s that show indication of involvement in responding to Fe, P, and/or N stress; 2: Determine if disrupting transcription of selected RING-type E3s cause differential growth under the deficiency or excess of Fe, P, and/or N; 3: Determine if the expression of selected RING-type E3s changes under the deficiency or excess of Fe, P, and/or N; 4: Find out if the decreased expression of three RING-type E3s of interest interferes with any major Fe, P, and/or N uptake or stress response mechanisms; and 5: Identify the possible roles that the three E3s of interest play in Fe, P, and/or N stress response.

This research aims to advance our understanding of the mechanisms which regulate ubiquitin ligase activity and engagement with substrates under varying levels of nutrient availability. When considering the rapidly changing status of the Earth's climate, greater knowledge of the role of the UPS in nutrient acquisition may assist with understanding how nutrient homeostasis can be maintained to mitigate the negative impact of abiotic stresses intensified by climate change. The UPS is a system that is highly conserved among eukaryotes. Therefore, knowledge gained maybe applied to crop species and will also be of interest to researchers in other areas of research beyond the plant sciences.

CHAPTER 2: *Arabidopsis* E3s ATL12 and ARI12 are involved in regulating the response to Fe stress

***Arabidopsis* E3s ATL12 and ARI12 are involved in regulating the response to Fe stress**

Erin MacKinnon and Sophia L. Stone

ABSTRACT

In eukaryotic cells, ubiquitin ligases (E3s) play an essential role in promoting stress tolerance through governing the ubiquitin (Ub) dependent degradation of signalling/regulatory proteins in response to environmental stimuli. Ub-mediated degradation via the 26S proteasome, or the Ubiquitin Proteasome System (UPS), is utilized by plants to alter the proteome in response to stress and is emerging as a significant regulator in iron (Fe) stress response pathways. Fe is an essential micronutrient and its uptake, as a heavy metal, is strictly regulated. In *Arabidopsis thaliana* the regulation of Fe uptake when exposed to toxic Fe levels (++Fe) can be partially attributed to the RING-type E3s BTSL1/2 and IDF1, which mediate the degradation of the major transcriptional regulator of Fe starvation responsive genes, FIT, and the high affinity Fe transporter, IRT1, respectively. Here we analyze the roles of two other RING-type E3s, ATL12 and ARI12, in the Fe stress response. Results show that FIT-regulated *ATL12* is involved in regulating *FIT* expression via interfering with jasmonic acid (JA) signalling under Fe deficiency (-Fe). *ATL12* loss-of-function mutants expressed lower levels of *FIT* and *IRT1* transcript levels, as well as IRT1 protein levels, under -Fe. ARI12 is likely involved in attenuating the IDR under sufficient and excess Fe levels (++Fe), with *ARI12* loss-of-function mutants having a higher tolerance to -Fe and having a higher tissue Fe content than WT under ++Fe. Both *ATL12* and *ARI12* mutants exhibited decreased sensitivity under -Fe and *ARI12* mutants exhibited decreased sensitivity on ++Fe, suggesting that ATL12 and ARI12 are regulators of the Fe stress response.

INTRODUCTION

Iron (Fe) is an essential micronutrient for all plants and its uptake, as a heavy metal, is strictly regulated. Optimal Fe levels are essential for a variety of processes including chlorophyll biosynthesis, nitrogen (N) fixation, DNA replication and repair, and the electron transport chain (Pushnik et al., 2008; Zhang, 2014). However, exposure to high Fe levels will cause toxic Fe accumulation inside the plant cells, increasing cell death and stunting plant growth due to the formation of reactive oxygen species (ROS), inhibiting growth and the development of sufficient root architecture, which impacts the uptake of other essential nutrients (Becker and Asch, 2005; Sachdev et al., 2021). There are two main forms of Fe available to plants in soil: ferric iron (Fe^{3+}), and the more readily available form, ferrous iron (Fe^{2+}). And although the micronutrient is abundant in most well-aerated soils, the bioavailability of Fe is relatively low because it primarily forms insoluble ferric oxides and hydroxide minerals, such as goethite (FeOOH) and hematite (Fe_2O_3) at neutral pH levels (Kobayashi and Nishizawa, 2012). To compensate for this, non-grass plants utilize a reduction-based strategy (Strategy I) to increase Fe solubility by decreasing the pH of the rhizosphere and reducing Fe^{3+} to its more soluble form Fe^{2+} . This is achieved through the sequential actions of multiple proteins in the root epidermal cell. In Arabidopsis, low Fe activates the FER-like iron deficiency induced transcription factor (FIT), a major regulator among a group of basic helix-loop-helix (bHLH) transcription factors that control the expression of approximately 500 Fe-deficiency responsive genes (Colangelo and Guerinot, 2004; Mai et al., 2016). FIT promotes the expression of *Ferric Reduction Oxidase 2 (FRO2)*, and *Iron-Regulated Transporter 1 (IRT1)*, a high-affinity iron transporter. IRT1 forms a plasma membrane (PM)-localized complex with H^+ -ATPase 2 (AHA2), which mediates the excretion of protons to decrease rhizosphere pH

(Connolly et al., 2003; Santi and Schmidt 2009; Martín-Barranco et al., 2020). These two processes allow for the solubilization and chelation of insoluble Fe^{3+} ; the Fe^{3+} is then reduced to Fe^{2+} by FRO2, and the Fe^{2+} can then be imported by IRT1. There are other, more elusive, regulators and mechanisms, including the bHLH transcription factor POPEYE (PYE), another major regulator of Fe deficiency response which negatively regulating the expression of *bHLH Ibs* (Pu and Liang, 2023). A second strategy (Strategy II-like) is coming to light in dicots involving PM-localized protein ATP-binding cassette g37 ABCG37/PDR9 secreting Fe mobilizing coumarins (FMC) into the rhizosphere and chelating Fe^{3+} , and evidence suggests that Fe^{3+} -FMC complexes are up taken via an unknown ATP-dependent mechanism (Fourcroy et al., 2014; Li et al., 2023).

When Fe levels are sufficient or high, a problem increased by anaerobic and acidic soil conditions, these responses must be suppressed to limit Fe uptake. The activation and deactivation of these Fe stress response mechanisms are coordinated by an intricate network of hormones and signalling molecules. Research shows that Fe deficiency increases production of the hormone ethylene in *Arabidopsis* and *Solanum lycopersicum* (tomato), which increases the expression of *FIT* and downstream target genes involved in the Fe-deficiency response Strategy I such as FRO2 and IRT1 (Hindt and Guerinot, 2012). Direct interactions between FIT and ethylene signalling pathway transcription factors, ETHYLENE INSENSITIVE3 (EIN3) and ETHYLENE INSENSITIVE3-LIKE1 (EIL1), limits proteasomal degradation of FIT under Fe deficiency (Lingam et al., 2011). Another signalling molecule which works to decrease the proteasomal degradation of FIT is nitric oxide (NO), which accumulates under Fe deficiency (Romera et al., 2011). Ethylene and NO work together to positively regulate the Fe-deficiency response, and studies demonstrate that NO enhances ethylene production and vice versa (Garcia et al., 2010; Garcia et al., 2011). These signalling molecules work downstream of the plant growth hormone,

auxin. In *Arabidopsis*, low Fe levels promotes auxin synthesis, which enhances expression of *FIT* and *FIT*-regulated genes, and increases NO levels (Chen et al., 2010). These signalling pathways promote Fe uptake, but under excess or sufficient Fe levels, these pathways must be deactivated, and transcription of Fe-deficiency response genes must be negatively regulated. Two hormonal signalling pathways are known to negatively regulate the Fe-deficiency response, one involving cytokinin (CK), and the second involving jasmonates, such as jasmonic acid (JA). Previous research demonstrates that JA signalling promotes the expression of *bHLH IVa* genes, which form heterodimers with *FIT* to promote the proteasomal degradation of *FIT* (Goossens et al., 2017; Cui et al., 2018; Shikha et al., 2023). In contrast, CKs act independently of *FIT* to negatively regulate *FIT*-regulated genes *IRT1* and *FRO2*, reducing the activity of Fe-deficiency response proteins via inhibiting their expression at the transcriptional level (Séguéla et al., 2008).

To maintain Fe homeostasis, plants must regulate the abundance of all the transporters, enzymes, ion channels, signalling proteins, and transcription regulators involved in Fe acquisition. Plants utilize mechanisms such as the Ubiquitin Proteasome System (UPS) to mediate the turnover of negative or positive regulators of Fe deficiency response genes when Fe levels are low or high, respectively. Target proteins are tagged for degradation by the 26S proteasome via ubiquitination, which involves the attachment of ubiquitin (Ub) via the sequential action of three enzymes: the E1, E2, and E3. The E3s control substrate selection, directly interacting with the target to mediate ubiquitination. The UPS is quickly emerging as a significant regulator of Fe uptake in plants. For example, under Fe sufficient and excess conditions, *IRT1* is ubiquitinated by the RING-type E3 *IRT1* Degradation Factor 1 (*IDF1*), to limit uptake of Fe (Barberon et al., 2011; Shin et al., 2013; Dubeaux et al., 2018). Sufficient Fe also promotes the ubiquitination of *FIT* by the RING E3s *BRUTUS* (*BTS*)-Like 1 and 2 (*BTSL1/BTSL2*), and of *bHLH105* and *bHLH115*, two *bHLH*

transcription factors involved in FIT activation, by the RING-type E3 BTS (Rodríguez-Celma et al., 2019; Selote et al., 2015). The Arabidopsis genome is estimated to encode for over 1500 single subunit E3s or components of E3 complexes, including approximately 500 RING-type E3s (Vierstra, 2012; Callis 2014). Results of microarray analysis shows that 66 of these RING E3s are differently expressed under Fe deficiency, suggesting potential involvement in the Fe deficiency response. In this article we investigate the roles of two of these E3s, ATL12 and ARI12, and provide evidence of involvement in maintaining Fe homeostasis in Arabidopsis. Our results indicate that ATL12 is involved in a feedback loop with FIT, with *ATL12* loss-of-function mutants exhibiting lower levels of *FIT*. *ATL12* loss-of-function mutants exhibit an abnormal response to Fe deficiency, possibly because ATL12 plays a role in the JA signalling pathway which regulates the IDR. Our results suggest that ARI12 is an Fe excess response gene, as *ARI12* expression significantly decreases under Fe deficiency, it likely targets an unknown IDR protein to limit Fe uptake when Fe levels are sufficient. *ARI12* loss-of-function mutants demonstrate an increased tolerance to Fe deficiency and contain significantly higher Fe levels after exposure to excess Fe, further supporting this theory.

MATERIALS AND METHODS

Plant growth conditions

14 candidate RING-type E3s were selected for this project (APPENDIX A). *Arabidopsis thaliana* ecotype Columbia (*Col-0*) (wild type, WT), and SALK T-DNA insertion mutant seeds (Table 1) were obtained from the Arabidopsis Biological Resource Center (ABRC, <https://abrc.osu.edu/>). Seeds were surface-sterilized with 50% (v/v) bleach for 10 minutes at room temperature. Seeds were then rinsed thoroughly with double-distilled H₂O then plated on solid ½ Murashige and Skoog (MS) medium containing 0.8% agar and 1% sucrose. Seeds were then stratified at 4°C in the dark for 72 hours, and then were grown under continuous light at 22°C. 10-day-old seedlings were transferred from the ½ MS medium to soil and grown with photoperiodic cycles of 16 hours light and 8 hours dark at 22°C.

Gene	Gene Name	Mutant: SALK Line
At2g22680	WAVH1	SALK_149664 (<i>wavh1-1</i>), SALK_041291 (<i>wavh1-2</i>)
At2g20030	ATL12	SALK_066923 (<i>atl12-1</i>), SALK_201056 (<i>atl12-2</i>)
At2g31780	ARI11	CS24734
At1g14260	ERiN1	SALK_118406
At1g05880	ARI12	SALK_033142 (<i>ari12-1</i>), SALK_034258 (<i>ari12-2</i>)
At1g70910	DEP	SALK_141707
At5g01070	ERiN2	SALK_086525
At2g38920	ERiN3	SALK_129778
At4g09110	ATL35	SALK_065995
At1g18910	BTSL2	SALK_048470
At5g03180	ERiN4	SALK_023683
At5g06490	ATL71	CS863433
At5g37910	SINA-like 9	SALK_023901
At5g58580	ATL63	SALK_139444

Table 1. The 14 selected candidate RING-type E3s and the corresponding T-DNA insertion mutant SALK lines which were ordered from ABRC (<https://abrc.osu.edu/>).

Nutrient media preparation

For nutrient sufficient conditions (control, +), ½ MS media was used. For excess iron conditions (++Fe), ½ MS media was supplemented with 300µM Ferric-ethylenediaminetetraacetic acid (Fe-EDTA; Sigma-Aldrich; <https://www.sigmaaldrich.com>). Iron deficiency (-Fe) was simulated using Fe-free ½ MS media supplemented with 150µM of 3-9(2-Pyridyl)-5,6-diphenyl-1,2,4-triazine-p,p'disulfonic acid monosodium salt hydrate (FerroZine; Sigma-Aldrich; <https://www.sigmaaldrich.com>). Phosphorus (P) and nitrogen (N) excess conditions were simulated using ½ MS media supplemented with 4.375 mM KH₂PO₄ and 60 mM NH₄NO₃, respectively (Sigma-Aldrich; <https://www.sigmaaldrich.com>). P deficiency (-P) was simulated with Phosphate-free media supplemented with 10 µM KH₂PO₄, N deficiency (-N) was simulated with Nitrogen-free media supplemented with 20 µM NH₄NO₃. All MS salts were ordered from Caisson Labs (www.caissonlabs.com). Composition of all nutrient treatment media can be viewed in Table 2.

Nutrient treatment	Media composition
Control	NO ₃ ⁻ (10.0 mM), NH ₄ ⁺ (2.0 mM), PO ₄ ³⁻ (1.25 mM), K ⁺ (2.0 mM), Mg ²⁺ (0.5 mM), Ca ²⁺ (0.5 mM), SO ₄ ²⁻ (0.5 mM), Fe ²⁺ /Fe ³⁺ (50 µM), Mn ²⁺ (0.55 µM), Zn ²⁺ (0.55 µM), Cu ²⁺ (0.08 µM), MoO ₄ ²⁻ (0.04 µM), H ₂ BO ₃ ⁻ /BO ₃ ³⁻ (2.7 µM), 0.05% MES (w/v), 1% sucrose (w/v), 0.8% agar (w/v)
Fe deficient (-Fe)	NO ₃ ⁻ (10.0 mM), NH ₄ ⁺ (2.0 mM), PO ₄ ³⁻ (1.25 mM), K ⁺ (2.0 mM), Mg ²⁺ (0.5 mM), Ca ²⁺ (0.5 mM), SO ₄ ²⁻ (0.5 mM), Mn ²⁺ (0.55 µM), Zn ²⁺ (0.55 µM), Cu ²⁺ (0.08 µM), MoO ₄ ²⁻ (0.04 µM), H ₂ BO ₃ ⁻ /BO ₃ ³⁻ (2.7 µM), + 150 µM FerroZine, 0.05% MES (w/v), 1% sucrose (w/v), 0.8% agar (w/v)
Fe excess (++Fe)	NO ₃ ⁻ (10.0 mM), NH ₄ ⁺ (2.0 mM), PO ₄ ³⁻ (1.25 mM), K ⁺ (2.0 mM), Mg ²⁺ (0.5 mM), Ca ²⁺ (0.5 mM), SO ₄ ²⁻ (0.5 mM), Fe ²⁺ /Fe ³⁺ (50 µM), Mn ²⁺ (0.55 µM), Zn ²⁺ (0.55 µM), Cu ²⁺ (0.08 µM), MoO ₄ ²⁻ (0.04 µM), H ₂ BO ₃ ⁻ /BO ₃ ³⁻ (2.7 µM), + 300 µM Fe-EDTA, 0.05% MES (w/v), 1% sucrose (w/v), 0.8% agar (w/v)
P deficient (-P)	NO ₃ ⁻ (10.0 mM), NH ₄ ⁺ (2.0 mM), K ⁺ (2.0 mM), Mg ²⁺ (0.5 mM), Ca ²⁺ (0.5 mM), SO ₄ ²⁻ (0.5 mM), Fe ²⁺ /Fe ³⁺ (50 µM), Mn ²⁺ (0.55 µM), Zn ²⁺ (0.55 µM),

	Cu ²⁺ (0.08 μM), MoO ₄ ²⁻ (0.04 μM), H ₂ BO ₃ ⁻ /BO ₃ ³⁻ (2.7 μM), + 10 μM KH ₂ PO ₄ , 0.05% MES (w/v), 1% sucrose (w/v), 0.8% agar (w/v)
P excess (++P)	NO ₃ ⁻ (10.0 mM), NH ₄ ⁺ (2.0 mM), PO ₄ ³⁻ (1.25 mM), K ⁺ (2.0 mM), Mg ²⁺ (0.5 mM), Ca ²⁺ (0.5 mM), SO ₄ ²⁻ (0.5 mM), Fe ²⁺ /Fe ³⁺ (50 μM), Mn ²⁺ (0.55 μM), Zn ²⁺ (0.55 μM), Cu ²⁺ (0.08 μM), MoO ₄ ²⁻ (0.04 μM), H ₂ BO ₃ ⁻ /BO ₃ ³⁻ (2.7 μM), + 4.375 mM KH ₂ PO ₄ , 0.05% MES (w/v), 1% sucrose (w/v), 0.8% agar (w/v)
N deficient (-N)	PO ₄ ³⁻ (1.25 mM), K ⁺ (2.0 mM), Mg ²⁺ (0.5 mM), Ca ²⁺ (0.5 mM), SO ₄ ²⁻ (0.5 mM), Fe ²⁺ /Fe ³⁺ (50 μM), Mn ²⁺ (0.55 μM), Zn ²⁺ (0.55 μM), Cu ²⁺ (0.08 μM), MoO ₄ ²⁻ (0.04 μM), H ₂ BO ₃ ⁻ /BO ₃ ³⁻ (2.7 μM), + 20 μM NH ₄ NO ₃ , 0.05% MES (w/v), 1% sucrose (w/v), 0.8% agar (w/v)
N excess (++N)	NO ₃ ⁻ (10.0 mM), NH ₄ ⁺ (2.0 mM), PO ₄ ³⁻ (1.25 mM), K ⁺ (2.0 mM), Mg ²⁺ (0.5 mM), Ca ²⁺ (0.5 mM), SO ₄ ²⁻ (0.5 mM), Fe ²⁺ /Fe ³⁺ (50 μM), Mn ²⁺ (0.55 μM), Zn ²⁺ (0.55 μM), Cu ²⁺ (0.08 μM), MoO ₄ ²⁻ (0.04 μM), H ₂ BO ₃ ⁻ /BO ₃ ³⁻ (2.7 μM), + 60 mM NH ₄ NO ₃ , 0.05% MES (w/v), 1% sucrose (w/v), 0.8% agar (w/v)

Table 2. Nutrient composition of the seven nutrient treatments used to analyze plant response under iron (Fe), phosphorus (P), and nitrogen (N) deficiency and excess. All MS salts were obtained from Caisson Labs (<https://caissonlabs.com>) and supplemental nutrients were obtained from Sigma-Aldrich (<https://www.sigmaaldrich.com>).

PCR genotyping

Arabidopsis thaliana Columbia (*Col-0*) seeds harbouring transfer-DNA (T-DNA) insertions within the 14 E3 genes of interest were ordered from the Arabidopsis Biological Resource Center (ABRC; <https://abrc.osu.edu/>) (Table 1). To identify homozygous mutants, polymerase chain reaction (PCR) utilizing gene specific primers flanking the T-DNA insertion site, along with primers targeting the T-DNA border, were used for genotyping plants. The National Center for Biotechnology Information (NCBI) online primer-BLAST tool (<https://www.ncbi.nlm.nih.gov/tools/primer-blast/>) was used to design gene specific primers (Table 3). Small leaf samples were used in PCR reactions utilizing the Phire[®] Plant Direct PCR kit (Thermo Scientific; <https://www.thermofisher.com>). The presence of the WT allele was indicated by a ~1Kb band amplified by the gene specific primers. A ~0.5Kb band amplified by a

forward gene specific primer and T-DNA specific primer, described by Salk Institute Genomic Analysis Laboratory (SIGnAL; <https://www.salk.edu>) LBb1.3 (5'-ATTTTGCCGATTTCGGAAC-3'), indicates the presence of mutant allele. Heterozygotes were identified by the presence of both alleles. Homozygous mutant plants confirmed by two independent PCR reactions were grown for eight weeks and seeds were harvested for use in further experiments. Disrupted E3 expression was confirmed using reverse-transcriptase (RT)-PCR.

Mutant: SALK line	F primer (5'-3')	R primer (5'-3')
SALK_149664	TCCGGAATCGGCTATCGTTG	CTATTAGCCGCCGAGACTCC
SALK_066923	ACAAGGGCTTGAATGTTCTGT	GACCGATCAAATGGTCCCCA
CS24734	CATGTGGGGCCAGAGAAA	CCCGTCTTCGACATAAGACCT
SALK_118406	CGCTATATACATCTATTTGCAGGTG	AGCAGCAGAGCGGAAAAATG
SALK_033142	TTATCAATGTGAAGCGGTGA	CCGAACATTAAGGGATCTTGT
SALK_141707	GGAACCGAAACAAGTCACCT	TGAGTTCCTTTCAAACCGGA
SALK_086525	CAGCAATCTCAAACCTCGCCG	AGCTAATTGAGAAAGCGTGTGA
SALK_129778	TTGCCATAATCTCTAACCTTGTC	TGGAGAAGTGTGCGCTTCGTT
SALK_065995	ACATGTCCTATCTGTCGTGCT	TGCGGTCTACGGATTCTGAC
SALK_048470	GGTGACGTACTTCATTTGACG	GGAAGCTATAATCTGTTGCGA
SALK_023683	TGAATTGAGAAAGAGAGAGAGAGA	AGCATGCTTGCATACTTCTGT
CS863433	TCATTCAAGCATTCAACATGCCA	CGGGAAAAGGGAACAACGTC
SALK_023901	TCCGGAATCGGCTATCGTTG	CTATTAGCCGCCGAGACTCC
SALK_139444	ACAAGGGCTTGAATGTTCTGT	GACCGATCAAATGGTCCCCA
SALK_041291	TCCCAATATCCCCAATCTTCCAC	CCGGAGAGAGCTTAACGTCC
SALK_201056	CGTTGTTTCGGATGCTGTGT	TCTGACTTCTTTTTCTGATGGGC
SALK_034258	GAGATGCTGGAGTTGACGTT	TACCATCTTAAGTGAGAAAGCAGA

Table 3. All E3-specific primer pairs used for PCR genotyping T-DNA insertion SALK-line mutants from ABRC (<https://abrc.osu.edu/>). Primers were created using NCBI (www.ncbi.nlm.nih.gov) primer blast tool to amplify a ~1Kb band flagging each T-DNA insertion site. Primer pairs were ordered from IDT (www.idtdna.com). To detect the presence of a T-DNA insertion the E3-specific F primers were used with the T-DNA specific primer designed by Salk Institute Genomic Analysis Laboratory (SIGnAL) LBb1.3 (5'-ATTTTGCCGATTTCGGAAC-3').

RT-PCR analysis

RT-PCR was used to analyze gene transcript levels in homozygous mutant plants and WT. Total RNA was extracted from leaves using TRIzolTM (Invitrogen; <https://www.thermofisher.com>).

Purity and concentration of RNAs were measured. cDNA synthesis was carried out using the iScriptTM gDNA Clear cDNA Synthesis Kit (Bio-Rad; <https://www.bio-rad.com>). Synthesized cDNA was then used in PCRs carried out using DreamTaq PCR Green Master Mix (Thermo Scientific; <https://www.thermofisher.com>) with gene specific primers designed using the NCBI online primer-BLAST tool (<https://www.ncbi.nlm.nih.gov/tools/primer-blast/>) (Table 4).

Gene	F primer (5'-3')	R primer (5'-3')
WAVH1	TAGAGTGCCGGTGGATTTGG	GCGATAACCGTTTCGAGCTG
ATL12	AGACGACCTCTCTGTGTTGG	TTCTCGCTCAAGCAACAACG
ARI11	GAAATGGCAATCGGTGGAGC	GCTTGTTCGCTCTTGACTA
ERiN1	TGCATTTTTCCGCTCTGCTG	AACTGGCAGCTCGGAGTAAG
ARI12	AATGGCATCCTATCCAGGGG	TACACTTGGGACAAGGCACC
DEP	CCAAGGCTCCAAGATCCCAA	GTGCTGTTCTCCAACAAGC
ERiN2	TTTCCGGCCTCTACGTCATC	GCAATGTGCCGATACTTGGT
ERiN3	GCTTCTTTCATCAGCTCCTCG	GTTCTGGAGAAGTGTCGCT
ACT1	ACGGATGCGCTGATGAAGAT	TCACTTGCCCATCAGGTAGC
IRT1	TCTCTCCAGCAACTTCAACTG	CCGGAGGCCGAAACACTTAAT
AtFER1	GAAAAGAGAAGCTTACTTGATTTGC	TCCAGGAAAGTTGGCGGC
AtIPS1	GGCTGATTCAGACTGCGAGTT	CACACAAAGAACACACAACGC
PHO2	AGCGACGATTGTGTCTGCAT	GTTGTGAAGGCTGTCAATGCT
NRT1.7	AGGCACTTTCACGGTCTCTC	TCGCGAAAACGATCCCTGTT
NLA	GTCTAGGCAAGGACAAGCGT	CGAAAGTCAAAGCGCAACCA
FIT	TCTTGGTTCGATCCAACTTCG	CGTTGGAGTCTAAGTCAGGCA
IDF1	CCCTATCCCTACAAATCGGACA	CAAGATGCGTGAAGAGGCTT
FRO2	TGCTCGATCTTGTCTTGCCA	GATGCGAGAATTGCACCGAG
URI	ACCAGCAGAGATTAAGGTCAATG	TGTAGGACATGGAGCTGGGA
PYE	ACGAGATTGAAGCTAGAGCGA	TGTGTCTGGGGATCAGGTTG

Table 4. All gene-specific primer pairs used in RT-PCR. Each primer pair was created using NCBI (www.ncbi.nlm.nih.gov) primer blast tool to amplify a ~200bp portion of the gene exon. Primer pairs were ordered from IDT (www.idtdna.com).

Stress assays – phenotypic analysis

Seeds harvested from homozygous mutants for all eight mutant lines were sterilized and stratified to initiate germination, then were grown on ½ MS media for five days under continuous light. Seedlings were then transferred to different nutrient treatment media in a sterile laminar flow station. All instruments and surfaces used for seedling transfer were sterilized with 50% bleach and 75% ethanol, then further sterilized under ultraviolet (UV) light. Seedlings were grown for 10 days on nutrient treatments: control, excess iron (++Fe), deficient iron (-Fe), excess phosphorus (++P), phosphorus deficient (-P), excess nitrogen (++N), and nitrogen deficient (-N). After 10 days photos were taken of seedlings and fresh weight was measured. Fresh weight was determined through weighing groups of seedlings. Root length was measured through analysis of the photos using ImageJ® image analysis software (<http://imagej.net>). Stress assays were repeated for mutant lines which showed differential growth under one or more nutrient stresses. RT-PCR was then used to determine any changes in E3 expression in WT plants when exposed to the nutrient stress under which the mutant for that E3 showed differential growth, and three E3s of interest were selected for further analysis. Results for all eight mutant lines can be viewed in APPENDIX B.

Electrolyte leakage

Electrolytes leakage (EL) assays were performed as previously described by Dionisio-Sese and Tobita (1998). Seedlings were grown under nutrient sufficient conditions for five days, then were exposed to -Fe, ++Fe, or + conditions for two, four, and six days. After the end of each treatment period, 50mg of fresh leaf tissue was collected from each group. Leaf samples were thoroughly rinsed then submerged in 5mL of ddH₂O and incubated for 2h at 32°C. Initial electrical conductivity (EC1) was measured using an electrical conductivity meter (HACH Pocket Pro

Conductivity meter; <https://www.hach.com>). Then, to release all electrolytes, the samples were autoclaved at 121°C for 20min. Samples were then cooled to 25°C, and final electrical conductivity values (EC2) were then measured. EL values were calculated, relative to fresh weight of leaves (FW), using the equation below:

$$EL/FW = ((EC1/EC2) \times 50) / FW$$

Rhizosphere acidification assay

For rhizosphere acidification assays liquid -Fe media was made with the same components as described in Table 1 minus the agar. Bromocresol purple (BP) was added to the liquid medias (0.006% w/v) to act as a pH indicator; the pH of the starting solution was adjusted to 6.5 instead of the standard 5.7. 10-day-old seedlings were grown in -Fe BP media for 12 hours under continuous light in a 12-well plate; every well was filled with 0.5mL of BP media and contained two, four or six seedlings. BP changes colour from purple to yellow when the pH decreases. Therefore, a colour change from purple to yellow after 12 hours indicates acidification. Absorbance at 589nm after the 12-hour period was measured to determine the degree of colour change.

Determination of Ferric Chelate Reductase 2 (FRO2) activity

FRO2 activity assays were performed as described by Yi and Guerinot (1996). Roots from 15-day-old seedlings grown under control, ++Fe, and -Fe were washed with 0.5mM calcium sulfate (CaSO₄) then rinsed with ddH₂O five times. Roots from 10 seedlings were weighed and placed in a test tube containing 1.4mL of solution of 0.1mM Fe-EDTA and 0.3mM FerroZine. Each sample was left in the dark at 25°C for 30 minutes. FRO2 activity was then determined via

spectrophotometry, measuring the absorbance (A) at 562nm and quantified using a molar extinction coefficient of $28.6\text{mM}^{-1}\text{cm}^{-1}$ as in the following equation:

$$((A/28.6)\times 700)/(FW(\text{roots})/2)$$

The Fe^{2+} forms a purple complex with the ferrozine as Fe^{3+} is reduced by FRO2; at a wavelength of 562nm the concentration of the complex is directly proportional to the absorbance (Gibbs, 1976).

Fe deficient and excess soil assays

Fe deficiency was induced through the addition of lime (CaCO_3) to the soil to increase alkalinity. Seedlings were grown on $\frac{1}{2}$ MS media for two weeks then transferred to soil supplemented with the 0%, 0.5%, 0.75%, and 1% (w/w) of CaCO_3 . All treatments were watered every week. Images were captured weekly for 4 weeks. Fe excess was induced through the addition of Fe-EDDHA to water. Plants were watered weekly with water supplemented with 0%, 1%, and 5% Fe-EDDHA (w/v). Seedlings were grown on $\frac{1}{2}$ MS media for two weeks then transferred to soil. All treatments were watered every week. Images were captured weekly for 3 weeks.

Fe content quantification

Fe content was quantified using methods described by Gautam et al. (2022). Seedlings were grown on control media for five days, then transferred to control, -Fe, and ++Fe media for seven days. Whole seedlings from approximately 40 seedlings from each treatment for each genotype were harvested and rinsed with ddH₂O. Samples were dried in an oven at 60-65°C for 2 days. Dry weight was recorded. Samples were digested via adding 225 μl nitric acid (65%) and incubating at 95°C for 6 hours (vortexing samples every hour), then adding 150 μl hydrogen peroxide (30%) to each

sample and samples were incubated at 56°C for 2 hours. 225 µl ddH₂O was added to fully digested samples. 245 µl of assay solution (1mM C₂₄H₁₄N₂Na₂O₆S₂ · 3H₂O, 0.6mM CH₃COONa, 0.48mM [NH₃OH]⁺Cl⁻, 100ml ddH₂O) was added to samples and absorbance was measured at 535nm. Values obtained were analyzed against a standard curve which was created using six standards (Table 5); spectrophotometer was zeroed using 0 µg Fe standard.

	Fe content	+ FeCl ₃ (50mM)	+ nitric acid	+ H ₂ O ₂	+ ddH ₂ O
STD1	1.25 µg	0.45 µl	225 µl	150 µl	225 µl
STD2	2.5 µg	0.9 µl	225 µl	150 µl	225 µl
STD3	5 µg	1.79 µl	225 µl	150 µl	225 µl
STD4	10 µg	3.58 µl	225 µl	150 µl	225 µl
STD5	20 µg	7.17 µl	225 µl	150 µl	225 µl
STD6	40 µg	14.34 µl	225 µl	150 µl	225 µl
STD7	100 µg	35.8 µl	225 µl	150 µl	225 µl
STD8	300 µg	107.4 µl	225 µl	150 µl	225 µl
STD9	700 µg	250.6 µl	225 µl	150 µl	225 µl
Blank	0 µg	0 µl	225 µl	150 µl	225 µl

Table 5. Standards used in iron (Fe) content quantification assay.

IRT1 immunoblot

Total protein was prepared from the roots of seedlings grown in iron-sufficient and iron-deficient conditions. Extracts were prepared by grinding roots on ice in a protein extraction buffer (50mM Tris, (pH 7.5; 1M), 10% glycerol, 100mM KCl (1M). Total protein content was measured via Bradford assay. Approximately 25 µg of total protein extracts were resolved on SDS-PAGE gel. The immunoblot was probed with the immunogen affinity purified IRT1 polyclonal antibody, which was raised in rabbits against the KLH-conjugated synthetic peptide derived from Arabidopsis IRT1 sequence, in a 1:5000 dilution (Agrisera; <https://www.agrisera.com>). Secondary antibody used was goat anti-rabbit IgG (H&L), HRP conjugated polyclonal antibody from Agrisera, in a 1:10000 dilution.

RESULTS

Confirming homozygous atl12-1 and ari12-1 loss-of-function mutants

Mutant seeds, SALK_066923 (*atl12-1*) and SALK_201056 (*atl12-2*), harbouring a T-DNA insertion in *ATL12*, and SALK_033142 (*ari12-1*) and SALK_034258 (*ari12-2*), harbouring a T-DNA insertion in *ARI12*, were obtained from ABRC. Homozygous *atl12-1*, *atl12-2*, *ari12-1*, and *ari12-2* individuals were found using PCR genotyping (Figure 1, Figure S1). After confirming homozygosity, the reduction of *ATL12* (*atl12-1* plant #4), *ARI12* (*ari12-1* plant #4), *ATL12* (*atl12-2* plant #1), and *ARI12* (*ari12-2* plant #3) transcript levels, compared to wild type (WT), was confirmed using qualitative RT-PCR (Figure 1, Figure S1).

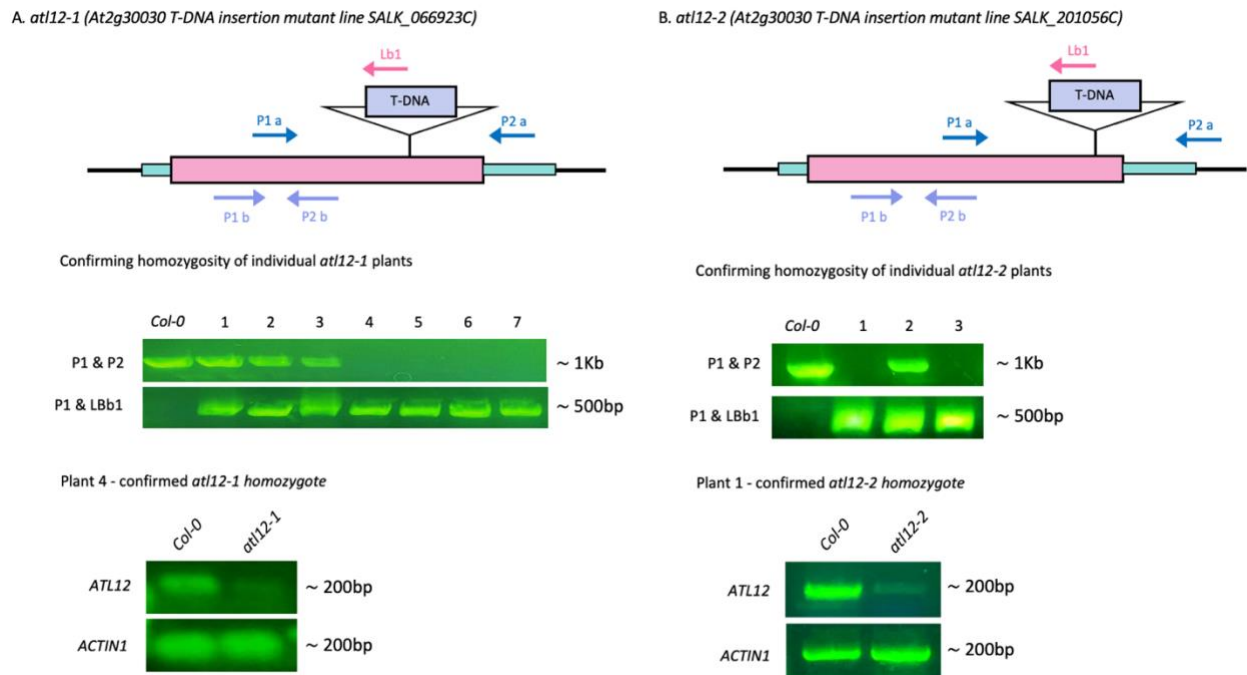


Figure 1. Schematics of *ATL12* and *ARI12* with location of T-DNA insertions and primer pairs used for PCR genotyping (P1a and P2a) and for analysis of E3 gene expression to determine knock-down expression (P2b and P2b). PCR genotyping was visualized using gel electrophoresis. **(A)** *ATL12* SALK_066923 T-DNA insertion mutant. Plant 4 (*atl12-1a*), 5, 6, and 7 were determined to be homozygous *atl12-1*. **(B)** *ARI12* SALK_033142 T-DNA insertion mutant. Plant 3 (*ari12-1a*) and 4 were determined to be homozygous *ari12-1*. Qualitative RT-PCR visualized using gel

electrophoresis showing expression of ATL12 is knocked down in *atl12-1* **(A)**, and ARI12 is knocked down in *ari12-1* **(B)**.

ATL12 and ARI12 are involved in plant response to Fe stress

WT, *atl12-1*, and *ari12-1* seedlings were grown on Fe sufficient (control, 75 μ M Fe) media for five days then exposed to Fe deficiency (-Fe, 0 μ M Fe), or excess Fe (++Fe, 375 μ M Fe) for 10 days. At the end of the 10-day treatment period root length and fresh weight was measured. There were no significant differences in fresh weight or root length between WT and *atl12-1* under +, -Fe, or ++Fe. There were no differences in fresh biomass between WT and *ari12-1* or *atl12-1* under all conditions tested (Figure 2A and B). *atl12-1* plants exhibited significantly longer roots than WT under -Fe (Figure 2A). Under -Fe and ++Fe *ari12-1* plants exhibited significantly longer roots than WT (Figure 2B). These results were confirmed using the alternate mutants *atl12-2* (Figure S4A) and *ari12-2* (Figure S4B).

ATL12 and *ARI12* transcript levels were determined using qualitative RT-PCR and WT seedlings that were exposed to the three Fe treatments for 10 days. Results showed that *ATL12* transcript levels increased during exposure to -Fe, while *ARI12* transcript levels decreased when seedlings were exposed to -Fe and upregulated in response to ++Fe (Figure 2C). These results demonstrate that ATL12 and ARI12 are involved in plant response to Fe stress.

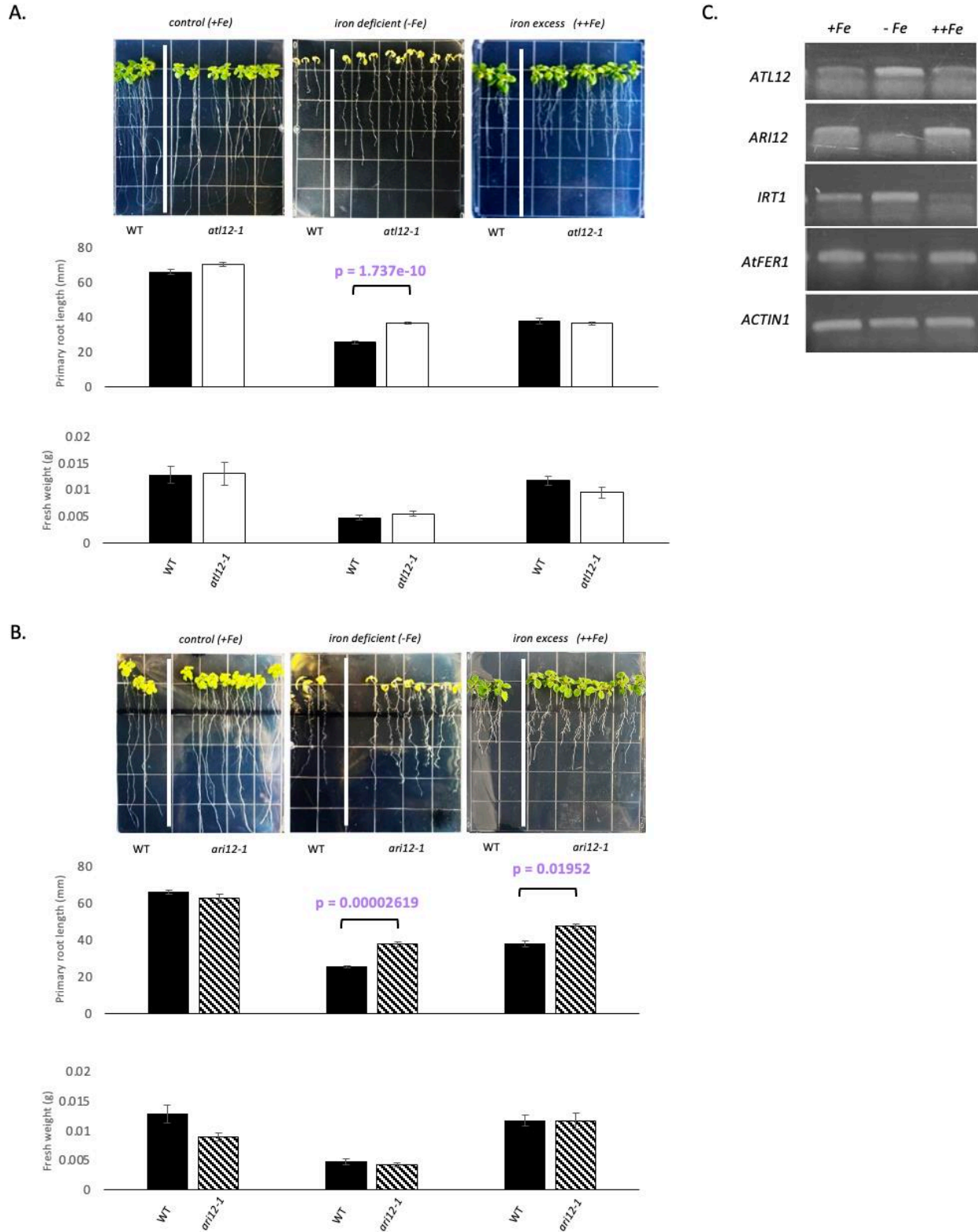


Figure 2. (A) 15-day old *atl12-1* and WT seedlings that were grown for five days on nutrient sufficient (control, +Fe) media then 10 days on +Fe, Fe deficient (-Fe), and Fe excess (++Fe) media. Primary root lengths and fresh weight were measured at the end of the 10-day treatment period

using ImageJ® (<http://imagej.net>). Mutants exhibited significantly longer roots than WT on -Fe ($p = 1.737e-10$) and showed no significant difference on +Fe. Analysis was done using One-Way ANOVA Tukey comparison. Error bars indicate \pm SE from three trials with at least three replicates per trial (≥ 72). **(B)** 15-day old *ari12-1* and WT seedlings that were grown for five days on +Fe media then 10 days on +Fe, -Fe, and ++Fe media. Primary root lengths were measured at the end of the 10-day treatment period using ImageJ® (<http://imagej.net>). Mutants exhibited significantly longer roots than WT on -Fe ($p = 0.00002619$) and ++Fe ($p = 0.01952$) and showed no significant difference on +Fe. Analysis was done using One-Way ANOVA Tukey comparison. Error bars indicate \pm SE from three trials with at least three replicates per trial (≥ 72). **(e)** cDNA was synthesized from RNA extracted from WT seedlings that were grown on +Fe for five days then for 10 days on +Fe, -Fe, and ++Fe. *IRT1* and *AtFER1* were used as positive control genes to confirm that the nutrient stress treatments were effective, *ACTIN* was used as a control for cDNA concentration. Expression of *ATL12* significantly increased when exposed to -Fe. Expression of *ARI12* significantly decreased under -Fe and increased under ++Fe. All segments of cDNA amplified are ≈ 200 bp.

atl12-1 plants exhibit higher rates of survival on Fe deficient soil

To examine the response of *atl12-1* and *ari12-1* to Fe deficiency on soil, two-week old plants were transferred to soil supplemented with 0%, 0.5%, 0.75%, and 1% (w/w) CaCO. Plants were watered once per week and photos were taken every week for four weeks. Survival rates of the plants among the four CaCO treatments were calculated at the end of the four weeks (Figure 3b). Survival rates of all plants were 100% on the control (0% CaCO) soil, and survival rate of WT and *ari12-1* decreased with increasing CaCO concentrations. Survival rate of *atl12-1* plants remained at 100% on 0.5% CaCO soil and decreased slightly on 0.75% and dropped to 60% on 1% CaCO soil. However, survival rates of *atl12-1* on these treatments were significantly higher than WT and *ari12-1* (Figure 3B). The six-week-old *atl12-1* plants also appeared larger than WT and *ari12-1* plants after growing on CaCO-supplemented soil for four weeks (Figure 3A). These results indicate that loss of *ATL12* function increases plant success on Fe deficient soil.

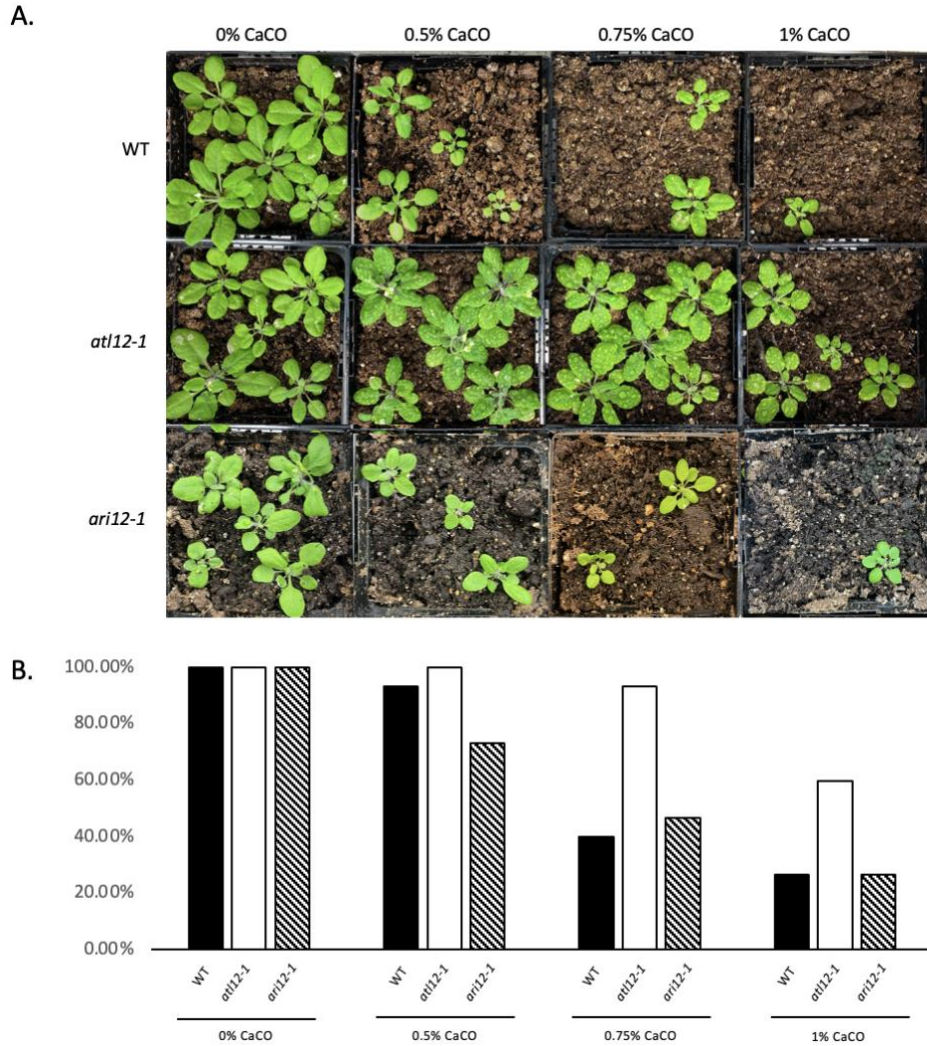


Figure 3. Varying concentrations (0% (control), 0.5%, 0.75%, and 1% (w/w)) of lime (CaCO) were added to soil to simulate iron deficiency through significantly increasing the alkalinity of the soil. **(A)** Two-week old WT, *atl12-1*, and *ari12-1* seedlings were transferred to the control or the CaCO supplemented soil and grown for four weeks. Plants were watered once a week and images were taken every week. Images shown were taken at four weeks. **(B)** Survival rates of WT, *atl12-1*, and *ari12-1* on all treatments were calculated after four weeks (n = 25).

ari12-1 exhibits slightly increased survival rates on Fe excess soil

To determine if adult plants exhibited differential growth under excess Fe, two-week old WT and *ari12-1* plants were transferred to soil supplemented with 0%, 1%, and 5% (w/v) Fe-EDDHA to induce Fe toxicity. Survival rates of the plants among the three treatments were calculated after

the three weeks (Figure 4A). Survival rates of all plants were 100% on the control (0% Fe-EDDHA) soil, and survival rate of WT and *ari12-1* decreased with the increasing Fe concentrations. Survival rates of *ari12-1* on these treatments were slightly higher than WT. The five-week-old WT and *ari12-1* plants grown on ++Fe soil for three weeks appeared larger than plants grown on control (Figure 4B). The slightly higher survival rate of *ARI12* loss-of-function mutants on Fe excess soil indicates that *ARI12* may be involved in plant response to excess Fe.

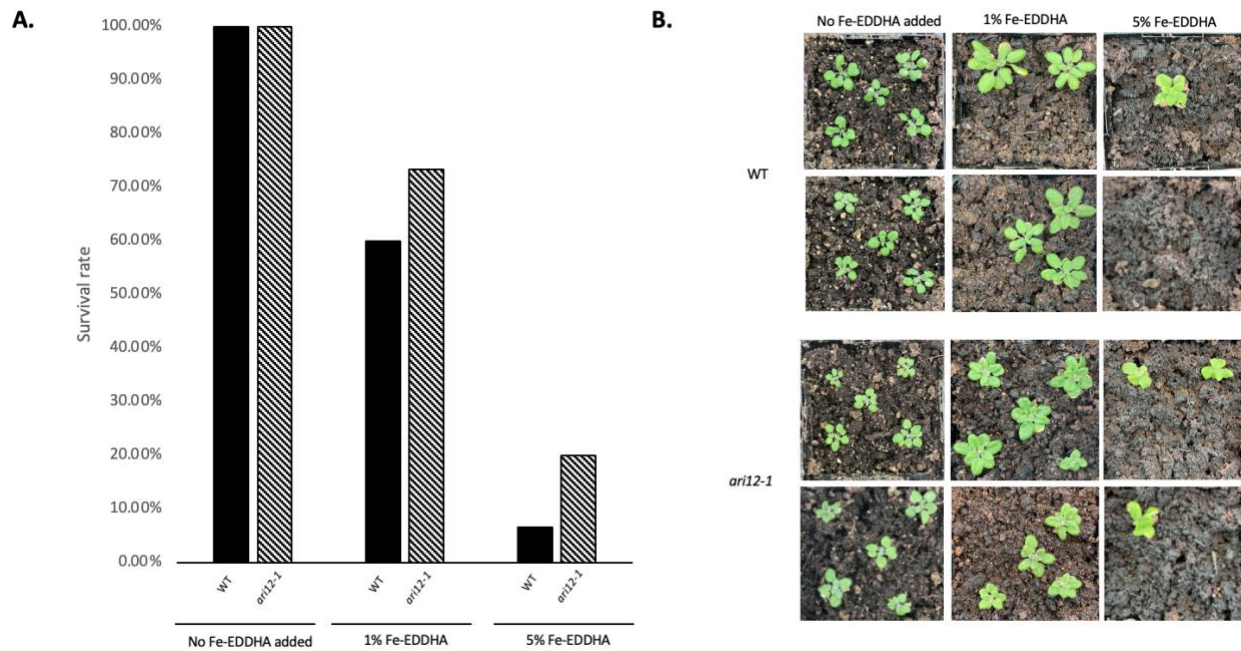


Figure 4. Soil and water were supplemented with varying concentrations of Fe-EDDHA (0% (control), 1%, and 5% Fe-EDDHA) to expose mature WT and *ari12-1* plants to iron excess (++Fe) conditions. **(A)** Survival rates of WT and *ari12-1* on all treatments were calculated after three weeks (n = 25). **(B)** Two-week old WT and *ari12-1* seedlings were transferred to the control or the Fe-EDDHA supplemented soil and grown for three weeks. Images shown were taken at three weeks.

Analyzing AHA2 and FRO2 activity of *atl12-1* and *ari12-1*

When exposed to Fe deficiency, plants excrete protons and phenolic chelating compounds to decrease the pH of the rhizosphere and increase Fe^{3+} reduction rates to increase Fe uptake. These two actions are dependent on the activity of AHA2 and FRO2 proteins in the plasma membrane of the root cells (Connolly et al., 2003; Santi and Schmidt 2009; Martín-Barranco et al., 2020). AHA2 activity was determined by measuring rhizosphere acidification (RA) abilities and FRO2 activity was determined by measuring Fe^{3+} to Fe^{2+} reduction rates using spectrophotometry. No significant differences in RA abilities were found amongst WT, *atl12-1*, and *ari12-1* (Figure 5A). There were also no significant differences in Fe^{3+} reduction rates (Figure 5B). These results indicate FRO2 and AHA2 activity are not disrupted in the *ATL12* and *ARI12* loss-of-function mutants.

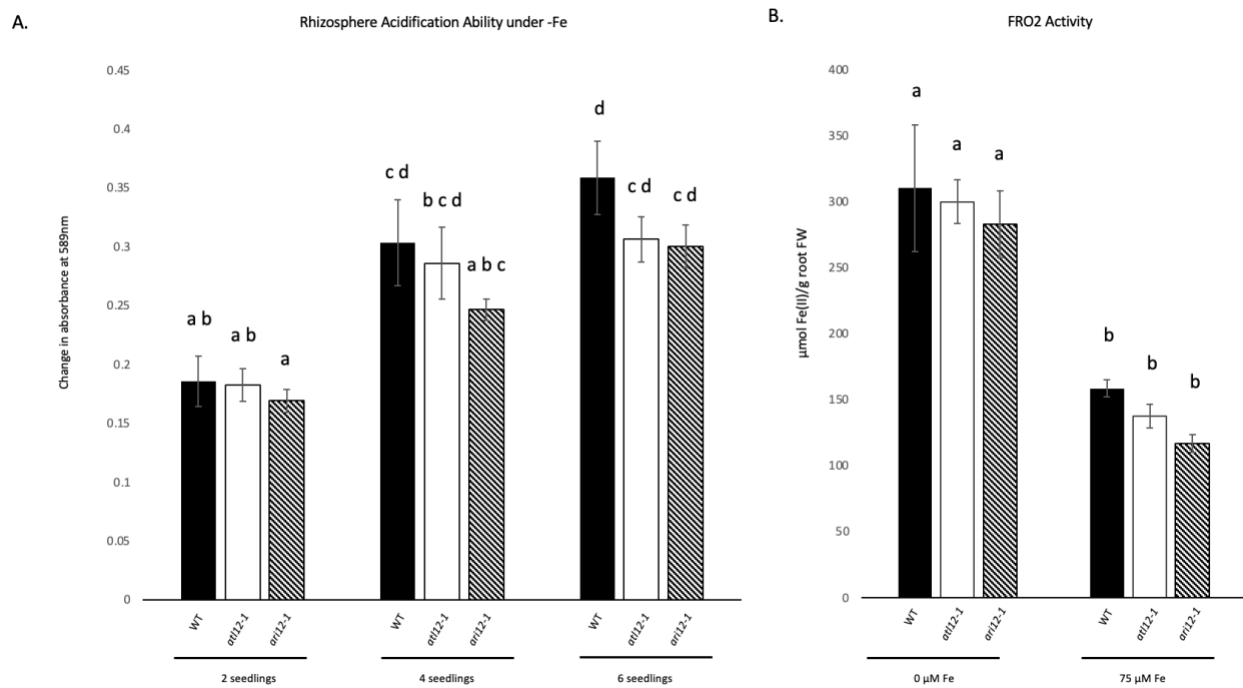


Figure 5. (A) Rhizosphere acidification abilities were measured using bromocresol purple (BP) as a pH indicator. 10-day old WT, *atl12-1*, and *ari12-1* seedlings were transferred to 500 μl aliquots of liquid -Fe media (0 μM Fe) that was supplemented with 0.006 (w/v) BP and adjusted to a pH of 6.5, in groups of 2, 4, and 6. Seedlings were left under continuous light for 12 hours. Absorbance

of the liquid at 589nm was measured after the 12-hour period to gauge the change in colour; purple to yellow indicating acidification. Different letters indicate p-value <0.05 using One-Way ANOVA Tukey comparison. Error bars indicate \pm SE from four trials with three technical replicates per trial. **(B)** FRO2 activity was measured by reduction rate of Fe(III) to Fe(II). Different letters indicate p-value <0.05 using One-Way ANOVA Tukey comparison. Error bars indicate \pm SE from three trials with three technical replicates per trial.

*No significant difference in electrolyte leakage levels in *atl12-1* or *ari12-1**

When a plant is exposed to external abiotic and biotic stresses, including over-exposure to heavy metals and micronutrient deficiency, cell death is imminent. The integrity of the cell walls of these dead and damaged plant cells will be compromised, causing K⁺ ions and other electrolytes to leak out of the cells (Demidchik et al., 2014). Studies show high EL levels are linked to the generation of reactive oxygen species (ROS) and the activation of programmed cell death (PCD) (Demidchik et al., 2014). The quantity of ions leaked from a plant can be used as a proxy for the severity of cell death and can be used to estimate stress tolerance. Plants exhibiting higher levels of EL are at increased risk of experiencing heavy metal toxicity, since the cell wall acts as a physical barrier in limiting metal uptake (Hall, 2002). The level of cell damage is also relevant to the maintenance of nutrient homeostasis because the cell wall is essential to nutrient signalling and transport (Ogden et al., 2018). There were no significant differences in EL levels in loss-of-function mutants compared to WT (Figure 6). This indicates that *atl12-1* and *ari12-1* do not have a higher level of cell damage compared to WT.

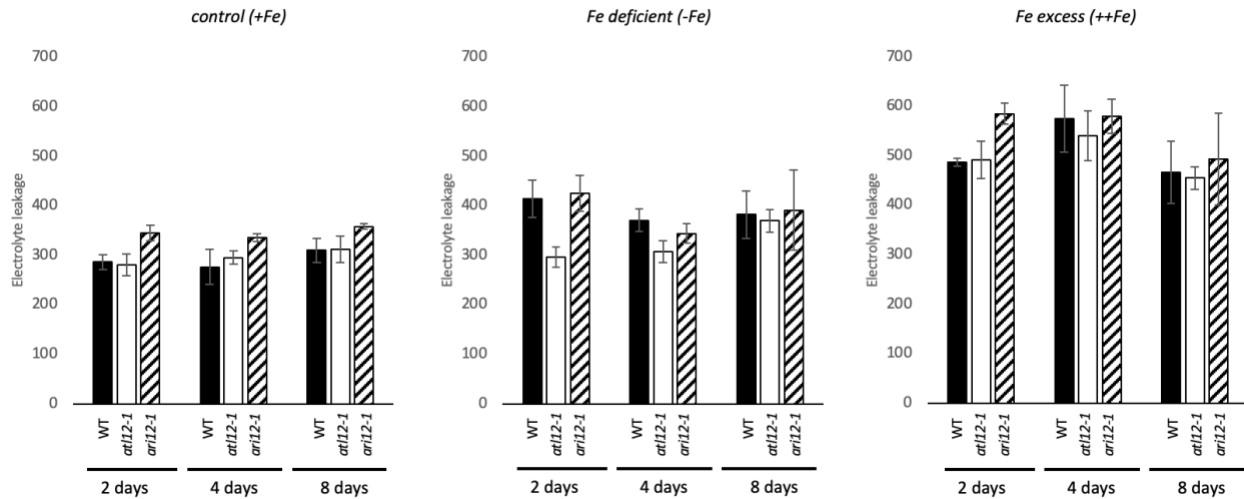


Figure 6. Electrolyte leakage (EL) was measured as described by Dionisio-Sese and Tobita (1998). Seedlings were grown on nutrient sufficient (control) media for five days then transferred to iron deficient media (-Fe), or iron excess media (++)Fe for two, four, and eight days. EL was measured for each group at the end of each treatment period. Analysis was done using One-Way ANOVA Tukey comparison. Error bars indicate \pm SE from two trials with at three technical replicates per trial.

atl12-1 display lower levels of *FIT* and *IRT1* under Fe deficiency

FIT regulates hundreds of Fe-deficiency response genes in Arabidopsis including *IRT1*, the major Fe transporter, which is strongly upregulated by *FIT* when the plants are exposed to Fe deficiency (Vert et al., 2002; Colangelo and Gueriot, 2004). Under severe Fe deficiency, *atl12-1* plants displayed a significantly different phenotype than WT, suggesting that the loss of *ATL12* function impacts the Fe deficiency response. To determine *FIT* and *IRT1* levels in *atl12-1* plants, RT-PCR was performed using RNA extracted out of 15-day old seedlings grown under control then transferred to -Fe conditions for 10 days. Results showed that *FIT* and *IRT1* levels in *atl12-1* were not upregulated under -Fe as observed in WT (Figure 7A). The impacted upregulation of *IRT1* levels was confirmed using western blotting (WB), which showed lower *IRT1* protein abundance in the roots of *atl12-1* under -Fe compared to WT (Figure 7B).

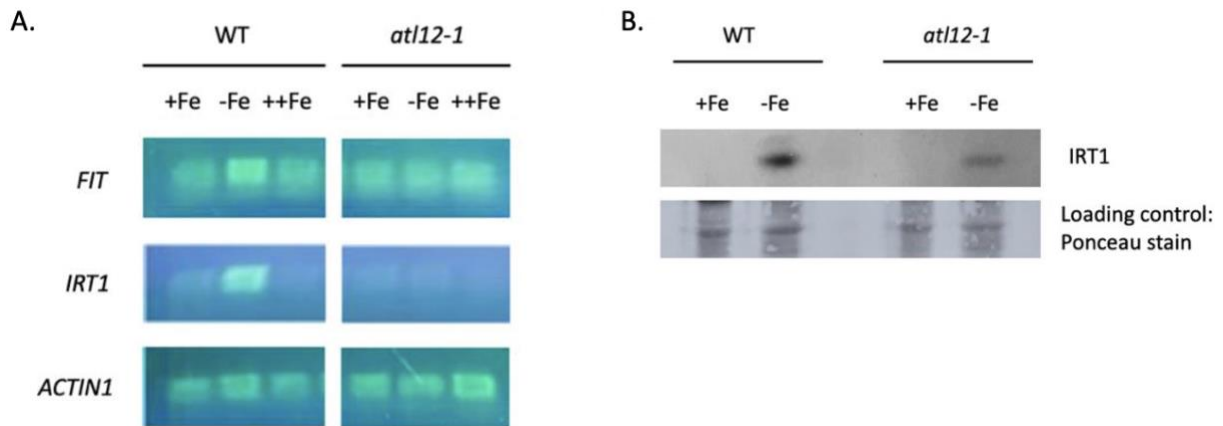


Figure 7. (A) RT-PCR analysis was performed using cDNA synthesized from RNA that was extracted from WT and *atl12-1* plants exposed to iron (Fe) sufficiency (control, +Fe), Fe deficiency (-Fe), or Fe excess (++Fe) for 10 days after being grown on control for five days. PCRs were run using primer pairs that flagged a ~ 200bp segment of *ACTIN1*, *FIT*, and *IRT1*. Gel electrophoresis was used to visualize gene levels. All segments of cDNA amplified are ≈200bp. **(B)** The abundance of IRT1 proteins in WT and *atl12-1* roots under -Fe were determined by western blot (WB) analysis with anti-IRT1 antibodies. Ponceau staining was used as a loading control. Protein was extracted from seedlings that were grown on +Fe for one week and then transferred to either +Fe or -Fe for five days.

ARI12 loss-of-function mutants have higher Fe content after exposure to excess Fe

Maintaining an optimal level of internal Fe is vital to plant survival as exposure to excess levels is toxic and cause cell death. *ATL12* and *ARI12* loss-of-function mutants show significantly different phenotypes and levels of Fe stress responsive genes, which may increase or decrease Fe uptake abilities under specific conditions. *atl12-1* plants show less IRT1 under -Fe than WT (Figure 7) suggesting that *atl12-1* has lower Fe uptake capabilities under -Fe. There was no significant difference in whole seedling Fe content of WT, *atl12-1*, and *ari12-1*, under -Fe for seven days (Figure 8A). However, *ari12-1* seedlings exposed to ++Fe contained a significantly higher concentration of Fe than WT and *atl12-1* ($p = 0.001006$) (Figure 8A), suggesting an impact on Fe

uptake or regulation in the absence of proper *ARI12* expression. After exposure to ++Fe for seven days leaves of *ari12-1* were also noticeably larger than WT (Figure 8B).

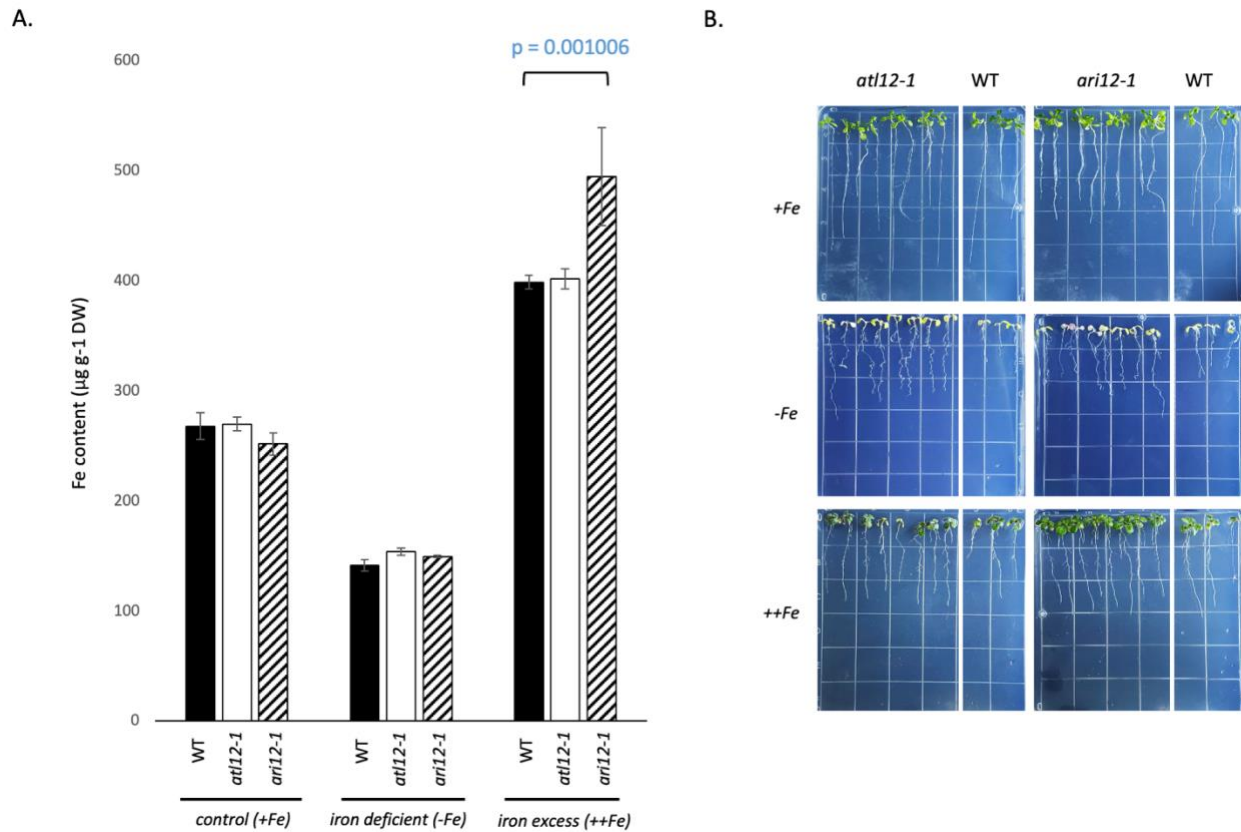


Figure 8. Fe content in whole seedlings was quantified using methods described by Gautam et al. (2022). Seedlings were grown under control/Fe sufficiency (+Fe) for five days then transferred to +Fe, iron deficient (-Fe), or iron excess (++Fe) for One week **(A)** Visualization of Fe content across all groups, p-value <0.05 using One-Way ANOVA Tukey comparison. Error bars indicate \pm SE from two trials with three technical replicates per trial. **(B)** Representative images of WT, *atl12-1*, and *ari12-1* seedlings on control (+Fe), (-Fe), and (++Fe), at the end of the treatment period.

DISCUSSION

ATL12 participates in a feedback loop with FIT

Previous work has established *Arabidopsis Toxicos en Levadura 12* (*ATL12*) as a RING-type E3 involved in a variety of defense responses, including the response to salt and ABA stress, and has been theorized to be involved in signal crosstalk between chitin-induced, NADPH oxidase-mediated, and hormonal defense response pathways (Kong and Ramonell, 2022; Kong, et al., 2021). Our research suggests that the function of *ATL12* is not limited to the roles it plays in these pathways, and results indicate that it plays a significant role in the response to Fe deficiency. *ATL12* was previously determined to be one of the approximately 450 *FIT*-regulated genes in the *Arabidopsis* genome (Colangelo and Guerinot, 2004; Mai et al., 2016). This information already suggests a role in the iron deficiency response (IDR) because *FIT* is established as the most significant regulator of IDR genes, with *FIT* mutants exhibiting impaired growth and severe chlorosis under sufficient Fe levels (Maurer et al., 2014).

When exposed to severe Fe deficiency, WT exhibits a significant increase in *ATL12* transcript levels, likely due to upregulation by *FIT*, indicating involvement of the E3 in the IDR. *ATL12* loss-of-function mutants demonstrated decreased sensitivity to Fe deficiency, exhibiting significantly longer roots and higher rates of survival on Fe deficient soil compared to WT. These results on their own suggest that *ATL12* is a negative regulator of the IDR. When exposed to Fe deficiency, *atl12-1* also exhibited significantly lower *FIT* and *IRT1* expression. Lower accumulation of *IRT1* proteins under Fe deficiency is also exhibited and can likely be attributed to the lower levels of *IRT1* in *atl12-1*. The increased root length and increased survival rate of *atl12-1* under Fe deficiency, while simultaneously expressing lower levels of *FIT* and *IRT1*

presents two interesting theories: 1) *ATL12* is involved in a feedback loop with *FIT*; and 2) *ATL12* is involved in sensing and/or signalling of Fe levels.

ATL12 both being regulated by *FIT* and seeming to play a role in regulating *FIT* levels, with a decrease in *ATL12* expression decreasing *FIT* expression, suggests that these two genes might participate in a feedback loop with each regulating the other under low Fe levels (Figure 10A). There are many signalling pathways which work to regulate *FIT* levels. For example, nitric oxide (NO) signalling modulates *FIT* transcription, inhibiting *FIT* degradation and promoting *FIT* stability under Fe deficiency (Meiser et al., 2011; Lei et al., 2020). In contrast, the phytohormone jasmonic acid (JA) acts as a negative regulator of the Fe deficiency response, through promoting the expression of *bHLH IVa* genes that form heterodimers with *FIT* to promote *FIT* degradation (Cui et al., 2018; Lei et al., 2020). Interplay between NO and plant hormones (including JA, abscisic acid (ABA), brassinosteroids (BR), and CK) have been established as vital to IDR signalling (Brumbarova et al., 2015; Jeong and Guerinot, 2009; Li et al., 2016). Jasmonates, such as JA, have been thoroughly studied in *Arabidopsis*, and have been established as an important regulator of defense gene expression, growth, and fertility in plants (Devoto and Turner, 2002; Huot et al., 2014; Campos et al., 2016; Li et al., 2022). Cui et al. (2018) demonstrate that JA negatively impacts Fe uptake via repressing the expression of multiple IDR genes (*FIT*, *bHLH38*, *bHLH39*, *bHLH100*, and *bHLH101*) and promoting the proteasomal degradation of *FIT*. However, studies demonstrate that Fe deficiency increases JA synthesis, which positively regulates the IDR in rice during the early stages of Fe deficiency (Kobayashi et al., 2016). No research sites an increase or decrease in JA synthesis in response to Fe deficiency in *Arabidopsis*. Research has shown that *ATL12* expression is upregulated in response to JA, suggesting that *ATL12* plays a role in JA signalling (Kong et al., 2021). It is possible that JA upregulates *ATL12* to counteract the

negative regulation of *FIT* under Fe deficiency (Figure 9A). This would explain the upregulation of *ATL12* under Fe deficiency, and the increase in *ATL12* levels in response to increased JA levels. This would also explain the lower *FIT* levels in *ATL12* loss-of-function mutants under Fe deficiency (Figure 9B). The molecular mechanisms which regulate Fe uptake are not entirely clear. JA upregulates the transcription factors *bHLH19* and *bHLH20*, which promote *FIT* degradation (Cui et al., 2018). *JASMONATE RESISTANT 1* (*JAR1*) catalyzes the formation of the conjugate jasmonyl-isoleucine (JA-Ile) from JA, which promotes *JASMONATE INSENSITIVE 1* (*MYC2*) (Staswick and Tiryaki, 2004; Schuman et al., 2018). *MYC2* represses *bHLH19* and *bHLH20* and upregulates *bHLH18* and *bHLH25*, two other transcription factors which promote *FIT* degradation (Cui et al., 2018). *MYC2* also represses the expression of *FIT* and *bHLH Ib* transcription factors (*bHLH38*, *bHLH39*, *bHLH100*, and *bHLH101*) (Cui et al., 2018). Further investigation is needed to determine where *ATL12* fits into this complex network.

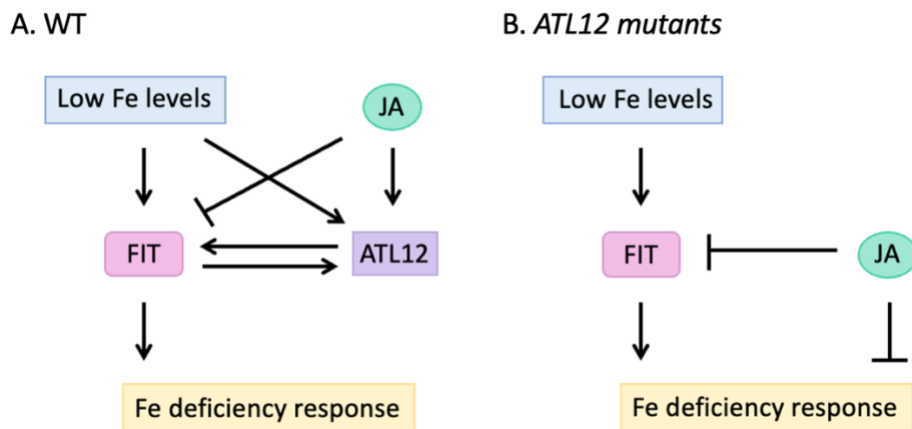


Figure 9. (A) Simplified representation of the possible crosstalk between *ATL12*, *FIT*, and JA. In Arabidopsis wild type (WT), *ATL12* and *FIT* possibly operate in a positive feedback loop to promote the Fe deficiency response. Low Fe levels also promotes JA to keep the Fe deficiency response under control. **(B)** If this feedback loop occurs, then in *ATL12* mutants, *ATL12* expression is knocked-down/out, and so *ATL12* cannot promote the expression of *FIT*, decreasing the intensity of the Fe deficiency response.

The longer roots exhibited by *ATL12* loss-of-function mutants indicate that the seedlings might be implementing a foraging strategy to increase Fe uptake, manipulating root system architecture (RSA) to explore the soil to physically search for Fe. This has been observed in *Arabidopsis* under mild Fe deficiency, but severe Fe deficiency usually arrests PR elongation and LR emergence to reduce nutrient demand (Seguela et al., 2008; Li et al., 2016). Loss of *ATL12* function may affect the ability to differentiate between mild and severe Fe deficiency, therefore affecting which response is activated. If this is true, then the *atl12-1* plants are responding how they would to milder Fe deficiency. The results of Fe content quantification shows that Fe levels in *atl12-1* and WT are not significantly different, suggesting that spending energy on increasing PR length is just as effective in increasing Fe uptake as the arrest of root growth to conserve nutrients. *ATL12* mutants also exhibited a significantly higher survival rate on Fe deficient soil. The CaCO treated soil simulates Fe deficiency via increasing the alkalinity of the soil, reducing the bioavailability of Fe, therefore specifically testing the plants RA and Fe³⁺ reduction abilities. Results show that the activity FRO2 and AHA2, two proteins vital to the functioning of these IDR mechanisms, are not significantly different in *atl12-1* and WT. However, *atl12-1* plants demonstrate higher rates of survival on the Fe deficient soil. These results suggest that *Arabidopsis* plants which increase PR growth to forage for Fe in exchange for a higher nutrient demand, are more successful than those that limit PR growth to conserve nutrients under Fe deficiency. The simultaneous lack of difference in Fe content and significant difference in *FIT* and *IRT1* levels between WT and *atl12-1* also indicates that other Fe deficiency response mechanisms not regulated by *FIT* are successfully up-taking Fe.

ARI12 is involved in the attenuation of the Fe deficiency response

Arabidopsis ARI12 is an RBR-type E3 which expression data suggests plays a role in Fe stress response, with microarray assays showing decreased levels of *ARI12* in WT when exposed to Fe deficiency. *ARI12* is known to be upregulated by the RING-type E3 CONSTITUTIVELY PHOTOMORPHOGENIC 1 (COP1) under UV-B exposure (Xie and Hauser, 2012; Xie et al., 2015). In the dark, COP1 also targets a protein that is possibly involved in Fe uptake, ELONGATED HYPOCOTYL 5 (HY5) (Srivastava et al., 2015; Xiao et al., 2022). In the light, HY5 proteins accumulate and regulate the expression of over 3000 genes, including those involved in nutrient uptake (Gangappa and Botto, 2016; Xiao et al. 2022). In tomato, HY5 directly activates the expression of the FIT ortholog, *FER*, in the roots, promoting downstream targets like *FRO2*, *IRT1*, and *NRAMP1*, to increase Fe uptake (Guo et al., 2021; Srivastava et al., 2015; Xiao et al., 2021). In Arabidopsis, HY5 has been reported to directly activate the transcription factor ABI5, a master regulator of the ABA signalling pathway (Bhagat et al., 2021; Chen and Xiong, 2008). ABA signalling is involved in reutilization and transport of Fe under Fe deficient conditions, significantly contributing to maintaining Fe homeostasis (Lei et al., 2014; Schwarz and Bauer, 2020). Research suggests that this interaction between HY5 and ABI5 fine tunes stress and developmental response in Arabidopsis (Bhagat et al., 2021). If ARI12 does play a role in Fe stress response it is possible that COP1 regulates the abundance of ARI12 under these conditions, as it does under UV-B exposure. This could establish COP1 as a regulator of the IDR, regulating ARI12, and possibly HY5, under Fe specific conditions. Our results suggest ARI12 is also involved in the Fe stress response, but the role of COP1, HY5, or ABA signalling remains unknown and cannot be expanded upon. The involvement of these genes would be an interesting avenue for future research into the IDR in Arabidopsis.

Our results demonstrate that *ARI12* levels in WT significantly decrease when exposed to Fe deficiency and increase when exposed to excess Fe. These results suggest that under Fe deficiency the expression of *ARI12* is repressed to allow its target protein to accumulate as part of the IDR, and under Fe sufficiency *ARI12* expression increases to reduce levels of the IDR protein. This creates a hypothesis that ARI12 is involved in the attenuation of the IDR, through targeting an unknown IDR related protein for proteasomal degradation (Figure 10A). This means that in *ARI12* loss-of-function mutants, the IDR proteins accumulate under Fe sufficiency (Figure 10B). This would also cause higher accumulation of the IDR protein in *ari12-1* when exposed to Fe deficiency, which would generate a higher tolerance to low Fe levels. This is supported by the decreased sensitivity of the *ari12-1* plants grown under Fe deficiency, which exhibit significantly longer roots than WT. The over-accumulation of the unknown IDR would also cause increased Fe uptake, and Fe content quantification shows that *ARI12* mutants contained a significantly higher Fe content than WT after being exposed to excess Fe for 10 days, supporting this theory. An analysis by Mladek et al. (2003) presents evidence that *ARI12* is expressed in the roots specifically, which when considered with our results supports the theory that it may be involved in the acquisition of Fe from the soil.

Our results suggest that the E3 ARI12 ubiquitinates a substrate involved in the IDR in the absence of low Fe stress, however, further investigation must be performed to pinpoint possible substrates and regulators of ARI12. Further analysis is also required to determine if the IDR protein is directly ubiquitinated for degradation by ARI12, or if ARI12 targets a protein that transcriptionally regulates the IDR protein.

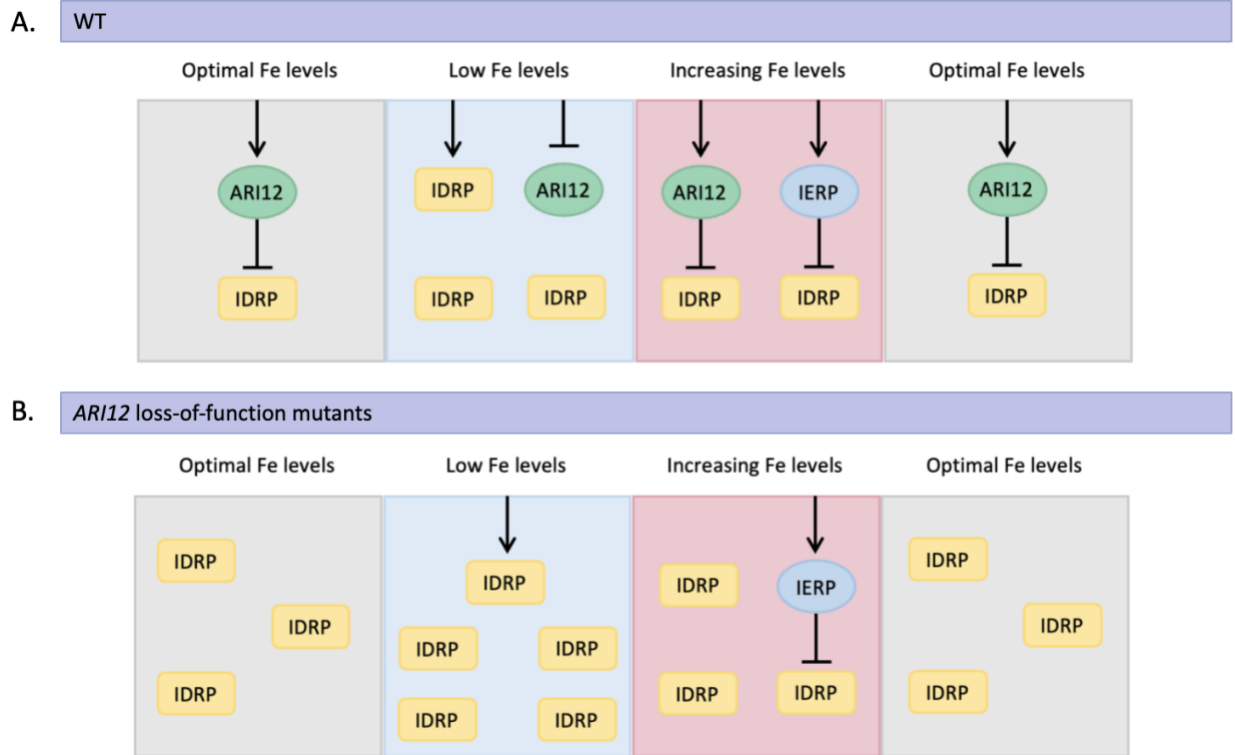


Figure 10. Simplified schematics of the possible role *ARI12* plays in attenuating the Iron Deficiency Response (IDR). **(A)** Under sufficient iron (Fe) levels, *ARI12* targets an unknown IDR Protein (IDRP) to inhibit the response. Low Fe (-Fe) levels decreases *ARI12* expression to allow its target protein to accumulate as part of the IDR. When Fe levels increase again, *ARI12* and an unknown Iron Excess Response Protein (IERP) targets the IDRP to attenuate the IDR and avoid toxic Fe accumulation. When external Fe levels are optimal again, *ARI12* works to mediate homeostasis of the IDR. **(B)** In *ari12-1* mutants, knocked-down *ARI12* expression causes accumulation of the IDRP under Fe sufficient conditions, causing increased Fe uptake under -Fe and excess Fe (++Fe).

Future directions

The strict regulation of Fe uptake in *Arabidopsis* is the result of many complex signalling networks which function to activate or deactivate the IDR in the absence or presence of sufficient Fe levels, respectively. This study demonstrated that the RING-type E3 ATL12 and the RBR-type E3 *ARI12* are involved in regulating the IDR in two unconnected ways. Importantly, results indicates that ATL12 possibly participates in a feedback loop with FIT under Fe deficiency.

However, many questions must be answered to understand exactly how this possible feedback loop operates. Considering our results as well as those of previous studies, it is possible that JA upregulates *ATL12* to attenuate the negative regulation of FIT by the JA signalling pathway. At a molecular level it seems that loss of *ATL12* function would increase sensitivity to Fe, but *ATL12* mutants grow in contradiction to this theory. The longer roots exhibited by *atl12-1* and *atl12-2* under severe Fe deficiency suggests that *ATL12* may play a role in limiting PR elongation to conserve nutrients under severe Fe deficiency. Under Fe deficiency *atl12-1* plants are more successful, which may be a result of the longer PR increasing Fe uptake although *FIT*, *IRT1* levels, and *IRT1* protein levels are lower. This may also be an indication that loss of *ATL12* function causes a disconnect in Fe level sensing or signalling, which could be traced back to the JA signalling pathway. Nonetheless, further research is necessary to confirm the theories discussed in this paper. These results may also aid in future studies of JA signalling and its significance in the IDR. Less is known of *ARI12*, but our results suggests that it works to attenuate the IDR in the absence of stress. This may explain the high Fe content in *ari12-1* plants exposed to excess Fe, and the increased tolerance to severe Fe deficiency. Pinpointing the specific roles of these E3s is heavily reliant on further studies determining the substrate(s) which they target for ubiquitination and the conditions under which the E3s ubiquitinate the substrates. Further investigation of these two E3s is necessary to fully understand their roles in maintaining Fe homeostasis. Our findings will serve as an aid to future studies of *ATL12* and *ARI12* as well as those focusing on the IDR and JA signalling.

SUPPLEMENTARY MATERIAL

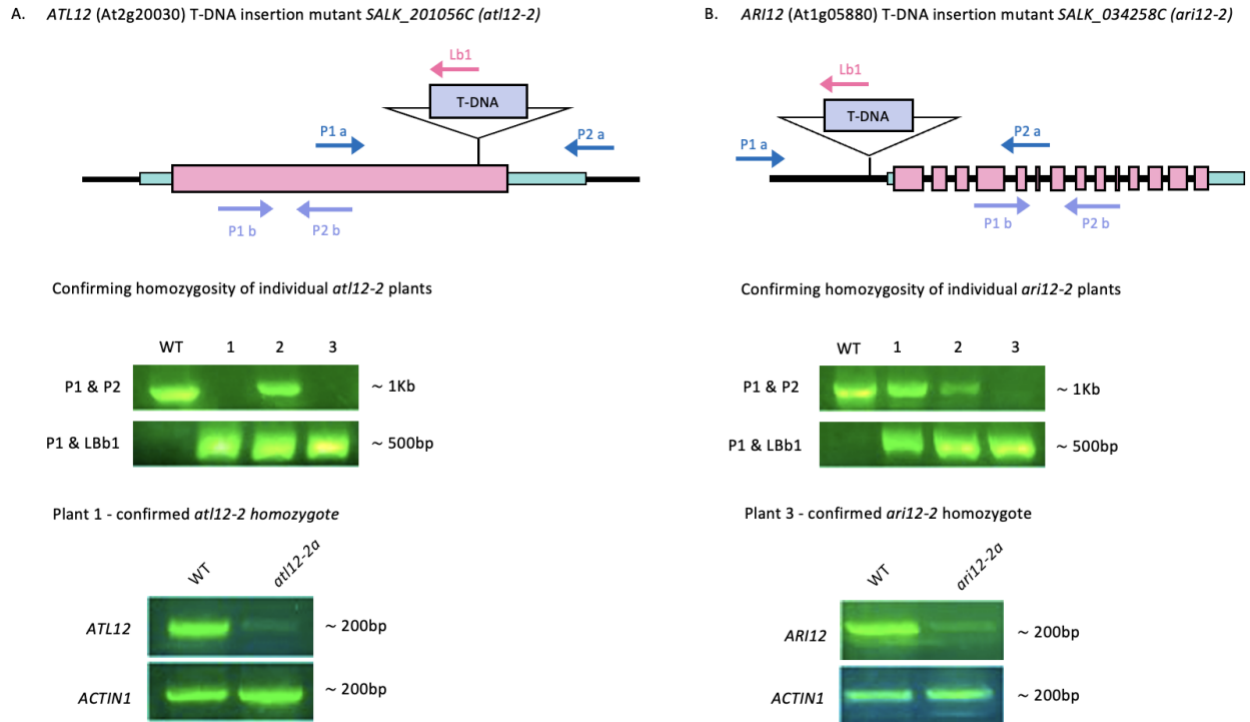


Figure S1. Schematics of *ATL12* and *ARI12* with location of T-DNA insertions and primer pairs used for PCR genotyping (P1a and P2a) and for analysis of E3 gene expression to determine knock-down expression (P2b and P2b). PCR genotyping was visualized using gel electrophoresis. **(A)** *ATL12* *SALK_201056* T-DNA insertion mutant. Plant 1 (*atl12-2a*), and 3 were determined to be homozygous *atl12-2*. **(B)** *ARI12* *SALK_034258* T-DNA insertion mutant. Plant 3 (*ari12-2a*) was determined to be homozygous *ari12-2*. Qualitative RT-PCR visualized using gel electrophoresis showing lower expression of *ATL12* in *atl12-2* **(A)**, and *ARI12* in *ari12-2* **(B)**.

ATL12 (At2g20030) T-DNA insertion mutant SALK-line 066923C (*atl12-1*)

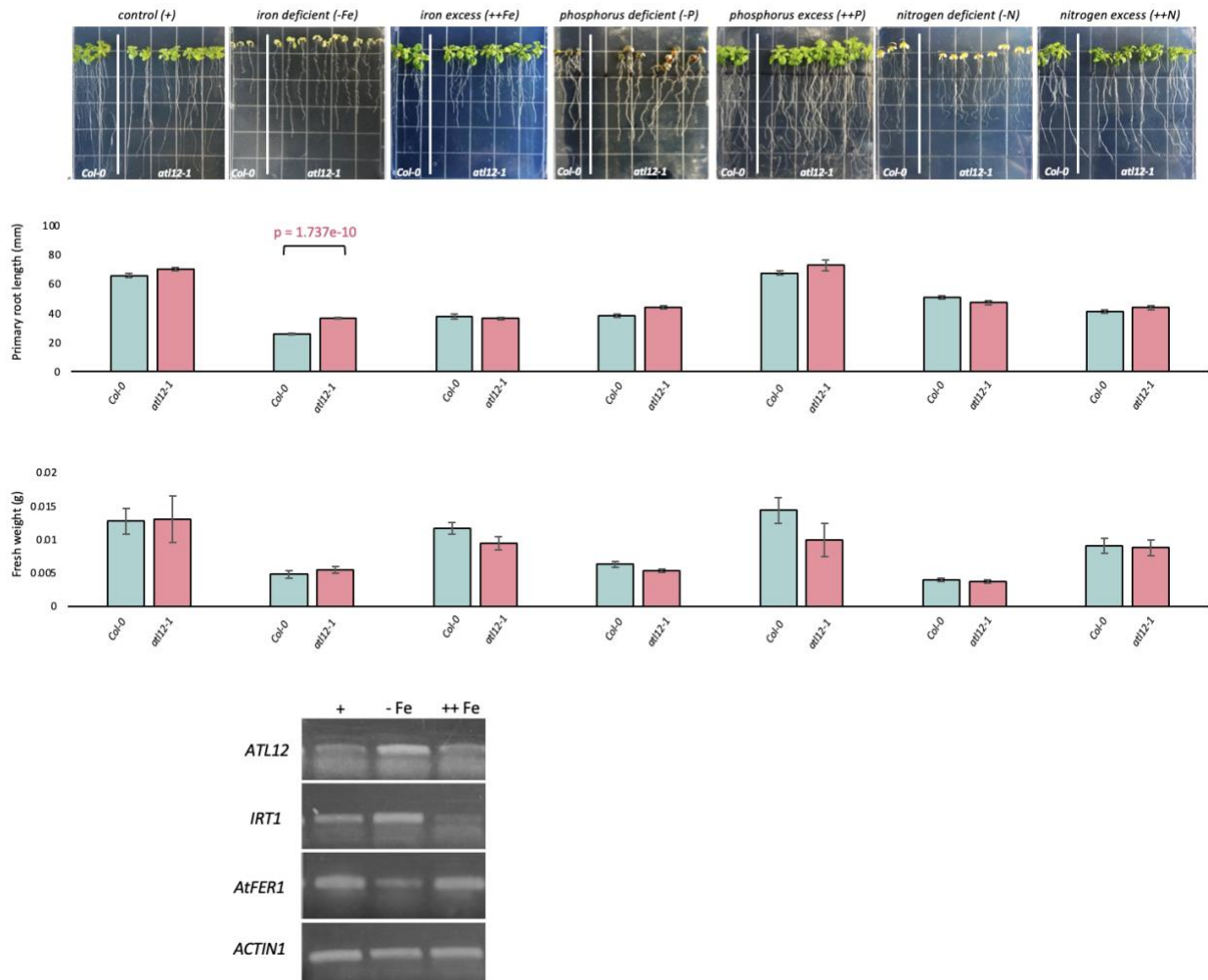


Figure S2. 15-day old *atl12-1* and wild type (WT, *Col-0*) seedlings that were grown for five days on nutrient sufficient (control) media then 10 days on +, Fe deficient (-Fe), Fe excess (++Fe), P deficient (-P), P excess (++P), N deficient (-N), and N excess (++N) media. Primary root lengths and fresh weight were measured at the end of the 10-day treatment period using ImageJ® (<http://imagej.net>). Analysis was done using One-Way ANOVA Tukey comparison. Error bars indicate \pm SE from at least one trial with at least three replicates per trial (≥ 24). cDNA was synthesized from RNA extracted from WT seedlings that were grown on control for five days then for 10 days on control, -Fe, and ++Fe. All segments of cDNA amplified are \approx 200bp.

ARI12 (At1g05880) T-DNA insertion mutant SALK_033142C

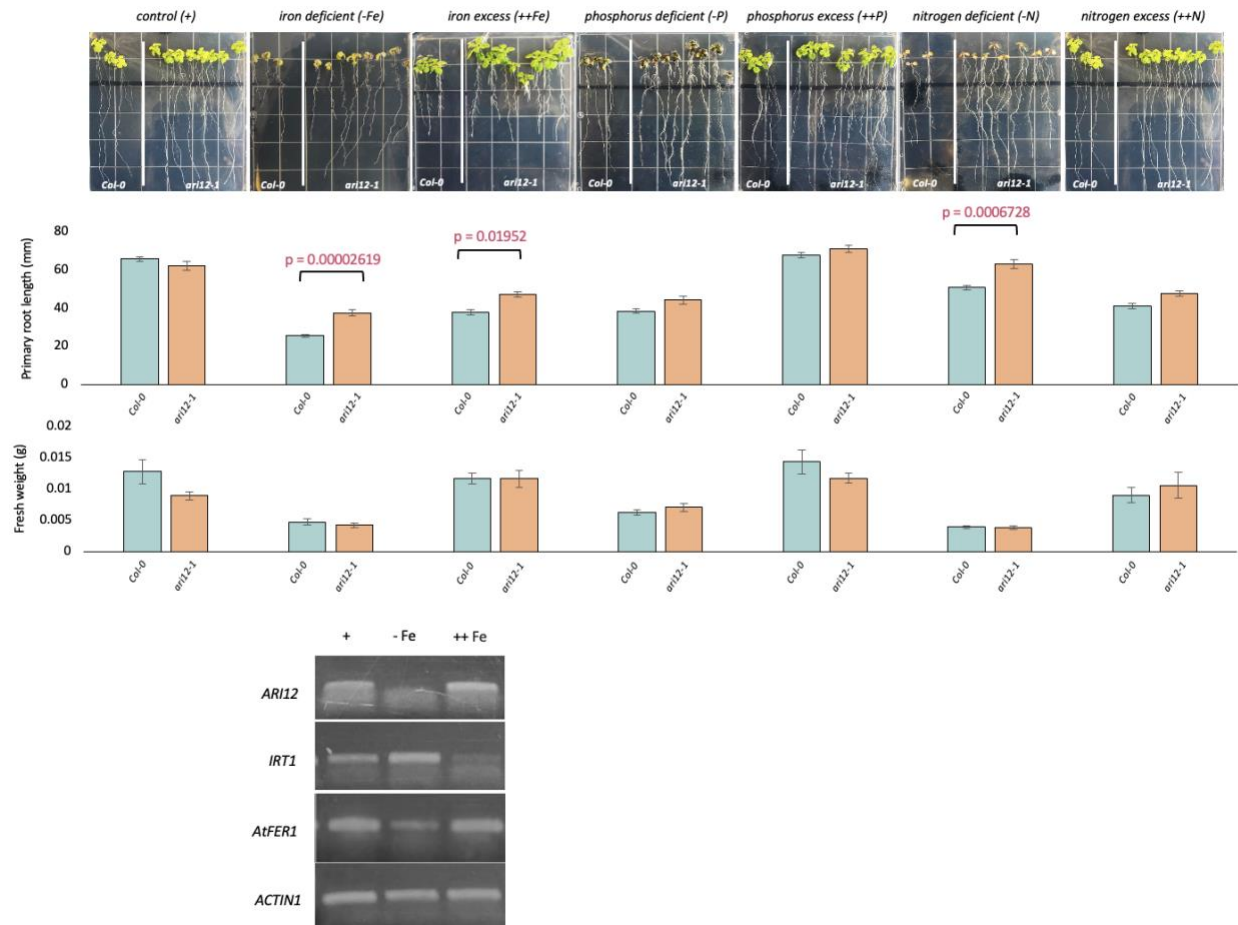


Figure S3. 15-day old *ari12-1* and wild type (WT, *Col-0*) seedlings that were grown for five days on nutrient sufficient (control) media then 10 days on control, Fe deficient (-Fe), Fe excess (++Fe), P deficient (-P), P excess (++P), N deficient (-N), and N excess (++N) media. Primary root lengths and fresh weight were measured at the end of the 10-day treatment period using ImageJ® (<http://imagej.net>). Analysis was done using One-Way ANOVA Tukey comparison. Error bars indicate \pm SE from at least one trial with at least three replicates per trial (≥ 24). *ARI12* loss-of-function mutants showed differential phenotypes under -Fe, ++Fe and -N, and the involvement of *ARI12* in Fe stress response was selected for further investigation. cDNA was synthesized from RNA extracted from WT seedlings that were grown on control for five days then for 10 days on control, -Fe, and ++Fe. All segments of cDNA amplified are ≈ 200 bp.

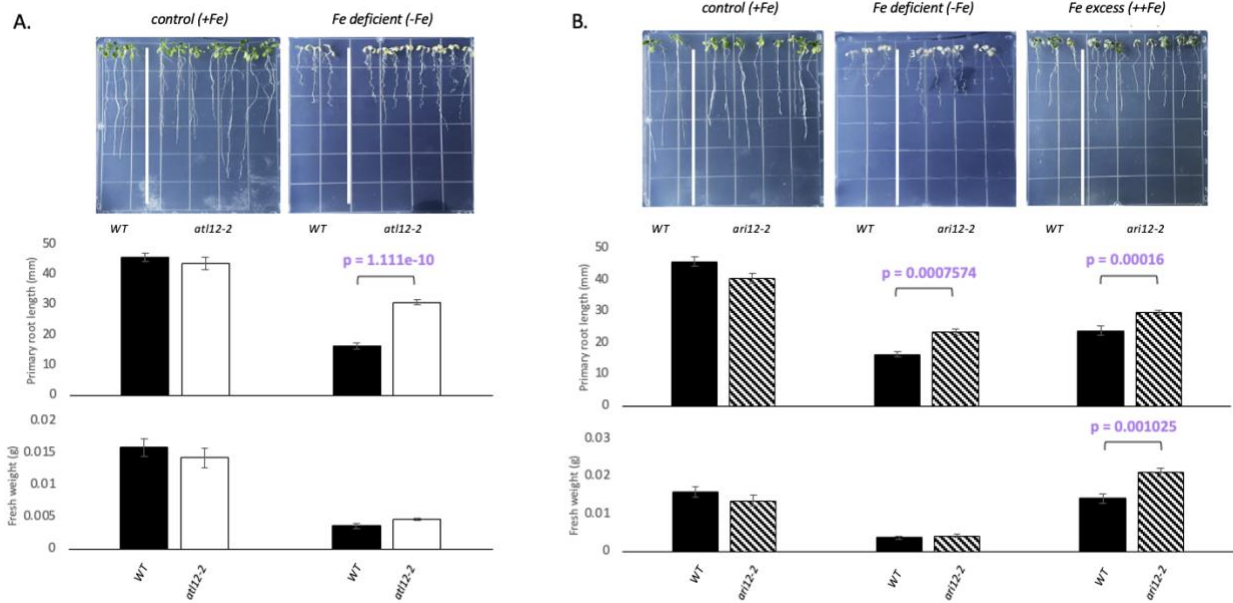


Figure S4. (A) 12-day old *at/12-2* and WT seedlings that were grown for five days on nutrient sufficient (control) media then 7 days on iron deficient (-Fe) media. Primary root lengths and fresh weight were measured at the end of the week-long treatment period using ImageJ® (<http://imagej.net>). Mutants exhibited significantly longer roots than WT on -Fe ($p = 1.111e-10$) and showed no significant difference on control. **(B)** 12-day old *ari12-2* and *Col-0* seedlings that were grown for five days on nutrient sufficient (control) media then 7 days on iron deficient (-Fe) or iron excess (++) media. Primary root lengths were measured at the end of the week-long treatment period using ImageJ® (<http://imagej.net>). *ARI12* mutants exhibited significantly longer roots than WT on -Fe ($p = 0.0007574$) and ++Fe ($p = 0.00162$) and showed no significant difference on control. *ari12-2* also exhibited a heavier fresh weight on ++Fe ($p = 0.001025$). Analysis was done using One-Way ANOVA Tukey comparison. Error bars indicate \pm SE from one trial with four replicates per trial ($n \geq 32$).

CHAPTER 3: RING-type E3 WAVH1 is required for optimal root growth and gravitropism under nitrogen deficiency in *Arabidopsis thaliana*

RING-type E3 WAVH1 is required for optimal root growth and gravitropism under nitrogen limitation in *Arabidopsis thaliana*

Erin MacKinnon and Sophia L. Stone

ABSTRACT

Ubiquitination is a post-translational modification which eukaryotes use to alter their proteome through mediating protein degradation, interaction, and activity. Substrate protein selection and the attachment of ubiquitin (Ub) is facilitated by the ubiquitin ligases (or E3s), many of which are involved in mediating nutrient stress responses. The wavy growth 3 (WAV3) E3 ligase family is an established group of gravitropism-regulating proteins in *Arabidopsis*, and a role for WAV3 Homolog 1 (WAVH1) in influencing root gravitropism and RSA modulation is coming to light. Here we demonstrate a role for WAVH1 in regulating root growth patterns under severe N limitation. *WAVH1* loss-of-function mutants (*wavh1-1*) demonstrate significantly lower lateral root (LR) emergence under N sufficient and deficient conditions, and lower primary root (PR) growth under severe N limitation compared to wild type (WT). Under severe N limitation *WAVH1* mutants also demonstrate severely impacted root gravitropic abilities, with mutants exhibiting a significantly larger root reflex angle in response to a 90° rotation. These significant differences are removed when treated with brassinazole (BRZ) a brassinosteroid (BR) biosynthesis inhibitor. In this paper we demonstrate that the E3 ligase WAVH1 is required for proper root gravitropism and manipulation of root system architecture (RSA) under severe N limitation, and we discuss a model in which WAVH1 plays a role in BR signalling to regulate root growth.

INTRODUCTION

Plant success is largely dependent on the availability of nutrients in the soil, as well as the ability to uptake those nutrients. Nitrogen (N) and phosphorus (P) are the two macronutrients required in the largest amount by plants, making the molecular mechanisms and strategies that govern the uptake of N and P, vital to plant success. N is a major component of amino acids, nucleotides, and chlorophyll, heavily contributing to photosynthetic processes and fruiting success; it is essential for the metabolism of sugar, controlling sugar levels which regulate the expression of genes vital for various developmental and physiological processes (Sato et al., 2009; Zhang et al. 2020). Inadequate levels of N inhibit development and reduce biomass, and because N content and photosynthetic capacity are positively correlated, N deficiency causes a decrease in photosynthetic rates (Sage and Pearcy, 1987; Khamis et al., 1990; Costa et al., 2002). P is vital to plant growth and development as it is a component of key macromolecules, such as proteins, nucleic acids and the energy units ATP and ADP (Elser, 2012; Plaxon et al., 2015; Khan et al., 2023). Sufficient levels are required to support photosynthetic processes, metabolism of nitrogen, carbohydrates, and fat, and other ATP-dependent pathways (López-Arredondo et al., 2014). P deficiency decreases leaf surface area, in turn decreasing CO₂ acquisition (Høgh-Jensen et al., 2002). Low soil N and P are two of the major limiting factors for crop yield, as they are required in large amounts but are often present in small quantities locally (Begum et al., 2015; Mussarat et al., 2021). To limit the impact of low N and P, the agricultural industry uses \approx 90 million tonnes of nitrogenous fertilizers and \approx 45 million tonnes of phosphorus fertilizers annually (Good et al., 2004; Walsh et al., 2023). Studies suggest that up to 70% of added N and P are not used by crops due to leaching, formation of insoluble compounds, or low nutrient use efficiency (Anas et al.,

2020; Brownlie et al., 2021). These added nutrients cost the agricultural industry millions of dollars and cause 78% of global ocean and freshwater eutrophication every year, therefore a better understanding of plant uptake and use of N and P is emerging as an important topic from both an economical and environmental standpoint (Masclaux-Daubresse et al., 2010; Poore and Nemecek, 2018).

The availability of N and P in the soil is influenced by multiple factors, including soil particle size, microbes, water content, temperature, aeration, as well as other nutrients present (Fageria and Baligar, 2005; Jackson, 2020). Plants uptake the two inorganic forms of N, nitrate (NO_3^-) and ammonium (NH_4^+), and organic forms of N, such as the amino acids in the soil and urea (Zhang et al., 2020; Muratore et al., 2021). The main forms of P available are the inorganic orthophosphates: H_2PO_4^- and HPO_4^{2-} , and while soil inorganic P (Pi) levels may be high, its reactivity makes it unavailable when soil conditions are not optimal (Holford, 1997; Mehra et al., 2017). If soil pH is too low, P reacts with organic matter, as well as aluminum (Al), and iron (Fe), to form insoluble compounds; a soil pH too high will bind to calcium (Ca) and magnesium (Mg), to form low-solubility phosphates (López-Bucio et al., 2002; Baccari and Krouma, 2023). Soil conditions will never truly be optimal, and so plants have evolved a plethora of strategies and molecular mechanisms to increase the uptake of N and P when external levels are depleted or unavailable, including influencing the pH of the rhizosphere, and manipulating root system architecture (RSA) (López-Bucio et al., 2002; Giehl and Wirén, 2014; Jing et al., 2010; MacKinnon and Stone 2022).

Plants have evolved different strategies adapted to tolerating different degrees of N and P deficiency, involving increasing root surface area to forage for nutrients under mild deficiency and arresting root growth to conserve nutrients when deficiency is severe (López-Bucio et al., 2002;

Jia et al., 2020). The nutrient foraging strategy that plants implement through spending energy on increasing primary root (PR) length, and lateral root (LR) length and emergence, is dependent on the crosstalk between various signalling pathways that detect N and P levels and activate the correct molecular mechanisms to trigger the appropriate response (Sugimura et al., 2022). Brassinosteroids (BR) are emerging as a key regulator in altering RSA under N and P deficient conditions (Jia et al., 2020; Pandey et al., 2020; Manghwar et al., 2022).

BRs regulate root growth through the activity of multiple signalling proteins, including a protein complex that involves the leucine-rich repeat receptor-like protein kinase (LRR-RLK) BRASSINOSTEROID-INSENSITIVE 1 (BRI1) interacting with BRI1-ASSOCIATED KINASE RECEPTOR 1 (BAK1) to modulate BR signalling in *Arabidopsis* (Li et al., 2002; Mao and Li, 2020). Mild N deficiency upregulates *BAK1* and promotes BR-induced auxin transport in roots, stimulating root cell division to enhance PR elongation and LR emergence (Perrot-Rechenmann, 2010; Jia et al., 2019; Jia et al., 2020). PR elongation and LR emergence is dependent on BRASSINOSTEROID-SIGNALLING KINASE 3 (BSK3) (Jia et al., 2019; Jia et al., 2020). Under mild N deficiency, BSK3 mediates BR signalling downstream of BR receptors, with studies showing *BSK3* loss-of-function mutants demonstrate decreased BR responses under low N compared to WT (Ren et al., 2019). Under severe N deficiency, shootward auxin transport is promoted to inhibit LR emergence and PR growth and conserve nutrients (Krouk et al., 2010; Giehl and Wirén, 2014; Jian et al., 2018; Mounier et al., 2014; Liu and Wirén, 2022). Root growth is also arrested under severe P deficiency through the inhibition of BR biosynthesis and signalling, which suggests that BR signalling also plays a role in promoting the more exploratory RSA that *Arabidopsis* demonstrates under mild P deficiency (Singh et al., 2018; Zhang et al., 2021).

Ubiquitination is a major regulator of the N and P deficiency response through directly regulating the abundance of transporters, enzymes, ion channels, and transcription regulators (e.g., transcription factors, co-activators, and repressors) involved nutrient uptake and stress response (Zelazny et al., 2011; Yates and Sadanandom, 2013). There are multiple E3s which have been identified as regulators of N uptake in plants. For example, in *Oryza sativa* (rice) the RING-type E3 NRT1.1B interacting protein 1 (OsNBIP1) targets the repressor protein SPX4 for degradation via the 26S proteasome, alleviating the inhibition of NIN-like protein 3 (NLP3) which promotes the expression of multiple N-responsive genes (Hu et al., 2019). In *Arabidopsis thaliana* (Arabidopsis) the RING-type E3 Nitrogen Limitation Adaptation (NLA) mediates the Ub-dependent degradation of nitrate transporter 1.7 (NRT1.7) in response to high N levels to decrease source-to-sink mobilization of NO_3^- (Peng et al., 2007; Fan et al., 2009; Kant et al., 2011; Liu et al., 2017; Hannam et al., 2018; Sakuraba, 2022). Under N deficiency, NLA protein levels decrease via miRNA-dependent translational repression, promoting N mobilization (Peng et al., 2007; Liu et al., 2017).

NLA also plays a role in regulating P homeostasis, ubiquitinating the PHOSPHATE TRANSPORTER 1 (PHT1) family of transporters at the PM to limit uptake under P excess (Kant et al., 2011; Lin et al., 2013; Park et al., 2014). In rice and Arabidopsis, the expression of Pi-starvation induced (PSI) genes are regulated by a family of Phosphate Starvation Response (PHR) transcription factors (Bustos et al., 2010). OsSPX4 interacts with OsPHR2 to repress the transcription of many PSI genes under Pi sufficiency (Lv et al., 2014). Under Pi-starvation, OsSPX4 is ubiquitinated by the RING-type E3s SPX4 degradation E3 ligases 1 and 2 (SDEL1/2), activating OsPHR2 and upregulating PSI genes (Hu et al., 2019; Ruan et al., 2019). Under Pi-starvation, the F-Box E3 Phosphate Response Ubiquitin E3 Ligase 1 (PRU1) promoting the Ub-

dependent degradation of WRKY6, a transcription factor that inhibits the transcription of transporter *Phosphate 1 (PHO1)* (Hamburger, 2002; Chen et al. 2009; Lin et al., 2013; Ye et al., 2018).

In the Arabidopsis genome, there are over 470 genes which encode for RING-type E3s, and additional E3s may be involved in maintaining N and P homeostasis (Stone et al., 2005). According to microarray analysis 25 RING-type E3s showed differential expression under low-P or low-N levels, which suggests a role in nutrient stress response. Here we provide evidence that indicates that the RING-type E3 WAVH1, a member of the wavy growth 3 (WAV3) family, is involved in modulating RSA specifically under N deficiency. Results demonstrate that loss of WAVH1 function limits PR elongation and LR emergence and inhibits gravitropic abilities under severe N deficiency, possibly interfering with BR signalling. *WAVH1* loss-of-function mutants also differently express multiple genes involved in plant response to N limitation *NRT1.1*, *BSK2*, *NLP6*, and *TCP20*. This suggests that WAVH1 plays a role in plant response to N limitation.

MATERIALS AND METHODS

Plant growth conditions

14 candidate RING-type E3s were selected for this project (APPENDIX A). *Arabidopsis thaliana* ecotype Columbia (*Col-0*) (wild type, WT), and SALK T-DNA insertion mutant seeds (Table 1) were obtained from the Arabidopsis Biological Resource Center (ABRC, <https://abrc.osu.edu/>). Seeds were surface-sterilized with 50% (v/v) bleach for 10 minutes at room temperature. Seeds were then rinsed thoroughly with double-distilled H₂O then plated on solid ½ Murashige and Skoog (MS) medium containing 0.8% agar and 1% sucrose. Seeds were then stratified at 4°C in the dark for 72 hours, and then were grown under continuous light at 22°C. 10-day-old seedlings were transferred from the ½ MS medium to soil and grown with photoperiodic cycles of 16 hours light and 8 hours dark at 22°C.

Gene	Gene Name	Mutant: SALK Line
At2g22680	WAVH1	SALK_149664 (<i>wavh1-1</i>), SALK_041291 (<i>wavh1-2</i>)
At2g20030	ATL12	SALK_066923 (<i>atl12-1</i>), SALK_201056 (<i>atl12-2</i>)
At2g31780	ARI11	CS24734
At1g14260	ERiN1	SALK_118406
At1g05880	ARI12	SALK_033142 (<i>ari12-1</i>), SALK_034258 (<i>ari12-2</i>)
At1g70910	DEP	SALK_141707
At5g01070	ERiN2	SALK_086525
At2g38920	ERiN3	SALK_129778
At4g09110	ATL35	SALK_065995
At1g18910	BTSL2	SALK_048470
At5g03180	ERiN4	SALK_023683
At5g06490	ATL71	CS863433
At5g37910	SINA-like 9	SALK_023901
At5g58580	ATL63	SALK_139444

Table 1. The 14 selected candidate RING-type E3s and the corresponding T-DNA insertion mutant SALK lines which were ordered from ABRC (<https://abrc.osu.edu/>).

Nutrient media preparation

For nutrient sufficient conditions (control, +), ½ MS media was used. For excess iron conditions (++Fe), ½ MS media was supplemented with 300µM Ferric-ethylenediaminetetraacetic acid (Fe-EDTA; Sigma-Aldrich; <https://www.sigmaaldrich.com>). Iron deficiency (-Fe) was simulated using Fe-free ½ MS media supplemented with 150µM of 3-9(2-Pyridyl)-5,6-diphenyl-1,2,4-triazine-p,p'disulfonic acid monosodium salt hydrate (FerroZine; Sigma-Aldrich; <https://www.sigmaaldrich.com>). Phosphorus (P) and nitrogen (N) excess conditions were simulated using ½ MS media supplemented with 4.375 mM KH₂PO₄ and 60 mM NH₄NO₃, respectively (Sigma-Aldrich; <https://www.sigmaaldrich.com>). P deficiency (-P) was simulated with Phosphate-free media supplemented with 10 µM KH₂PO₄, N deficiency (-N) was simulated with Nitrogen-free media supplemented with 20 µM NH₄NO₃. All MS salts were ordered from Caisson Labs (www.caissonlabs.com). Composition of all nutrient treatment media can be viewed in Table 2.

Nutrient treatment	Media composition
Control	NO ₃ ⁻ (10.0 mM), NH ₄ ⁺ (2.0 mM), PO ₄ ³⁻ (1.25 mM), K ⁺ (2.0 mM), Mg ²⁺ (0.5 mM), Ca ²⁺ (0.5 mM), SO ₄ ²⁻ (0.5 mM), Fe ²⁺ /Fe ³⁺ (50 µM), Mn ²⁺ (0.55 µM), Zn ²⁺ (0.55 µM), Cu ²⁺ (0.08 µM), MoO ₄ ²⁻ (0.04 µM), H ₂ BO ₃ ⁻ /BO ₃ ³⁻ (2.7 µM), 0.05% MES (w/v), 1% sucrose (w/v), 0.8% agar (w/v)
Fe deficient (-Fe)	NO ₃ ⁻ (10.0 mM), NH ₄ ⁺ (2.0 mM), PO ₄ ³⁻ (1.25 mM), K ⁺ (2.0 mM), Mg ²⁺ (0.5 mM), Ca ²⁺ (0.5 mM), SO ₄ ²⁻ (0.5 mM), Mn ²⁺ (0.55 µM), Zn ²⁺ (0.55 µM), Cu ²⁺ (0.08 µM), MoO ₄ ²⁻ (0.04 µM), H ₂ BO ₃ ⁻ /BO ₃ ³⁻ (2.7 µM), + 150 µM FerroZine, 0.05% MES (w/v), 1% sucrose (w/v), 0.8% agar (w/v)
Fe excess (++Fe)	NO ₃ ⁻ (10.0 mM), NH ₄ ⁺ (2.0 mM), PO ₄ ³⁻ (1.25 mM), K ⁺ (2.0 mM), Mg ²⁺ (0.5 mM), Ca ²⁺ (0.5 mM), SO ₄ ²⁻ (0.5 mM), Fe ²⁺ /Fe ³⁺ (50 µM), Mn ²⁺ (0.55 µM), Zn ²⁺ (0.55 µM), Cu ²⁺ (0.08 µM), MoO ₄ ²⁻ (0.04 µM), H ₂ BO ₃ ⁻ /BO ₃ ³⁻ (2.7 µM), + 300 µM Fe-EDTA, 0.05% MES (w/v), 1% sucrose (w/v), 0.8% agar (w/v)
P deficient (-P)	NO ₃ ⁻ (10.0 mM), NH ₄ ⁺ (2.0 mM), K ⁺ (2.0 mM), Mg ²⁺ (0.5 mM), Ca ²⁺ (0.5 mM), SO ₄ ²⁻ (0.5 mM), Fe ²⁺ /Fe ³⁺ (50 µM), Mn ²⁺ (0.55 µM), Zn ²⁺ (0.55 µM),

	Cu ²⁺ (0.08 μM), MoO ₄ ²⁻ (0.04 μM), H ₂ BO ₃ ⁻ /BO ₃ ³⁻ (2.7 μM), + 10 μM KH ₂ PO ₄ , 0.05% MES (w/v), 1% sucrose (w/v), 0.8% agar (w/v)
P excess (++P)	NO ₃ ⁻ (10.0 mM), NH ₄ ⁺ (2.0 mM), PO ₄ ³⁻ (1.25 mM), K ⁺ (2.0 mM), Mg ²⁺ (0.5 mM), Ca ²⁺ (0.5 mM), SO ₄ ²⁻ (0.5 mM), Fe ²⁺ /Fe ³⁺ (50 μM), Mn ²⁺ (0.55 μM), Zn ²⁺ (0.55 μM), Cu ²⁺ (0.08 μM), MoO ₄ ²⁻ (0.04 μM), H ₂ BO ₃ ⁻ /BO ₃ ³⁻ (2.7 μM), + 4.375 mM KH ₂ PO ₄ , 0.05% MES (w/v), 1% sucrose (w/v), 0.8% agar (w/v)
N deficient (-N)	PO ₄ ³⁻ (1.25 mM), K ⁺ (2.0 mM), Mg ²⁺ (0.5 mM), Ca ²⁺ (0.5 mM), SO ₄ ²⁻ (0.5 mM), Fe ²⁺ /Fe ³⁺ (50 μM), Mn ²⁺ (0.55 μM), Zn ²⁺ (0.55 μM), Cu ²⁺ (0.08 μM), MoO ₄ ²⁻ (0.04 μM), H ₂ BO ₃ ⁻ /BO ₃ ³⁻ (2.7 μM), + 20 μM NH ₄ NO ₃ , 0.05% MES (w/v), 1% sucrose (w/v), 0.8% agar (w/v)
N excess (++N)	NO ₃ ⁻ (10.0 mM), NH ₄ ⁺ (2.0 mM), PO ₄ ³⁻ (1.25 mM), K ⁺ (2.0 mM), Mg ²⁺ (0.5 mM), Ca ²⁺ (0.5 mM), SO ₄ ²⁻ (0.5 mM), Fe ²⁺ /Fe ³⁺ (50 μM), Mn ²⁺ (0.55 μM), Zn ²⁺ (0.55 μM), Cu ²⁺ (0.08 μM), MoO ₄ ²⁻ (0.04 μM), H ₂ BO ₃ ⁻ /BO ₃ ³⁻ (2.7 μM), + 60 mM NH ₄ NO ₃ , 0.05% MES (w/v), 1% sucrose (w/v), 0.8% agar (w/v)

Table 2. Nutrient composition of the seven nutrient treatments used to analyze plant response under iron (Fe), phosphorus (P), and nitrogen (N) deficiency and excess. All MS salts were obtained from Caisson Labs (<https://caissonlabs.com>) and supplemental nutrients were obtained from Sigma-Aldrich (<https://www.sigmaaldrich.com>).

PCR genotyping

Arabidopsis thaliana Columbia (*Col-0*) seeds harbouring transfer-DNA (T-DNA) insertions within the 14 E3 genes of interest were ordered from the Arabidopsis Biological Resource Center (ABRC; <https://abrc.osu.edu/>) (Table 1). To identify homozygous mutants, polymerase chain reaction (PCR) utilizing gene specific primers flanking the T-DNA insertion site, along with primers targeting the T-DNA border, were used for genotyping plants. The National Center for Biotechnology Information (NCBI) online primer-BLAST tool (<https://www.ncbi.nlm.nih.gov/tools/primer-blast/>) was used to design gene specific primers (Table 3). Small leaf samples were used in PCR reactions utilizing the Phire[®] Plant Direct PCR kit (Thermo Scientific; <https://www.thermofisher.com>). The presence of the WT allele was indicated by a ~1Kb band amplified by the gene specific primers. A ~0.5Kb band amplified by a

forward gene specific primer and T-DNA specific primer, described by Salk Institute Genomic Analysis Laboratory (SIGnAL; <https://www.salk.edu>) LBb1.3 (5'-ATTTTGCCGATTCGGAAC-3'), indicates the presence of mutant allele. Heterozygotes were identified by the presence of both alleles. Homozygous mutant plants confirmed by two independent PCR reactions were grown for eight weeks and seeds were harvested for use in further experiments. Disrupted E3 expression was confirmed using reverse-transcriptase (RT)-PCR.

Mutant: SALK line	F primer (5'-3')	R primer (5'-3')
SALK_149664	TCCGGAATCGGCTATCGTTG	CTATTAGCCGCCGAGACTCC
SALK_066923	ACAAGGGCTTGAATGTTCTGT	GACCGATCAAATGGTCCCCA
CS24734	CATGTGGGGCCAGAGAAA	CCCGTCTTCGACATAAGACCT
SALK_118406	CGCTATATACATCTATTTGCAGGTG	AGCAGCAGAGCGGAAAAATG
SALK_033142	TTATCAATGTGAAGCGGTGA	CCGAACATTAAGGGATCTTGT
SALK_141707	GGAACCGAAACAAGTCACCT	TGAGTTCCTTTCCAAACCGGA
SALK_086525	CAGCAATCTCAAACCTCGCCG	AGCTAATTGAGAAAGCGTGTGA
SALK_129778	TTGCCATAATCTCTAACCTTGTC	TGGAGAAGTGTGCGCTTCGTT
SALK_065995	ACATGTCCTATCTGTCGTGCT	TGCGGTCTACGGATTCTGAC
SALK_048470	GGTGACGTACTTCATTTGACG	GGAAGCTATAATCTGTTGCGA
SALK_023683	TGAATTGAGAAAGAGAGAGAGAGA	AGCATGCTTGCATACTTCTGT
CS863433	TCATTCAAGCATTCAACATGCCA	CGGGAAAAGGGAACAACGTC
SALK_023901	TCCGGAATCGGCTATCGTTG	CTATTAGCCGCCGAGACTCC
SALK_139444	ACAAGGGCTTGAATGTTCTGT	GACCGATCAAATGGTCCCCA
SALK_041291	TCCAATATCCCCAATCTTCCAC	CCGGAGAGAGCTTAACGTCC
SALK_201056	CGTTGTTTCGGATGCTGTGT	TCTGACTTCTTTTTCTGATGGGC
SALK_034258	GAGATGCTGGAGTTGACGTT	TACCATCTTAAGTGAGAAAGCAGA

Table 3. All E3-specific primer pairs used for PCR genotyping T-DNA insertion SALK-line mutants from ABRC (<https://abrc.osu.edu/>). Primers were created using NCBI (www.ncbi.nlm.nih.gov) primer blast tool to amplify a ~1Kb band flagging each T-DNA insertion site. Primer pairs were ordered from IDT (www.idtdna.com). To detect the presence of a T-DNA insertion the E3-specific F primers were used with the T-DNA specific primer designed by Salk Institute Genomic Analysis Laboratory (SIGnAL) LBb1.3 (5'-ATTTTGCCGATTCGGAAC-3').

RT-PCR analysis

RT-PCR was used to analyze gene transcript levels in homozygous mutant plants and WT. Total RNA was extracted from leaves using TRIzolTM (Invitrogen; <https://www.thermofisher.com>). Purity and concentration of RNAs were measured. cDNA synthesis was carried out using the iScriptTM gDNA Clear cDNA Synthesis Kit (Bio-Rad; <https://www.bio-rad.com>). Synthesized cDNA was then used in PCRs carried out using DreamTaq PCR Green Master Mix (Thermo Scientific; <https://www.thermofisher.com>) with gene specific primers designed using the NCBI online primer-BLAST tool (<https://www.ncbi.nlm.nih.gov/tools/primer-blast/>) (Table 4).

Gene	F primer (5'-3')	R primer (5'-3')
WAVH1	TAGAGTGCCGGTGGATTTGG	GCGATAACCGTTTCGAGCTG
ATL12	AGACGACCTCTCTGTGTTGG	TTCTCGCTCAAGCAACAACG
ARI11	GAAATGGCAATCGGTGGAGC	GCTTGTTGCGCTCTTGACTA
ERiN1	TGCATTTTTCCGCTCTGCTG	AACTGGCAGCTCGGAGTAAG
ARI12	AATGGCATCCTATCCAGGGG	TACACTTGGGACAAGGCACC
DEP	CCAAGGCTCCAAGATCCCAA	GTGCTGTTCTCCAACAAGC
ERiN2	TTCCGGCCTCTACGTCATC	GCAATGTGCCGATACTTGGT
ERiN3	GCTTCTTTCATCAGCTCCTCG	GTTCTGGAGAAGTGTCGCT
ACT1	ACGGATGCGCTGATGAAGAT	TCACTTGCCCATCAGGTAGC
IRT1	TCTCTCCAGCAACTTCAACTG	CCGGAGGCCGAAACACTTAAT
AtFER1	GAAAAGAGAAGCTTACTTGATTTGC	TCCAGGAAAGTTGGCGGC
AtIPS1	GGCTGATTCAGACTGCGAGTT	CACACAAAGAACACACAACGC
PHO2	AGCGACGATTGTGTCTGCAT	GTTGTGAAGGCTGTCAATGCT
NRT1.7	AGGCACTTTCACGGTCTCTC	TCGCGAAAACGATCCCTGTT
NLA	GTCTAGGCAAGGACAAGCGT	CGAAAGTCAAAGCGCAACCA
TCP20	CCCTACCTTGAGCTTGAGCC	GGGTTTCTGGTTTTGATTTTCTT
NLP6	CGATGGAAGCTGTATGGGGA	ATGGGTAGTCGGTTTTGCAG
NLP7	TTGCCTCTCGCTCAGACTTG	CCTGGCCTTCTGGAGATGG
BAK1	ATCATCATTGCGAGGCGAG	TGGACTIONGCAAACTCATGGAC
BSK2	TGCTTCTCATGTCTTAATGGGCT	TCCTGCACTTGTTGTGTCCA
BSK3	TCTCCAACAGTGTGTGCTCG	TTCGAGCCCTCTTTCAGTGC
NRT1.1	AGTCGCACAATCCGAGACAT	CCGAAGAAAAGCCCCAAACC

Table 4. All gene-specific primer pairs used in RT-PCR. Each primer pair was created using NCBI (www.ncbi.nlm.nih.gov) primer blast tool to amplify a ~200bp portion of the gene exon. Primer pairs were ordered from IDT (www.idtdna.com).

Stress assays – phenotypic analysis

Seeds harvested from homozygous mutants for all eight mutant lines were sterilized and stratified to initiate germination, then were grown on ½ MS media for five days under continuous light. Seedlings were then transferred to different nutrient treatment media in a sterile laminar flow station. All instruments and surfaces used for seedling transfer were sterilized with 50% bleach and 75% ethanol, then further sterilized under ultraviolet (UV) light. Seedlings were grown for 10 days on nutrient treatments: control, excess iron (++Fe), deficient iron (-Fe), excess phosphorus (++P), phosphorus deficient (-P), excess nitrogen (++N), and nitrogen deficient (-N). After 10 days photos were taken of seedlings and fresh weight was measured. Fresh weight was determined through weighing groups of seedlings. Root length was measured through analysis of the photos using ImageJ® image analysis software (<http://imagej.net>). Stress assays were repeated for mutant lines which showed differential growth under one or more nutrient stresses. RT-PCR was then used to determine any changes in E3 expression in WT plants when exposed to the nutrient stress under which the mutant for that E3 showed differential growth, and three E3s of interest were selected for further analysis. Results for all eight mutant lines can be viewed in APPENDIX B.

Root gravitropism assays

Five-day-old seedlings were transferred from ½ MS media to +, -N, and -P treatments. Seedlings were grown for three days before rotating 90°. After three days images were captured and analyzed using ImageJ® image analysis software (<http://imagej.net>) to determine the angle of bending of the primary root.

Lugol's staining

Roots of seedlings grown for 10 days on N sufficient media (control, +N) and -N media were submerged in Lugol's iodine staining reagent (Sigma; <https://www.sigmaaldrich.com>) for 30 seconds then rinsed with ddH₂O. Stained roots were then mounted on slides using 50% glycerol and analyzed under a microscope at 100X to view starch levels at the root tip to view starch accumulation.

Hormone treatments

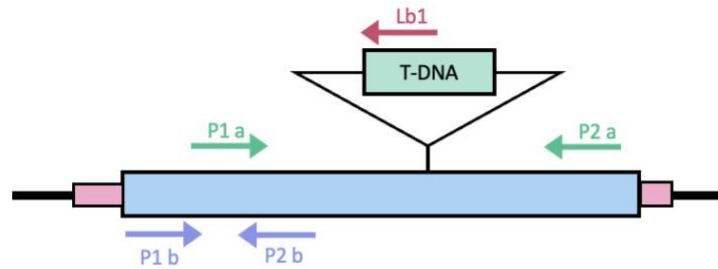
WT and *wavh1-1* seedlings were grown on N sufficient media (control, +N) media for five days and then transferred to media of different N availabilities (+N, and -N) containing 0nm, 0.1nm, or 1nm epibrassinolide brassinosteroids (BL) (Sigma-Aldrich; <https://www.sigmaaldrich.com>) or 1μM brassinazole (BRZ), a brassinosteroid biosynthesis inhibitor (Sigma-Aldrich; <https://www.sigmaaldrich.com>). LR emergence and length, and PR length was assessed.

RESULTS

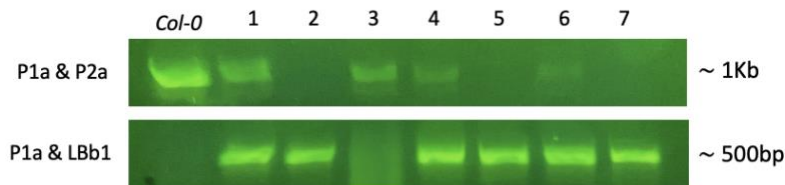
Finding homozygous wavh1-1 knock-down mutants

SALK_149664 and SALK_018439 seeds were obtained from ABRC, harbouring a T-DNA insertion in the WAVH1 gene (Figure 1, Figure S1). Homozygosity of *wavh1-1* and one *wavh1-2* individuals were found using PCR genotyping. Lower expression of *WAVH1* was confirmed in *wavh1-1a* (plant #2, Figure 1) and *wavh1-2a* (plant #4, Figure S1) using qualitative RT-PCR analysis. Seeds were harvested from all homozygous individuals, and progeny of *wavh1-1a* were used for further experiments.

WAVH1 (At2g22680) T-DNA insertion mutant SALK_149664C (*wavh1-1*)



Confirming homozygosity of individual *wavh1-1* plants



Plant 2 (*wavh1-1a*) – confirmed *wavh1-1* homozygote

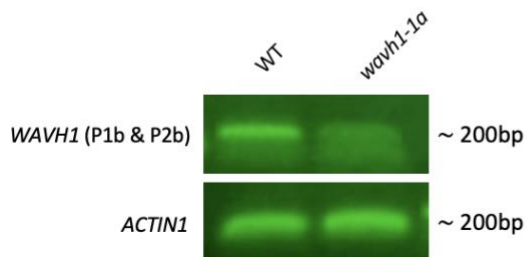


Figure 1. Schematics of *WAVH1* gene with location of T-DNA insertion (SALK_149664) and primer pairs used for PCR genotyping (P1a and P2a) and RT-PCR (P2b and P2b). PCR genotyping visualized using gel electrophoresis. Plant 2, 5, and 7 determined to be homozygous *wavh1-1*. Qualitative RT-PCR was used to confirm lower *WAVH1* expression in *wavh1-1a* (plant 2).

Increased root sensitivity of wavh1-1, and differential expression of WAVH1 in WT, under N and P deficiency

WT and *wavh1-1* seeds were grown on ½ MS media, and five-day old seedlings were transferred to different treatments (control (+), phosphorus deficiency (-P), excess phosphorus (++P), nitrogen deficiency (-N), and excess nitrogen (++N)) for ten days (Figure 2). *WAVH1* loss-of-function mutants showed no significant difference compared to WT on control. Under -P, ++P, and -N conditions, *wavh1-1* plants exhibited significantly shorter primary roots compared to WT (Figure 2A). Also, no significant differences were observed in *wavh1-1* biomass across all treatments compared to WT (Figure 2A). The significant difference in PR length of *WAVH1* loss-of-function mutants under -P and -N was confirmed using a second mutant line, *wavh1-2* (Figure S3).

WAVH1 expression in WT was analyzed to confirm its involvement in P and/or N stress response. Expression of *WAVH1* in WT was examined across all five nutrient treatments using RT-PCR analysis. *WAVH1* transcript levels decrease under -P (Figure 2C) and -N (Figure 2C).

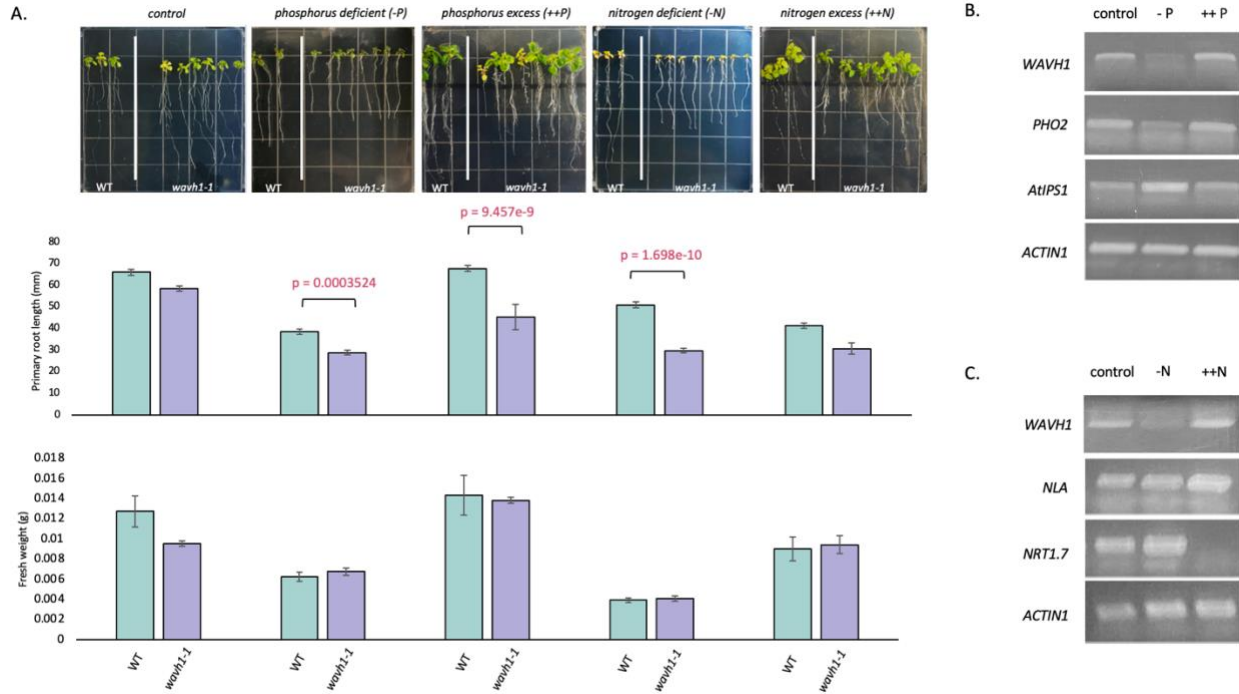


Figure 2. (A) 15-day old *wavh1-1* seedlings exhibit significantly increased root sensitivity compared to WT under phosphorus deficiency (-P) and nitrogen deficiency (-N). Seedlings were grown for five days on nutrient sufficient media then transferred to -P, ++P, -N, and ++N media for 10 days. Graphs show primary root length and fresh weight. Error bars indicate \pm SE from at least three trials with at least three replicates per trial ($n \geq 65$). **(B)** RT-PCR showing *WAVH1* transcript levels in WT seedlings exposed to control, -P, and ++P for 10 days. P-responsive *PHO2* and *AtIPS1* were used as positive controls. *ACTIN1* was used as a loading control. **(C)** RT-PCR showing *WAVH1* transcript levels in WT seedlings exposed to control, -N, and ++N for 10 days. N-responsive *NLA* and *NRT1.7* were used as positive controls. *ACTIN1* was used as a loading control. All segments of cDNA amplified are \approx 200bp.

Under nitrogen deficiency, wavh1-1 exhibits impaired root gravitropic response

The gravitropic abilities of *WAVH1* loss-of-function mutants were analyzed because the WAV3 family of E3s are known to play significant roles in regulating gravitropic responses in Arabidopsis (Mochizuki et al., 2005; Sakai et al., 2011). We measured root reflex angle of *wavh1-1* and WT seedlings in response to a 90° rotation under nutrient sufficient, P deficient, and N deficient conditions. There was no significant difference in root gravitropic abilities of *wavh1-1* and WT

seedlings under nutrient sufficient conditions (Figure 3). Under severe N limitation, *wavh1-1* exhibited a significantly higher root reflex angle compared to WT following a 90° rotation, indicating that *WAVHI* loss-of-function mutants have a significantly impaired root gravitropic response (Figure 3). Gravitropic abilities were unaffected by P deficiency as there were no significant differences between *wavh1-1* and WT under -P conditions.

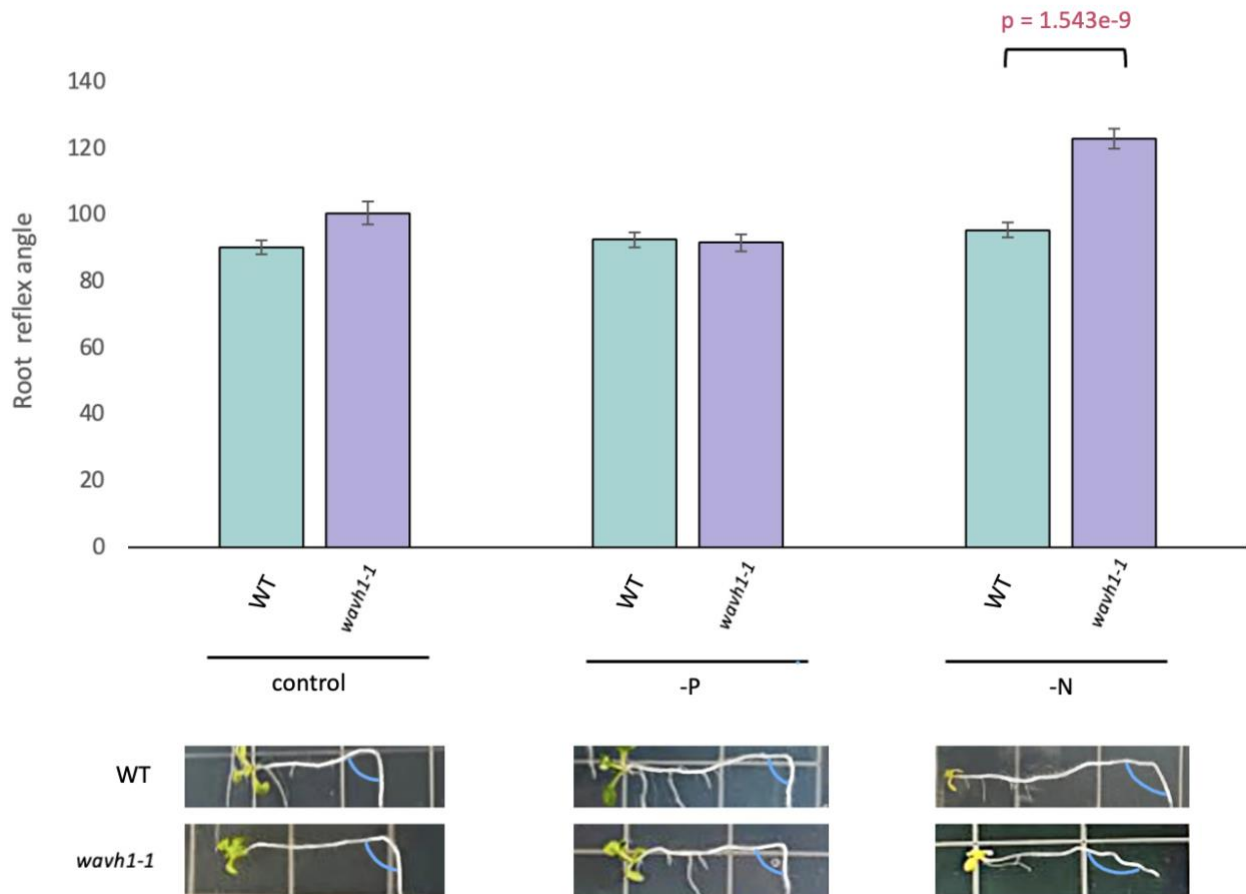


Figure 3. WT and *wavh1-1* seedlings were grown for five days on nutrient sufficient media, then transferred to control, -P, or -N. After growing for three days the media plates were tilted 90° and seedlings grew for another three days. Root reflex angles were measured using ImageJ® (<http://imagej.net>). *wavh1-1* displayed significantly larger angles of root curvature compared to WT. Below the graph are representative photos of WT and *wavh1-1* under each nutrient treatment three days after tilting 90°. *WAVHI* mutants display a much more obtuse angle of descent following tilting. Analysis was done using One-Way ANOVA Tukey comparison. Error bars indicate \pm SE from two trials with at least three replicates per trial ($n \geq 24$).

Lugol's staining was used to visualize starch granule accumulation in *wavh1-1* root tips under N limitation after a 90° turn, as starch levels and accumulation patterns could provide insight as to why *WAVHI* loss-of-function mutants exhibit an impaired gravitropic response under N deficient conditions. Root tips were viewed at 100X. Results showed that there was no significant difference in starch levels, although it did reveal a level of starch accumulation in the separating layer of root cap cells in *wavh1-1* not seen in WT (Figure 4). This starch accumulation in *wavh1-1* is observed under N sufficient and deficient conditions, and there does seem to be a slightly higher level of cell disorganization in the root tips of the *WAVHI* mutants under N sufficient conditions.

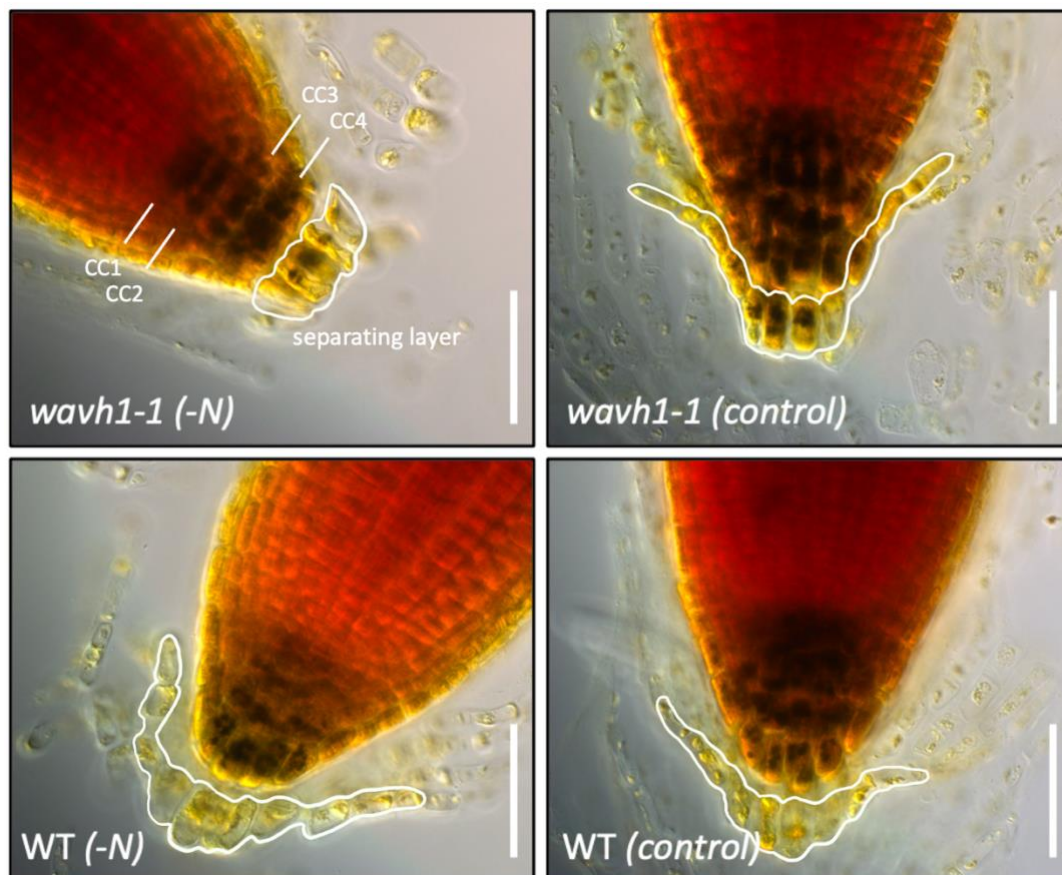


Figure 4. Lugol's staining assay used to visualize starch levels in the columella cells (CC) of WT and *wavh1-1* seedlings that were grown on nitrogen (N) sufficiency (control) for five days then

transferred to control or N deficiency (-N) for one week. Seedlings were turned 90° on day three of the treatment period. Root tips were submerged in Lugol's iodine stain for 30 seconds and then rinsed with ddH₂O. Images were captured at 100X. Scale bar = 50µm. The CC layers from CC1 to CC4 are indicated.

NRT1.1, TCP20, NLP6, and BSK2 are differently expressed in wavh1-1

To further investigate the role of WAVH1 in the N deficiency response, transcript levels of multiple N limitation responsive genes were analyzed using RT-PCR. *NRT1.1*, *TCP20*, and *NLP6* levels are significantly lower in the *WAVH1* loss-of-function mutants compared to WT under N deficiency. These genes were selected for analysis because they are known to regulate root growth in response to N deficiency. *BSK2* is significantly lower in *wavh1-1* under N sufficient conditions compared to WT. *BSK2* was selected for analysis because it is known to interact with WAVH1, and it is homologous to *BSK3*, which is known to play a role in plant response to N limitation.

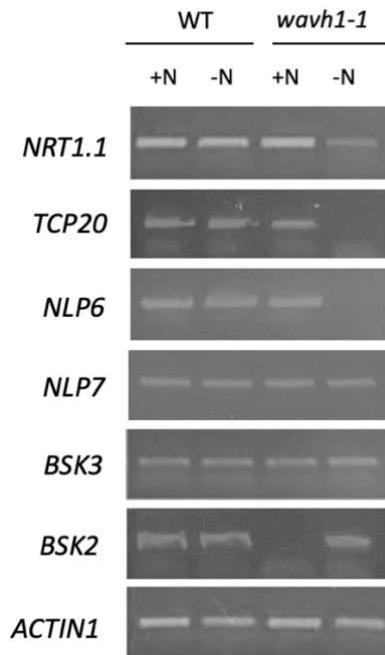


Figure 5. RT-PCR analysis showing transcript levels of *NRT1.1*, *TCP20*, *NLP6*, *NLP7*, *BSK3*, *BSK2*, and *ACTIN1* in WT and *wavh1-1* plants exposed to N sufficiency (control, +N) or N deficiency (-N).

Gel electrophoresis was used to visualize expression levels. All segments of cDNA amplified are ≈200bp.

Loss of WAVH1 function negatively impacts lateral root emergence under severe N limitation

RSA manipulation is a significant part of the N deficiency response in Arabidopsis, therefore, to further analyze the role of WAVH1 in the N deficiency response we analyzed *wavh1-1* root growth more in depth. Analysis of lateral roots under nitrogen sufficiency and deficiency shows that *wavh1-1* plants exhibit a significantly lower level of lateral root (LR) emergence than WT under control and -N (Figure 6A and D), while maintaining a similar average LR length (Figure 6B). When comparing LR emergence between N sufficient (control) and deficient conditions, *wavh1-1* exhibits a higher percent decrease in LR emergence compared to WT. Analysis of LR number per cm of primary root (PR) reveals no significant difference between WT and *wavh1-1* (Figure 6C).

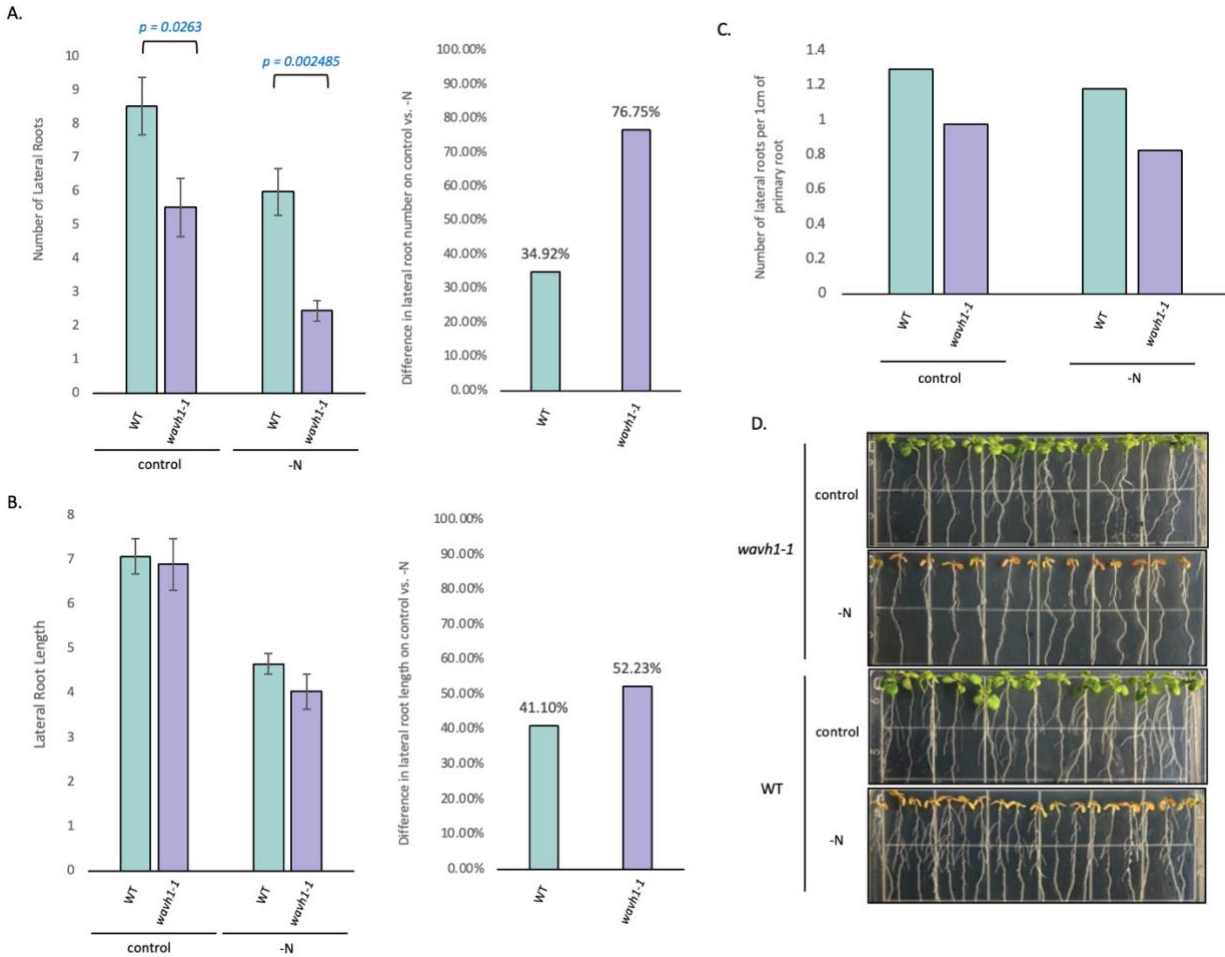


Figure 6. (A) Analysis of lateral root (LR) number on WT and *wavh1-1* seedlings that were grown for five days on N sufficient media (control) then transferred to control or N deficient media (-N) for 10 days. *WAVH1* mutants demonstrated a significantly higher percent decrease in LR emergence when exposed to -N than WT. Analysis was done using One-Way ANOVA Tukey comparison. Error bars indicate \pm SE from three trials with at least three replicates per trial ($n \geq 50$). **(B)** Analysis LR length on WT and *wavh1-1* seedlings that were grown for five days on control then transferred to control or -N media for 10 days. Roots were measured using ImageJ® (<http://imagej.net>). There was no significant difference in LR length. Analysis was done using One-Way ANOVA Tukey comparison. Error bars indicate \pm SE from two trials with at least three replicates per trial ($n \geq 25$). **(C)** Further analysis of LR number done factoring in average primary root (PR) length, which is significantly shorter in *wavh1-1*. Done to confirm that difference in LR emergence was not simply because of shorter PRs. **(D)** WT and *wavh1-1* seedlings that were grown on control media for five days then transferred to control or -N for then days. Images were captured at the end of the 10-day treatment period.

Impact of excess brassinosteroids and brassinosteroid biosynthesis inhibition on *wavh1-1* root growth under severe N limitation

Brassinosteroids play a key role in regulating the changes to RSA under N deficient conditions, and so to further investigate the role of WAVH1 in root growth under N limitation the effect of excess BL and BRZ on root growth was analyzed. On nutrient sufficient media, the addition of 0.1nm BL slightly but insignificantly decreases the primary root length of WT ($p = 0.05867$) and *wavh1-1* ($p = 0.9912$). The addition of 1nm BL significantly decreases primary root growth in WT ($p = 1.346e-11$) and *wavh1-1* ($p = 1.472e-11$) to a similar degree. Under severe N limitation, the addition of 0.1nm and 1nm BL had no effect on primary root length of WT or *wavh1-1* seedlings, and the significant difference between primary root length of WT and *wavh1-1* shown on -N was maintained throughout all N deficient treatments (Figure 7).

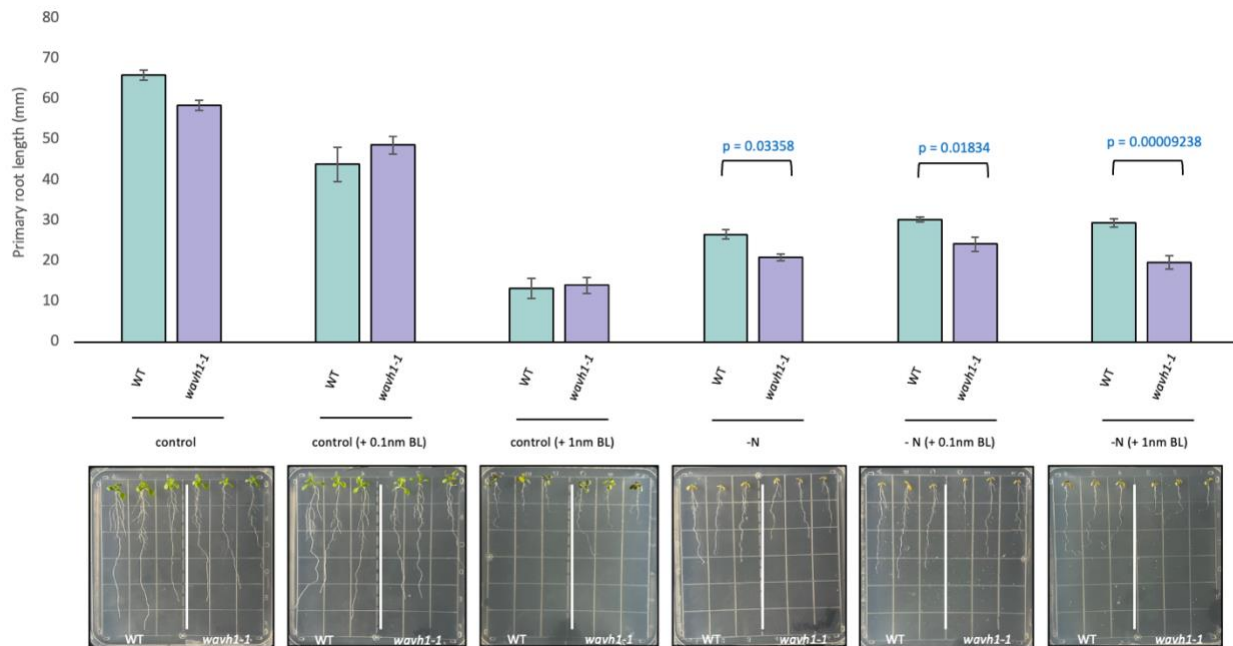


Figure 7. Analysis of primary root (PR) growth under varying levels of epibrassinolide brassinosteroids (BL) exposure, under N sufficiency (control) and deficiency (-N). Seedlings were growth on control for five days then transferred to treatments and grown for one week. Roots were measured using ImageJ® (<http://imagej.net>). Analysis was done using One-Way ANOVA

Tukey comparison. Error bars indicate \pm SE from two trials with at least three replicates per trial ($n \geq 18$).

The addition of 1nm of BL has a severe impact on the PR growth path under severe N deficiency. Although there was no significant difference calculated between WT and *wavh1-1*, *wavh1-1* has a less predictable PR growth pattern, with PR length divided by distance travelled exhibiting a larger range than WT. *WAVHI* loss-of-function mutants also seemed to demonstrate more impaired root gravitropic abilities than WT when treated with 1nm BL, with the PR of multiple *WAVHI* mutants starting to grow upwards or forming loops.

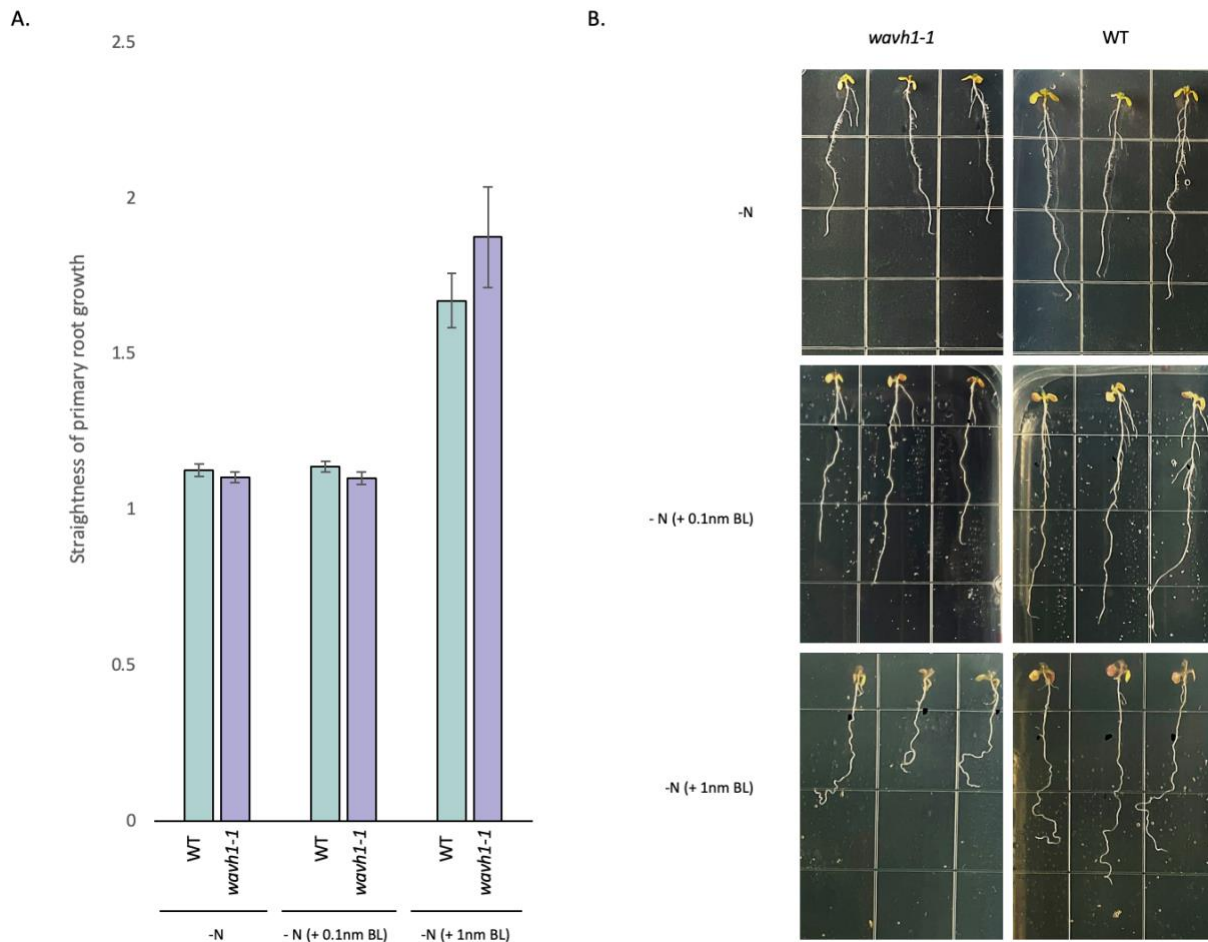


Figure 8. (A) Analysis of straightness of primary root (PR) growth by dividing PR length by the length of a straight line from the root tip to the start of the root. Roots were measured using

ImageJ® (<http://imagej.net>). Analysis was done using One-Way ANOVA Tukey comparison. Error bars indicate \pm SE from two trials with at least three replicates per trial ($n \geq 18$). **(B)** Images of seedling growth under varying levels of epibrassinolide brassinosteroids (BL) exposure, under severe nitrogen deficiency (-N). Seedlings were growth on control for five days then transferred to -N and grown for one week.

The addition of brassinosteroid inhibitor brassinazole (BRZ) causes a significant decrease in primary root length in WT and *wavh1-1* under both N sufficient (control) and N deficient conditions (Figure 9). Under severe N limitation, the presence of BRZ removes the significant difference in primary root length between WT and *wavh1-1* seen under severe N limitation without BRZ (Figure 9B). Under nutrient sufficiency the presence of BRZ inhibits LR emergence to a similar degree in WT and *wavh1-1* (Figure 9C). Under N deficiency WT exhibits a significant decrease in LR emergence in response to BRZ ($p = 0.000007$). BRZ showed no significant impact on LR emergence in *wavh1-1* ($p = 0.6341$). The addition of BRZ under severe N deficiency also seems to reduce the significant difference in LR emergence observed between *wavh1-1* and WT under severe N deficiency in the absence of BRZ (Figure 9C).

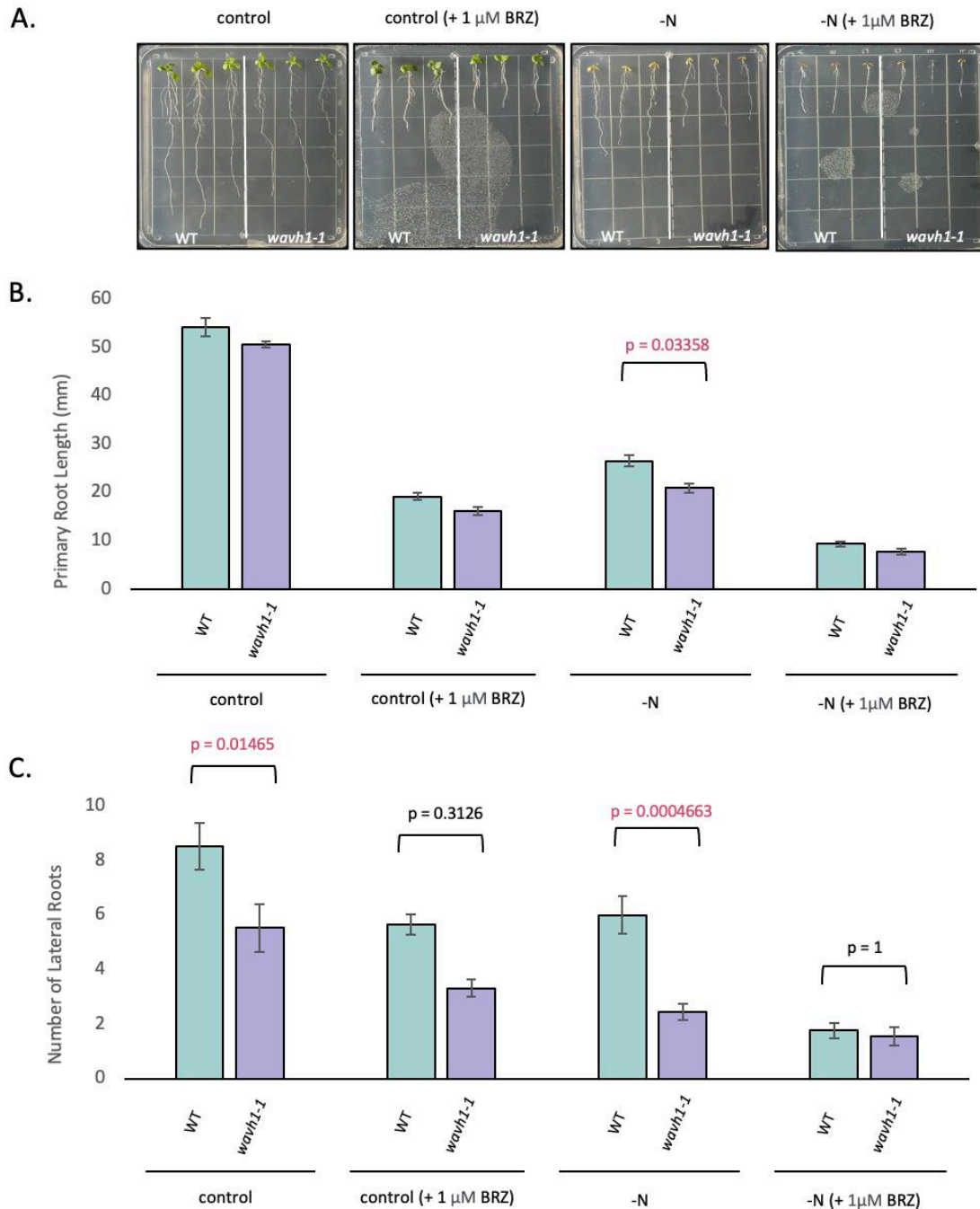


Figure 9. (A) Seedlings that were grown on nitrogen sufficient media (control) for five days then were exposed to different nitrogen (N) and brassinazole (BRZ) levels for one week. **(B)** Analysis of primary root (PR) length of WT and *wavh1-1* grown under different levels of N and BRZ. Analysis was done using One-Way ANOVA Tukey comparison. Error bars indicate \pm SE from two trials with at least three replicates per trial ($n \geq 18$). Roots were measured using ImageJ® (<http://imagej.net>). **(C)** Analysis of lateral root (LR) emergence of WT and *wavh1-1* grown under different levels of N and BRZ. Analysis was done using One-Way ANOVA Tukey comparison. Error bars indicate \pm SE from two trials with at least three replicates per trial ($n \geq 18$).

BRZ has no significant effect on the root gravitropic abilities of WT or *wavh1-1* under nutrient sufficiency (Figure 10). However, BRZ was found to increase the root reflex angle of *wavh1-1* seedlings under severe N limitation (Figure 10). In fact, in the presence of BRZ, the root reflex angle of *wavh1-1* was not significantly different from WT.

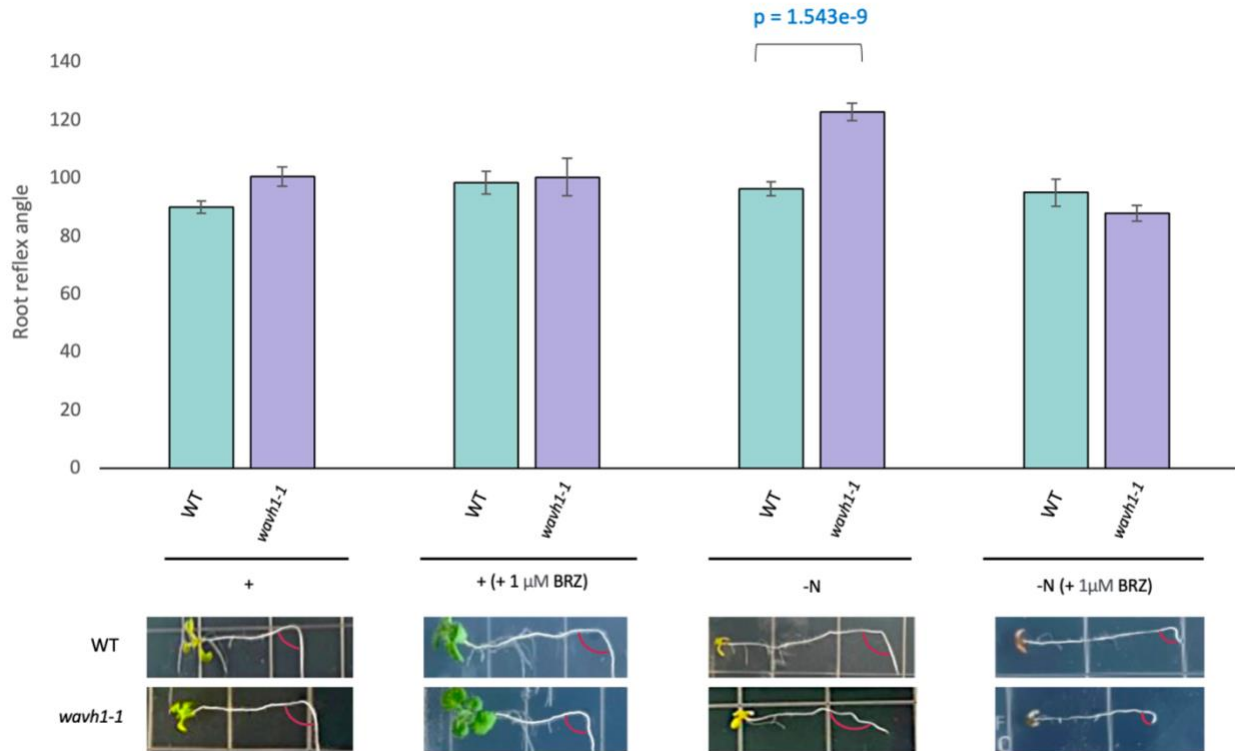


Figure 10. WT and *wavh1-1* grown on nitrogen sufficient media (control) for five days then were transferred to media of different nitrogen (N) and brassinazole (BRZ) levels for six days. Seedlings grew for three days then were turned 90° and grew for another three days. Images were captured at the end of the six day treatment period. Root reflex angles were measured using ImageJ® (<http://imagej.net>). Analysis was done using One-Way ANOVA Tukey comparison. Error bars indicate \pm SE from at least two trials with at least three replicates per trial ($n \geq 18$).

DISCUSSION

The WAV3 family of ubiquitin ligases contains 3 WAV3 homologs; WAVH1, WAVH2, and EMBRYO DEVELOPMENT ARREST 40 (EDA40). Not much is known of the specific functions of these E3s, but studies show that they play significant roles in controlling root growth patterns in Arabidopsis, specifically influencing gravitropic responses (Mochizuki et al., 2005; Sakai et al., 2011). A study conducted by Sakai et al., (2011) demonstrates that the WAV3 family of E3s control gravitropism likely via regulating auxin signalling/transport. Research has established WAVH1 as a protein that induces a weak gravitropic response compared to its homologs WAV3 and WAVH2, which induce moderate and strong responses, respectively (Mochizuki et al., 2005; Sakai et al., 2011). However, our results suggest that WAVH1 is heavily involved in regulating root growth patterns under N limitation, with *WAVH1* loss-of-function mutants demonstrating severely impaired gravitropic abilities, lower LR emergence, and shorter PR length under severe N limitation. The hypersensitivity of *wavh1-1* to severe N deficiency suggests that WAVH1 is a positive regulator of root growth under N limitation. *WAVH1* expression in WT goes down under N limitation, suggesting that a substrate of WAVH1 accumulates as part of the N limitation response. Also, *WAVH1* is expressed under sufficient and excess N levels, which suggests that the E3 may play a role in the attenuation of the N limitation response to maintain N homeostasis.

The crosstalk between brassinosteroid (BR) and auxin signalling is vital to RSA modulation in response to N limitation. Results indicate that WAVH1 does play a role in BR signalling and/or BR biosynthesis under N limitation. *wavh1-1* exhibited significantly shorter PR length and lower LR emergence when exposed to severe N limitation compared to WT, and the

addition of the BR biosynthesis inhibitor BRZ alleviates these significant differences. This suggests that the *WAVH1* mutants exhibit impaired root growth due to an abnormality in the BR signalling pathway. It is possible WT PR and LR growth is impacted more significantly by the addition of BRZ because BR biosynthesis or signalling is already being inhibited to an unknown extent when *WAVH1* transcription is disrupted. Mild N limitation activates a foraging strategy, upregulating BAK1 and promoting BR-induced auxin transport in roots, stimulating root cell division to enhance PR elongation and LR emergence (Devi et al., 2022; Jia et al., 2019; Jia et al., 2020; Perrot-Rechenmann, 2010). BRs regulate this process through the activity of multiple signalling proteins, including a protein complex that involves the leucine-rich repeat receptor-like protein kinase (LRR-RLK) BRI1 interacting with BAK1 to modulate BR signalling in Arabidopsis (Li et al., 2002; Mao and Li, 2020). This process is dependent on BSK3 (Jia et al., 2019; Jia et al., 2020).

Studies suggest BSK3 mediates BR signalling downstream of BR receptors under N deficiency, with results showing *BSK3* loss-of-function mutants demonstrate impaired BR responses under N limitation (Ren et al., 2019). Previous research demonstrates that *WAVH1* interacts with BSK2, a BR signalling kinase homologous to BSK3 (Arabidopsis Interactome Mapping Consortium). Not much is known about BSK2, however, it is a substrate of BRI1, and is known to mediate signal transduction from BRI1 (Tang et al., 2009). Our results show that *BSK2* is expressed under N sufficiency and deficiency in WT, but *wavh1-1* only expresses *BSK2* under N deficiency. This suggests that *WAVH1* may not only interact with BSK2, but it may also be involved in the regulation of *BSK2*. Under sufficient and deficient N levels *wavh1-1* shows significantly lower LR emergence, with a significantly higher percent decrease in LR emergence from sufficiency to deficiency than WT. It is possible that *WAVH1* targets a regulator of *BSK2* to

regulate the BR-mediated process of directing auxin to the LR primordium to promote emergence under N sufficient conditions, leading to the significantly lower LR count in *wavh1-1* under N sufficiency. It is also possible that *BSK2* is promoted by another regulator to promote the shootward transport of auxin, which limits LR emergence under N limitation. This would explain why *BSK2* is still expressed in *wavh1-1* under N limitation. Of course, further exploration into the WAVH1 and BSK2 interaction as well as how WAVH1 influences *BSK2* transcript levels is necessary to draw any conclusions. Furthermore, the same study that determined an interaction between WAVH1 and BSK2 determined an interaction between BSK2 and COPPER AMINE OXIDASE ZETA (CuAOZ), a protein involved in LR emergence (Arabidopsis Interactome Mapping Consortium; Qu et al., 2017). This further links BSK2 to LR emergence, presenting another interesting interaction to explore in the future.

The lower LR emergence in *wavh1-1* under sufficient N levels likely impacts the acquisition of other nutrients as well, which could contribute to the decreased stress tolerance. *WAVH1* mutants also expressed lower levels of the N limitation responsive gene *TEOSINTE BRANCHEDI/CYCLOIDEA/PROLIFERATING CELL FACTOR 1-20 (TCP20)*, which plays a role in controlling PR growth under severe N limitation (Guan et al., 2014). TCP20 interacts with NIN-LIKE PROTEIN 6 and 7 (NLP6/7) under N sufficient and deficient conditions, and *NLP6* levels were also lower in *wavh1-1*. The TCP20/NLP6 interaction is required for the expression of the Cell-Cycle Progression Gene (CYCB1;1) and is suggested to control the expression of *NRT1.1* (Guan et al., 2017; Konishi and Yanagisawa, 2019). And so, the lower levels of *TCP20* and *NLP6* may explain the lower levels of *NRT1.1* expressed in *wavh1-1* (Guan et al., 2014).

NRT1.1 is a NO₃⁻ transporter and sensor that is an established regulator of N homeostasis and demonstrates the ability to modulate auxin transport. Under mild N deficiency it promotes

auxin transport to LR primordium to promote LR emergence and under severe N limitation it promotes shootward auxin transport to inhibit LR emergence (Krouk et al., 2010; Giehl and Wirén, 2014; Mounier et al., 2014; Jian et al., 2018; Chai et al., 2022; Liu and Wirén, 2022). *NRT1.1* is upregulated by BRASSINAZOLE-RESISTANT 2/ BRI1 EMS SUPPRESSOR 1 (BZR2/BES1), a positive regulator of the BR signalling pathway, under N sufficient and deficient conditions (Chai et al., 2022). BZR2 mediates downstream BR responses like its homolog BZR1, which also mediates negative feedback regulation of BR biosynthesis (Yin et al. 2002; Sun et al., 2010). It is possible that the lower levels of *NRT1.1* expressed in *wavh1-1* interferes with N level these abilities, impacting root growth under severe N limitation.

Our results also show that the gravitropic response of *wavh1-1* is impacted under severe N limitation, with *wavh1-1* exhibiting a significantly higher root reflex angle in response to a 90° turn under N limitation. The activity of amyloplasts, the starch-accumulating plastids which move according to the direction of gravity in the differentiated columella cells (CCs) at the root tip, was analyzed using Lugol's staining (Blancaflor et al., 1998; Nakamura et al., 2019; Zluhan-Martínez et al., 2021). The movements of these amyloplasts trigger directional auxin transport from the CCs to promote differential cellular elongation of upper and lower flanks of the root elongation zone (EZ), facilitating the physical turning of the root tip in response to the gravitational shift (Nakamura et al., 2019; Su et al., 2020). Under N limitation Lugol's staining showed no difference in amyloplast activity between *wavh1-1* and WT, suggesting that the lower gravitropic response under N limitation may be caused by impaired cellular elongation or directional auxin transport in response to the gravitational shift. A previous study confirmed that WAVH1 interacts with the ribosome assembly factor ARABIDOPSIS ADENYLATE KINASE 6 (AAK6) (Arabidopsis Interactome Mapping Consortium), a protein required for cell generation and elongation (Slovak

et al., 2020). Not enough is known about AAK6 to draw any conclusions about its interaction with WAVH1, however, it would be interesting if future studies investigated this interaction and root gravitropism under N limitation. It is also possible that directional auxin transport is impacted in *wavh1-1*, this is supported by our previous results which suggest WAVH1 is involved in BR signalling, a process which influences auxin transport. Furthermore, when treated with 1 μ M of BRZ, the gravitropic abilities seem to be restored, with no significant difference between WT and *wavh1-1* root reflex angles under N sufficiency or limitation. Further exploration of these processes and WAVH1 is needed to determine the exact role of WAVH1 in the gravitropic response of roots under N limitation.

Another interesting observation in *wavh1-1* plants is the starch accumulated in the separating layer of CCs at the root tip. The starch accumulation in the separating layer of CCs is present in *wavh1-1* under sufficient and deficient N levels, so it is unlikely that this affects the gravitropic response. It is possible that this phenotype is a result of the loss of *WAVH1* function, but no conclusions can be drawn strictly from this information.

The role of WAVH1 is still unclear, however, our results indicate that WAVH1 does somehow influence LR emergence via BR signalling and auxin transport (Figure 11). It is also possible that its involvement in BR-signalling affects PR growth under severe P and N deficiency. Inhibition of BR biosynthesis alleviates the significant difference in PR length and LR emergence between WT and *wavh1-1* under severe N deficiency, further suggesting that WAVH1 is involved in regulating BR signalling when N levels are low.

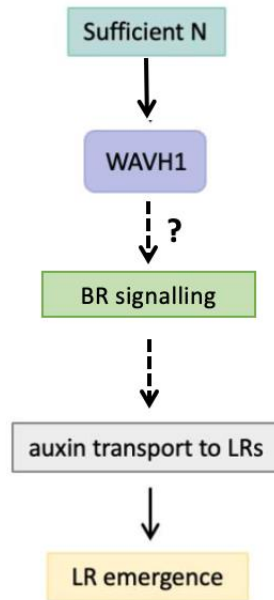
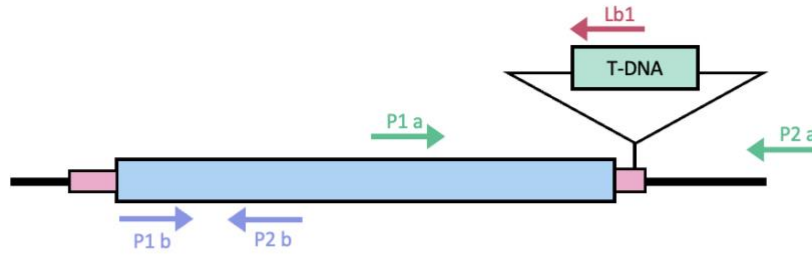


Figure 11. Simplified representation of how the WAVH1 might influence LR emergence in WT. In this model, WAVH1 targets a regulator of BR signalling, promoting LR emergence under nitrogen (N) sufficient conditions. In *WAVH1* loss-of-function mutants this interaction would be inhibited causing lower LR emergence.

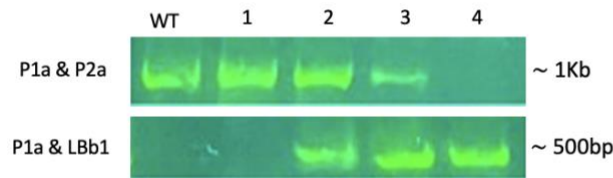
Further research is required to confirm these theories and to determine what specific ways WAVH1 is involved in the interplay between auxin transport and BR signalling that impacts RSA under severe N deficiency. Furthermore, additional work must be done to determine the exact function of WAVH1 in the root gravitropic response under severe N limitation. As a RING-type E3, discovering potential substrates of WAVH1 and whether the substrate is ubiquitinated and targeted for proteasomal degradation is vital to understanding the role of WAVH1 in N stress response. This study will serve to aid future studies that investigate the role of WAVH1 as well as BR signalling in the N deficiency response.

SUPPLEMENTARY MATERIAL

WAVH1 (At2g22680) T-DNA insertion mutant *SALK_018439C* (*wavh1-2*)



Confirming homozygosity of individual *wavh1-2* plants



Plant 4 (*wavh1-2a*) – confirmed *wavh1-2* homozygote

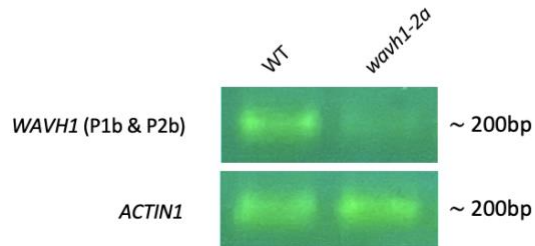


Figure S1. Schematics of *WAVH1* gene with location of T-DNA insertion (*SALK_018439*) and primer pairs used for PCR genotyping (P1a and P2a) and RT-PCR (P2b and P2b). PCR genotyping visualized using gel electrophoresis. Plant 4 was determined to be homozygous *wavh1-2*. Qualitative RT-PCR was used to confirm lower *WAVH1* expression in *wavh1-2a* (plant 4).

WAVH1 (At2g22680) T-DNA insertion mutant SALK_149664C

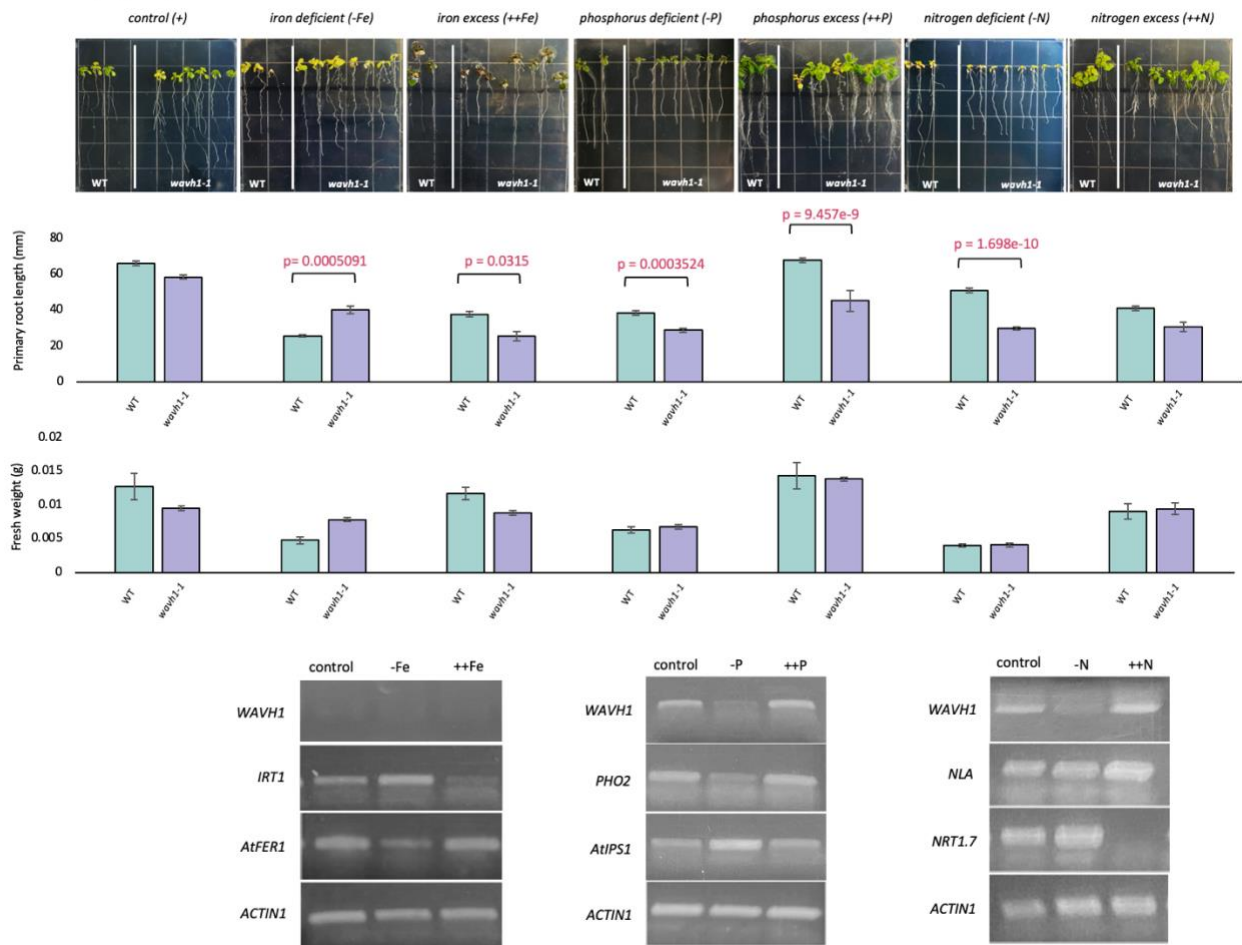


Figure S2. 15-day old *wavh1-1* and wild type (WT, *Col-0*) seedlings that were grown for five days on nutrient sufficient (control, +) media then 10 days on +, Fe deficient (-Fe), Fe excess (++Fe), P deficient (-P), P excess (++P), N deficient (-N), and N excess (++N) media. Primary root lengths and fresh weight were measured at the end of the 10-day treatment period using ImageJ® (<http://imagej.net>). Analysis was done using One-Way ANOVA Tukey comparison. Error bars indicate \pm SE from at least one trial with at least three replicates per trial (≥ 24). *WAVH1* mutants showed a differential phenotype under -Fe, ++Fe, -P, ++P, and -N. *WAVH1* expression under Fe, P, and N stresses were analyzed. cDNA was synthesized from RNA extracted from WT seedlings that were grown on control for five days then for 10 days on +, -P, ++P, -N, and ++N; all segments of cDNA amplified are ≈ 200 bp.

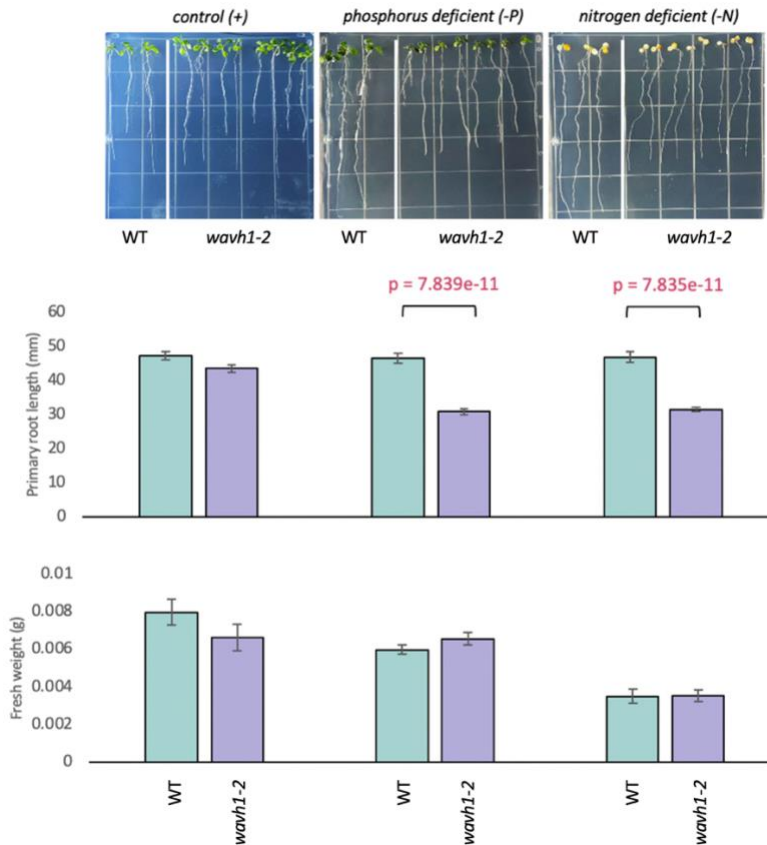


Figure S3. 12-day old *wavh1-2* plants exhibit significantly increased root sensitivity compared to wild type (WT, *Col-0*) under phosphorus deficiency (-P) and nitrogen deficiency (-N). Plants were grown for five days on nutrient sufficient $\frac{1}{2}$ MS media then transferred to -P and -N media for one week. Fresh weight was measured, and primary root lengths were measured using ImageJ® (<http://imagej.net>) to confirm previous results. Analysis was done using One-Way ANOVA Tukey comparison. Error bars indicate \pm SE from one trial with four biological replicates ($n \geq 30$).

Electrolyte leakage

Electrolyte leakage assays were performed as previously described by Dionisio-Sese and Tobita (1998). Five-day-old WT seedlings and seedlings from mutant lines of interest were transferred to +, -P, or -N conditions. After exposure to stress for four, six, and 10 days, seedlings were used to collect 100mg of fresh leaf tissue. Shoot samples were thoroughly rinsed then submerged in 10mL of ddH₂O and incubated for 2h at 32°C. Initial electrical conductivity (EC₁) was measured using an electrical conductivity meter (HACH Pocket Pro Conductivity meter; <https://www.hach.com>).

Then, to release all electrolytes, the samples were autoclaved at 121°C for 20min. Samples were then cooled to 25°C, and final electrical conductivity values (EC2) were then measured. Electrolyte leakage (EL) were calculated, relative to fresh weight of leaves (FW), using the equation below:

$$EL/FW = ((EC1/EC2) \times 100) / FW$$

When a plant is exposed to external abiotic and biotic stresses, including over-exposure to heavy metals and micronutrient deficiency, cell death is imminent. The integrity of the cell walls of these dead and damaged plant cells will be compromised, causing K⁺ ions and other electrolytes to leak out of the cells (Demidchik et al., 2014). Studies show high EL levels are linked to the generation of reactive oxygen species (ROS) and the activation of programmed cell death (PCD). The quantity of ions leaked from a plant can be used as a proxy for the severity of cell death and can be used to estimate stress tolerance. The level of cell damage is also relevant to the maintenance of nutrient homeostasis because the cell wall is essential to nutrient signalling and transport (Ogden et al., 2018). There were no significant differences in EL levels in *WAVHI* loss-of-function mutants compared to WT (Figure S4). This indicates that *wavh1-1* do not have a higher level of cell damage compared to WT.

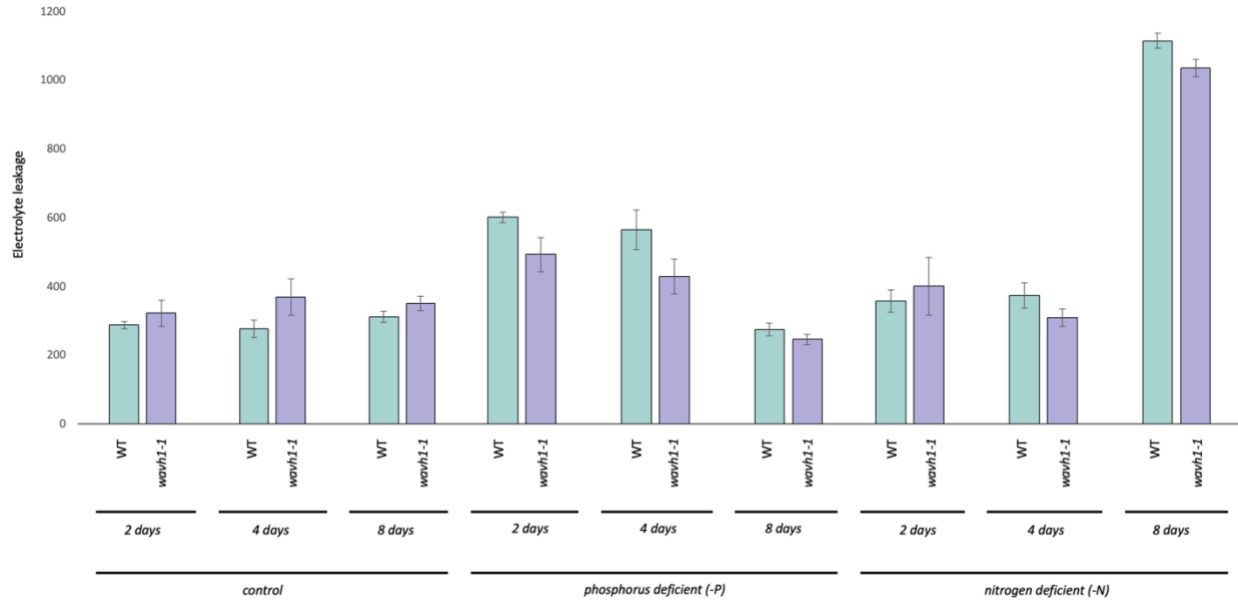


Figure S4. Electrolyte leakage (EL) was measured as described by Dionisio-Sese and Tobita (1998). Seedlings were grown on nutrient sufficient (control) media for five days then transferred to control media, phosphorus deficient media (-P), or nitrogen deficient media (-N) for two, four, and eight days. EL was measured for each group at the end of each treatment period. Analysis was done using One-Way ANOVA Tukey comparison. Error bars indicate \pm SE from one trial with at least three biological replicates per trial.

Rhizosphere acidification

Rhizosphere acidification assays were performed on the mutant lines that showed differential growth and gene expression under low phosphorus stress. Liquid phosphorus deficient media was made with the same components as the -P treatment outlines in Table 2, minus the agar. Bromocresol purple (BP) was added to the liquid medias (0.006% w/v) to act as a pH indicator; the pH of the starting solution was adjusted to 6.5. 10-day-old seedlings were put in -P BP media. Seedlings were grown in the BP media for 12 hours under continuous light in a 12-well plate; every well was filled with 0.5mL of BP media and contained two, four and six seedlings from selected mutant lines. BP changes colour from purple to yellow when the pH decreases. Therefore, a colour change from purple to yellow after 12 hours indicates acidification by the seedlings.

Absorbance at 590nm of all liquid media after the 12-hour period was measured to further analyze the degree of colour change and compare the acidification abilities of *wavh1-1* to WT under phosphorus deficiency.

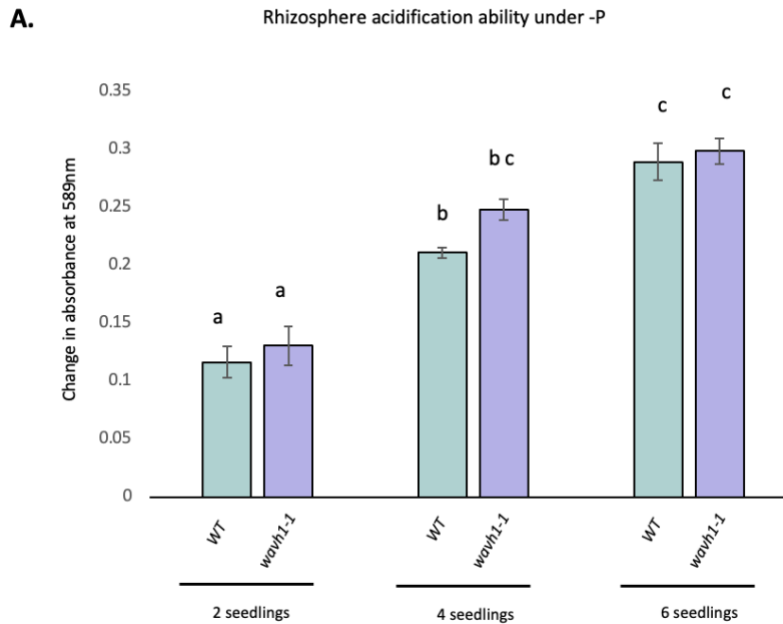


Figure S5. Rhizosphere acidification abilities were measured using bromocresol purple (BP) as a pH indicator. 10-day old WT and *wavh1-1* seedlings were transferred to 500 μ l aliquots of liquid -P media (20 μ M P) that was supplemented with 0.006 (w/v) BP and adjusted to a pH of 6.5, in groups of 2, 4, and 6. Seedlings were left under continuous light for 12 hours. Absorbance of the liquid at 589nm was measured after the 12-hour period to gauge the change in colour; purple to yellow indicating acidification. Different letters indicate p-value <0.05 using One-Way ANOVA Tukey comparison. Error bars indicate \pm SE from three trials with at least two technical replicates per trial.

CHAPTER 4: CONCLUSIONS AND FUTURE DIRECTIONS

Ubiquitination is an important post-translational modification used to regulate many nutrient stress response pathways through inducing proteasomal degradation of target proteins or provoking nonproteolytic outcomes such as controlling gene expression and trafficking. The E3 Ub ligases play a central role in this process through directly mediating the transfer of Ub to transporters, enzymes, ion channels, signalling proteins (e.g., kinases and receptors), and transcription regulators (e.g., transcription factors, co-activators, and repressors). Eight RING-type and RBR-type E3s which indicated possible involvement in Fe, PO₄⁻, or NO₃⁻ stress response were selected for analysis. The eight candidate E3s were analyzed under nutrient sufficiency as well as deficient and excess levels of Fe, P, and N. Three of these E3s, ATL12, ARI12, and WAVH1, were investigated further.

In Chapter 2 I present a theory that ATL12, a FIT-regulated RING-type E3, is involved in a feedback loop with FIT. Previous studies demonstrate that *ATL12* expression is upregulated when JA levels are increased, and I propose a model in which JA, Fe deficiency, and FIT and JA upregulates *ATL12* to mitigate the negative regulation of the IDR when external Fe levels are low. JA is an established regulator of the IDR through repressing the expression of multiple IDR genes and promoting the degradation of FIT. Our model suggests that ATL12 attenuates this negative regulation under Fe deficiency. However, many important questions need to be addressed to further understand the role of this E3. For example, it is unknown what substrate(s) ATL12 is targeting. Further analysis of ATL12 activity is necessary to pinpoint its role in the IDR, which should include finding proteins that ATL12 interacts with, confirming whether ATL12 ubiquitinates found proteins, and if the outcome of confirmed ubiquitination is proteasomal

degradation. Finding substrates that *ATL12* targets for degradation will greatly increase our current understanding of the molecular mechanisms that govern the IDR. It is also unclear if increased JA levels directly upregulates *ATL12* or if the increase in JA levels causes a regulator of *ATL12* to promote *ATL12* levels, and it is unconfirmed what the exact outcome of this upregulation of *ATL12* is.

In Chapter 2 I also explored the role of *ARI12*, an RBR-type E3, in the response to Fe stress. Our results suggest that *ARI12* targets an unknown IDR protein under Fe sufficient conditions to maintain the vital homeostasis of Fe. *ARI12* loss-of-function mutants were found to have a higher tissue Fe content when exposed to excess Fe, suggesting that *ARI12* is needed to limit Fe uptake under excess Fe levels. *ARI12* expression was found to decrease under Fe deficiency, which suggests that the protein *ARI12* targets accumulates under Fe deficiency as part of the IDR. *ARI12* is specifically expressed in the roots, which further suggests that it is involved in regulating Fe uptake. Much work is still needed to understand the functional specificities of this RBR-type E3 and how it works to attenuate the IDR when Fe levels are sufficient. The next step in pinpointing the role of *ARI12* in the response to Fe stress is finding the substrates which it ubiquitinates.

In Chapter 3, I investigated the role of *WAVH1*, a RING-type E3 and member of the *WAV3* family of gravitropism-involved E3s. Previous studies establish *WAVH1* as having a weak impact on gravitropism, however, I conclude that *WAVH1* is necessary for proper gravitropic abilities specifically under severe N limitation. My results also indicate that *WAVH1* is involved in modulating RSA under severe N limitation and is possibly involved in a BR signalling pathway which mediates auxin transport. Results indicate that *WAVH1* does play a role in the interplay of auxin and BR signalling in roots, specifically in regulating root growth under N deficiency, and I

propose a theoretical model where WAVH1 is somehow involved in promoting LR emergence under N sufficient conditions. Further research is required to determine the intricacies of how WAVH1 works to regulate root growth and gravitropism under N deficiency, and in what manner/under what conditions it is interacting with its known interactors BSK2 and AAK6. The next step is determining the substrates which WAVH1 ubiquitinates. These results will also aid in future studies focusing on changes in RSA under severe N limitation, as well as the complex interplay of auxin and BR signalling that contributes to root responses under N limitation.

This research contributes to the knowledge of E3 ubiquitin ligases and their roles in nutrient stress response in plants and will serve to aid future studies that further investigate ATL12, ARI12, and WAVH1, as well as the molecular mechanisms regulating plant response to Fe, P, and N stress. Our results will also assist in filling gaps that exist in the current knowledge of Fe, P, and N stress response through proposing multiple models which attempt to explain the possible involvement of ATL12, ARI12, and WAVH1. These results may contribute to the understanding of molecular responses in an emerging research area with potential significance in improving nutrient use efficiency and uptake in crop species. The UPS is highly conserved among eukaryotes, and therefore this knowledge can be applied other species and will be of interest to researchers in other fields of research beyond the plant sciences.

REFERENCES

- Adams, E.H.G., & Spoel, S.H. (2018). The ubiquitin-proteasome system as a transcriptional regulator of plant immunity. *J. Exp. Bot.*, *69*(19), 4529-4537.
- Agorio, A., Giraudat, J., Bianchi, M.W., Marion, J., Espagne, C., Castaings, L., Lelièvre, F., Curie, C., Thomine, S., & Merlot, S. (2017). Phosphatidylinositol 3-phosphate-binding protein AtPH1 controls the localization of the metal transporter NRAMP1 in Arabidopsis. *Proc. Natl. Acad. Sci. U.S.A.*, *114*(16), 3354-3363.
- Ahanger, M.A., & Ahmad, P. (2019). Role of mineral nutrients in abiotic stress tolerance: revisiting the associated signaling mechanisms. *Plant Signal. Mol.*, *23*(15), 269-285.
- Almagro, A., Lin, S.H., & Tsay, Y.F. (2008). Characterization of the Arabidopsis nitrate transporter NRT1.6 reveals a role of nitrate in early embryo development. *The Plant Cell*, *20*(12), 3289-3299.
- Anas, M., Liao, F., Verma, K.K., Sarwar, M.A., Mahmood, A., Chen, Z.L., Li, Q., Zeng, X.P., Liu, Y., & Li, Y.R. (2020). Fate of nitrogen in agriculture and environment: agronomic, eco-physiological and molecular approaches to improve nitrogen use efficiency. *Biol. Res.*, *53*(1), 47.
- Arabidopsis Interactome Mapping Consortium. (2011). Evidence for network evolution in an Arabidopsis interactome map. *Science*, *333*(6042), 601-7.
- Aung, M.S., Kobayashi, T., Masuda, H., & Nishizawa, N.K. (2018). Rice HRZ ubiquitin ligases are crucial for the response to excess iron. *Physiol. Plant.*, *163*, 282-296.
- Ayadi, A., David, P., Arrighi, J.F., Chiarenza, S., Thibaud, M.C., Nussaume, L., & Marin, E. (2015). Reducing the genetic redundancy of Arabidopsis PHOSPHATE TRANSPORTER1 transporters to study phosphate uptake and signaling. *Plant Physiol.*, *167*, 1511-1526.
- Baccari, B., & Krouma, A. (2023). Rhizosphere Acidification Determines Phosphorus Availability in Calcareous Soil and Influences Faba Bean (*Vicia faba*) Tolerance to P Deficiency. *Sustainability*, *15*(7), 6203.
- Barberon, M., Zelazny, E., Robert, S., Conéjéro, G., Curie, C., Friml, J., & Vert, G. (2011). Monoubiquitin-dependent endocytosis of the iron-regulated transporter 1 (IRT1) transporter controls iron uptake in plants. *Proc. Natl. Acad. Sci. U. S. A.*, *108*, 450-458.
- Bard J., Goodall E., Greene E., Jonsson E., Dong K., & Martin A. (2018). Structure and function of the 26S proteasome. *Annu. Rev. Biochem.*, *87*, 697-724.
- Bari, R., Datt, P.B., Stitt, M., & Scheible, W.R. (2006). PHO2, microRNA399, and PHR1 define a phosphate-signaling pathway in plants. *Plant Physiol.*, *141*, 988-999.

- Becker, M., & Asch, F. (2005). Iron toxicity in rice - conditions and management concepts. *J. Plant Nutr. Soil Sci.*, 168, 558-573.
- Begum, M.A., Islam, A., Ahmed, Q.M., Islam, A., & Rahman, M. (2015). Effect of nitrogen and phosphorus on the growth and yield performance of soybean. *Res. Agric. Livest. Fish*, 2, 35-42.
- Bhagat, P.K., Verma, D., Sharma, D., & Sinha, A.K. (2021). HY5 and ABI5 transcription factors physically interact to fine tune light and ABA signaling in *Arabidopsis*. *Plant Mol. Biol.*, 107, 117-127.
- Blancaflor, E.B., Fasano, J.M., & Gilroy, S. (1998). Mapping the functional roles of cap cells in the response of *Arabidopsis* primary roots to gravity. *Plant Physiol.*, 116(1), 213-22.
- Brown, C.E., Pezeshki, S.R., & DeLaune, R.D. (2006). The effects of salinity and soil drying on nutrient uptake and growth of *Spartina alterniflora* in a simulated tidal system. *Environ. Exp. Bot.*, 58, 140-148.
- Brownlie, W.J., Sutton, M.A., Reay, D.S., Heal, K.V., Hermann, L., Kabbe, C., & Spears, B.M. (2021) Global actions for a sustainable phosphorus future. *Nat. Food*, 2(2), 71-74.
- Brumbarova, T., Bauer, P., & Ivanov, R. (2015). Molecular mechanisms governing *Arabidopsis* iron uptake. *Trends in Plant Science*, 20, 124-133.
- Bustos, R., Castrillo, G., Linhares, F., Puga, M.I., Rubio, V., Pérez-Pérez, J., Solano, R., Leyva, A., Paz-Ares, J. (2010). A central regulatory system largely controls transcriptional activation and repression responses to phosphate starvation in *Arabidopsis*. *PLoS Genet.*, 6(9), 1001102.
- Callis, J. (2014). The ubiquitination machinery of the ubiquitin system. *Arabidopsis Book*, 12, 0174.
- Campos, M.L., Yoshida, Y., Major, I.T., de Oliveira Ferreira, D., Weraduwage, S.M., Froehlich, J.E., Johnson, B.F., Kramer, D.M., Jander, G., Sharkey, T.D., & Howe, G.A. (2016). Rewiring of jasmonate and phytochrome B signalling uncouples plant growth-defense tradeoffs. *Nat. Commun.*, 7, 12570.
- Castaigns, L., Caquot, A., Loubet, S., & Curie, C. (2016). The high-affinity metal transporters NRAMP1 and IRT1 team up to take up iron under sufficient metal provision. *Sci. Rep.*, 6, 37222.
- Chai, S., Chen, J., Yue, X., Li, C., Zhang, Q., de Dios, V.R., Yao, Y., & Tan, W. (2022). Interaction of BES1 and LBD37 transcription factors modulates brassinosteroid-regulated root forging response under low nitrogen in *Arabidopsis*. *Front. Plant Sci.*, 13, 998961.

- Chen, H., & Xiong, L. (2008). Role of HY5 in abscisic acid response in seeds and seedlings. *Plant Signal Behav.*, 3(11), 986-8.
- Chen, W.W., Yang, J.L., Qin, C., Jin, C.W., Mo, J.H., Ye, T., & Zheng, S.J. (2010). Nitric oxide acts downstream of auxin to trigger root ferric-chelate reductase activity in response to iron deficiency in *Arabidopsis*. *Plant Physiol.*, 154, 810-819.
- Chen, Y.F., Li, L. Q., Xu, Q., Kong, Y.H., Wang, H., & Wu, W.H. (2009). The WRKY6 transcription factor modulates PHOSPHATE1 expression in response to low pi stress in *Arabidopsis*. *Plant Cell*, 21, 3554-3566.
- Cheng, M.C., Hsieh, E.J., Chen, J.H., Chen, H.Y., & Lin, T.P. (2016). Arabidopsis RGLG2, Functioning as a RING E3 Ligase, Interacts with AtERF53 and Negatively Regulates the Plant Drought Stress Response. *Plant Physiol.*, 170(2), 1162-3.
- Colangelo, E.P., & Guerinot, M.L. (2004). The essential basic helix-loop-helix protein FIT1 is required for the iron deficiency response. *Plant Cell.*, 16(12), 3400-12.
- Connolly, E.L., Campbell, N.H., Grotz, N., Prichard, C.L., & Guerinot, M.L. (2003). Overexpression of the FRO2 ferric chelate reductase confers tolerance to growth on low iron and uncovers posttranscriptional control. *Plant Physiol.*, 133, 1102-1110.
- Costa, C., Dwyer, L.M., Stewart, D.W., & Smith, D.L. (2002). Nitrogen effects on grain yield and yield components of leafy and nonleafy maize genotypes. *Crop Science*, 42(5), 1556-1563.
- Cui, Y., Chen, C.L., Cui, M., Zhou, W.J., Wu, H.L., & Ling, H.Q. (2018). Four IVa bHLH Transcription Factors Are Novel Interactors of FIT and Mediate JA Inhibition of Iron Uptake in *Arabidopsis*. *Mol. Plant.*, 11(9), 1166-1183.
- Curie, C., Alonso, J. M., Le Jean, M., Ecker, J. R., & Briat, J. F. (2000). Involvement of NRAMP1 from *Arabidopsis thaliana* in iron transport. *Biochem. J.*, 347(3), 749-755.
- Demidchik, V., Straltsova, D., Medvedev, S.S., Pozhvanov, G.A., Sokolik, A., & Yurin, V. (2014). Stress-induced electrolyte leakage: the role of K⁺-permeable channels and involvement in programmed cell death and metabolic adjustment. *J. Exp. Bot.*, 65(5), 1259-70.
- Devi, L.L., Pandey, A., Gupta, S., & Singh, A.P. (2022). The interplay of auxin and brassinosteroid signaling tunes root growth under low and different nitrogen forms. *Plant Physiol.*, 189(3), 1757-1773.
- Devoto, A., Nieto-Rostro, M., Xie, D., Ellis, C., Harmston, R., Patrick, E., Davis, J., Sherratt, L., Coleman, M., & Turner, J.G. (2002). COI1 links jasmonate signalling and fertility to the SCF ubiquitin-ligase complex in *Arabidopsis*. *Plant J.*, 32, 457-466.

- Dionisio-Sese, M., & Tobita, S. (1998). Antioxidant responses of rice seedlings to salinity stress. *Plant Science*, *135*(1), 1-9.
- Dittmar, G., and Winklhofer, K.F. (2020). Linear ubiquitin chains: cellular functions and strategies for detection and quantification. *Front. Chem.*, *7*, 915.
- Dubeaux, G., Neveu, J., Zelazny, E., & Vert, G. (2018). Metal sensing by the IRT1 transporter-receptor orchestrates its own degradation and plant metal nutrition. *Mol. Cell*, *69*, 953–964.
- Duc, C., Cellier, F., Lobréaux, S., Briat, J.F., & Gaymard, F. (2009). Regulation of iron homeostasis in *Arabidopsis thaliana* by the clock regulator time for coffee. *J. Biol. Chem.*, *284*(52), 36271-36281.
- Duncan, L.M., Piper, S., Dodd, R.B., Saville, M.K., Sanderson, C.M., Luzio, J.P., & Lehner, P.J. (2006). Lysine-63-linked ubiquitination is required for endolysosomal degradation of class I molecules. *EMBO J.*, *25*, 1635–1645.
- Eckardt, N.A., Cutler, S., Juenger, T.E., Marshall-Colon, A., Udvardi, M., & Verslues, P.E. (2023). Focus on climate change and plant abiotic stress biology. *The Plant Cell*, *35*(1), 1-3.
- Elser, J.J. (2012). Phosphorus: a limiting nutrient for humanity? *Curr. Opin. Biotechnol.*, *23*(6), 833-8.
- Fageria, N.K., & Baligar, V.C. (2005). Enhancing nitrogen use efficiency in crop plants. *Advances in Agronomy*, *88*, 97-185.
- Fan, S.C., Lin, C.S., Hsu, P.K., Lin, S.H., & Tsay, Y.F. (2009). The *Arabidopsis* nitrate transporter NRT1.7, expressed in phloem, is responsible for source-to-sink remobilization of nitrate. *Plant Cell*, *21*, 2750-2761.
- Fourcroy, P., Sisó-Terraza, P., Sudre, D., Savirón, M., Reyt, G., Gaymard, F., Abadía, A., Abadía, J., Álvarez-Fernández, A., & Briat, J.F. (2014). Involvement of the ABCG37 transporter in secretion of scopoletin and derivatives by *Arabidopsis* roots in response to iron deficiency. *New Phytol.*, *201*(1), 155-167.
- Gangappa S. N., Botto J. F. (2016). The multifaceted roles of HY5 in plant growth and development. *Mol. Plant* *9* 1353-1365.
- García, M.J., Lucena, C., Romera, F.J., Alcántara, E., & Pérez-Vicente, R. (2010). Ethylene and nitric oxide involvement in the up-regulation of key genes related to iron acquisition and homeostasis in *Arabidopsis*. *J. Exp. Bot.*, *61*(14), 3885-99.

- García, M.J., Suárez, V., Romera, F.J., Alcántara, E., & Pérez-Vicente, R. (2011). A new model involving ethylene, nitric oxide and Fe to explain the regulation of Fe-acquisition genes in Strategy I plants. *Plant Physiol. Biochem.*, 49(5), 537-44.
- Gautam, C.K., Tsai, H.H., & Schmidt, W. (2022). A Quick Method to Quantify Iron in *Arabidopsis* Seedlings. *Bio. Protoc.* 12(5), 4342.
- Gelybó, G., Tóth, E., Farkas, C., Horel, Á., Kása, I., & Bakacsi, Z. (2018). Potential impacts of climate change on soil properties. *Agrochem. Soil Sci.* 67, 121-141.
- Gibbs, C.R. (1976). Characterization and application of ferrozine iron reagent as a ferrous iron indicator. *Anal. Chem.* 48, 1197-1201.
- Giehl, R.F., & von Wirén, N. (2014). Root nutrient foraging. *Plant Physiol.*, 166(2), 509-17.
- Good, A.G., Shrawat, A.K., & Muench, D.G. (2004). Can less yield more? Is reducing nutrient input into the environment compatible with maintaining crop production? *Trends in Plant Science.*, 9, 597-605.
- Goossens, J., Mertens, J., & Goossens, A. (2017). Role and functioning of bHLH transcription factors in jasmonate signalling. *J. Exp. Bot.*, 68(6), 1333-1347.
- Grillet, L., Lan, P., Li, W., Mokkalapati, G., & Schmidt, W. (2018). IRON MAN is a ubiquitous family of peptides that control iron transport in plants. *Nature Plants*, 4, 953-963.
- Grotz, N., Fox, T., Connolly, E., Park, W., Guerinot, M.L., & Eide, D. (1998). Identification of a family of zinc transporter genes from *Arabidopsis* that respond to zinc deficiency. *Proc. Natl. Acad. Sci. U S A.*, 95(12), 7220-4.
- Guan, P., Ripoll, J.J., Wang, R., Vuong, L., Bailey-Steinitz, L.J., Ye, D., & Crawford, N.M. (2017). Interacting TCP and NLP transcription factors control plant responses to nitrate availability. *Proc. Natl. Acad. Sci. U S A.*, 114(9), 2419-2424.
- Guan, P., Wang, R., Nacry, P., Breton, G., Kay, S.A., Pruneda-Paz, J.L., Davani, A., & Crawford, N.M. (2014). Nitrate foraging by *Arabidopsis* roots is mediated by the transcription factor TCP20 through the systemic signaling pathway. *Proc. Natl. Acad. Sci. U S A.*, 111(42), 15267-72.
- Guo, Z., Xu, J., Wang, Y., Hu, C., Shi, K., Zhou, J., Xia, X., Zhou, Y., Foyer, C.H., & Yu, J. (2021). The phyB-dependent induction of HY5 promotes iron uptake by systemically activating FER expression. *EMBO Rep.*, 22, 51944.
- Hall, J.L. (2002). Cellular mechanisms for heavy metal detoxification and tolerance. *Journal of Experimental Botany*, 53(366), 1-11.

- Hamburger, D., Rezzonico, E., MacDonald-Comber Petétot, J., Somerville, C., & Poirier, Y. (2002). Identification and characterization of the Arabidopsis PHO1 gene involved in phosphate loading to the xylem. *Plant Cell*, *14*, 889-902.
- Hannam, C., Gidda, S. K., Humbert, S., Peng, M., Cui, Y., Dyer, J. M., Rothstein, S.J., & Mullen, R.T. (2018). Distinct domains within the nitrogen limitation adaptation protein mediate its subcellular localization and function in the nitrate-dependent phosphate homeostasis pathway. *Botany*, *96*, 79-96.
- Harish, H., Aslam, S., Chouhan, S., Pratap, Y., & Lalotra, S. (2023). Iron toxicity in plants: A Review. *International journal of environment and climate change* *13*(8), 1894-1900.
- Haynes R.J., & Swift R.S. (1986). Effects of soil acidification and subsequent leaching on levels of extractable nutrients in a soil. *Plant Soil*, *95*, 327-336.
- He, J., Wang, M., Li, S., Chen, L., Zhang, K., & She, J. (2023). Cryo-EM structure of the plant nitrate transporter AtCLCa reveals characteristics of the anion-binding site and the ATP-binding pocket. *J. Biol. Chem.*, *299*(2), 102833.
- He, Q., Lu, H., Guo, H., Wang, Y., Zhao, P., Li, Y., Wang, F., Xu, J., Mo, X., & Mao, C. (2021). OsbHLH6 interacts with OsSPX4 and regulates the phosphate starvation response in rice. *Plant J.*, *105*(3), 649-667.
- Hikosaka, K. (2004). Interspecific difference in the photosynthesis-nitrogen relationship: patterns, physiological causes, and ecological importance. *J. Plant Res.*, *117*, 481-494.
- Hindt, M.N., & Guerinot, M.L. (2012). Getting a sense for signals: regulation of the plant iron deficiency response. *Biochim. Biophys. Acta.*, *1823*, 1521-1530.
- Høgh-Jensen, H., Schjoerring, J., & Soussana, J.F. (2002). The influence of phosphorus deficiency on growth and nitrogen fixation of white clover plants. *Ann. Bot.* *90*(6), 745-53.
- Holford, I.C.R. (1997). Soil phosphorus: its measurement, and its uptake by plants. *Aust. J. Soil Res.*, *35*, 227-239.
- Hsieh, E.J., Cheng, M.C., & Lin T.P. (2013). Functional characterization of an abiotic stress-inducible transcription factor AtERF53 in *Arabidopsis thaliana*. *Plant Mol. Biol.*, *82*, 223-237.
- Hu, B., Jiang, Z., Wang, W., Qiu, Y., Zhang, Z., Liu, Y., Li, A., Gao, X., Liu, L., Qian, Y., Huang, X., Yu, F., Kang, S., Wang, Y., Xie, J., Cao, S., Zhang, L., Wang, Y., Xie, Q., Kopriva, S., & Chu, C. (2019). Nitrate–NRT1.1B–SPX4 cascade integrates nitrogen and phosphorus signalling networks in plants. *Nat. Plants*, *5*, 401-413.

- Huot, B., Yao, J., Montgomery, B.L., & He, S.Y. (2014). Growth-defense tradeoffs in plants: a balancing act to optimize fitness. *Mol. Plant.*, 7(8), 1267-1287.
- Ichami, S.M., Karuku, G.N., Sila, A.M., Ayuke, F.O., & Shepherd, K.D. (2022). Spatial approach for diagnosis of yield-limiting nutrients in smallholder agroecosystem landscape using population-based farm survey data. *PLoS One*. 17(2), 0262754.
- Jackson, R.S. (2020). Chapter 5 - Site selection and climate. In R. S. Jackson (Ed.), *Wine science* (5th ed., pp. 331-374). *Academic Press*.
- Jeong, J., & Guerinot, M.L. (2009). Homing in on iron homeostasis in plants. *Trends Plant Sci.*, 14(5), 280-5.
- Jia, Z., Giehl, R.F.H., Meyer, R.C., Altmann, T., & von Wirén, N. (2019). Natural variation of BSK3 tunes brassinosteroid signaling to regulate root foraging under low nitrogen. *Nat. Commun.* 10, 2378.
- Jia, Z., Giehl, R.F.H., & von Wirén, N. (2020). The Root Foraging Response under Low Nitrogen Depends on *DWARF1*-Mediated Brassinosteroid Biosynthesis. *Plant Physiol.*, 183(3), 998-1010.
- Jian, S., Liao, Q., Song, H., Liu, Q., Lepo, J.E., Guan, C., Zhang, J., Ismail, A.M., & Zhang, Z. (2018). NRT1.1-related NH₄⁺ toxicity is associated with a disturbed balance between NH₄⁺ uptake and assimilation. *Plant Physiol.*, 178, 1473-1488
- Jiang, Y., Li, Y., Zeng, Q., Wei, J., & Yu, H. (2017). The effect of soil pH on plant growth, leaf chlorophyll fluorescence and mineral element content of two blueberries. *Acta. Hortic.*, 1180, 269-276.
- Jiménez-López, D., Muñoz-Belman, F., González-Prieto, J.M., Aguilar-Hernández, V., & Guzmán, P. (2018). Repertoire of plant RING E3 ubiquitin ligases revisited: New groups counting gene families and single genes. *PLoS ONE*, 13.
- Jing, J., Rui, Y., Zhang, F., Rengel, Z., & Shen, J. (2010). Localized application of phosphorus and ammonium improves growth of maize seedlings by stimulating root proliferation and rhizosphere acidification. *Field Crops Research.*, 119, 355-364.
- Kant, S., Peng, M., & Rothstein, S.J. (2011). Genetic regulation by NLA and MicroRNA827 for maintaining nitrate-dependent phosphate homeostasis in Arabidopsis. *PLoS Genet.*, 7, 1002021.
- Khamis, S., Lamaze, T., Lemoine, Y., & Foyer, C. (1990). Adaptation of the photosynthetic apparatus in maize leaves as a result of nitrogen limitation. *Plant Physiol.*, 94, 1436-1443.

- Khan, F., Siddique, A.B., Shabala, S., Zhou, M., & Zhao, C. (2023). Phosphorus Plays Key Roles in Regulating Plants' Physiological Responses to Abiotic Stresses. *Plants (Basel)*, 12(15), 2861.
- Kiba, T., Feria-Bourrellier, A.B., Lafouge, F., Lezhneva, L., Boutet-Mercey, S., Orsel, M., Bréhaut, V., Miller, A., Daniel-Vedele, F., Sakakibara, H., & Krapp, A. (2012). The Arabidopsis nitrate transporter NRT2.4 plays a double role in roots and shoots of nitrogen-starved plants. *Plant Cell*, 24(1), 245-58.
- Kiba, T., & Krapp, A. (2016). Plant Nitrogen Acquisition Under Low Availability: Regulation of Uptake and Root Architecture, *Plant and Cell Physiology*, 57(4), 707-714.
- Kobayashi, T., Itai, R.N., Senoura, T., Oikawa, T., Ishimaru, Y., Ueda, M., Nakanishi, H., & Nishizawa, N.K. (2016). Jasmonate signaling is activated in the very early stages of iron deficiency responses in rice roots. *Plant Mol. Biol.*, 91(4-5), 533-47.
- Kobayashi, T., & Nishizawa, N.K. (2012). Iron uptake, translocation, and regulation in higher plants. *Annu. Rev. Plant Biol.*, 63, 131-52.
- Kobayashi, T., Nagasaka, S., Senoura, T., Itai, R. N., Nakanishi, H., and Nishizawa, N. K. (2013). Iron-binding haemerythrin RING ubiquitin ligases regulate plant iron responses and accumulation. *Nat. Commun.*, 4, 2792.
- Komander D. (2010). Mechanism, specificity and structure of the deubiquitinases. *Subcell. Biochem.* 54, 69-87.
- Kong, F., Guo, T., & Ramonell, K.M. (2021). *Arabidopsis Toxicos en Levadura 12 (ATL12)*: A Gene Involved in Chitin-Induced, Hormone-Related and NADPH Oxidase-Mediated Defense Responses. *J. Fungi (Basel)*, 7(10), 883.
- Kong, F., Ramonell, K.M. (2022). *Arabidopsis Toxicos en Levadura 12* Modulates Salt Stress and ABA Responses in *Arabidopsis thaliana*. *International Journal of Molecular Sciences*, 23(13), 7290.
- Konishi, M., & Yanagisawa, S. (2019). The role of protein-protein interactions mediated by the PB1 domain of NLP transcription factors in nitrate-inducible gene expression. *BMC Plant Biol.*, 19(1), 90.
- Kosarev, P., Mayer, K.F., & Hardtke, C.S. (2002). Evaluation and classification of RING-finger domains encoded by the Arabidopsis genome. *Genome Biol.*, 3.
- Kosarev, P., Mayer, K.F.X., & Hardtke, C.S. (2002). Evaluation and classification of RING-finger domains encoded by the Arabidopsis genome. *Genome Biol.*, 3(4), 0016.1-0016.12.

- Krapp, A., David, L.C., Chardin, C., Girin, T., Marmagne, A., Leprince, A.S., Chaillou, S., Ferrario-Méry, S., Meyer, C., & Daniel-Vedele, F. (2014). Nitrate transport and signalling in Arabidopsis. *J. Exp. Bot.*, *65*(3), 789-98.
- Krouk, G., Lacombe, B., Bielach, A., Perrine-Walker, F., Malinska, K., Mounier, E., Hoyerova, K., Tillard, P., Leon, S., Ljung, K., Zazimalova, E., Benkova, E., Nacry, P., & Gojon, A. (2010). Nitrate-regulated auxin transport by NRT1.1 defines a mechanism for nutrient sensing in plants. *Dev. Cell.*, *18*(6), 927-37.
- Lanquar, V., Lelièvre, F., Bolte, S., Hamès, C., Alcon, C., Neumann, D., Vansuyt, G., Curie, C., Schröder, A., Krämer, U., Barbier-Brygoo, H., & Thomine, S. (2005). Mobilization of vacuolar iron by AtNRAMP3 and AtNRAMP4 is essential for seed germination on low iron. *EMBO J.*, *24*(23), 4041-51.
- Lei, R., Li, Y., Cai, Y., Li, C., Pu, M., Lu, C., Yang, Y., & Liang, G. (2020). bHLH121 functions as a direct link that facilitates the activation of FIT by bHLH IVc transcription factors for maintaining Fe homeostasis in Arabidopsis. *Molecular Plant*, *13*, 634-649.
- Lei, G.J., Zhu, X.F., Wang, Z.W., Dong, F., Dong, N.Y., & Zheng, S.J. (2014). Abscisic acid alleviates iron deficiency by promoting root iron reutilization and transport from root to shoot in Arabidopsis. *Plant Cell Environ.*, *37*(4), 852-63.
- Lezhneva, L., Kiba, T., Feria-Bourrellier, A.B., Lafouge, F., Boutet-Mercey, S., Zoufan, P., Sakakibara, H., Daniel-Vedele, F., & Krapp, A. (2014). The Arabidopsis nitrate transporter NRT2.5 plays a role in nitrate acquisition and remobilization in nitrogen-starved plants. *Plant J.*, *80*(2), 230-41.
- Li, X., Zhang, H., Ai, Q., Liang, G., & Yu, D. (2016). Two bHLH transcription factors, bHLH34 and bHLH104, regulate iron homeostasis in *Arabidopsis thaliana*. *Plant Physiology*, *170*, 2478-2493.
- Li, C., Xu, M., Cai, X., Han, Z., Si, J., & Chen, D. (2022). Jasmonate Signaling Pathway Modulates Plant Defense, Growth, and Their Trade-Offs. *Int. J. Mol. Sci.*, *23*(7), 3945.
- Li, G., Kronzucker, H.J., & Shi, W. (2016). The Response of the Root Apex in Plant Adaptation to Iron Heterogeneity in Soil. *Front. Plant Sci.*, *7*, 344.
- Li, J., Cao, X., Jia, X., Liu, L., Cao, H., Qin, W., & Li, M. (2021). Iron Deficiency Leads to Chlorosis Through Impacting Chlorophyll Synthesis and Nitrogen Metabolism in *Areca catechu* L. *Front. Plant Sci.*, *12*, 710093.
- Li, J., Wang, Y., Zheng, L., Li, Y., Zhou, X., Li, J., Gu, D., Xu, E., Lu, Y., Chen, X., & Zhang, W. (2019). The Intracellular Transporter AtNRAMP6 Is Involved in Fe Homeostasis in Arabidopsis. *Front. Plant Sci.*, *10*, 1124.

- Li, J., Wen, J., Lease, K.A., Doke, J.T., Tax, F.E., & Walker, J.C. (2002). BAK1, an Arabidopsis LRR receptor-like protein kinase, interacts with BRI1 and modulates brassinosteroid signaling. *Cell*, *110*(2), 213-22.
- Li, M., Watanabe, S., Gao, F., & Dubos, C. (2023). Iron Nutrition in Plants: Towards a New Paradigm? *Plants*, *12*(2), 384.
- Li, Y., Lu, C.K., Li, C.Y., Lei, R.H., Pu, M.N., Zhao, J.H., Peng, F., Ping, H.Q., Wang, D., & Liang, G. (2021). Iron man interacts with Brutus to maintain iron homeostasis in Arabidopsis. *Proc. Natl. Acad. Sci.*, *118*, 2109063118.
- Liao, Q., Zhou, T., Yao, J.Y., Han, Q.F., Song, H.X., Guan, C.Y., Hua, Y.P., & Zhang, Z.H. (2018). Genome-scale characterization of the vacuole nitrate transporter Chloride Channel (CLC) genes and their transcriptional responses to diverse nutrient stresses in allotetraploid rapeseed. *PLoS One*, *13*(12), 0208648.
- Lin, W.Y., Huang, T.K., & Chiou, T.J. (2013). Nitrogen limitation adaptation, a target of microRNA827, mediates degradation of plasma membrane-localized phosphate transporters to maintain phosphate homeostasis in Arabidopsis. *Plant Cell*, *25*, 4061-4074.
- Lingam, S., Mohrbacher, J., Brumbarova, T., Potuschak, T., Fink-Straube, C., Blondet, E., Genschik, P., & Bauer, P. (2011). Interaction between the bHLH transcription factor FIT and ETHYLENE INSENSITIVE3/ETHYLENE INSENSITIVE3-LIKE1 reveals molecular linkage between the regulation of iron acquisition and ethylene signaling in Arabidopsis. *Plant Cell*, *23*(5), 1815-29.
- Liu, Y., & von Wirén, N. (2022). Integration of nutrient and water availabilities via auxin into the root developmental program. *Curr. Opin. Plant Biol.*, *65*, 102117.
- Liu, W., Sun, Q., Wang, K., Du, Q., & Li, W. (2017). Nitrogen limitation adaptation (NLA) is involved in source-to-sink remobilization of nitrate by mediating the degradation of NRT1.7 in Arabidopsis. *New Phytol.*, *214*, 734-744.
- López-Arredondo, D. L., Leyva-González, M.A., González-Morales, S.I., López-Bucio, J., & Herrera-Estrella, L. (2014). Phosphate nutrition: improving low-phosphate tolerance in crops. *Annu. Rev. Plant Biol.*, *65*, 95-123.
- López-Bucio, J., Hernández-Abreu, E., Sánchez-Calderón, L., Nieto-Jacobo, M.F., Simpson, J., & Herrera-Estrella, L. (2002). Phosphate availability alters architecture and causes changes in hormone sensitivity in the Arabidopsis root system. *Plant Physiol.*, *129*, 244-256
- Ludewig, U., Neuhäuser, B., & Dynowski, M. (2007). Molecular mechanisms of ammonium transport and accumulation in plants. *FEBS Lett.*, *581*, 2301-2308.

- Lv, Q., Zhong, Y., Wang, Y., Wang, Z., Zhang, L., Shi, J., Wu, Z., Liu, Y., Mao, C., Yi, K., & Wu, P. (2014). SPX4 Negatively Regulates Phosphate Signaling and Homeostasis through Its Interaction with PHR2 in Rice. *Plant Cell*, *26*, 1586-1597.
- MacKinnon, E., & Stone, S.L. (2022). The Ubiquitin Proteasome System and Nutrient Stress Response. *Front. Plant Sci.*, *13*, 867419.
- Mai, H.J., Pateyron, S., & Bauer, P. (2016). Iron homeostasis in *Arabidopsis thaliana*: transcriptomic analyses reveal novel FIT-regulated genes, iron deficiency marker genes and functional gene networks. *BMC Plant Biol.*, *16*, 211.
- Manghwar, H., Hussain, A., Ali, Q., & Liu, F. (2022). Brassinosteroids (BRs) role in plant development and coping with different stresses. *Int. J. Mol. Sci.*, *23*, 1012.
- Mao, J., & Li, J. (2020). Regulation of Three Key Kinases of Brassinosteroid Signaling Pathway. *Int. J. Mol. Sci.*, *21*(12), 4340.
- Marín, I. (2010). Diversification and Specialization of Plant RBR Ubiquitin Ligases. *PLoS One*, *5*(7), 11579.
- Martín-Barranco, A., Spielmann, J., Dubeaux, G., Vert, G., & Zelazny, E. (2020). Dynamic control of the high-affinity iron uptake complex in root epidermal cells. *Plant Physiol.*, *184*, 1236-1250.
- Masclaux-Daubresse, C., Daniel-Vedele, F., Dechorgnat, J., Chardon, F., Gaufichon, L., & Suzuki, A. (2010). Nitrogen uptake, assimilation and remobilization in plants: challenges for sustainable and productive agriculture. *Ann. Bot.*, *105*, 1141-1157.
- Maurer, F., Naranjo Arcos, M.A., Bauer, P. (2014). Responses of a triple mutant defective in three iron deficiency-induced basic helix-loop-helix genes of the subgroup Ib(2) to iron deficiency and salicylic acid. *PLoS One*, *9*, 99234.
- Mehra, P., Pandey, B.K., & Giri, J. (2017). Improvement in phosphate acquisition and utilization by a secretory purple acid phosphatase (OsPAP21b) in rice. *Plant Biotechnol J.*, *15*(8), 1054-1067.
- Meiser, J., Lingam, S., & Bauer, P. (2011). Posttranslational regulation of the iron deficiency basic helix-loop-helix transcription factor FIT is affected by iron and nitric oxide. *Plant Physiology*, *157*, 2154-2166.
- Melo, F.V., Oliveira, M.M., Saibo, N., & Lourenço, T.F. (2021). Modulation of abiotic stress responses in Rice by E3-ubiquitin ligases: a promising way to develop stress-tolerant crops. *Front. Plant Sci.* *12*, 640193.
- Miricescu, A., Goslin, K., & Graciet, E. (2018). Ubiquitylation in plants: signaling hub for the integration of environmental signals. *J. Exp. Biol.*, *69*, 4511-4527.

- Mladek, C., Guger, K., & Hauser, M.T. (2003). Identification and characterization of the ARIADNE gene family in Arabidopsis. A group of putative E3 ligases. *Plant Physiol.*, *131*(1), 27-40.
- Młodzińska, E., & Zboińska, M. (2016). Phosphate uptake and allocation—A closer look at Arabidopsis thaliana L. and Oryza sativa L. *front. Plant Sci.*, *7*, 1198.
- Mochizuki, S., Harada, A., Inada, S., Sugimoto-Shirasu, K., Stacey, N., Wada, T., Ishiguro, S., Okada, K., & Sakai, T. (2005). The Arabidopsis WAVY GROWTH 2 protein modulates root bending in response to environmental stimuli. *Plant Cell.*, *17*(2), 537-47.
- Mounier, E., Pervent, M., Ljung, K., Gojon, A., & Nacry, P. (2014). Auxin-mediated nitrate signaling by NRT1.1 participates in the adaptive response of Arabidopsis root architecture to the spatial heterogeneity of nitrate availability. *Plant Cell Environ.*, *37*, 162-174.
- Muratore, C., Espen, L., & Prinsi, B. (2021). Nitrogen Uptake in Plants: The Plasma Membrane Root Transport Systems from a Physiological and Proteomic Perspective. *Plants (Basel)*, *10*(4), 681.
- Mussarat, M., Shair, M., Muhammad, D., Mian, I.A., Khan, S., Adnan, M., Fahad, S., Dessoky, E.S., Sabagh, A.E.L., Zia, A., Khan, B., Shahzad, H., Anwar, S., Ilahi, H., Ahmad, M., Bibi, H., Adnan, M., & Khan, F. (2021). Accentuating the Role of Nitrogen to Phosphorus Ratio on the Growth and Yield of Wheat Crop. *Sustainability*, *13*(4), 2253.
- Nagarajan, V.K., Jain, A., Poling, M.D., Lewis, A.J., Raghothama, K.G., & Smith, A.P. (2011). Arabidopsis Pht1;5 mobilizes phosphate between source and sink organs and influences the interaction between phosphate homeostasis and ethylene signaling. *Plant Physiol.*, *156*(3), 1149-63.
- Nakamura, M., Nishimura, T., & Morita, M.T. (2019). Bridging the gap between amyloplasts and directional auxin transport in plant gravitropism. *Curr. Opin. Plant Biol.*, *52*, 54-60.
- Neina, D. (2019). The role of soil pH in plant nutrition and soil remediation. *Appl. Environ. Soil Sci.*, *2019*, 1-9.
- Ogden, M., Hoefgen, R., Roessner, U., Persson, S., & Khan, G.A. (2018). Feeding the Walls: How Does Nutrient Availability Regulate Cell Wall Composition? *Int. J. Mol. Sci.*, *19*(9), 2691.
- Pandey, A., Devi, L.L., & Singh, A.P. (2020). Review: emerging roles of brassinosteroid in nutrient foraging. *Plant Sci.*, *296*, 110474.

- Park, B.S., Seo, J.S., & Chua, N. (2014). Nitrogen limitation adaptation recruits phosphate2 to target the phosphate transporter PT2 for degradation during the regulation of Arabidopsis phosphate homeostasis. *Plant Cell*, 26, 454-464.
- Peng, M., Hannam, C., Gu, H., Bi, Y.M., & Rothstein, S.J. (2007). A mutation in NLA, which encodes a RING-type ubiquitin ligase, disrupts the adaptability of Arabidopsis to nitrogen limitation. *The Plant J.*, 50, 320-337.
- Perrot-Rechenmann, C. (2010). Cellular Responses to Auxin: Division versus Expansion. *Cold Spring Harb. Perspect. Biol.*, 2(5), 001446.
- Petit, J.M., van Wuytswinkel, O., Briat, J.F., & Lobréaux, S. (2001). Characterization of an iron-dependent regulatory sequence involved in the transcriptional control of AtFer1 and ZmFer1 plant ferritin genes by iron. *J. Biol. Chem.*, 276(8), 5584-90.
- Pickart, C.M., & Eddins, M.J. (2004). Ubiquitin: structures, functions, mechanisms. *Biochim Biophys. Acta.*, 1695(1-3), 55-72.
- Plaxton, W.C., & Lambers, H. (2015). Phosphorus Metabolism in Plants. *Phosphorus metab. Plants.*, 48, 1-449.
- Poore, J., & Nemecek, T. (2018). Reducing food's environmental impacts through producers and consumers. *Science*, 360(6392), 987-992.
- Pregitzer, K.S., & King J.S. (2005). "Effects of soil temperature on nutrient uptake," in *Nutrient acquisition by plants*. ed. BassiriRad H. (Berlin, Heidelberg: Springer), 277-310.
- Pu, M.N., & Liang, G. (2023). The transcription factor POPEYE negatively regulates the expression of bHLH Ib genes to maintain iron homeostasis. *J. Exp. Bot.*, 74(8), 2754-2767.
- Pushnik, J.C., Miller, G.W., & Manwaring, J.H. (2008). The role of iron in higher plant chlorophyll biosynthesis, maintenance, and chloroplast biogenesis. *J. Plant Nutr.*, 7, 733-758.
- Qu, Y., Wang, Q., Guo, J., Wang, P., Song, P., Jia, Q., Zhang, X., Kudla, J., Zhang, W., Zhang, Q. (2017). Peroxisomal CuAO ζ and its product H₂O₂ regulate the distribution of auxin and IBA-dependent lateral root development in Arabidopsis. *J. Exp. Bot.*, 68(17), 4851-4867.
- Ren, H., Willige, B.C., Jaillais, Y., Geng, S., Park, M.Y., Gray, W.M., & Chory, J. BRASSINOSTEROID-SIGNALING KINASE 3, a plasma membrane-associated scaffold protein involved in early brassinosteroid signaling. *PLoS Genet.*, 15(1), 1007904.

- Riaz, N., & Guerinot, M.L. (2021). All together now: regulation of the iron deficiency response. *J. Exp. Bot.*, 72(6):2045-2055.
- Rodríguez-Celma, J., Connorton, J.M., Kruse, I., Green, R.T., Franceschetti, M., Chen, Y.T., Cui, Y., Ling, H.Q., Yeh, K.C., & Balk, J. (2019). Arabidopsis BRUTUS-LIKE E3 ligases negatively regulate iron uptake by targeting transcription factor FIT for recycling. *PNAS*, 116, 17584-17591.
- Romera, F.J., García, M.J., Alcántara, E., & Pérez-Vicente, R. (2011). Latest findings about the interplay of auxin, ethylene and nitric oxide in the regulation of Fe deficiency responses by Strategy I plants. *Plant Signal Behav.*, 6(1), 167-70.
- Ruan, W., Guo, M., Wang, X., Guo, Z., Xu, Z., Xu, L., Zhao, H., Sun, H., Yan, C., & Yi, K. (2019). Two RING-Finger Ubiquitin E3 Ligases Regulate the Degradation of SPX4, An Internal Phosphate Sensor, for Phosphate Homeostasis and Signaling in Rice. *Mol. Plant.*, 12(8), 1060-1074.
- Sachdev, S., Ansari, S.A., Ansari, M.I., Fujita, M., & Hasanuzzaman, M. (2021). Abiotic Stress and Reactive Oxygen Species: Generation, Signaling, and Defense Mechanisms. *Antioxidants (Basel)*. 10(2), 277.
- Sadanandom, A., Bailey, M., Ewan, R., Lee, J., & Nelis, S. (2012). The ubiquitin-proteasome system: central modifier in plant signaling. *New Phytol.*, 196, 13-28.
- Sadowski, M., & Sarcevic, B. (2010). Mechanisms of mono- and poly-ubiquitination: Ubiquitination specificity depends on compatibility between the E2 catalytic core and amino acid residues proximal to the lysine. *Cell Div.* 5, 19.
- Sage, R.G., & Percy, R.W. (1987). The nitrogen use efficiency of C₃ and C₄ plants. II. Leaf nitrogen effects on the gas exchange characteristics of *Chenopodium album* (L.) and *Amaranthus retroflexus* (L.). *Plant Physiol.*, 84, 959-963.
- Sakai, T., Mochizuki, S., Haga, K., Uehara, Y., Suzuki, A., Harada, A., Wada, T., Ishiguro, S., & Okada, K. (2012). The wavy growth 3 E3 ligase family controls the gravitropic response in Arabidopsis roots. *Plant J.*, 70(2), 303-14.
- Sakuraba, Y. (2022). Molecular basis of nitrogen starvation-induced leaf senescence. *Front Plant Sci.*, 13, 1013304.
- Santi, S., & Schmidt, W. (2009). Dissecting iron deficiency-induced proton extrusion in Arabidopsis roots. *New Phytol.*, 183, 1072-1084.
- Sato, T., Maekawa, S., Yasuda, S., Domeki, Y., Sueyoshi, K., Fujiwara, M., Fukao, Y., Goto, D.B., & Yamaguchi, J. (2011). Identification of 14-3-3 proteins as a target of ATL31 ubiquitin ligase, a regulator of the C/N response in Arabidopsis. *Plant J.*, 68, 137-146.

- Sato, T., Maekawa, S., Yasuda, S., Sonoda, Y., Katoh, E., Ichikawa, T., Nakazawa, M., Seki, M., Shinozaki, K., Matsui, M., Goto, D.B., Ikeda, A., & Yamaguchi, J. (2009). CNI1/ATL31, a RING-type ubiquitin ligase that functions in the carbon/nitrogen response for growth phase transition in Arabidopsis seedlings. *Plant J.*, *60*, 852-864.
- Schmidt, C., & Schroeder, J.I. (1994). Anion Selectivity of Slow Anion Channels in the Plasma Membrane of Guard Cells: Large Nitrate Permeability. *Plant Physiology*, *106*(1), 383-391.
- Schroeder, J.I., & Keller, B.U. (1992). Two types of anion channel currents in guard cells with distinct voltage regulation. *Proceedings of the National Academy of Sciences, USA*, *89*, 5025-5029.
- Schuman, M.C., Meldau, S., Gaquerel, E., Diezel, C., McGale, E., Greenfield, S., & Baldwin, I.T. (2018). The Active Jasmonate JA-Ile Regulates a Specific Subset of Plant Jasmonate-Mediated Resistance to Herbivores in Nature. *Front. Plant Sci.*, *9*, 787.
- Schwarz, B., & Bauer, P. (2020). FIT, a regulatory hub for iron deficiency and stress signaling in roots, and FIT-dependent and -independent gene signatures. *J. Exp. Bot.*, *71*(5), 1694-1705.
- Séguéla, M., Briat, J.F., Vert, G., & Curie, C. (2008). Cytokinins negatively regulate the root iron uptake machinery in Arabidopsis through a growth-dependent pathway. *Plant J.*, *55*(2), 289-300.
- Seguela, M., Briat, J.F., Vert, G., & Curie, C. (2008). Cytokinins negatively regulate the root iron uptake machinery in *Arabidopsis* through a growth-dependent pathway. *Plant J.*, *55*, 289-300.
- Selote, D., Samira, R., Matthiadis, A., Gillikin, J.W., & Long, T.A. (2015). Iron-binding E3 ligase mediates iron response in plants by targeting basic helix-loop-helix transcription factors. *Plant Physiol.*, *167*, 273-286.
- Shikha, D., Jakhar, P., & Satbhai, S.B. (2023). Role of jasmonate signaling in the regulation of plant responses to nutrient deficiency. *J. Exp. Bot.*, *74*(4), 1221-1243.
- Shin, R., Jez, J.M., Basra, A., Zhang, B., & Schachtman, D.P. (2011). 14-3-3 proteins fine-tune plant nutrient metabolism. *FEBS Lett.*, *585*(1), 143-7.
- Shin, H., Shin, H.S., Dewbre, G.R., & Harrison, M.J. (2004). Phosphate transport in Arabidopsis: Pht1;1 and Pht1;4 play a major role in phosphate acquisition from both low- and high-phosphate environments. *Plant J.* *39*, 629-642.
- Shin, L.J., Lo, J.C., Chen, G.H., Callis, J., Fu, H., & Yeh, K.C. (2013). IRT1 degradation factor1, a ring E3 ubiquitin ligase, regulates the degradation of iron-regulated transporter1 in Arabidopsis. *Plant Cell*, *25*, 3039-3051.

- Singh, A.P., Fridman, Y., Holland, N., Ackerman-Lavert, M., Zananiri, R., Jaillais, Y., Henn, A., & Savaldi-Goldstein, S. (2018). Interdependent Nutrient Availability and Steroid Hormone Signals Facilitate Root Growth Plasticity. *Dev. Cell.*, 46(1), 59-72.
- Slovak, R., Setzer, C., Roiuk, M., Bertels, J., Göschl, C., Jandrasits, K., Beemster, G.T.S., & Busch, W. (2020). Ribosome assembly factor Adenylate Kinase 6 maintains cell proliferation and cell size homeostasis during root growth. *New Phytol.*, 225(5), 2064-2076.
- Smith, M.R., Reis Hodecker, B.E., Fuentes, D., Merchant, A. (2022). Investigating Nutrient Supply Effects on Plant Growth and Seed Nutrient Content in Common Bean. *Plants (Basel)*, 11(6), 737.
- Srivastava, A.K., Senapati, D., Srivastava, A., Chakraborty, M., Gangappa, S.N., & Chattopadhyay, S. (2015). Short Hypocotyl in White Light1 Interacts with Elongated Hypocotyl5 (HY5) and Constitutive Photomorphogenic1 (COP1) and Promotes COP1-Mediated Degradation of HY5 during Arabidopsis Seedling Development. *Plant Physiol.*, 169(4), 2922-34.
- Staswick, P.E., & Tiryaki, I. (2004). The oxylipin signal jasmonic acid is activated by an enzyme that conjugates it to isoleucine in Arabidopsis. *Plant Cell*, 16, 2117-2127.
- Stone, S.L., & Callis, J. (2007). Ubiquitin ligases mediate growth and development by promoting protein death. *Curr. Opin. Plant Biol.*, 10, 624-632.
- Stone S.L. (2019). Role of the ubiquitin proteasome system in plant response to abiotic stress. *Int. Rev. Cell Mol. Biol.* 343, 66-95.
- Stone, S.L., Hauksdóttir, H., Troy, A., Herschleb, J., Kraft, E., & Callis, J. (2005). Functional analysis of the RING-type ubiquitin ligase family of Arabidopsis. *Plant Physiol.*, 137(1), 13-30.
- Su, S.H., Keith, M.A., & Masson, P.H. (2020). Gravity Signaling in Flowering Plant Roots. *Plants (Basel)*, 9(10), 1290.
- Sugimura, Y., Kawahara, A., Maruyama, H., & Ezawa, T. (2022). Plant Foraging Strategies Driven by Distinct Genetic Modules: Cross-Ecosystem Transcriptomics Approach. *Front Plant Sci.*, 13, 903539.
- Sun, Y., Fan, X.Y., Cao, D.M., Tang, W., He, K., Zhu, J.Y., He, J.X., Bai, M.Y., Zhu, S., Oh, E., Patil, S., Kim, T.W., Ji, H., Wong, W.H., Rhee, S.Y., & Wang, Z.Y. (2010). Integration of brassinosteroid signal transduction with the transcription network for plant growth regulation in Arabidopsis. *Dev. Cell.*, 19(5), 765-77.

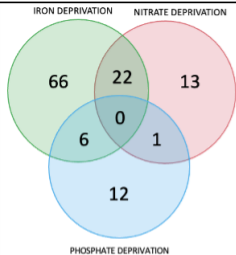
- Tang, W., Kim, T.W., Oses-Prieto, J.A., Sun, Y., Deng, Z., Zhu, S., Wang, R., Burlingame, A.L., & Wang, Z.Y. (2008). BSKs mediate signal transduction from the receptor kinase BRI1 in Arabidopsis. *Science*, 321(5888), 557-60.
- Tarantino, D., Petit, J.M., Lobreaux, S., Briat, J.F., Soave, C., & Murgia, I. (2003). Differential involvement of the IDRS cis-element in the developmental and environmental regulation of the AtFer1 ferritin gene from Arabidopsis. *Planta*, 217(5), 709-16.
- Thomine, S., Lelièvre, F., Debarbieux, E., Schroeder, J.I., & Barbier-Brygoo, H. (2003). AtNRAMP3, a multispecific vacuolar metal transporter involved in plant responses to iron deficiency. *Plant J*, 34, 685-695
- Thrower, J.S., Hoffman, L., Rechsteiner, M., & Pickart, C.M. (2000). Recognition of the polyubiquitin proteolytic signal. *EMBO J*, 19, 94-102.
- Tripathi, R., Tewari, R., Singh, K.P., Keswani, C., Minkina, T., Srivastava, A.K., De Corato, U., & Sansinenea, E. (2022). Plant mineral nutrition and disease resistance: A significant linkage for sustainable crop protection. *Front. Plant Sci.*, 13, 883970.
- Trujillo, M., & Shirasu, K. (2010). Ubiquitin in plant immunity. *Curr. Opin. Plant Biol.*, 13, 402-408.
- Varadan, R., Walker, O., Pickart, C., & Fushman, D. (2002). Structural properties of Polyubiquitin chains in solution. *J. Mol. Biol.*, 324, 637-647.
- Vert, G., Briat, J.F., Curie, C. (2001). Arabidopsis IRT2 gene encodes a root-periphery iron transporter. *Plant J*, 26(2), 181-9.
- Vert, G., Grotz, N., Dédaldéchamp, F., Gaymard, F., Guerinot, M.L., Briat J.F., & Curie, C. (2002). IRT1, an Arabidopsis transporter essential for iron uptake from the soil and for plant growth. *Plant Cell*, 14, 1223-1233.
- Vierstra, R.D. (2009). The ubiquitin-26S proteasome system at the nexus of plant biology. *Nat. Rev. Mol. Cell Biol.*, 10, 385-397.
- Vierstra, R.D. (2012). The expanding universe of ubiquitin and ubiquitin-like modifiers. *Plant Physiol.*, 160, 2-14.
- Walsh, M., Schenk, G. & Schmidt, S. (2023). Realising the circular phosphorus economy delivers for sustainable development goals. *npj Sustain. Agric.*, 1, 2.
- Xiao, Y., Chu, L., Zhang, Y., Bian, Y., Xiao, J., Xu, D. (2022). HY5: A Pivotal Regulator of Light-Dependent Development in Higher Plants. *Front. Plant Sci.*, 12, 800989.

- Xie, L., Lang-Mladek, C., Richter, J., Nigam, N., Hauser, M.T. (2015). UV-B induction of the E3 ligase ARIADNE12 depends on CONSTITUTIVELY PHOTOMORPHOGENIC 1. *Plant Physiol. Biochem.*, 93, 18-28.
- Xie, L., & Hauser, M.T. (2012). Induction of *ARI12* upon broad band UV-B radiation is suppressed by UVR8 and cryptochromes. *Plant Signal. Behav.*, 7, 1411-1414.
- Yasuda, S., Sato, T., Maekawa, S., Aoyama, S., Fukao, Y., & Yamaguchi, J. (2014). Phosphorylation of Arabidopsis ubiquitin ligase ATL31 is critical for plant carbon/nitrogen nutrient balance response and controls the stability of 14-3-3 proteins. *J. Biol. Chem.*, 289(22), 15179-93.
- Yasuda, S., Aoyama, S., Hasegawa, Y., Sato, T., & Yamaguchi, J. (2017). Arabidopsis CBL-interacting protein kinases regulate carbon/nitrogen-nutrient response by phosphorylating ubiquitin ligase ATL31. *Mol. Plant*, 10, 605-618.
- Yates, G., & Sadanandom, A. (2013). Ubiquitination in plant nutrient utilization. *Front. Plant Sci.*, 4, 452.
- Ye, Q., Wang, H., Su, T., Wu, W.H., & Chen, Y.F. (2018). The ubiquitin E3 ligase PRU1 regulates WRKY6 degradation to modulate phosphate homeostasis in response to low-pi stress in Arabidopsis. *Plant Cell*, 30, 1062-1076.
- Yi, Y., & Guerinot, M.L. (1996). Genetic evidence that induction of root Fe(III) chelate reductase activity is necessary for iron uptake under iron deficiency. *Plant J.*, 10(5), 835-44.
- Yin, Y., Wang, Z.Y., Mora-Garcia, S., Li, J., Yoshida, S., Asami, T., & Chory, J. (2002). BES1 accumulates in the nucleus in response to brassinosteroids to regulate gene expression and promote stem elongation. *Cell.*, 109, 181-191.
- Yuan, L., Loqué, D., Kojima, S., Rauch, S., Ishiyama, K., Inoue, E., Takahashi, H., & von Wirén, N. (2007). The organization of high-affinity ammonium uptake in Arabidopsis roots depends on the spatial arrangement and biochemical properties of AMT1-type transporters. *Plant Cell.*, 19(8), 2636-52.
- Zahra, N., Hafeez, M.B., Shaukat, K., Wahid, A., & Hasanuzzaman, M. (2021). Fe toxicity in plants: Impacts and remediation. *Physiologia Plantarum*, 173(1), 201-222.
- Zelazny, E., Barberon, M., Curie, C., & Vert, G. (2011). Ubiquitination of transporters at the forefront of plant nutrition. *Plant Signal. Behav.*, 6(10), 1597-9.
- Zhang, C. (2014). Essential functions of iron-requiring proteins in DNA replication, repair and cell cycle control. *Protein Cell*, 5, 750-760.

- Zhang, H., Yang, Y., Sun, C., Liu, X., Lv, L., Hu, Z., Yu, D., & Zhang, D. (2020). Up-regulating *GmETO1* improves phosphorus uptake and use efficiency by promoting root growth in soybean. *Plant Cell Environ.*, 43(9), 2080-2094.
- Zhang, Z., Hu, B., & Chu, C. (2020). Towards understanding the hierarchical nitrogen signalling network in plants. *Curr. Opin. Plant Biol.*, 55, 60-65.
- Zheng, Z.L. (2009). Carbon and nitrogen nutrient balance signaling in plants. *Plant Signal Behav.*, 4(7), 584-91.
- Zluhan-Martínez, E., López-Ruíz, B.A., García-Gómez, M.L., García-Ponce, B., de la Paz Sánchez, M., Álvarez-Buylla, E.R., & Garay-Arroyo, A. (2021). Integrative Roles of Phytohormones on Cell Proliferation, Elongation and Differentiation in the *Arabidopsis thaliana* Primary Root. *Front. Plant Sci.*, 12.

APPENDIX A: Selecting candidate RING-type E3s

This project started with 14 E3s that were selected based on microarray expression data obtained from public databases (Figure A1; Figure A2). These 14 E3s showed a decrease or increase in gene expression in wild type *Arabidopsis thaliana* ecotype Columbia (WT, *Col-0*), when exposed to iron (Fe), phosphate (PO₄⁻), or nitrate (NO₃⁻) deficiency, and some had known interactors (Table A1; Table A2). SALK T-DNA insertion mutant seeds (Table A3) for each of the 14 E3s were obtained from the Arabidopsis Biological Resource Center (ABRC, <https://abrc.osu.edu/>). Homozygous T-DNA loss-of-function mutants were found for eight of the 14 E3s. These eight E3s moved on to further analysis.



	Heat	Cold	Salt	Dehydration	Hypoxia	Iron deprivation (94)	Nitrate deprivation (36)	Phosphate deprivation (19)	Ozone	UV-b	Genotoxic	Bacteria	Fungi	Virus	Chitin	fig22
Abscisic acid (ABA)	39	38	54	51	21	40	14	16	40	15	19	54	53	4	14	16
Heat		33	44	42	24	32	10	12	29	19	21	41	39	2	12	8
Cold			50	40	15	38	13	10	31	22	21	44	45	1	11	9
Salt				57	23	61	20	12	42	29	31	67	73	4	13	18
Dehydration					19	43	13	14	32	22	25	55	55	2	15	13
Hypoxia						20	4	8	18	9	23	20	24	2	6	5
Iron deprivation							22	6	25	23	22	41	55	2	5	7
Nitrate deprivation								1	6	6	8	13	22	0	1	1
Phosphate deprivation									13	4	6	13	13	2	12	6
Ozone										12	13	68	51	2	16	24
UV-b											14	22	20	1	2	6
Genotoxic												26	26	3	3	6
Bacteria													74	4	18	23
Fungi														4	15	21
Virus															2	1
Chitin																6

Figure A1. Compilation of data from microarray analysis showing number of RING-type E3s that showed differential gene expression under various abiotic and biotic stresses. Two expression databases were used: Toronto BAR (<https://bar.utoronto.ca>) and Expression Atlas (<https://www.ebi.ac.uk/gxa/plant/experiments>).

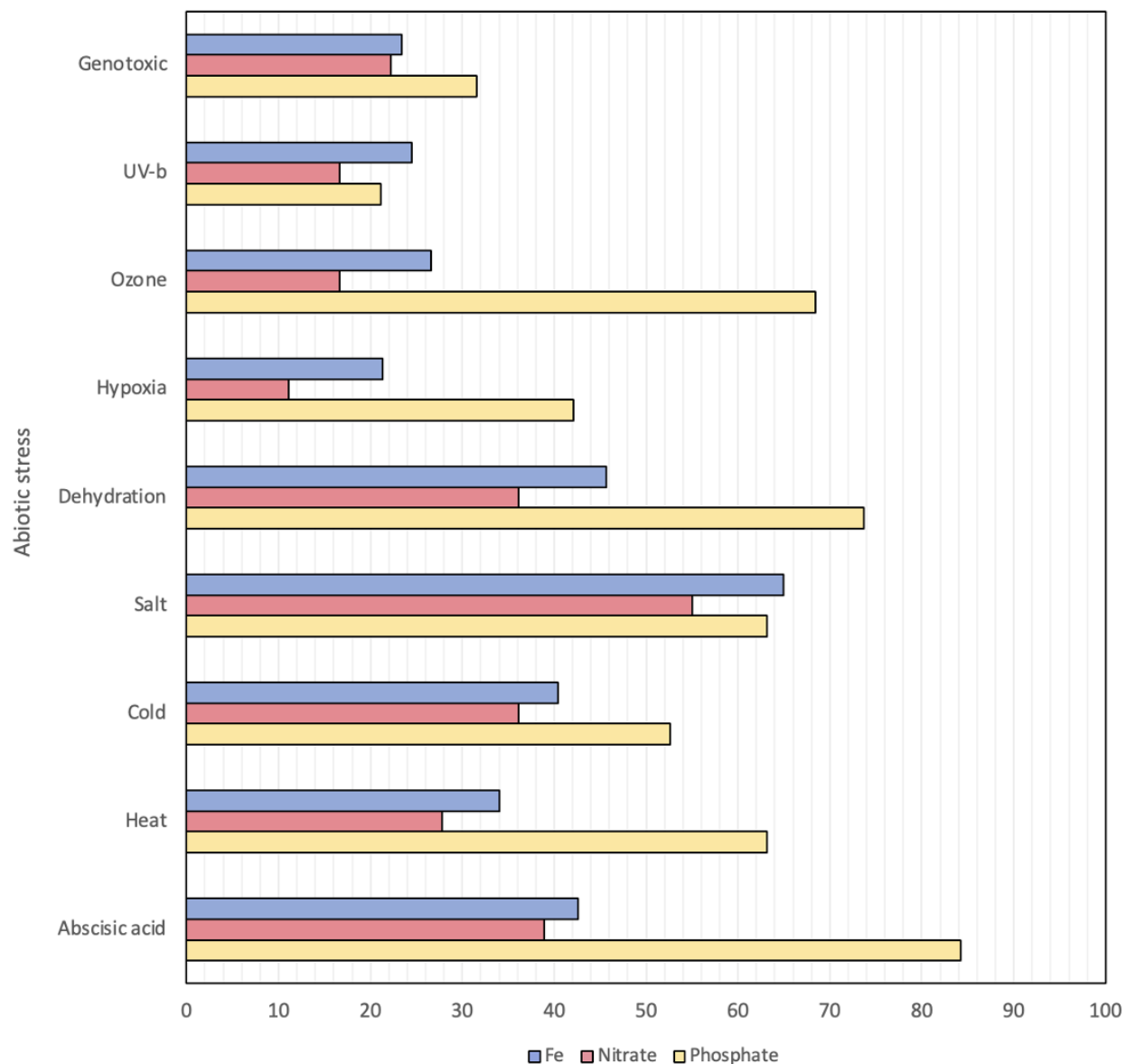


Figure A2. Graph showing the percent of RING-Type E3s that were found to be differently expressed under iron (Fe), nitrate (NO_3^-), or phosphate (PO_4^-) deficiency as well as another abiotic stress. E.g. 84.2% of E3s that were differently expressed under PO_4^- deficiency were differently expressed under abscisic acid (ABA) stress.

RING E3	Gene name	Fe Deprivation	N limitation	P Deprivation
At2g22680	WAVH1			
At2g20030	ATL12			

At2g31780	ARI11			
At1g14260	ERiN1			
At1g05880	ARI12			
At1g70910	DEP			
At5g01070	ERiN2			
At2g38920	ERiN3			
At4g09110	ATL35			
At1g18910	BTSL2			
At5g03180	ERiN4			
At5g06490	ATL71			
At5g37910	SINA-like 9			
At5g58580	ATL63			

Table A1. Microarray analysis of E3 gene expression under iron (Fe), phosphate (PO₄⁻), and nitrate (NO₃⁻) deprivation; blue indicates a decrease and red indicates an increase in gene expression in wild type *Arabidopsis thaliana* ecotype Columbia.

RING E3		Interactors found	FIT regulated
At2g22680	WAVH1	ACBP4, At3g03000, AAK6, BSK2, KNAT1, MAP70-5	
At2g20030	ATL12	GRF3	yes
At2g31780	ARI11		
At1g14260	ERiN1	At1g29060, At1g63110, At2g27290, At3g12180, At3g66654, At4g20790, At5g49540, At5g59650, HHP4, MKK10, RBL11, UBC34, VPS60.1, FRD3	
At1g05880	ARI12	ARI12	
At1g70910	DEP	HSP23.6-MITO	
At5g01070	ERiN2		
At2g38920	ERiN3		
At4g09110	ATL35		yes
At1g18910	BTSL2		yes

At5g03180	ERiN4	At1g19240, At2g42390, D6PK, ROP10, FRB3	
At5g06490	ATL71		yes
At5g37910	SINA-like 9		
At5g58580	ATL63		

Table A2. Interaction data gathered using the public interaction databases BioGRID (<https://thebiogrid.org/>) and IntAct (<https://www.ebi.ac.uk/intact/home>) for all 14 candidate RING-type E3s selected for this project.

Gene	Gene Name	SALK Line
At2g22680	WAVH1	SALK_149664 (<i>wavh1-1</i>), SALK_041291 (<i>wavh1-2</i>)
At2g20030	ATL12	SALK_066923 (<i>atl12-1</i>), SALK_201056 (<i>atl12-2</i>)
At2g31780	ARI11	CS24734
At1g14260	ERiN1	SALK_118406
At1g05880	ARI12	SALK_033142 (<i>ari12-1</i>), SALK_034258 (<i>ari12-2</i>)
At1g70910	DEP	SALK_141707
At5g01070	ERiN2	SALK_086525
At2g38920	ERiN3	SALK_129778
At4g09110	ATL35	SALK_065995
At1g18910	BTSL2	SALK_048470
At5g03180	ERiN4	SALK_023683
At5g06490	ATL71	CS863433
At5g37910	SINA-like 9	SALK_023901
At5g58580	ATL63	SALK_139444

Table A3. The 14 selected candidate RING-type E3s which are possibly involved in maintaining nutrient homeostasis, and the corresponding T-DNA insertion mutant SALK lines which were ordered from ABRC (<https://abrc.osu.edu/>).

APPENDIX B: Phenotypic analysis of RING-type E3 mutants in nutrient stress assays

Eight SALK T-DNA insertion mutant lines, each targeting one of eight candidate RING-type E3s, were put through stress assays where they were exposed to sufficient, deficient, and excess levels of iron (Fe), phosphorus (P), and nitrogen (N). All eight mutant lines showed some sort of differential growth when compared to wild type *Arabidopsis thaliana* ecotype Columbia (WT, *Col-0*) phenotypically on at least one of the six nutrient stress treatments. Three of the eight E3s were selected for further analysis and were discussed in Chapter 1 and 2. Stress assay results for the other five are included in this appendix.

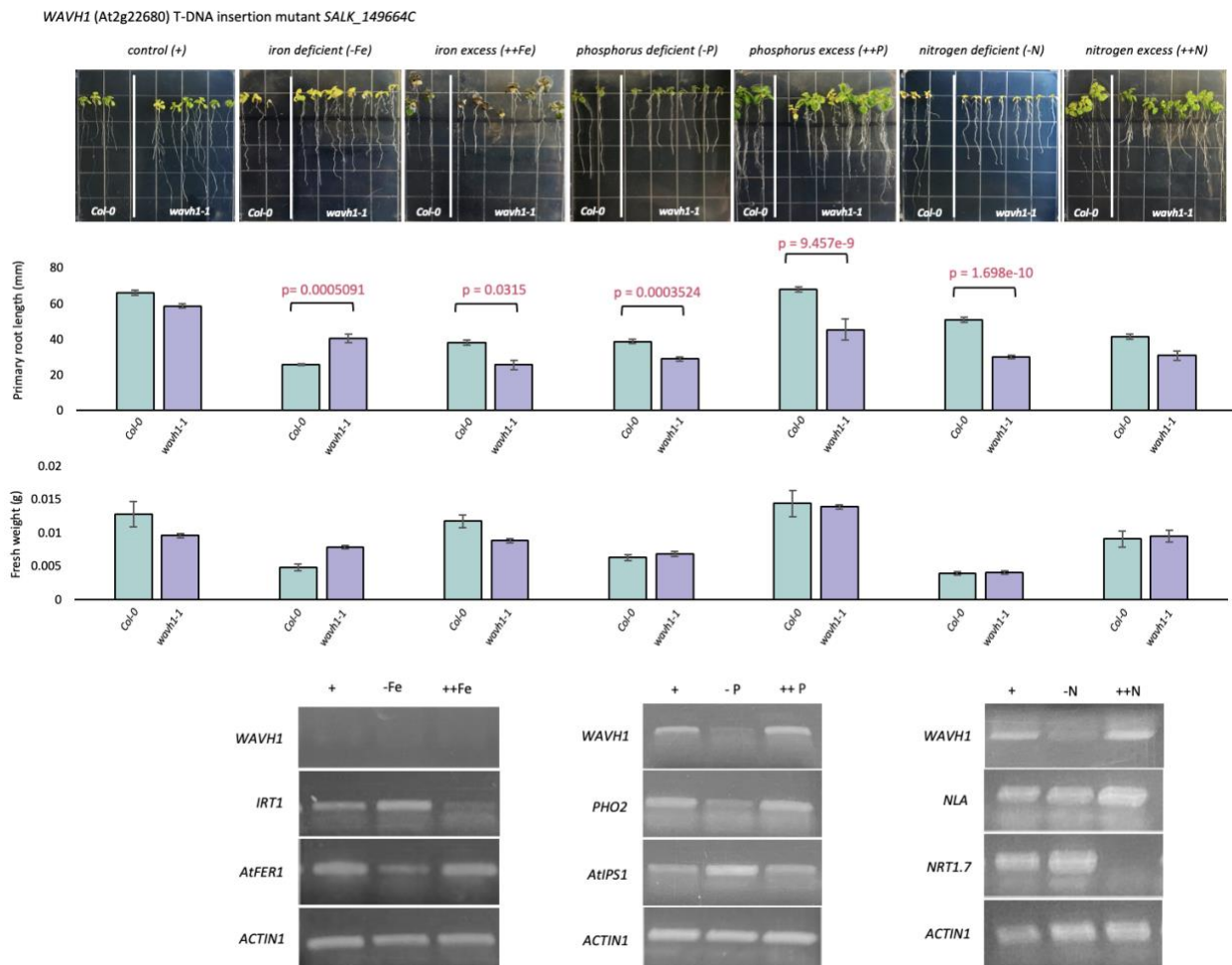


Figure B1. 15-day old *wavh1-1* and wild type (*Col-0*, WT) seedlings that were grown for five days on nutrient sufficient (control, +) media then 10 days on control, Fe deficient (-Fe), Fe excess (++Fe), P deficient (-P), P excess (++P), N deficient (-N), and N excess (++N) media. Primary root lengths and fresh weight were measured at the end of the 10-day treatment period using ImageJ®

(<http://imagej.net>). Analysis was done using One-Way ANOVA Tukey comparison. Error bars indicate \pm SE from at least one trial with at least three replicates per trial (≥ 24). *WAVH1* loss-of-function mutants showed a differential phenotype under -Fe, ++Fe, -P, ++P, and -N. *WAVH1* expression was analyzed using RNA extracted from WT seedlings that were grown on control for five days then for 10 days on control, -Fe, ++Fe, -P, ++P, -N, and ++N.

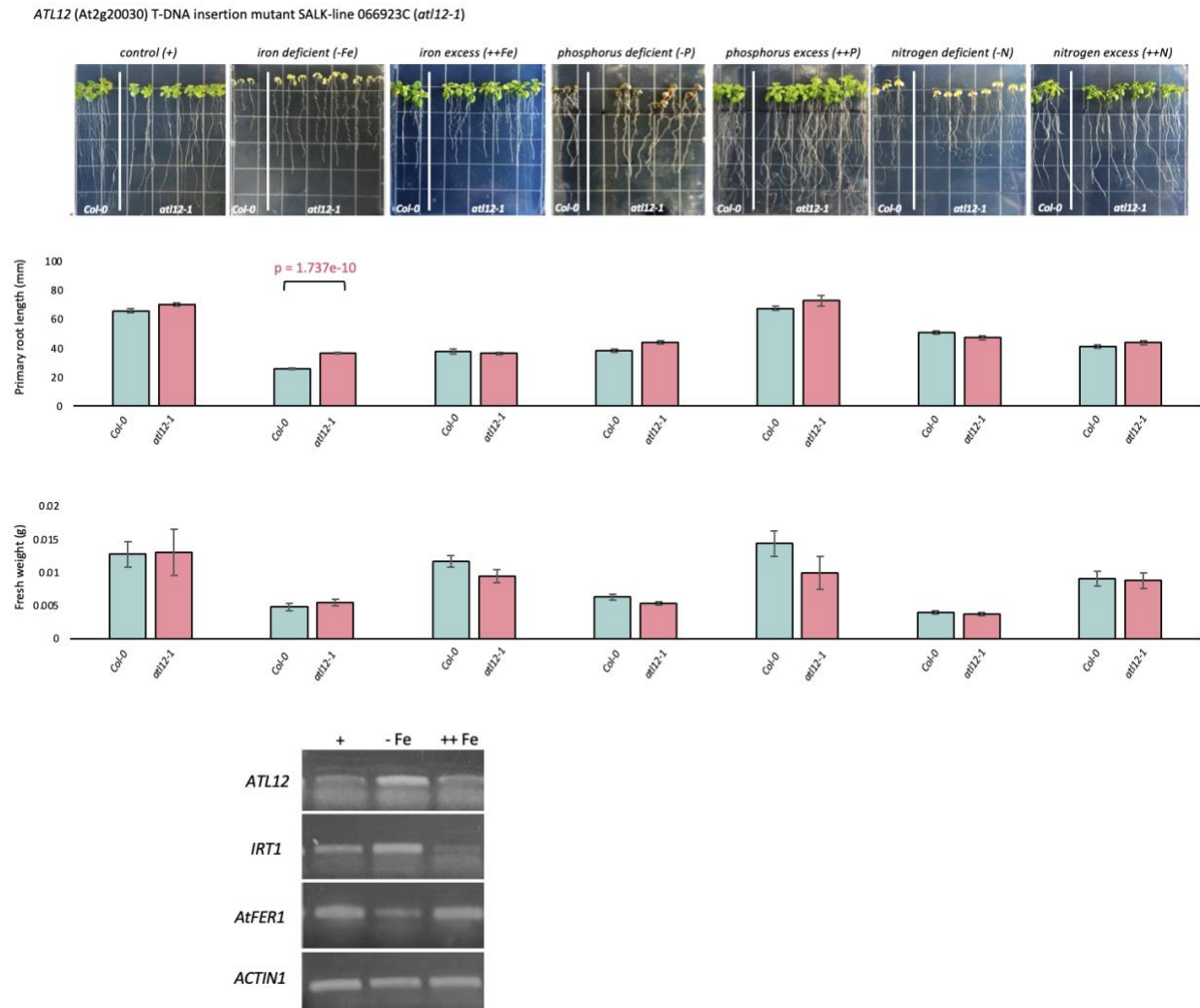


Figure B2. 15-day old *atl12-1* and wild type. (*Col-0*, WT) seedlings that were grown for five days on nutrient sufficient (control, +) media then 10 days on control, Fe deficient (-Fe), Fe excess (++Fe), P deficient (-P), P excess (++P), N deficient (-N), and N excess (++) media. Primary root lengths and fresh weight were measured at the end of the 10-day treatment period using ImageJ® (<http://imagej.net>). Analysis was done using One-Way ANOVA Tukey comparison. Error bars indicate \pm SE from at least one trial with at least three replicates per trial (≥ 24). *ATL12* loss-of-

function mutants showed a differential phenotype under -Fe. *ATL12* expression was analyzed using RNA extracted from WT seedlings that were grown on control for five days then for 10 days on control, -Fe and ++Fe.

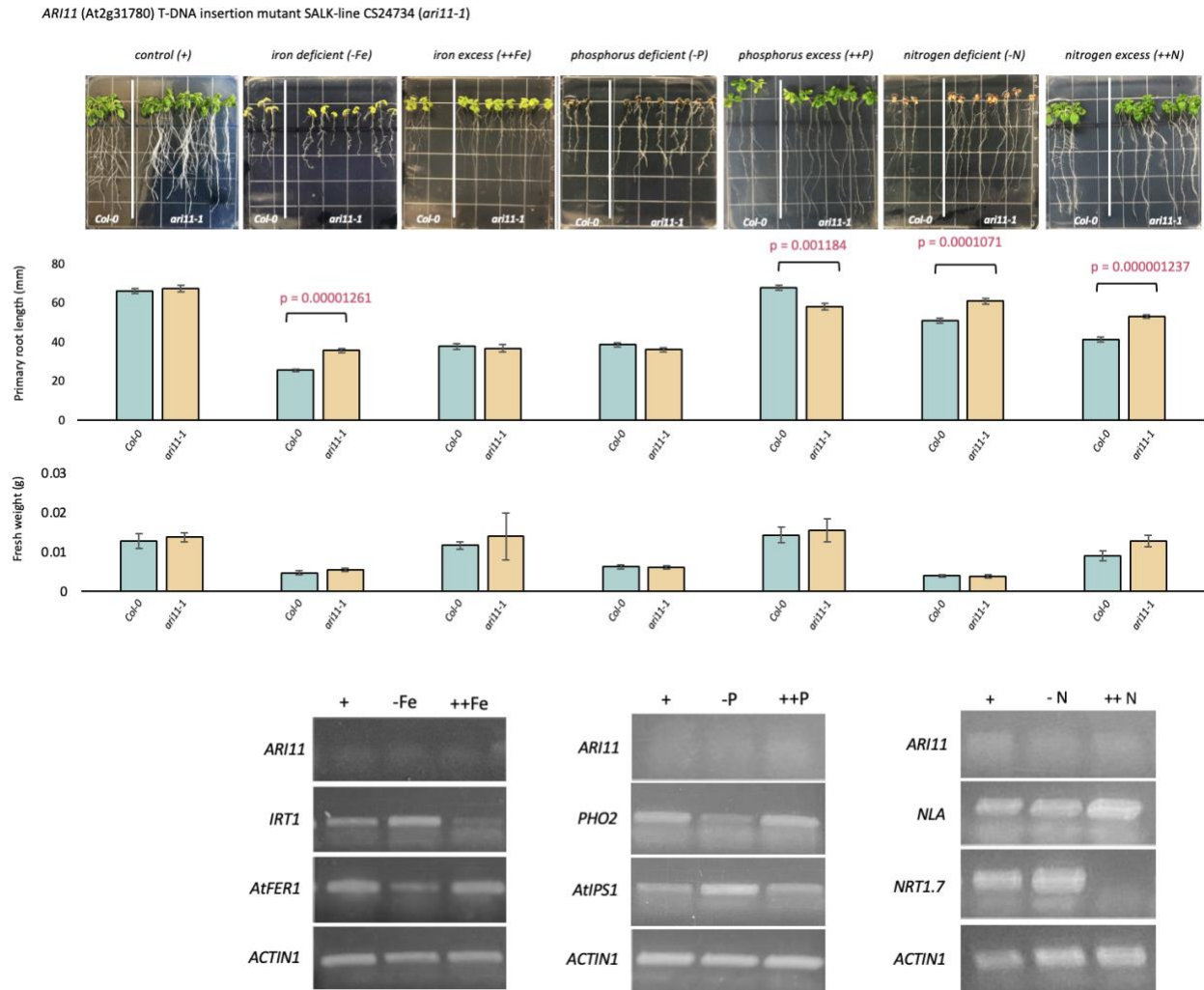


Figure B3. 15-day old *ari11-1* and wild type. (*Col-0*, WT) seedlings that were grown for five days on nutrient sufficient (control, +) media then 10 days on control, Fe deficient (-Fe), Fe excess (++Fe), P deficient (-P), P excess (++P), N deficient (-N), and N excess (++N) media. Primary root lengths and fresh weight were measured at the end of the 10-day treatment period using ImageJ® (<http://imagej.net>). Analysis was done using One-Way ANOVA Tukey comparison. Error bars indicate \pm SE from at least one trial with at least three replicates per trial (≥ 24). *WAVH1* loss-of-function mutants showed a differential phenotype under -Fe, ++P, -N, and ++N. *ARI11* expression was analyzed using RNA extracted from WT seedlings that were grown on control for five days then for 10 days on control, -Fe, ++Fe, -P, ++P, -N, and ++N.

At1g14260 T-DNA insertion mutant SALK-line 118406C (*erin1-1*)

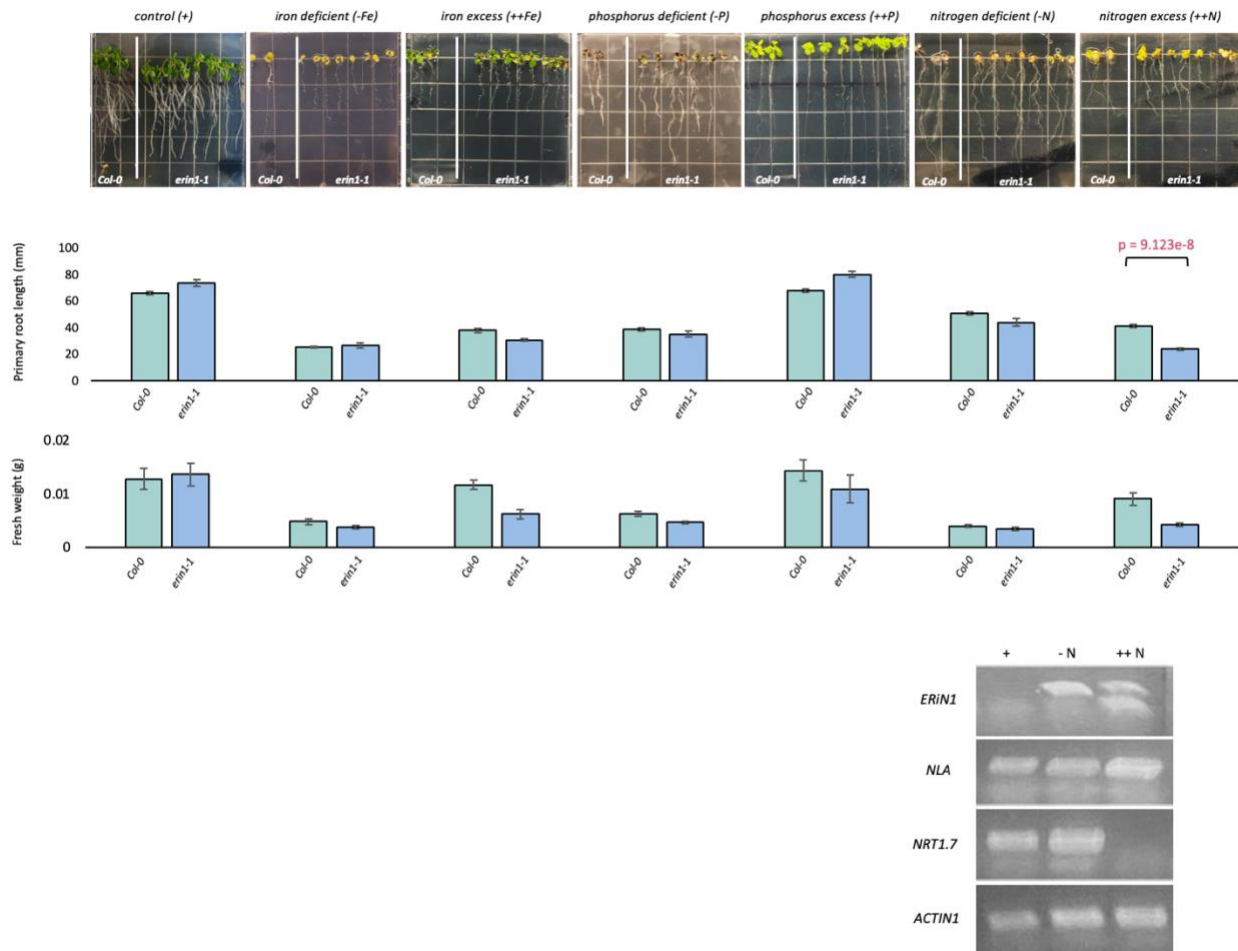


Figure B4. 15-day old *erin1-1* and wild type (*Col-0*, WT) seedlings that were grown for five days on nutrient sufficient (control, +) media then 10 days on control, Fe deficient (-Fe), Fe excess (++Fe), P deficient (-P), P excess (++P), N deficient (-N), and N excess (++N) media. Primary root lengths and fresh weight were measured at the end of the 10-day treatment period using ImageJ® (<http://imagej.net>). Analysis was done using One-Way ANOVA Tukey comparison. Error bars indicate \pm SE from at least one trial with at least three replicates per trial (≥ 24). *ERIN1* loss-of-function mutants showed a differential phenotype under ++N. *ERIN1* expression was analyzed using RNA extracted from WT seedlings that were grown on control for five days then for 10 days on control, -N, and ++N.

ARI12 (At1g05880) T-DNA insertion mutant SALK_033142C

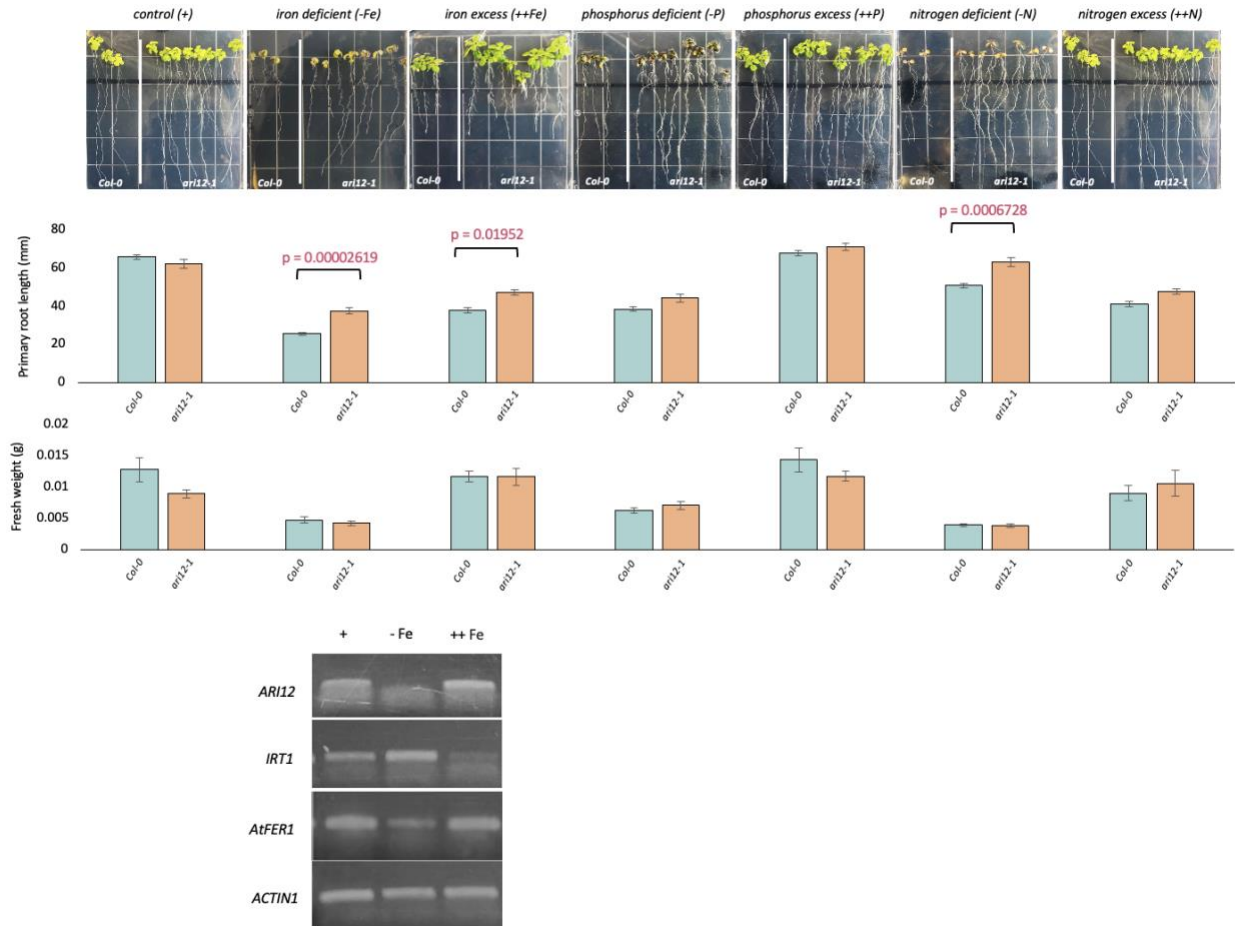


Figure B5. 15-day old *ari12-1* and wild type. (*Col-0*, WT) seedlings that were grown for five days on nutrient sufficient (control, +) media then 10 days on control, Fe deficient (-Fe), Fe excess (++Fe), P deficient (-P), P excess (++P), N deficient (-N), and N excess (++N) media. Primary root lengths and fresh weight were measured at the end of the 10-day treatment period using ImageJ® (<http://imagej.net>). Analysis was done using One-Way ANOVA Tukey comparison. Error bars indicate \pm SE from at least one trial with at least three replicates per trial (≥ 24). *ARI12* loss-of-function mutants showed a differential phenotype under -Fe, ++Fe, and -N. *ARI12* expression was analyzed using RNA extracted from WT seedlings that were grown on control for five days then for 10 days on control, -Fe, and ++Fe.

DEP (At1g70910) T-DNA insertion mutant SALK_141707C

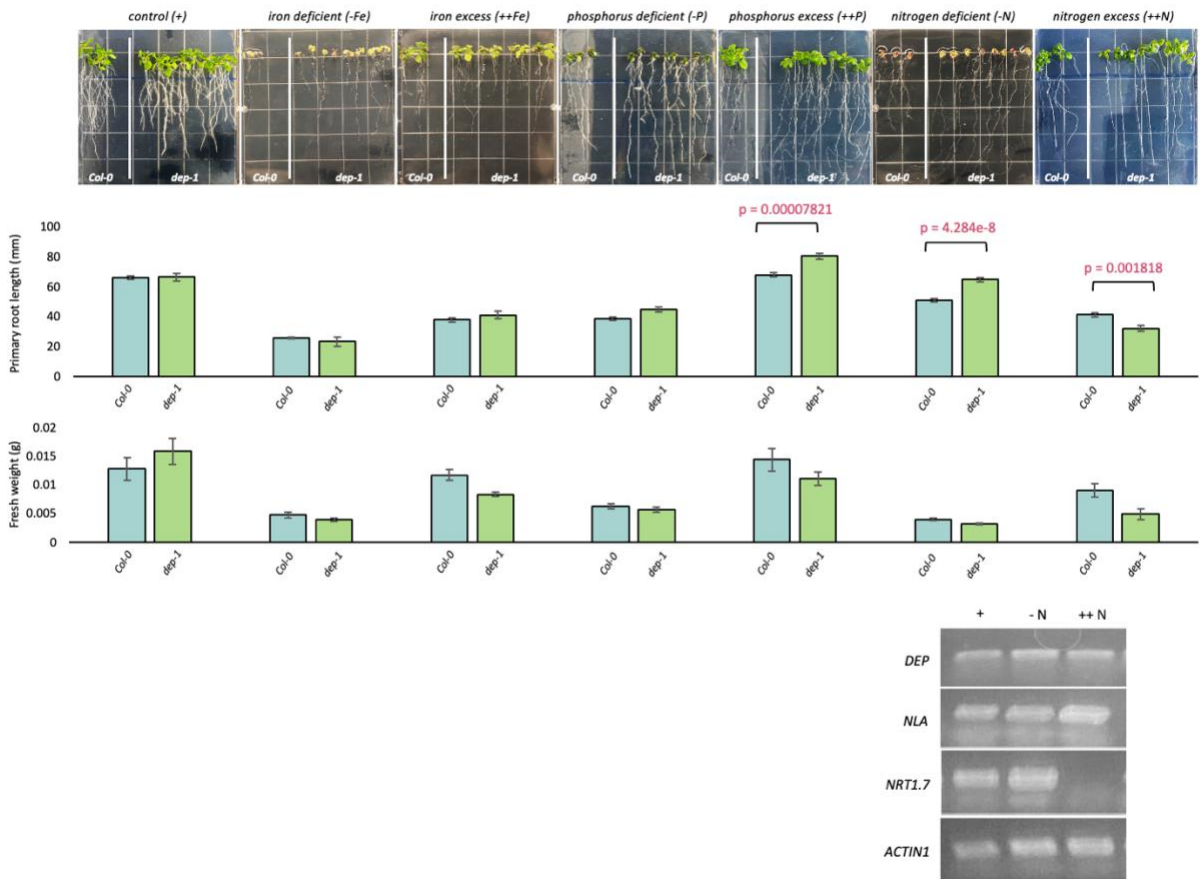


Figure B6. 15-day old *dep1-1* and wild type (*Col-0*, WT) seedlings that were grown for five days on nutrient sufficient (control, +) media then 10 days on control, Fe deficient (-Fe), Fe excess (++Fe), P deficient (-P), P excess (++P), N deficient (-N), and N excess (++N) media. Primary root lengths and fresh weight were measured at the end of the 10-day treatment period using ImageJ® (<http://imagej.net>). Analysis was done using One-Way ANOVA Tukey comparison. Error bars indicate \pm SE from at least one trial with at least three replicates per trial (≥ 24). *DEP1* loss-of-function mutants showed a differential phenotype under ++P, -N, and ++N. *DEP1* expression was analyzed using RNA extracted from WT seedlings that were grown on control for five days then for 10 days on control, -N, and ++N.

At5g01070 T-DNA insertion mutant SALK-line 086525C (*erin2-1*)

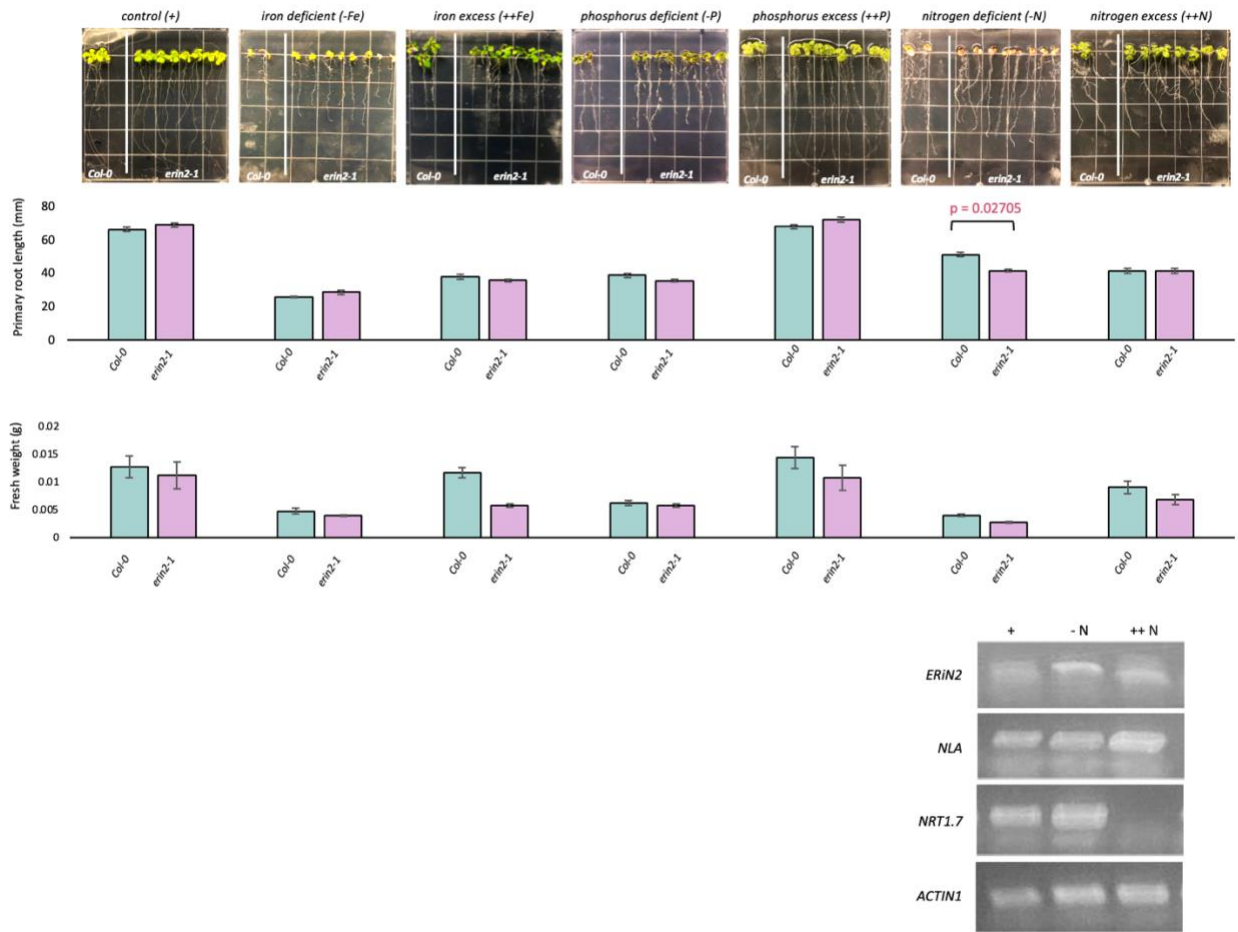


Figure B7. 15-day old *erin2-1* and wild type (*Col-0*, WT) seedlings that were grown for five days on nutrient sufficient (control, +) media then 10 days on control, Fe deficient (-Fe), Fe excess (++Fe), P deficient (-P), P excess (++P), N deficient (-N), and N excess (++N) media. Primary root lengths and fresh weight were measured at the end of the 10-day treatment period using ImageJ® (<http://imagej.net>). Analysis was done using One-Way ANOVA Tukey comparison. Error bars indicate \pm SE from at least one trial with at least three replicates per trial (≥ 24). *ERIN2* loss-of-function mutants showed a differential phenotype under -N. *ERIN2* expression was analyzed using RNA extracted from WT seedlings that were grown on control for five days then for 10 days on control, -N, and ++N.

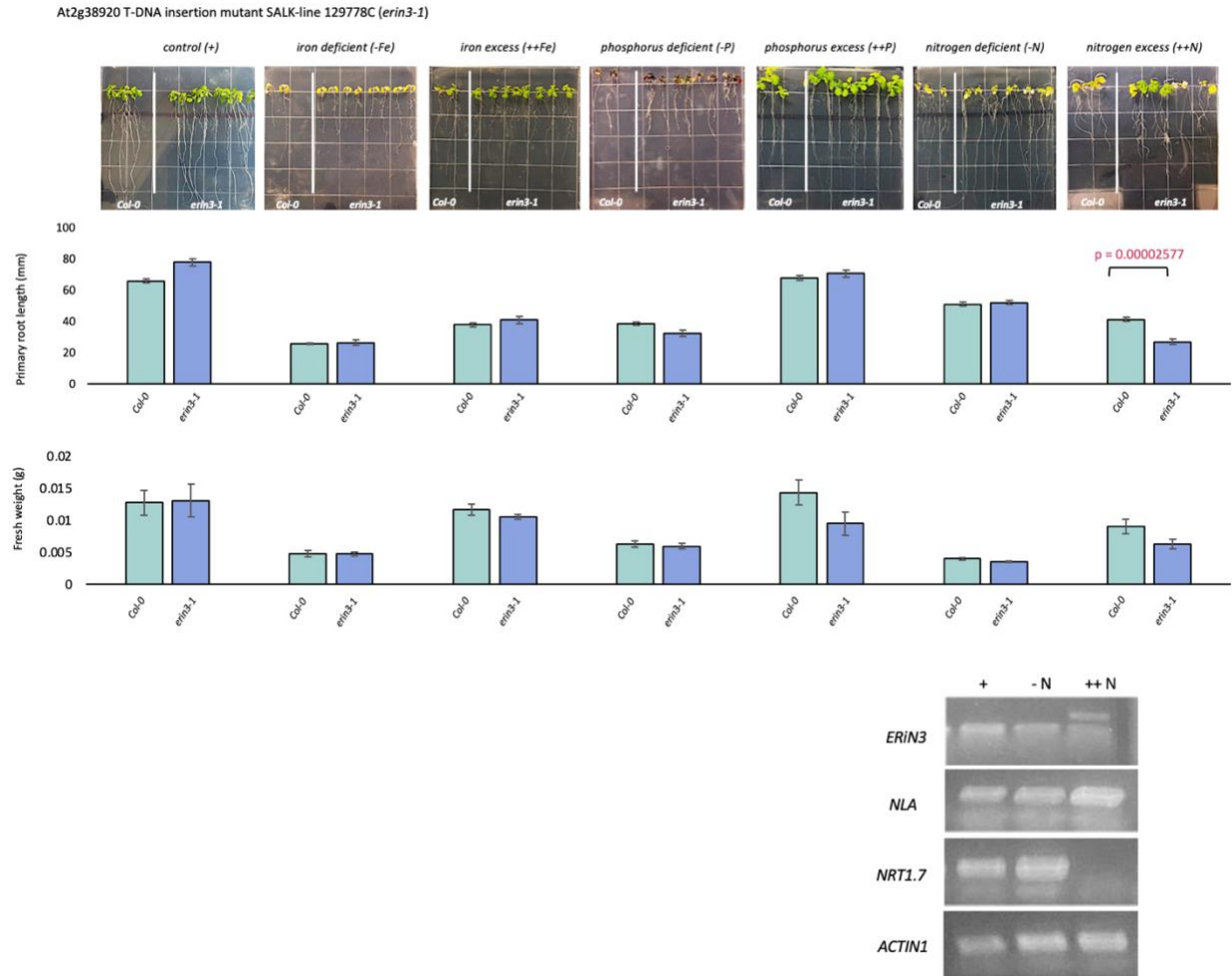


Figure B8. 15-day old *erin3-1* and wild type (*Col-0*, WT) seedlings that were grown for five days on nutrient sufficient (control, +) media then 10 days on control, Fe deficient (-Fe), Fe excess (++Fe), P deficient (-P), P excess (++P), N deficient (-N), and N excess (++N) media. Primary root lengths and fresh weight were measured at the end of the 10-day treatment period using ImageJ® (<http://imagej.net>). Analysis was done using One-Way ANOVA Tukey comparison. Error bars indicate \pm SE from at least one trial with at least three replicates per trial (≥ 24). *ERIN3* loss-of-function mutants showed a differential phenotype under ++N. *ERIN3* expression was analyzed using RNA extracted from WT seedlings that were grown on control for five days then for 10 days on control, -N, and ++N.

APPENDIX C: Review Article: The Ubiquitin Proteasome System and Nutrient Stress

Response

The Ubiquitin Proteasome System and Nutrient Stress Response

*Erin Mackinnon and Sophia L. Stone**

Department of Biology, Dalhousie University, Halifax, NS, Canada

Plants utilize different molecular mechanisms, including the Ubiquitin Proteasome System (UPS) that facilitates changes to the proteome, to mitigate the impact of abiotic stresses on growth and development. The UPS encompasses the ubiquitination of selected substrates followed by the proteasomal degradation of the modified proteins. Ubiquitin ligases, or E3s, are central to the UPS as they govern specificity and facilitate the attachment of one or more ubiquitin molecules to the substrate protein. From recent studies, the UPS has emerged as an important regulator of the uptake and translocation of essential macronutrients and micronutrients. In this review, we discuss select E3s that are involved in regulating nutrient uptake and responses to stress conditions, including limited or excess levels of nitrogen, phosphorus, iron, and copper.

Keywords: ubiquitination, 26S proteasome, ubiquitin ligase, protein degradation, abiotic stress, nutrient stress, nutrient uptake

IMPACT OF ENVIRONMENTAL FACTORS ON NUTRIENT ACQUISITION

Plants must cope with external factors that impact the uptake of nutrients, which are essential for growth, development, and yield. Climate change poses additional challenges to the availability and acquisition of nutrients, further impacting plant health. According to the Intergovernmental Panel on Climate Change (IPCC), global temperature is projected to increase 1.0°C (highest mitigation efforts) to 5.7°C (lowest mitigation efforts) by the end of this century (IPCC, 2021). With climate change, extreme weather events occur more frequently, and the duration and timing of these events become more erratic. High temperatures contribute to drought conditions in many habitats (Mimura, 2013). Increased water vapor in the atmosphere from high temperatures contributes to flooding (Sun et al., 2007; O'Gorman and Schneider, 2009). Rapid warming of the arctic and atmospheric pressure changes cause disruptions to the polar vortex, leading to irregular temperature/weather patterns and colder climates in ecosystems that are not acclimated to low temperatures (Cohen et al., 2020; Overland, 2021). In addition to directly affecting plant health, these climatic shifts affect growth *via* the alteration of soil properties such as pH, which, among other issues, impacts the acquisition of nutrients.

Soil temperature and moisture are two important determinants in the availability and uptake of nutrients. Temperature extremes impact nutrient acquisition by influencing root growth, soil microbial diversity, diffusion of nutrients across the soil, and the level of

nutrients available for uptake (Baon et al., 1994; Pregitzer and King, 2005; Yan et al., 2013; Gelybó et al., 2018; Maharajan et al., 2021). For example, low temperatures reduce phosphorus (P) uptake in corn (*Zea mays*; Mackay and Barber, 1984; McCallister et al., 1997; Maharajan et al., 2021). Similarly, elevated temperature has been shown to decrease P uptake in wheat (*Triticum aestivum*; Kumar et al., 2012; Maharajan et al., 2021). Elevated temperatures and heavy rain caused by climate change has made P deficiency one of the leading restrictive factors for crop growth (López-Arredondo et al., 2014). Root colonization by arbuscular mycorrhizal fungi such as *Glomus mosseae* has been shown to promote uptake of nutrients including P in barley (*Hordeum vulgare*) and zinc (Zn) in red clover (*Trifolium pratense*; Baon et al., 1994; Chen et al., 2003; Wu and Zou, 2010). Low temperature has been shown to reduce mycorrhizal formation limiting the beneficial effects of the fungus on nutrient uptake (Baon et al., 1994; Wu and Zou, 2010). High temperatures contribute to dry soil conditions, which reduces the rate of nutrient diffusion from the rhizosphere to the absorbing surface of the roots (Pregitzer and King, 2005).

Soil salinity is one of the major abiotic factors limiting crop production. Plants grown under high salinity conditions display reduced content and uptake of essential nutrients including P, Zn, nitrogen (N), potassium (K), calcium (Ca), and iron (Fe; Brown et al., 2006; Bano and Fatima, 2009; Etesami and Noori, 2019). Water logging increases soil leaching resulting in loss of nutrient cations and salts, as well as higher soil acidification (Karmakar et al., 2016; Gelybó et al., 2018). Erosion caused by heavy rainfall also depletes soil nutrients (Yao et al., 2021). Plants have an optimal soil pH range for maximum growth, and pH above or below this range has been shown to influence nutrient uptake and content (Islam et al., 1980; Haynes and Swift, 1986; Neina, 2019). Blueberry (*Vaccinium* spp.) grown in soil with pH above optimal (4.0–5.5) had reduced micronutrient (copper [Cu], manganese [Mn], Zn, and Fe), and macronutrient (magnesium [Mg], K, P, Ca) content in leaves (Jiang et al., 2017). Soil pH is also a major determinant of the level of nutrients available for use by plants. For example, Zn and Cu are more readily available in acidic soils (Kabata-Pendias, 2004). Nutritional status is not only essential to plant health but is also important for coping with adverse environments as the detrimental effects of abiotic stresses may be minimized by optimizing nutrition, which influences water circulation, photosynthesis, and other physiological processes (Ahanger and Ahmad, 2019).

Climate change, in addition to the increasing global population, puts immense pressure on agricultural productivity, increasing the urgency for understanding the molecular basis for plant response to abiotic stresses. Plants rely heavily on regulatory mechanisms such as the ubiquitin proteasome system (UPS) to maintain cellular homeostasis and continued growth under adverse conditions. The UPS is used to regulate the function of proteins involved in generating the cellular changes required to respond to the changing environment and mitigate the negative impact of stress (Miricescu et al., 2018; Stone, 2019). This review will discuss the role of the UPS in facilitating nutrient uptake, as well as various components of the UPS which have known or predicted roles in responding to nutrient stress.

THE UBIQUITIN PROTEASOME SYSTEM

The UPS involves the ubiquitination of a selected substrate followed by proteasomal degradation of the modified protein (**Figure 1A**). Ubiquitination is the covalent attachment of ubiquitin (Ub), a small, highly conserved protein, to substrates. The conjugation process requires the sequential actions of three types of enzymes: ubiquitin activating enzyme (E1), ubiquitin conjugating enzyme (E2), and ubiquitin ligase (E3). Degradation of the ubiquitinated protein is accomplished by the 26S proteasome, a large multi-catalytic multi-subunit complex. The system allows plants to efficiently regulate almost every aspect of cellular function *via* the degradation of numerous proteins including enzymes, transporters, ion channels, signaling proteins (e.g., kinases and receptors), and transcription regulators (e.g., transcription factors, co-activators, and repressors; Trujillo and Shirasu, 2010; Sadanandom et al., 2012; Adams and Spoel, 2018; Stone, 2019). In response to external stimuli, ubiquitination can be promoted or inhibited leading to increased degradation or stabilization of a substrate protein, respectively. These changes in protein abundance may facilitate or prohibit cellular responses.

The E1 initiates the enzymatic cascade, creating a thioester bond between the active site cysteine and the C-terminal glycine residue of Ub in an ATP-dependent reaction (**Figure 1A**). Ubiquitin is then transferred from the E1 to the active site cysteine of the E2, forming a thioester linked E2-Ub intermediate. The E3 mediates transfer of Ub from the E2 to the substrate, *via* the formation of an isopeptide bond between the Ub C-terminal carboxyl group and the amino group of a residue on the substrate, typically a lysine side chain. Substrate specificity is attributed to a large and diverse collection of E3s. For example, the *Arabidopsis thaliana* (*Arabidopsis*) genome is estimated to encode for over 1,500 single subunit E3s or components of E3 complexes (Vierstra, 2012). Single subunit ubiquitin ligases include enzymes that utilize a Really Interesting New Gene (RING), Homologous to E6AP C-Terminus (HECT), or U-box domain to interact with the E2-Ub intermediate (**Figure 1B**). Complex E3s such as the Cullin (Cul)-RING ubiquitin ligases (CRLs) consists of a scaffold Cul protein interacting with a substrate- recognition component, with or without an adaptor subunit, and an E2-binding RING-Box (Rbx) protein (**Figure 1B**). Except for the single subunit HECT-type and RING-in-between-RING (RBR)-type E3s that accept Ub from the E2, ubiquitin ligases facilitate the transfer of Ub from the E2 directly to the substrate (**Figure 1B**). The pervasiveness of ubiquitin-dependent regulation is due in part to a single E3 regulating the abundance of multiple substrates. Additionally, depending on the environment, multiple E3s may target a particular substrate for ubiquitination.

The conjugation cascade can result in monoubiquitination (attachment of one Ub), multi-monoubiquitination (attachment of a single Ub to two or more sites), or polyubiquitination (attachment of a polyubiquitin chain) of the substrate (**Figure 1A**). There is a degree of structural plasticity in polyubiquitination due to flexibility of chain conformations caused by the different linkages used to generate Ub chains. Ub-Ub linkages can be created using eight different attachment sites, including seven lysine residues (6, 11, 27, 29, 33, 48, and 63) and the N-terminal methionine of ubiquitin (Dittmar and Winklhofer, 2020). The different chain configurations influence the fate of the modified substrate. For example, a chain created using 63-lysine is linked to non-proteasomal outcomes such as endocytosis, while a chain

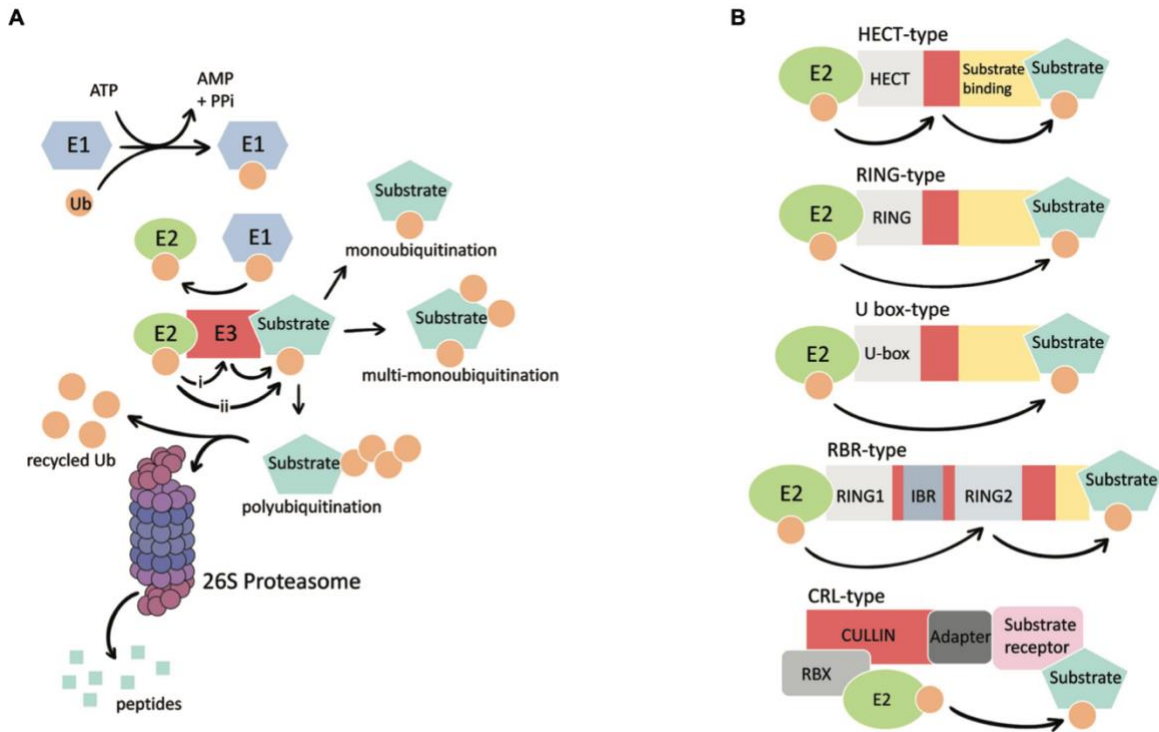


FIGURE 1 | (A) A simplified outline of the ubiquitin proteasome system. The E1, E2, and E3 enzymes facilitate attachment of one or more ubiquitin (Ub) molecules to the target substrate. Ubiquitination of the target occurs through transfer of Ub from the E2 to the E3 active cysteine prior to attachment to the substrate (i) or direct transfer of Ub to the substrate (ii). The conjugation cascade results in the monoubiquitination (one Ub at one site), multi-monoubiquitination (multiple Ubs at different sites), or polyubiquitination (multiple Ubs forming a chain) of the substrate. Polyubiquitinated substrates are recognized and degraded by the 26S proteasome. Ub is removed from the substrate and recycled. **(B)** Schematics representation of different E3 types. E3s utilize a RING (Really Interesting New gene), HECT (Homologous to E6AP C-terminus), or U-box domain to interact with the E2. Single subunit HECT and RING-in-between-RING (RBR) type E3s accept the Ub from the E2. Complex E3 Cullin (Cul)-RING ubiquitin ligases (CRLs) utilize different subunits to interact with the E2 and substrate.

generated using 48-lysine serves as a signal for degradation by the 26S proteasome (Thrower et al., 2000; Varadan et al., 2002; Duncan et al., 2006). The attachment of Ub is reversible *via* the actions of deubiquitylating enzymes (DUBs) that act as alternate regulators of ubiquitination, which cleave the isopeptide bond between Ub molecules to shorten chains and remove ubiquitin from substrate proteins (Komander, 2010). The best-known function of ubiquitination is targeting proteins to the 26S proteasome for degradation (**Figure 1A**).

The 26S proteasome is a compartmentalized complex composed of a hollow cylindrical 20S Core Particle (CP), which is capped at one or both ends by a 19S Regulatory Particle (RP);

Figure 1A; Bard et al., 2018). The CP consists of four stacked heptameric rings with protease activities found on the β subunits of the two inner rings. The RP recognizes and removes the ubiquitin/ ubiquitin chain from the substrate, unfolds, and directs the protein into the chamber of the CP for proteolysis. The removed ubiquitin molecules are recycled and the 26S proteasome expels the resulting peptides.

THE UPS AND NUTRIENT STRESS

The UPS is an important regulator of plant responses to abiotic stresses such as drought, heat, and salinity (Stone, 2019; Melo et al., 2021). The expression of genes that encode for components of the UPS are induced by abiotic stresses and mutations that hinder activity of ubiquitin enzymes or the proteasome have been shown to alter stress tolerance (Wang et al., 2009, 2019; Sun et al., 2020). Ubiquitin-dependent proteolysis is an important regulator of the acquisition of nutrients from the rhizosphere. Failure to properly regulate nutrient uptake is detrimental to growth and development, increases susceptibility to diseases, and reduces abiotic stress tolerance (Huber et al., 2012; Ahanger and Ahmad, 2019). The UPS is intricately involved in regulating nutrient acquisition *via* modulating the abundance of transcriptional regulators that control the expression of nutrient-responsive genes, components of nutrient signaling pathways, specialized channels, and transporters that uptake and translocate nutrients (**Table 1**). Factors such as nutrient deficiency may increase the ubiquitin- dependent degradation of a transcriptional repressor to promote the expression of nutrient stress-responsive genes or decrease the turnover of a membrane-bound transporter to enhance uptake. Alternatively, the UPS may promote the degradation of transcriptional activators and transporter proteins to attenuate the uptake of nutrients. Here, we describe some of the available evidence to illustrate the essential regulatory role of the UPS in the acquisition of macronutrients: N, P, and K; and micronutrients: Fe, Cu, and boron (B; **Table 1**).

TABLE 1 | Ubiquitin enzymes involved in nutrient uptake and stress response.

Ubiquitin enzymes	Function	Substrate (Known or potential)	Species	References
ATL8 (Arabidopsis Tóxicos en Levadura 8)	RING E3 Phosphate deficiency response	Unknown	<i>Arabidopsis thaliana</i>	Ramalah et al., 2022
ATL31 (Arabidopsis Tóxicos en Levadura 31)	RING E3 Carbon/Nitrogen balance	14-3-3 γ	<i>A. thaliana</i>	Sato et al., 2011
BTS (BRUTUS)	RING E3 Iron deficiency response	PYEL (Popeye-like)	<i>A. thaliana</i>	Selote et al., 2015
BTSL1/BTSL2 (BRUTUS-like 1/2)	RING E3 Iron deficiency response	FIT (FER-like iron deficiency-induced transcription factor)	<i>A. thaliana</i>	Rodríguez-Celma et al., 2019
CPN1 (Copine 1)	RING E3 Na ⁺ /K ⁺ Homeostasis	SKD1 (Suppressor of K ⁺ transport Growth Defect 1)	<i>Mesembryanthemum crystallinum</i>	Chiang et al., 2013
GmARI1 (<i>Glycine max</i> ARIADNE 1)	RBR E3 Aluminum toxicity	Unknown	<i>G. max</i>	Zhang et al., 2014
HRZ1/HRZ2 (Hemerythrin motif-containing RING- and Zinc-finger protein 1/2)	RING E3 Iron stress impacts zinc uptake	PR1 (Positive regulator of iron homeostasis 1)	<i>O. sativa</i>	Kobayashi et al., 2013
IDF1 (IRT1 degradation factor 1)	RING E3 Iron deficiency response	IRT1 (Iron-regulated transporter 1)	<i>A. thaliana</i>	Shin et al., 2013
NBIP1 (NRT1.1B interacting protein 1)	RING E3 Nitrogen stress	SPX4	<i>Oryza sativa</i>	Hu et al., 2019
NLA (Nitrogen limitation adaptation)	RING E3 Nitrate acquisition	NRT1.7 (Arabidopsis nitrate transporter 1.7)	<i>A. thaliana</i>	Liu et al., 2017
PIE1 (Pi starvation-induced E3 ligase)	RING E3 Phosphate acquisition	PHT1;4 (Phosphate transporter 1;4)	<i>A. thaliana</i>	Lin et al., 2013;
PHO2 (Phosphate 2)	UBC/E2 Phosphate deficiency response	ORE1	<i>A. thaliana</i>	Park et al., 2014
PRU1 (Phosphate response ubiquitin E3 ligase 1)	F-Box Pi-deficiency response	SPX2	<i>O. sativa</i>	Park et al., 2018
RGLG1/2 (RING Domain ligase1/2)	CRL E3 Iron deficiency response	WRKY6	<i>A. thaliana</i>	Yang et al., 2018
SDEL1/2 (SPX4 degradation E3 ligases 1/2)	RING E3 Phosphate deficiency response	Unknown	<i>A. thaliana</i>	Lin et al., 2013;
Unknown	RING E3 Boron stress	BOR1 (Boron transporter 1)	<i>A. thaliana</i>	Park et al., 2014
Unknown	Iron deficiency response	AHA2 (H ⁺ -ATPase2)	<i>A. thaliana</i>	Ye et al., 2018
Unknown	Iron deficiency response	FRO2 (Ferric chelate reductase 2)	<i>A. thaliana</i>	Ye et al., 2018
			<i>A. thaliana</i>	Pan et al., 2015
			<i>O. sativa</i>	Ruan et al., 2019
			<i>A. thaliana</i> , <i>O. sativa</i>	Yoshinari et al., 2021
			<i>A. thaliana</i>	Martin-Barranco et al., 2020
			<i>A. thaliana</i>	Martin-Barranco et al., 2020

Macronutrients

Primary macronutrients (e.g., N and P) are required in large amounts relative to secondary macronutrients (e.g., Ca and Mg) and essential micronutrients.

Nitrogen: N is a major component of amino acids, nucleotides, and chlorophyll. Low N availability limits growth, development, and yield. Plants uptake inorganic forms of N as nitrate (NO_3^-) and ammonium (H_4N^+). Soil amino acids serve as an organic N form (Zhang et al., 2020). Arabidopsis has four families of nitrate transporters including the NRT1 family, which are predominantly low-affinity transporters involved in the sensing, uptake, and translocation of NO_3^- (Tsay et al., 2007). The RING-type E3 Nitrogen Limitation Adaptation (NLA) is as a major component in the molecular machinery that regulates N deficiency response (Peng et al., 2007; Kant et al., 2011; Liu et al., 2017; **Figure 2A**). Under N deficiency, *nla* mutants display premature senescence indicating hypersensitivity to the stress (Peng et al., 2007). NLA, which is predominantly localized to the plasma membrane, mediates the ubiquitin-dependent degradation of NRT1.7 (Liu et al., 2017; Hannam et al., 2018; **Figure 2A**). The phloem expressed NRT1.7 is involved in source-to-sink remobilization of nitrate (Fan et al., 2009). *nrt1.7* mutants exhibited abnormally high levels of NO_3^- in senescent leaves, suggesting NRT1.7 is an important facilitator of phloem loading to remobilize nitrate. NLA levels decrease during exposure to N limiting conditions, allowing for the increase in NRT1.7 abundance, which promotes N mobilization (Liu et al., 2017). In rice (*Oryza sativa*), the RING-type E3 NRT1.1B interacting protein 1 (OsNBIP1) targets the repressor protein SPX4 (named after *Saccharomyces cerevisiae* SYG1 and PHO81 and mammalian XPR1 [SPX] domain-containing proteins) for proteasomal degradation, which alleviates inhibition of transcription factor NLP3 to promote expression of N-responsive genes (**Figure 2A**) (Hu et al., 2019). The perception of nitrate by the transreceptor OsNRT1.1B is suggested to recruit OsNBIP1, which then ubiquitinates SPX4 (**Figure 2A**). The RING-type E3s, Arabidopsis tóxicos en levadura (ATL) 6 and ATL31, were identified as negative regulators of the response to changes in the balance of available carbon (C) to N during seedling growth (Sato et al., 2009 and 2011). The strict coordination of C to N levels (termed the C/N response) is critical to seedling success, inhibiting post-germinative growth under high C/low N stress conditions (Sato et al., 2009). The C/N response is also vital to ecosystem success, as an ideal C/N ratio in plants is necessary to optimize CO_2 utilization (Zheng, 2009). The 14-3-3 protein, 14-3-3 χ , accumulates in response to C/N stress and promotes early seedling growth arrest (Sato et al., 2011). Under high C/low N conditions, phosphorylation stabilizes ATL31, which interacts

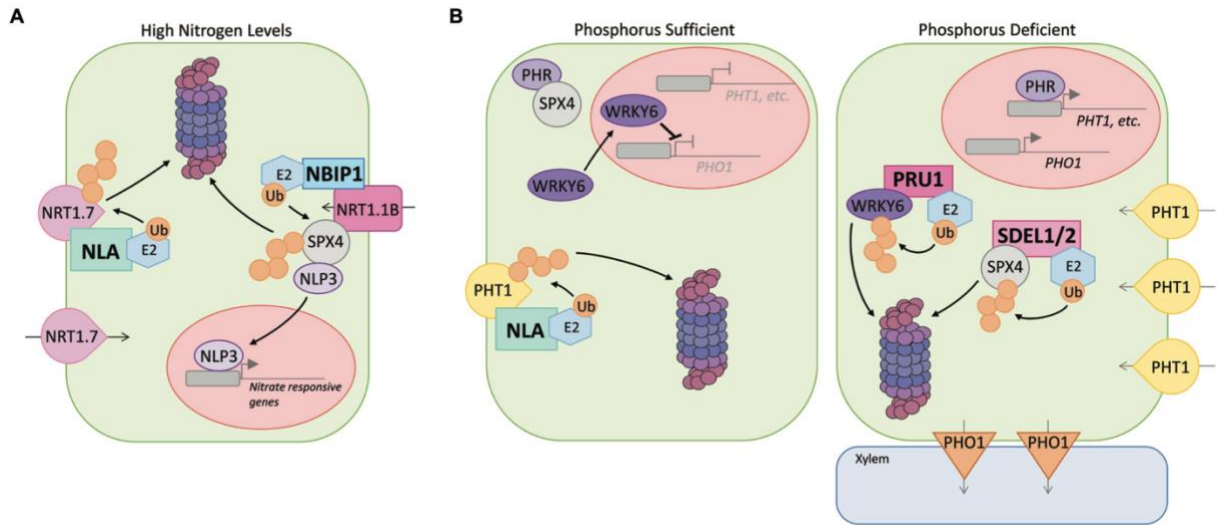


FIGURE 2 | Simplified representation of the role of select E3s from *Arabidopsis* and *Oryza Sativa* (rice) in regulating nutrient uptake. **(A)** Under high N, the E3 NLA mediate ubiquitin-dependent degradation of NRT1.7 nitrate transporter to avoid N overaccumulation. The transceptor NRT1.1B recruits the E3 NBIP1, which ubiquitinates SPX4 allowing the transcription factor NLP3 to enter the nucleus and promote expression of N-responsive genes. **(B)** Under Pi replete conditions, E3 NLA ubiquitinates PHT1 inorganic phosphate transporters facilitating degradation by the 26S proteasome to reduce uptake and prevent Pi overaccumulation. Under P limiting stress conditions, E3s SDEL1 and SDEL2 mediate the degradation of SPX4, which allows the transcription factor PHR1/2 to activate the expression of *PSI* genes such as *PHT1*. Also, the E3 PRU1 mediates degradation of the repressor WRKY6, which relieves inhibition of *PHO1* transcription. Increase in *PHO1* transporter abundance promotes loading of Pi into the root xylem.

with and mediates the proteasome-dependent degradation of 14-3-3 χ to attenuate the nutrient stress response (Yasuda et al., 2014 and 2017). Calcineurin B-Like (CBL)-Interacting Protein Kinase 14 (CIPK14), which is activated in a Ca²⁺-dependent manner *via* its association with CBL8, mediates phosphorylation of ATL31 under high C/low N stress, suggesting the involvement of Ca²⁺ signaling in the C/N response (Yasuda, 2017).

Phosphorus: P is a key component of macromolecules, and it plays a fundamental role in photosynthesis, metabolism of nitrogen, carbohydrates, and fat (López-Arredondo et al., 2014). Regulating the abundance of phosphate transporters is important as low P levels significantly reduce root growth and net photosynthesis, and high levels of the transporters cause toxic P accumulation in cells. For *Arabidopsis*, four families of Phosphate Transporters (PHTs), PHT1-PHT4, are involved in the intracellular transport and uptake of inorganic phosphate (Pi) from soil (Młodzińska and Zboińska, 2016). Of the nine PHT1 members, plasma membrane-localized PHT1;1, PHT1;2, PHT1;3 and PHT1;4 are primarily involved in

the acquisition of Pi (Shin et al., 2004; Ayadi et al., 2015). A family of Phosphate Starvation Response (PHR) transcription factors regulate the expression of *Pi-starvation- induced (PSI)* genes including *PHT1s* (Bustos et al., 2010). In rice, OsSPX4 interacts with OsPHR2 under Pi-replete conditions, inhibiting transcriptional activity (Lv et al., 2014; **Figure 2B**). The RING-type ubiquitin ligases, SPX4 degradation E3 ligases 1 (SDEL1) and SDEL2, accumulate under Pi-deficiency and mediate the ubiquitin-dependent proteasomal degradation of the repressor, which would allow OsPHR2 to enter the nucleus and promote expression of *PSI* genes (Ruan et al., 2019; **Figure 2B**).

Nitrate-induced degradation of SPX4, mediated by the E3 OsNBIP1, also contributes to the activation of OsPHR2 and expression of *PSI* genes (Hu et al., 2019). The E3 NLA is an important regulator of phosphate homeostasis, modulating the abundance of *PHT1s* at the plasma membrane (Kant et al., 2011; Lin et al., 2013). Under phosphate sufficient conditions, loss of *NLA* function results in accumulation of *PHT1s* and increased Pi content causing toxicity. *NLA*, along with the E2 Phosphate 2 (PHO2 [or UBC24]), has been shown to mediate the ubiquitin-dependent proteasomal degradation of *PHT1;4* to suppress Pi uptake under high phosphate conditions (Liu et al., 2012; Lin et al., 2013; Park et al., 2014; **Figure 2B**). *NLA* and PHO2 levels are kept low *via* the action of Pi starvation- induced microRNAs, allowing for the accumulation of phosphate transporters and increase Pi uptake (Bari et al., 2006; Kant et al., 2011; Lin et al., 2013). The increase in microRNAs under Pi-deficient conditions requires the transcription factor PHR1 (Bari et al., 2006). P homeostasis is also controlled *via* the activity of Phosphate Response Ubiquitin E3 Ligase 1 (PRU1), which promotes the ubiquitin-dependent degradation of WRKY6, a transcription factor known to inhibit transcription of *Phosphate 1 (PHO1)*; Chen et al., 2009; Lin et al., 2013; Ye et al., 2018; **Figure 2B**). *PHO1* is expressed under P deficiency and is involved in the translocation of phosphorus from root-to-shoot (Hamburger et al., 2002). PRU1 is a F-box protein, which function as the substrate-binding component for CRL E3 complexes (Ye et al., 2018). PRU1 promotes the proteasomal degradation of WRKY6 under low P stress to increase the abundance of *PHO1*, promoting the movement of the nutrient into root xylem (**Figure 2B**).

Potassium: K is an activator of many enzymes involved in protein synthesis, sugar transport, and metabolism of N and C (Tränkner et al., 2018). K also plays a key role in gas exchange and transpiration as optimal K levels are essential for stomatal opening and closing (Andrés et al., 2014). Maintaining K homeostasis is critical, as excess K negatively affects the uptake of other nutrients including N, Ca, and Mg (Tränkner et al., 2018). Plants uptake potassium ions (K^+) *via* Shaker-like K^+ channels, such as AKT1, and K^+ transporters including AtHAK5 (Gierth et al., 2005; Rubio et al., 2008; Pyo et al., 2010). Under K^+ replete conditions, uptake is dominated by ATK1 and other low-affinity K^+ uptake mechanisms (Rubio et al., 2010). K^+ deficiency induces the expression of AtHAK5, a high-affinity transporter essential for uptake under limiting conditions (Ahn et al., 2004; Gierth et al., 2005; Pyo et al., 2010). The extent to which ubiquitin-mediated processes are involved mediating K uptake is unclear. Salt stress induces the expression of Suppressor of K^+ transport Growth Defect 1 (SKD1), an AAA-type ATPase, which facilitates K^+ transport to maintain Na^+/K^+ homeostasis (Ho et al., 2010). Studies using the halophyte ice plant *Mesembryanthemum crystallinum* found that the SKD1 is ubiquitinated by the RING-type E3 Copine 1 (CPN1; Chiang et al., 2013). Under high

salt stress, SKD1 relocates from the cytosol to the plasma membrane where it interacts with CPN1 (Chiang et al., 2013; Jou et al., 2013).

Micronutrients

Plants require very small quantities of micronutrients; but extremely low levels will cause deficiencies, and excess nutrient levels are toxic. Therefore, maintaining optimal levels of these nutrients are critical for plant success.

Iron: Fe is necessary for chlorophyll biosynthesis, N fixation, DNA replication and repair, and the electron transport chain (Pushnik et al., 2008; Zhang, 2014). Excess Fe inhibits root growth, impacting the uptake of other nutrients, a problem increased by anaerobic and acidic soil conditions (Becker and Asch, 2005). Under Fe deficient conditions, expression of Iron-regulated Transporter 1 (IRT1) is upregulated in roots to promote the uptake of Fe^{2+} from the rhizosphere (Vert et al., 2002). IRT1 forms a plasma membrane-localized complex with H^+ -ATPase2 (AHA2), which mediates the extrusion of protons to acidify the rhizosphere and solubilize iron, and Ferric Chelate Reductase 2 (FRO2) that reduces Fe^{3+} to Fe^{2+} for import (Connolly et al., 2003; Santi and Schmidt, 2009; Martín-Barranco et al., 2020). IRT1 transports other essential cations, including Zn, Mn, cadmium (Cd), and cobalt (Co; Vert et al., 2002). The iron transporter is ubiquitinated at the plasma membrane by the RING-type E3 IRT1 Degradation Factor 1 (IDF1), which is suggested to promote endocytosis leading to vacuolar degradation as well as turnover by the proteasome (Barberon et al., 2011; Shin et al., 2013; Dubeaux et al., 2018). Increasing concentrations of non-iron metals, such as Zn, Mn, and Co, promotes the monoubiquitination of IRT1 followed by IDF1-mediated polyubiquitination using 63-lysine linkages to generate the chain (Barberon et al., 2011; Dubeaux et al., 2018). Both modifications, monoubiquitination and polyubiquitination, decrease the levels of IRT1 in the plasma membrane by promoting internalization and degradation in the vacuole. The switch to IDF1-mediated ubiquitination, in response to excess non-iron metals, is triggered by CIPK23-dependent phosphorylation of IRT1 (Dubeaux et al., 2018). AHA2 and FRO2 are also ubiquitinated; however, the modification is not induced by non-iron metals and does not promote internalization and degradation but is suggested to regulate enzyme function (Martín-Barranco et al., 2020). FER-like Iron Deficiency-induced Transcription Factor (FIT) is a key regulator among a group of basic helix-loop-helix (bHLH) transcription factors that control the expression of *IRT1* and other Fe-deficiency responsive genes (Cohen et al., 2004; Mai et al., 2016). Fe deficiency triggers a cascade of bHLH regulators that culminates in the expression and activation of FIT, which then promotes the transcription of genes involved in the mobilization and uptake of iron. Two bHLH transcription factors, bHLH105 and bHLH115, are ubiquitinated and targeted for proteasomal degradation by the RING-type E3 BRUTUS (BTS), which prohibits activation of the Fe-deficiency response in the absence of stress (Selote et al., 2015). Iron Mans (IMAs) are a family of peptides that bind to BTS under Fe-deficiency and disrupt the interaction with bHLH105 and bHLH115, allowing the transcription factors to accumulate and promote the stress response (Grillet et al., 2018; Li et al., 2021). BTS belongs to a family of hemerythrin-containing RING-type E3s, which include BRUTUS-LIKE1 (BTSL1) and BTSL2 and are similar to *O. sativa* Hemerythrin motif-containing RING- and Zinc- finger protein 1 (OsHRZ1) and

OsHRZ2 (Kobayashi et al., 2013; Rodríguez-Celma et al., 2019). BTSL1 and BTSL2 regulate FIT abundance *via* proteasome-dependent degradation (Rodríguez-Celma et al., 2019). BTS, OsHRZ1, and OsHRZ2 have been shown to bind Fe and Zn, suggesting that the E3s function as metal sensors as well as negative regulators of the Fe-deficiency response (Kobayashi et al., 2013; Selote et al., 2015; Rodríguez-Celma et al., 2019). OsHRZ1 and OsHRZ2 are also required for limiting metal uptake under excess iron stress, further suggesting a role for the E3s in iron sensing (Aung et al., 2018). The RING-type E3s Ring Domain Ligase1 (RGLG1) and RGLG2 are also involved in regulating responses to iron limiting condition; however, substrates are not known (Pan et al., 2015).

Copper: Regulation of Cu uptake is critical because it is a key component in numerous enzymatic activities and photosynthetic processes, and high concentrations are toxic to cells (Kumar et al., 2021). In Arabidopsis, Cu uptake is achieved by a family of five high-affinity transporters, Copper Transporter (COPT)1, COPT2, COPT3, COPT5, and COPT6 (Sancenón et al., 2003 and 2004; Jung et al., 2012). Although COPT1, COPT2, and COPT6 are plasma membrane localized they interact with two closely related ER-localized proteins, Ubiquitin-associated Domain-containing Protein 2a (UBAC2a) and UBAC2b (Li et al., 2021). *UBAC2* mutants accumulate less COPT1, COPT2, and COPT6 proteins, display reduced Cu root content, and increased sensitivity to Cu deficiency stress. COPT1 protein levels in *ubac2a/b* increase following inhibition of proteasome activity, suggesting regulation by the UPS. UBAC2a/b is suggested to interact with the newly synthesized COPT1 to prohibit degradation of the Cu transporter. The E3 that regulates COPT1 protein abundance is unknown.

Boron: B is required for synthesizing and maintaining structural integrity of cell walls and pollen viability (Camacho- Cristóbal et al., 2008). Insufficient or excess levels of boron are detrimental to crop yield and quality. Under B sufficient levels, passive transport through the cell membrane is the dominant uptake mechanism (Cervilla et al., 2009). In Arabidopsis, the uptake of B as boric acid under nutrient limiting conditions is dependent on boric acid channel protein Nodulin 26-like Intrinsic Protein5;1 (NIP5;1; Takano et al., 2006). Under B-deficiency, the boron transporter BOR1 is involved in xylem loading and translocation of B from root- to-shoot in Arabidopsis and rice (Takano et al., 2002; Nakagawa et al., 2007). Boron-induced ubiquitination of BOR1 does not target the transporter to the proteasome but promote endocytosis and vacuolar degradation (Kasai et al., 2011). High boron levels are suggested to induce a conformational change in BOR1 that triggers the attachment of a 63-lysine linked polyubiquitin chain at a previously inaccessible lysine on the C-terminal tail of the transporter (Yoshinari et al., 2021). The E3 responsible for BOR1 polyubiquitination is not yet identified.

CONCLUSION

Knowledge of ubiquitin-mediated processes involved in maintaining the homeostasis of nutrients such as iron and nitrogen is well established. The UPS regulates the presence of transporters at the plasma membrane that uptake nutrients from the rhizosphere, the abundance of transporters that translocate nutrients from the root to above ground organs. The UPS also modulates the levels of regulators that control transcription of genes involved in nutrient homeostasis. However, our understanding of how the UPS functions to regulate

the uptake of most nutrients, such as boron, zinc, and copper, is very limited. As research progresses the extent of ubiquitin-mediated regulation in sensing, uptake and translocations of nutrients will undoubtedly become more apparent. This may also lead to a better understanding of the mechanisms that regulate ubiquitin ligase activity and substrate engagement under different levels of nutrient availability. Considering climate change, more detailed knowledge of the role of ubiquitination in nutrient acquisition may assist with understanding how optimal nutrient status can be maintained to ameliorate the negative impact of abiotic and biotic stresses on growth and yield.

AUTHOR CONTRIBUTIONS

EM and SS conceptualize the topic. EM wrote the draft and made the figures. SS edited the draft and figures. All authors contributed to the article and approved the submitted version.

FUNDING

This work is supported by a Discovery grant from the Natural Sciences and Engineering Research Council of Canada (NSERC) to SLS. EM is supported by a Nova Scotia Graduate Scholarship (NSGS) and a graduate scholarship from Dalhousie University.

ACKNOWLEDGMENTS

The authors acknowledge the Natural Sciences and Engineering Research Council of Canada (NSERC) for providing support to SLS. Thanks to Dalhousie University and Nova Scotia Graduate Scholarship (NSGS) for supporting EM's graduate studies.

REFERENCES

- Adams, E. H. G., and Spoel, S. H. (2018). The ubiquitin-proteasome system as a transcriptional regulator of plant immunity. *J. Exp. Bot.* 69, 4529–4537. doi: 10.1093/jxb/ery216
- Ahanger, M. A., and Ahmad, P. (2019). Role of mineral nutrients in abiotic stress tolerance: revisiting the associated signaling mechanisms. *Plant Signal. Mol.* 269–285. doi: 10.1016/B978-0-12-816451-8.00016-2
- Andrés, Z., Pérez-Hormaeche, J., Leidi, E. O., Schlücking, K., Steinhorst, L., McLachlan, D. H., et al. (2014). Control of vacuolar dynamics and regulation of stomatal aperture by tonoplast potassium uptake. *PNAS* 111, E1806–E1814. doi: 10.1073/pnas.1320421111
- Aung, M. S., Kobayashi, T., Masuda, H., and Nishizawa, N. K. (2018). Rice HRZ ubiquitin ligases are crucial for the response to excess iron. *Physiol. Plant.* 163, 282–296. doi: 10.1111/ppl.12698
- Ayadi, A., David, P., Arrighi, J.-F., Chiarenza, S., Thibaud, M.-C., Nussaume, L., et al. (2015). Reducing the genetic redundancy of Arabidopsis PHOSPHATE TRANSPORTER1

transporters to study phosphate uptake and signaling. *Plant Physiol.* 167, 1511–1526. doi: 10.1104/pp.114.252338

Bano, A., and Fatima, M. (2009). Salt tolerance in *Zea mays* (L). Following inoculation with rhizobium and pseudomonas. *Biol. Fertil. Soils* 45, 405–413. doi: 10.1007/s00374-008-0344-9

Baon, J. B., Smith, S. E., and Alston, A. M. (1994). Phosphorus uptake and growth of barley as affected by soil temperature and mycorrhizal infection. *J. Plant Nutr.* 17, 479–492. doi: 10.1080/01904169409364742

Barberon, M., Zelazny, E., Robert, S., Conéjéro, G., Curie, C., Friml, J., et al. (2011). Monoubiquitin-dependent endocytosis of the iron-regulated transporter 1 (IRT1) transporter controls iron uptake in plants. *Proc. Natl. Acad. Sci. U. S. A.* 108, E450–E458. doi: 10.1073/pnas.1100659108

Bard, J., Goodall, E., Greene, E., Jonsson, E., Dong, K., and Martin, A. (2018). Structure and function of the 26S proteasome. *Annu. Rev. Biochem.* 87, 697–724. doi: 10.1146/annurev-biochem-062917-011931

Bari, R., Datt, P. B., Stitt, M., and Scheible, W. R. (2006). PHO2, microRNA399, and PHR1 define a phosphate-signaling pathway in plants. *Plant Physiol.* 141, 988–999. doi: 10.1104/pp.106.079707

Becker, M., and Asch, F. (2005). Iron toxicity in rice - conditions and management concepts. *J. Plant Nutr. Soil Sci.* 168, 558–573. doi: 10.1002/jpln.200520504

Brown, C. E., Pezeshki, S. R., and DeLaune, R. D. (2006). The effects of salinity and soil drying on nutrient uptake and growth of *Spartina alterniflora* in a simulated tidal system. *Environ. Exp. Bot.* 58, 140–148. doi: 10.1016/j.envexpbot.2005.07.006

Bustos, R., Castrillo, G., Linhares, F., Puga, M. I., Rubio, V., Pérez-Pérez, J., et al. (2010). A central regulatory system largely controls transcriptional activation and repression responses to phosphate starvation in *Arabidopsis*.

PLoS Genet. 6:e1001102. doi: 10.1371/journal.pgen.1001102 Camacho-Cristóbal, J. J., Rexach, J., and González-Fontes, A. (2008). Boron in plants: deficiency and toxicity. *J. Integr. Plant Biol.* 50, 1247–1255. doi:

10.1111/j.1744-7909.2008.00742.x

Cervilla, L. M., Rosales, M. A., Rubio-Wilhelmi, M. M., Sánchez-Rodríguez, E.,

Blasco, B., Ríos, J. J., et al. (2009). Involvement of lignification and membrane permeability in the tomato root response to boron toxicity. *Plant Sci: Int J Exp Plant Bio* 176, 545–552. doi: 10.1016/j.plantsci.2009.01.008

- Chen, B. D., Li, X. L., Tao, H. Q., Christie, P., and Wong, M. H. (2003). The role of arbuscular mycorrhiza in zinc uptake by red clover growing in a calcareous soil spiked with various quantities of zinc. *Chemosphere* 50, 839–846. doi: 10.1016/S0045-6535(02)00228-X
- Chen, Y. F., Li, L. Q., Xu, Q., Kong, Y. H., Wang, H., and Wu, W. H. (2009). The WRKY6 transcription factor modulates PHOSPHATE1 expression in response to low pi stress in Arabidopsis. *Plant Cell* 21, 3554–3566. doi: 10.1105/tpc.108.064980
- Chiang, C. P., Li, C. H., Jou, Y., Chen, Y. C., Lin, Y. C., Yang, F. Y., et al. (2013). Suppressor of K⁺ transport growth defect 1 (SKD1) interacts with RING-type ubiquitin ligase and sucrose non-fermenting 1-related protein kinase (SnRK1) in the halophyte ice plant. *J. Exp. Bot.* 64, 2385–2400. doi: 10.1093/jxb/ert097
- Cohen, J., Zhang, X., Francis, J., Jung, T., Kwok, R., Overland, J., et al. (2020). Divergent consensus on Arctic amplification influence on midlatitude severe winter weather. *Nature Climate Change*, 10, 20–29.
- Cohen, J., Zhang, X., Francis, J., Jung, T., Kwok, R., Overland, J., et al. (2004). The essential basic helix-loop-helix protein FIT1 is required for the iron deficiency response. *Plant Cell* 16, 3400–3412. doi: 10.1105/tpc.104.024315
- Connolly, E. L., Campbell, N. H., Grotz, N., Prichard, C. L., and Guerinot, M. L. (2003). Overexpression of the FRO2 ferric chelate reductase confers tolerance to growth on low iron and uncovers posttranscriptional control. *Plant Physiol.* 133, 1102–1110. doi: 10.1104/pp.103.02512
- Dittmar, G., and Winklhofer, K. F. (2020). Linear ubiquitin chains: cellular functions and strategies for detection and quantification. *Front. Chem.* 7, 915. doi: 10.3389/fchem.2019.00915
- Dubeaux, G., Neveu, J., Zelazny, E., and Vert, G. (2018). Metal sensing by the IRT1 transporter-receptor orchestrates its own degradation and plant metal nutrition. *Mol. Cell* 69, 953–964.e5. doi: 10.1016/j.molcel.2018.02.009
- Duncan, L. M., Piper, S., Dodd, R. B., Saville, M. K., Sanderson, C. M., Luzio, J. P., et al. (2006). Lysine-63-linked ubiquitination is required for endolysosomal degradation of class I molecules. *EMBO J.* 25, 1635–1645. doi: 10.1038/sj.emboj.7601056
- Etesami, H., and Noori, F. (2019). “Soil salinity as a challenge for sustainable agriculture and bacterial-mediated alleviation of salinity stress in crop plants,” in *Saline Soil-Based Agriculture by Halotolerant Microorganisms*. eds. M. Kumar, H. Etesami and V. Kumar (Singapore: Springer), 1–22. doi: 10.1007/978-981-13-8335-9_1
- Fan, S. C., Lin, C. S., Hsu, P. K., Lin, S. H., and Tsay, Y. F. (2009). The Arabidopsis nitrate transporter NRT1.7, expressed in phloem, is responsible for source-to-sink remobilization of nitrate. *Plant Cell* 21, 2750–2761. doi: 10.1105/tpc.109.067603

- Gao, F., Robe, K., Gaymard, F., Izquierdo, E., and Dubos, C. (2019). The transcriptional control of iron homeostasis in plants: a tale of bHLH transcription factors? *Front. Plant Sci.* 10:6. doi: 10.3389/fpls.2019.00006
- Gelybó, G., Tóth, E., Farkas, C., Horel, Á., Kása, I., and Bakacsi, Z. (2018). Potential impacts of climate change on soil properties. *Agrochem. Soil Sci.* 67, 121–141. doi: 10.1556/0088.2018.67.1.9
- Gierth, M., Maser, P., and Schroeder, J. I. (2005). The potassium transporter AtHAK5 functions in K⁺ deprivation-induced high-affinity K⁺ uptake and AKT1 K⁺ channel contribution to K⁺ uptake kinetics in Arabidopsis roots. *Plant Physiol.* 137, 1105–1114. doi: 10.1104/pp.104.057216
- Gojon, A. (2017). Nitrogen nutrition in plants: rapid progress and new challenges. *J. Exp. Bot.* 68, 2457–2462. doi: 10.1093/jxb/erx171
- Grillet, L., Lan, P., Li, W., Mokkaapati, G., and Schmidt, W. (2018). IRON MAN is a ubiquitous family of peptides that control iron transport in plants. *Nature Plants* 4, 953–963. doi: 10.1038/s41477-018-0266-y
- Hamburger, D., Rezzonico, E., MacDonald-Comber Petétot, J., Somerville, C., and Poirier, Y. (2002). Identification and characterization of the Arabidopsis PHO1 gene involved in phosphate loading to the xylem. *Plant Cell* 14, 889–902. doi: 10.1105/tpc.000745
- Hannam, C., Gidda, S. K., Humbert, S., Peng, M., Cui, Y., Dyer, J. M., et al. (2018). Distinct domains within the nitrogen limitation adaptation protein mediate its subcellular localization and function in the nitrate-dependent phosphate homeostasis pathway. *Botany* 96, 79–96. doi: 10.1139/cjb-2017-0149
- Haynes, R. J., and Swift, R. S. (1986). Effects of soil acidification and subsequent leaching on levels of extractable nutrients in a soil. *Plant Soil* 95, 327–336. doi: 10.1007/BF02374613
- Ho, L. W., Yang, T. T., Shieh, S. S., Edwards, G., and Yen, H. (2010). Reduced expression of a vesicle trafficking-related ATPase SKD1 decreases salt tolerance in Arabidopsis. *Func. Plant Bio.* 37, 962–973. doi: 10.1071/FP10049
- Hu, B., Jiang, Z., Wang, W., Qiu, Y., Zhang, Z., Liu, Y., et al. (2019). Nitrate–NRT1.1B–SPX4 cascade integrates nitrogen and phosphorus signalling networks in plants. *Nat Plants* 5, 401–413. doi: 10.1038/s41477-019-0384-1
- Huber, D., Römheld, V., and Weinmann, M. (2012). “Relationship between nutrition, plant diseases and pests,” in *Mineral Nutrition of Higher Plants*. ed. H. Marschner. 3rd Edn. (Beijing: Science Press), 283–298.

IPCC (2021). "Summary for policymakers in climate change 2021," in *The Physical Science Basis. Contribution of Working Group I to the Sixth Assessment Report of the Intergovernmental Panel on Climate Change*. eds. V. Masson-Delmotte, P. Zhai, A. Pirani, S. L. Connors, C. Péan and S. Bergeret al. (Cambridge, UK: Cambridge University Press) In Press.

Islam, A. K. M. S., Edwards, D. G., and Asher, C. J. (1980). pH optima for crop growth. *Plant Soil* 54, 339–357. doi: 10.1007/BF02181830

Jiang, Y., Li, Y., Zeng, Q., Wei, J., and Yu, H. (2017). The effect of soil pH on plant growth, leaf chlorophyll fluorescence and mineral element content of two blueberries. *Acta Hort.* 1180, 269–276. doi: 10.17660/ActaHortic.2017.1180.36

Jou, Y., Chiang, C. P., and Yen, H. E. (2013). Changes in cellular distribution regulate SKD1 ATPase activity in response to a sudden increase in environmental salinity in halophyte ice plant. *Plant Sign. Behav.* 8:e27433. doi: 10.4161/psb.27433

Jung, H. I., Gayomba, S. R., Rutzke, M. A., Craft, E., Kochian, L. V., and Vatamaniuk, O. K. (2012). COPT6 is a plasma membrane transporter that functions in copper homeostasis in Arabidopsis and is a novel target of SQUAMOSA promoter-binding protein-like 7. *J. Biol. Chem.* 287, 33252–33267. doi: 10.1074/jbc.M112.397810

Kabata-Pendias, A. (2004). Soil–plant transfer of trace elements—an environmental issue. *Geoderma* 122, 143–149. doi: 10.1016/j.geoderma.2004.01.004

Kant, S., Peng, M., and Rothstein, S. J. (2011). Genetic regulation by NLA and MicroRNA827 for maintaining nitrate-dependent phosphate homeostasis in Arabidopsis. *PLoS Genet.* 7:e1002021. doi: 10.1371/journal.pgen.1002021

Karmakar, R., Das, I., Dutta, D., and Rakshit, A. (2016). Potential effects of climate change on soil properties: a review. *Sci. Int.* 4, 51–73. doi: 10.3390/agriculture3030398

Kasai, K., Takano, J., Miwa, K., Toyoda, A., and Fujiwara, T. (2011). High boron-induced ubiquitination regulates vacuolar sorting of the BOR1 borate transporter in Arabidopsis thaliana. *J. Biol. Chem.* 286, 6175–6183. doi: 10.1074/jbc.M110.184929

Kobayashi, T., Nagasaka, S., Senoura, T., Itai, R. N., Nakanishi, H., and Nishizawa, N. K. (2013). Iron-binding haemerythrin RING ubiquitin ligases regulate plant iron responses and accumulation. *Nat. Commun.* 4:2792. doi: 10.1038/ncomms3792

Komander, D. (2010). Mechanism, specificity and structure of the deubiquitinases. *Subcell. Biochem.* 54, 69–87. doi: 10.1007/978-1-4419-6676-6_6

- Kumar, V., Pandita, S., Sidhu, G. P. S., Sharma, A., Khanna, K., Kaur, P., et al. (2021). Copper bioavailability, uptake, toxicity and tolerance in plants: A comprehensive review. *Chemosphere* 262:127810. doi: 10.1016/j.chemosphere.2020.127810
- Kumar, M., Swarup, A., Patra, A., Chandrakala, J. U., and Manjaiah, K. M. (2012). Effect of elevated CO₂ and temperature on phosphorus efficiency of wheat grown in an Inceptisol of subtropical India. *Plant Soil Environ.* 58, 230–235. doi: 10.17221/749/2011-PSE
- Li, Y., Lu, C. K., Li, C. Y., Lei, R. H., Pu, M. N., Zhao, J. H., et al. (2021). Iron man interacts with Brutus to maintain iron homeostasis in Arabidopsis. *Proc. Natl. Acad. Sci.* 118:e2109063118. doi: 10.1073/pnas.2109063118
- Li, X., Wang, Z., Fu, Y., Cheng, X., Zhang, Y., Fan, B., et al. (2021). Two ubiquitin-associated ER proteins interact with COPT copper transporters and modulate their accumulation. *Plant Physiol.* 187, 2469–2484. doi: 10.1093/plphys/kiab442
- Lin, W. Y., Huang, T. K., and Chiou, T. J. (2013). Nitrogen limitation adaptation, a target of microRNA827, mediates degradation of plasma membrane-localized phosphate transporters to maintain phosphate homeostasis in Arabidopsis. *Plant Cell* 25, 4061–4074. doi: 10.1105/tpc.113.116012
- Liu, T. Y., Huang, T. K., Tseng, C. Y., Lai, Y. S., Lin, S. I., Lin, W. Y., et al. (2012). PHO2-dependent degradation of PHO1 modulates phosphate homeostasis in Arabidopsis. *Plant Cell* 24, 2168–2183. doi: 10.1105/tpc.112.096636
- Liu, W., Sun, Q., Wang, K., Du, Q., and Li, W. (2017). Nitrogen limitation adaptation (NLA) is involved in source-to-sink remobilization of nitrate by mediating the degradation of NRT1.7 in Arabidopsis. *New Phytol.* 214, 734–744. doi: 10.1111/nph.14396
- López-Arredondo, D. L., Leyva-González, M. A., González-Morales, S. I., López-Bucio, J., and Herrera-Estrella, L. (2014). Phosphate nutrition: improving low-phosphate tolerance in crops. *Annu. Rev. Plant Biol.* 65, 95–123. doi: 10.1146/annurev-arplant-050213-035949
- Lv, Q., Zhong, Y., Wang, Y., Wang, Z., Zhang, L., Shi, J., et al. (2014). SPX4 negatively regulates phosphate signaling and homeostasis through its interaction with PHR2 in rice. *Plant Cell* 26, 1586–1597. doi: 10.1105/tpc.114.123208
- Mackay, A., and Barber, S. (1984). Soil temperature effects on root growth and phosphorus uptake by corn. *Soil Sci. Soc. America J.* 48, 818–823. doi: 10.2136/sssaj1984.03615995004800040024x
- Maharajan, T., Ceasar, S. A., Krishna, T. P. A., and Ignacimuthu, S. (2021). Management of phosphorus nutrient amid climate change for sustainable agriculture. *J. Environ. Qual.* 50, 1303–1324. doi: 10.1002/jeq2.20292

- Mai, H. J., Pateyron, S., and Bauer, P. (2016). Iron homeostasis in *Arabidopsis thaliana*: transcriptomic analyses reveal novel FIT-regulated genes, iron deficiency marker genes and functional gene networks. *BMC Plant Biol.* 16:211. doi: 10.1186/s12870-016-0899-9
- Martín-Barranco, A., Spielmann, J., Dubeaux, G., Vert, G., and Zelazny, E. (2020). Dynamic control of the high-affinity iron uptake complex in root epidermal cells. *Plant Physiol.* 184, 1236–1250. doi: 10.1104/pp.20.00234
- McCallister, D. L., Jawson, L., and Jawson, M. (1997). Soil temperature and fumigation effects on plant phosphorus uptake and related microbial properties. *J. Plant Nutr.* 20, 485–497. doi: 10.1080/01904169709365269
- Melo, F. V., Oliveira, M. M., Saibo, N., and Lourenço, T. F. (2021). Modulation of abiotic stress responses in Rice by E3-ubiquitin ligases: a promising way to develop stress-tolerant crops. *Front. Plant Sci.* 12:640193. doi: 10.3389/fpls.2021.640193
- Mimura, N. (2013). Sea-level rise caused by climate change and its implications for society. *Proc. Jpn. Acad. Ser. B Phys. Biol. Sci.* 89, 281–301. doi: 10.2183/pjab.89.281
- Miricescu, A., Goslin, K., and Graciet, E. (2018). Ubiquitylation in plants: signaling hub for the integration of environmental signals. *J. Exp. Biol.* 69, 4511–4527. doi: 10.1093/jxb/ery165
- Młodzińska, E., and Zboińska, M. (2016). Phosphate uptake and allocation—A closer look at *Arabidopsis thaliana* L. and *Oryza sativa* L. *front. Plant Sci* 7:1198. doi: 10.3389/fpls.2016.01198
- Nakagawa, Y., Hanaoka, H., Kobayashi, M., Miyoshi, K., Miwa, K., and Fujiwara, T. (2007). Cell-type specificity of the expression of OsBOR1, a rice efflux boron transporter gene, is regulated in response to boron availability for efficient boron uptake and xylem loading. *Plant Cell* 19, 2624–2635. doi: 10.1105/tpc.106.049015
- Neina, D. (2019). The role of soil pH in plant nutrition and soil remediation. *Appl. Environ. Soil Sci.* 2019, 1–9. doi: 10.1155/2019/5794869
- O’Gorman, P. A., and Schneider, T. (2009). The physical basis for increases in precipitation extremes in simulations of 21st-century climate change. *PNAS* 106, 14773–14777. doi: 10.1073/pnas.0907610106
- Overland, J. (2021). Rare events in the Arctic. *Clim. Chang.* 168, 1–13. doi: 10.1007/s10584-021-03238-2
- Pan, I. C., Tsai, H. H., Cheng, Y. T., Wen, T. N., Buckhout, T. J., and Schmidt, W. (2015). Post-transcriptional coordination of the *Arabidopsis* iron deficiency response is partially dependent on the E3 ligases ring domain ligase1 (RGLG1) and ring domain ligase2 (RGLG2). *Mol. Cell. Proteomics* 14, 2733–2752. doi: 10.1074/mcp.M115.048520

Park, B. S., Seo, J. S., and Chua, N. (2014). Nitrogen limitation adaptation recruits phosphate2 to target the phosphate transporter PT2 for degradation during the regulation of Arabidopsis phosphate homeostasis. *Plant Cell* 26, 454–464. doi: 10.1105/tpc.113.120311

Park, B. S., Yao, T., Seo, J. S., Wong, E. C. C., Mitsuda, N., Huang, C. H., et al. (2018). Arabidopsis NITROGEN LIMITATION ADAPTATION regulates ORE1 homeostasis during senescence induced by nitrogen deficiency. *Nature Plants* 4, 898–903. doi: 10.1038/s41477-018-0269-8

Peng, M., Hannam, C., Gu, H., Bi, Y.-M., and Rothstein, S. J. (2007). A mutation in NLA, which encodes a RING-type ubiquitin ligase, disrupts the adaptability of Arabidopsis to nitrogen limitation. *The Plant J.* 50, 320–337. doi: 10.1111/j. 1365-313X.2007.03050.x

Pregitzer, K. S., and King, J. S. (2005). “Effects of soil temperature on nutrient uptake,” in *Nutrient acquisition by plants*. ed. H. BassiriRad (Berlin, Heidelberg: Springer), 277–310.

Pushnik, J. C., Miller, G. W., and Manwaring, J. H. (2008). The role of iron in higher plant chlorophyll biosynthesis, maintenance, and chloroplast biogenesis. *J. Plant Nutr.* 7, 733–758. doi: 10.1080/01904168409363238

Pyo, Y. J., Gierth, M., Schroeder, J. I., and Cho, M. H. (2010). High-affinity K⁺ transport in Arabidopsis: AtHAK5 and AKT1 are vital for seedling establishment and postgermination growth under low-potassium conditions. *Plant Physiol.* 153, 863–875. doi: 10.1104/pp.110.154369

Ramaiah, M., Jain, A., Yugandhar, P., and Raghothama, K. G. (2022). ATL8, a RING E3 ligase, modulates root growth and phosphate homeostasis in Arabidopsis. *Plant Physiol. Biochem.* 179, 90–99. doi: 10.1016/j. plaphy.2022.03.019

Rodríguez-Celma, J., Connorton, J. M., Kruse, I., Green, R. T., Franceschetti, M., Chen, Y. T., et al. (2019). Arabidopsis BRUTUS-LIKE E3 ligases negatively regulate iron uptake by targeting transcription factor FIT for recycling. *PNAS* 116, 17584–17591. doi: 10.1073/pnas.1907971116

Ruan, W., Guo, M., Wang, X., Guo, Z., Xu, Z., Xu, L., et al. (2019). Two RING-finger ubiquitin E3 ligases regulate the degradation of SPX4, an internal phosphate sensor, for phosphate homeostasis and signaling in rice. *Mol. Plant* 12, 1060–1074. doi: 10.1016/j.molp.2019.04.003

Rubio, F., Alemain, F., Nieves-Cordones, M., and Martiñez, V. (2010). Studies on Arabidopsis AtHAK5, AtAKT1 double mutants disclose the range of concentrations at which AtHAK5, AtAKT1 and unknown systems mediate K uptake. *Physiol. Plant.* 139, 220–228. doi: 10.1111/j.1399-3054.2010.01354.x

- Rubio, F., Nieves-Cordones, M., Alemañ, F., and Martínez, V. (2008). Relative contribution of AtHAK5 and AtAKT1 to K⁺ uptake in the high-affinity range of concentrations. *Physiol. Plant.* 134, 598–608. doi: 10.1111/j.1399-3054.2008.01168.x
- Sadanandom, A., Bailey, M., Ewan, R., Lee, J., and Nelis, S. (2012). The ubiquitin- proteasome system: central modifier in plant signaling. *New Phytol.* 196, 13–28. doi: 10.1111/j.1469-8137.2012.04266.x
- Sancenón, V., Puig, S., Mateu-Andrés, I., Dorcey, E., Thiele, D. J., and Peñarrubia, L. (2004). The Arabidopsis copper transporter COPT1 functions in root elongation and pollen development. *J. Biol. Chem.* 279, 15348–15355. doi: 10.1074/jbc. M313321200
- Sancenón, V., Puig, S., Mira, H., Thiele, D. J., and Peñarrubia, L. (2003). Identification of a copper transporter family in Arabidopsis thaliana. *Plant Mol. Biol.* 51, 577–587. doi: 10.1023/A:1022345507112
- Santi, S., and Schmidt, W. (2009). Dissecting iron deficiency-induced proton extrusion in Arabidopsis roots. *New Phytol.* 183, 1072–1084. doi: 10.1111/j. 1469-8137.2009.02908.x
- Sato, T., Maekawa, S., Yasuda, S., Domeki, Y., Sueyoshi, K., Fujiwara, M., et al. (2011). Identification of 14-3-3 proteins as a target of ATL31 ubiquitin ligase, a regulator of the C/N response in Arabidopsis. *Plant J.* 68, 137–146. doi: 10.1111/j.1365-313X.2011.04673.x
- Sato, T., Maekawa, S., Yasuda, S., Sonoda, Y., Katoh, E., Ichikawa, T., et al. (2009). CNI1/ATL31, a RING-type ubiquitin ligase that functions in the carbon/nitrogen response for growth phase transition in Arabidopsis seedlings. *Plant J.* 60, 852–864. doi: 10.1111/j.1365-313X.2009.04006.x
- Selote, D., Samira, R., Matthiadis, A., Gillikin, J. W., and Long, T. A. (2015). Iron-binding E3 ligase mediates iron response in plants by targeting basic helix-loop-helix transcription factors. *Plant Physiol.* 167, 273–286. doi: 10.1104/ pp.114.250837
- Shin, L. J., Lo, J. C., Chen, G. H., Callis, J., Fu, H., and Yeh, K. C. (2013). IRT1 degradation factor1, a ring E3 ubiquitin ligase, regulates the degradation of iron-regulated transporter1 in Arabidopsis. *Plant Cell* 25, 3039–3051. doi: 10.1105/tpc.113.115212
- Shin, H., Shin, H.-S., Dewbre, G. R., and Harrison, M. J. (2004). Phosphate transport in Arabidopsis: Pht1;1 and Pht1;4 play a major role in phosphate acquisition from both low- and high-phosphate environments. *Plant J.* 39, 629–642. doi: 10.1111/j.1365-313X.2004.02161.x
- Stone, S. (2019). Role of the ubiquitin proteasome system in plant response to abiotic stress. *Int. Rev. Cell Mol. Biol.* 343, 66–95. doi: 10.1016/bs. ircmb.2018.05.012
- Sun, Y., Solomon, S., Dai, A., and Portmann, R. W. (2007). How often will it rain? *J. Clim.* 20, 4801–4818. doi: 10.1175/JCLI4263.1

Sun, Y., Zhao, J., Li, X., and Li, Y. (2020). E2 conjugases UBC1 and UBC2 regulate MYB42-mediated SOS pathway in response to salt stress in Arabidopsis. *New Phytol.* 227, 455–472. doi: 10.1111/nph.16538

Takano, J., Noguchi, K., Yasumori, M., Kobayashi, M., Gajdos, Z., Miwa, K., et al. (2002). Arabidopsis boron transporter for xylem loading. *Nature* 420, 337–340. doi: 10.1038/nature01139

Takano, J., Wada, M., Ludewig, U., Schaaf, G., Von Wirén, N., and Fujiwara, T. (2006). The Arabidopsis major intrinsic protein NIP5;1 is essential for efficient boron uptake and plant development under boron limitation. *Plant Cell* 18, 1498–1509. doi: 10.1105/tpc.106.041640

Thrower, J. S., Hoffman, L., Rechsteiner, M., and Pickart, C. M. (2000). Recognition of the polyubiquitin proteolytic signal. *EMBO J.* 19, 94–102. doi: 10.1093/emboj/19.1.94

Tränkner, M., Tavakol, E., and Jákl, B. (2018). Functioning of potassium and magnesium in photosynthesis, photosynthate translocation and photoprotection. *Physiol. Plant.* 163, 414–431. doi: 10.1111/ppl.12747

Trujillo, M., and Shirasu, K. (2010). Ubiquitin in plant immunity. *Curr. Opin. Plant Biol.* 13, 402–408. doi: 10.1016/j.pbi.2010.04.002

Tsay, Y. F., Chiu, C. C., Tsai, C. B., Ho, C. H., and Hsu, P. K. (2007). Nitrate transporters and peptide transporters. *FEBS Lett.* 581, 2290–2300. doi: 10.1016/j.febslet.2007.04.047

Varadan, R., Walker, O., Pickart, C., and Fushman, D. (2002). Structural properties of Polyubiquitin chains in solution. *J. Mol. Biol.* 324, 637–647. doi: 10.1016/s0022-2836(02)01198-1

Vert, G., Grotz, N., Dédaldéchamp, F., Gaymard, F., Guerinot, M. L., Briat, J. F., et al. (2002). IRT1, an Arabidopsis transporter essential for iron uptake from the soil and for plant growth. *Plant Cell* 14, 1223–1233. doi: 10.1105/tpc.001388

Vierstra, R. D. (2012). The expanding universe of ubiquitin and ubiquitin-like modifiers. *Plant Physiol.* 160, 2–14. doi: 10.1104/pp.112.200667

Wang, S., Kurepa, J., and Smalle, J. A. (2009). The Arabidopsis 26S proteasome subunit RPN1a is required for optimal plant growth and stress responses. *Plant Cell Physiol.* 50, 1721–1725. doi: 10.1093/pcp/pcp105

Wang, L., Wen, R., Wang, J., Xiang, D., Wang, Q., Zang, Y., et al. (2019). Arabidopsis UBC13 differentially regulates two programmed cell death pathways in responses to pathogen and low-temperature stress. *New Phytol.* 221, 919–934. doi: 10.1111/nph.15435

- Wu, Q.-S., and Zou, Y.-N. (2010). Beneficial roles of arbuscular mycorrhizas in citrus seedlings at temperature stress. *Sci. Hortic.* 125, 289–293. doi: 10.1016/j.scienta.2010.04.001
- Yan, Q. Y., Duan, Z. Q., Li, J. H., Li, X., and Dong, J. L. (2013). Cucumber growth and nitrogen uptake as affected by solution temperature and NO₃⁻: NH₄⁺ ratios during the seedling. *Korean J. Hort. Sci. Tech.* 31, 393–399. doi: 10.7235/hort.2013.12178
- Yang, J., Xie, M. Y., Wang, L., Yang, Z. L., Tian, Z. H., Wang, Z. Y., et al. (2018). A phosphate-starvation induced RING-type E3 ligase maintains phosphate homeostasis partially through OsSPX2 in rice. *Plant Cell Physiol.* 59, 2564–2575. doi: 10.1093/pcp/pcy176
- Yao, Y., Dai, Q., Gao, R., Gan, Y., and Yi, X. (2021). Effects of rainfall intensity on runoff and nutrient loss of gently sloping farmland in a karst area of SW China. *PLoS One* 16:E0246505. doi: 10.1371/journal.pone.0246505
- Yasuda, S., Aoyama, S., Hasegawa, Y., Sato, T., and Yamaguchi, J. (2017). Arabidopsis CBL-interacting protein kinases regulate carbon/nitrogen-nutrient response by phosphorylating ubiquitin ligase ATL31. *Mol. Plant* 10, 605–618. doi: 10.1016/j.molp.2017.01.005
- Yasuda, S., Sato, T., Maekawa, S., Aoyama, S., Fukao, Y., and Yamaguchi, J. (2014). Phosphorylation of Arabidopsis ubiquitin ligase ATL31 is critical for plant carbon/nitrogen nutrient balance response and controls the stability of 14-3-3 proteins. *J. Biol. Chem.* 289, 15179–15193. doi: 10.1074/jbc.M113.533133
- Ye, Q., Wang, H., Su, T., Wu, W. H., and Chen, Y. F. (2018). The ubiquitin E3 ligase PRU1 regulates WRKY6 degradation to modulate phosphate homeostasis in response to low-pi stress in Arabidopsis. *Plant Cell* 30, 1062–1076. doi: 10.1105/tpc.17.00845
- Yoshinari, A., Hosokawa, T., Beier, M. P., Oshima, K., Ogino, Y., Hori, C., et al. (2021). Transport-coupled ubiquitination of the borate transporter BOR1 for its boron-dependent degradation. *Plant Cell* 33, 420–438. doi: 10.1093/plcell/koaa020
- Zhang, C. (2014). Essential functions of iron-requiring proteins in DNA replication, repair and cell cycle control. *Protein Cell* 5, 750–760. doi: 10.1007/s13238-014-0083-7
- Zhang, Z., Hu, B., and Chu, C. (2020). Towards understanding the hierarchical nitrogen signalling network in plants. *Curr. Opin. Plant Biol.* 55, 60–65. doi: 10.1016/j.pbi.2020.03.006
- Zhang, X., Wang, N., Chen, P., Gao, M., Liu, J., Wang, Y., et al. (2014). Overexpression of a soybean ariadne-like ubiquitin ligase gene GmARI1 enhances aluminum tolerance in Arabidopsis. *PLoS One* 9:e111120. doi: 10.1371/journal.pone.0111120

Conflict of Interest: The authors declare that the research was conducted in the absence of any commercial or financial relationships that could be construed as a potential conflict of interest.

Publisher's Note: All claims expressed in this article are solely those of the authors and do not necessarily represent those of their affiliated organizations, or those of the publisher, the editors and the reviewers. Any product that may be evaluated in this article, or claim that may be made by its manufacturer, is not guaranteed or endorsed by the publisher.

Copyright © 2022 Mackinnon and Stone. This is an open-access article distributed under the terms of the Creative Commons Attribution License (CC BY). The use, distribution or reproduction in other forums is permitted, provided the original author(s) and the copyright owner(s) are credited and that the original publication in this journal is cited, in accordance with accepted academic practice. No use, distribution or reproduction is permitted which does not comply with these terms.